

**LATICES AS FLOCCULANTS IN SELECTIVE FLOCCULATION OF MINERAL
SUSPENSIONS**

by

YIHONG ZHAN

B.Sc. Xiamen University, 1983, M.Sc. University of Regina, 1990

**A THESIS SUBMITTED IN PARTIAL FULFILLMENT OF THE REQUIREMENT
FOR THE DEGREE OF DOCTOR OF PHILOSOPHY**

in

THE FACULTY OF GRADUATE STUDIES

(Department of Mining and Mineral Process Engineering)

**We accept this thesis as conforming
to the required standard**

THE UNIVERSITY OF BRITISH COLUMBIA

July 1999

© Yihong Zhan, 1999

In presenting this thesis in partial fulfilment of the requirements for an advanced degree at the University of British Columbia, I agree that the Library shall make it freely available for reference and study. I further agree that permission for extensive copying of this thesis for scholarly purposes may be granted by the head of my department or by his or her representatives. It is understood that copying or publication of this thesis for financial gain shall not be allowed without my written permission.

Department of Mining and Mineral process Engineering

The University of British Columbia
Vancouver, Canada

Date July 22, 1999

ABSTRACT

In contrast to polyelectrolyte flocculants, latices possess a certain degree of hydrophobicity, are compatible with flotation collectors and can be considered for use in a flotation circuit. In this study, three latices, polystyrene (PS), poly(2-ethylhexylmethacrylate) [P(EHMA)] and copoly(methyl acrylate - acrylic acid) [P(MAAA)] were prepared, characterized and tested in the flocculation and flotation of fine salt-type minerals (e.g., fluorite, apatite and calcite). PS and P(EHMA) latices were produced by emulsion polymerization with potassium oleate as an emulsifier. P(MAAA) latex was produced by emulsifier-free emulsion polymerization of methyl acrylate and acrylic acid in a molar ratio of 1.4 : 1. The surfaces of all latex particles contained carboxylic groups. While carboxylic groups were part of the adsorbed oleic acid on the surfaces of PS and P(EHMA) latices, carboxylic groups that were brought by one of the monomers (acrylic acid) were chemically bound to the surface of P(MAAA) latex. The particles of PS latex are rigid as characterized by the high glass transition temperature of the polymer while those of the P(EHMA) latex are relatively soft as characterized by the low glass transition temperature of the polymer. The affinity of the latices to the mineral surfaces is mainly due to the interaction between the carboxylic groups on the surface of latex particles and calcium sites on the mineral surfaces. The softness of the P(EHMA) latex probably facilitates the adhesion between the latex particles and mineral surfaces.

The flocculation results with all the tested latices reveal that, at a same dosage of latices and their natural pulp pH, the P(EHMA) latex produced a higher flocculation recovery of fluorite, apatite and calcite than the other two latices, polystyrene and P(MAAA). The P(EHMA) and P(MAAA) latices all exhibit a higher flocculation recovery of fluorite and apatite than calcite. The difference of degree of flocculation of fluorite,

apatite and calcite is even greater when the P(MAAA) latex was used. The chemically bound carboxylic groups on the surface of the P(MAAA) latex particles seem to play a major role in the interaction with the minerals. The carboxylic groups on the latex surface completely ionize at pH 9.2-9.5. At this pH and at a latex dosage of 2.2 kg/t, 90% of the apatite and only 5% of the calcite flocculated. At a lower dosage of 1.1 kg/t, 60% of apatite flocculated while calcite did not flocculate at all. While with the P(EHMA) latex, at a dosage of 1 kg/t, the flocculation recovery is about 90% for apatite and 45% for calcite.

The addition of small amounts of dispersants, sodium tripolyphosphate and sodium silicate increases the apatite recovery and the P_2O_5 grade in the selective flocculation with the P(MAAA) latex from apatite-calcite and apatite-silica mixtures. At a P(MAAA) dosage of 1.1 kg/t, pH around 9.1-9.4 and 4 ppm of sodium tripolyphosphate, 60% of the apatite can be recovered from a 1:1 apatite-calcite mixture, with a 33% P_2O_5 grade. At a higher dosage of P(MAAA) latex and the same other conditions the apatite recovery can be increased to 90% while the P_2O_5 grade was not significantly changed and remained at around 33%. However with sodium silicate utilized in the apatite-calcite mixture, at a P(MAAA) dosage of 1.1 kt/t, pH around 9.1-9.4 and 20 ppm of sodium silicate, 70% of apatite can be recovered, with a 29% of P_2O_5 grade. Further increasing the sodium silicate concentration to 30 ppm did not significantly change the apatite recovery and the P_2O_5 grade. For a 1:1 apatite-silica mixture, at a P(MAAA) dosage of 1.1 kg/t, pH around 9.1-9.3 and 20 ppm of sodium silicate, 80% of apatite can be recovered, with a 33% P_2O_5 grade. However with sodium tripolyphosphate utilized in the apatite-silica mixture, at a P(MAAA) dosage of 1.1 kt/t, pH around 9.1-9.3 and 2 ppm of sodium tripolyphosphate, 70% of apatite can be recovered at a 34% P_2O_5 grade. Further increase in the sodium tripolyphosphate concentration caused decrease of both grade and recovery. Deposition

tests with P(MAAA) latex revealed that the latex has the higher deposition density and deposition rate on fluorite and apatite surfaces than on calcite surfaces. This corroborates the flocculation tests.

The use of the P(MAAA) latex in the flotation of fine (100% -38 μm) apatite and phosphate ore was evaluated via Hallimond tube and batch flotation tests. The latex enhances the flotation of the fine apatite at pH around 9. This has been attributed to the formation of flocs that increase the particle-bubble collision probability. The flocs produced by the P(MAAA) latex are apparently strong enough to withstand the shearing force in a flotation cell.

TABLE OF CONTENTS

ABSTRACT-----	ii
TABLE OF CONTENTS-----	v
LIST OF TABLES-----	x
LIST OF FIGURES -----	xi
NOMENCLATURE-----	xvi
ACKNOWLEDGEMENTS-----	xviii
INTRODUCTION-----	1
CHAPTER 1 OBJECTIVES AND SCOPE-----	4
CHAPTER 2 BACKGROUND-----	7
CHAPTER 3 SUBJECT OVERVIEW -----	9
3.1 Surface Properties of Apatite, Fluorite and Calcite -----	9
3.1.1 Composition and Structure -----	9
3.1.2 Minerals/Water Interfaces-----	13
3.1.2.1 Fluorite/Water Interface-----	14
3.1.2.2 Calcite/Water Interface-----	15
3.1.2.3 Apatite/Water Interface -----	17
3.2 Flotation Beneficiation of Phosphate Ores-----	19
3.2.1 Flotation of Phosphate Ores Containing Siliceous Gangue-----	20
3.2.2 Flotation of Phosphate Ores Containing Calcareous Gangue -----	21
3.3 Fundamental Aspects of Flotation with Fatty Acids-----	24
3.3.1 Oleate Colloid Chemistry-----	24

3.3.2 Flotation with Fatty Acids -----	26
3.3.3 FTIR Studies on Adsorption Mechanism-----	29
3.3.4 Effects of Modifying Reagents -----	32
3.4 Selective Flocculation -----	38
3.4.1 Basic Principles-----	39
3.4.2 Stability of Mineral Suspensions -----	40
3.4.2.1 Electrical Double Layer-----	40
3.4.2.2 Stability of Mineral Suspensions -----	41
3.4.3 Dispersing Agents -----	45
3.4.4 Flocculants and Flocculation -----	46
3.4.5 Separation of Apatite from Carbonate and Silica by Selective Flocculation -----	51
3.5 Polymer Latices -----	53
3.5.1 Emulsion Polymerization -----	54
3.5.2 The Role of Surfactants -----	54
3.5.3 The Stability of Polymer Latices-----	56
3.5.4 The Glass Transition Temperature, T_g , of a Polymer -----	57
3.5.5 Surface Characterization of Latices-----	60
3.5.6 Methods of Latex Cleaning -----	62
3.6 Deposition of Colloidal Particles on Planar Surfaces -----	63
3.6.1 The Rotating Disc System -----	64
3.6.2 Deposition of Colloidal Particles on Planar System -----	67

CHAPTER 4 EXPERIMENTAL	71
4.1 Definition	71
4.2 Experimental Approach	71
4.3 Preparation of Mineral Samples	75
4.4 Chemicals	77
4.5 Experimental Setups and Methods	81
4.5.1 Preparation of Latices	81
4.5.2 Purification of Latices	84
4.5.2.1 Serum Replacement Technique	85
4.5.2.2 Ion-Exchange Resin	86
4.5.3 Characterization of Latices	87
4.5.3.1 Microelectrophoretic Mobility Measurements	87
4.5.3.2 Scanning Electron Microscope (SEM) Analysis	88
4.5.3.3 Contact Angle Measurement	88
4.5.4 Characterization of Mineral Samples	89
4.5.4.1 Infrared Spectroscopy	89
4.5.4.2 Surface Area Measurements	90
4.5.4.3 Electrokinetic Measurements	90
4.5.5 Microflotation Tests	90
4.5.6 Flocculation Tests	91
4.5.7 Batch Flotation Tests	94
4.5.8 Deposition of Latex Particles on Mineral Surfaces	94

4.5.9 2 ³ Factorial Design Experiments	96
CHAPTER 5 RESULTS AND DISCUSSION	100
5.1 Latex Characterization	100
5.1.1 Electrophoretic Mobility Measurements	100
5.1.2 Scanning Electron Microscope	100
5.1.3 Contact Angle Measurements	104
5.2 Characterization of Mineral Samples	109
5.2.1 FTIR Spectroscopy	109
5.2.2 Surface Area Measurements	114
5.2.3 Electrokinetic Measurements	116
5.3 Single Mineral Flocculation with Latices	116
5.3.1 Comparison of Effect of P(EHMA) and PS Latex Dosages	116
5.3.2 Effect of pH on Flocculation Using P(EHMA) Latex	121
5.3.3 Single Mineral Flocculation with the P(MAAA) Latex	125
5.4 Deposition of the Latices onto Mineral Surfaces	129
5.5 Selective Flocculation Using Latex P(MAAA)	133
5.6 Effect of Dispersing Agents	140
5.7 Microflotation	152
5.8 Batch Flotation	161
5.9 2 ³ Factorial Design Experiments	164
CHAPTER 6 GENERAL DISCUSSION	170
6.1 Effect of Characteristics of Latex Particles on Interaction with Mineral	

Surfaces -----	170
6.2 The Role of P(MAAA) Latex in Selective Flocculation of Apatite, Calcite and Silica-----	172
6.3 Loss of Selectivity in the Mixed Component Systems -----	173
6.4 The Role of Latex P(MAAA) in Flotation of Fine Apatite-----	175
CHAPTER 7 CONCLUSION -----	178
CHAPTER 8 SUGGESTION FOR FUTURE WORK -----	182
CHAPTER 9 REFERENCES-----	184
APPENDIX I Calculation of Mobility and Conversion of Mobility to Zeta Potential---	201
APPENDIX II Calculation of Standard Deviation and Interaction Effects Among Factors-----	205

LIST OF TABLES

Table	Page
3.1 Approximate values of glass transition temperature, T_g , for various polymers	59
4.1 Chemical Characterization of Mineral Samples	76
4.2 Compositions of the Phosphate Sample	76
4.3 Chemicals	79
4.4 Recipes and Conditions of Latices Preparation	83
4.5 Preparation of Polystyrene with Various Concentrations of Emulsifier	84
5.1 Effect of Emulsifier Concentration on the Size of Polystyrene Latex Particles	106
5.2 Contact Angles of the Latices	109
5.3 BET Surface Area Determination	114
5.4 Results of Flotation of Coarse and Fine Florida Phosphate	161
5.5 Results of Flotation of the Fine (-38 μm) Florida Phosphate in the Presence of Depressant and P(MAAA) Latex	163
5.6 Results and Calculations of Factorial Experiment on the Apatite-Calcite System	164
5.7 Results and Calculations of Factorial Experiment on the Apatite-Silica System	167

LIST OF FIGURES

Figure	Page
1.1 Structural formulas of (a) polystyrene (b) poly(2-ethylhexylmethacrylate) (c) poly(methyl acrylate-acrylic acid) (d) potassium oleate	5
3.1 Structure of apatite (Young, 1980; Montel et al, 1977) (a) apatite projected on ab plane (b) perspective drawing of Y-ion column	12
3.2 Domain diagram for oleic acid (Laskowski, 1988)	25
3.3 The effect of conditioning time and pH on the flotation response of fluorite at a concentration of sodium oleate of 10^{-5} M (Laskowski, 1994)	28
3.4 Ex-situ FTIR/IRS spectra of chemisorbed oleate and adsorbed calcium dioleate (Free and Mill, 1995)	31
3.5 Comparison of adsorption density verse oleate concentration for both in-situ and ex-situ FTIR adsorption analysis, pH9.5 to 10 (Free and Miller, 1995)	31
3.6 Schematic illustration of selective flocculation in a two-component ore	40
3.7 Schematic illustration of various types of latex particles surface: (a) smooth; (b) with nonionic chains; (c) with ionic chains	57
3.8 The flow pattern imposed by a rotating disc. The right-hand inset shows the stream lines below the disc. The left-hand inset shows the stream lines in an x, y plane and emphasises that v_z does not depend on the radial distance. The bottom inset shows the values of F (radial velocity) and H (velocity towards the disc) that are found in the diffusion layer	66
3.9 (a) Stagnation point flow collector. 1. colloidal dispersion; 2. entrance tube; 3. collector; 4. microscope; 5. Outflow tube; 6. Flow speed control valve; 7. Reservoir (b) stagnation point flow, two-dimensional schematic representation of fluid streamlines and coordinates system	70
4.1 A sketch of the experimental apparatus used to produce latices	81
4.2 A sketch of the filtration cell used for serum replacement of latices. (A)feed stream inlet; (B) polyacetal top plate; (C) Teflon-coated	

magnetic stirring bar; (D) polycarbonate reservoir; (E) ethyl-propylene copolymer O-ring; (F) polyethylene porous disc; (G) polyacetal bottom plate; (H) filtrate outlet	85
4.3 A sketch of the flocculation device	92
4.4 Diagram of the rotating disc apparatus. (A) constant speed motor with reduction gears; (B) roller bearing; (C) collect chuck; (D) cover; (E) glass dish containing dispersion; (F) Teflon disc; (G) deposition surface	96
5.1 Electrophoretic mobility of polystyrene latex particles (a) effect of emulsifier concentration on mobility of latex particles (b) effect of ion-exchange resin treatment on mobility of latex particles	102
5.2 Comparison of electrophoretic mobility of P(EHMA) and P(EHMA)-R latex particles	103
5.3 Electrophoretic mobility of P(MAAA) latex	103
5.4 SEM micrography of polystyrene latex	107
5.5 SEM micrography of P(EHMA) latex	107
5.6 SEM micrography of P(MAAA) latex	108
5.7 Diffuse reflectance FTIR spectra of fluorite (sample without mixed with KBr)	111
5.8 Diffuse reflectance FTIR spectra of fluorite (sample mixed with 50% KBr)	112
5.9 Diffuse reflectance FTIR spectra of apatite (sample mixed with 50% KBr)	113
5.10 Diffuse reflectance FTIR spectra of calcite (sample mixed with 50% KBr)	115
5.11 Zeta potential of fluorite, apatite, calcite and silica as function of pH	117
5.12 Effect of calcite supernatant on the zeta potential of apatite and apatite supernatant on the zeta potential of calcite	117
5.13 Effect of PS dosage on flocculation of fluorite	119
5.14 Effect of P(EHMA) dosage on flocculation of fluorite	119
5.15 Effect of P(EHMA) dosage on flocculation of apatite	120
5.16 Effect of P(EHMA) dosage on flocculation of calcite	120
5.17 Effect of pH on flocculation of fluorite with P(EHMA) latex	122
5.18 Effect of pH on flocculation of apatite with P(EHMA) latex	122
5.19 Effect of pH on flocculation of calcite with P(EHMA) latex	123

5.20 Effect of P(EHMA) latex dosage on flocculation of fluorite, apatite and calcite at their natural pH	126
5.21 Effect of pH on flocculation of fluorite, apatite and calcite with P(EHMA) latex	126
5.22 Effect of P(EHMA)-R dosage on flocculation of fluorite, apatite and calcite at their natural pH	127
5.23 Effect of pH on flocculation of apatite, fluorite and calcite with P(EHMA)-R latex	127
5.24 Effect of P(MAAA) dosage on flocculation of fluorite, apatite and calcite	128
5.25 Effect of pH on flocculation of apatite, fluorite and calcite with P(MAAA) latex	128
5.26 Deposition of P(MAAA) latex onto fluorite surface	132
5.27 Comparison of deposition of P(MAAA) latex onto fluorite, apatite and calcite surfaces	134
5.28 Deposition of P(MAAA) latex onto fluorite, apatite and calcite surfaces vs. the deposition time	134
5.29 Deposition of P(MAAA) latex onto fluorite, apatite and calcite surfaces vs. pH	135
5.30 Deposition of P(MAAA) latex onto apatite and calcite surfaces at two different pH level	135
5.31 Effect of P(MAAA) dosage on the selective flocculation of apatite from apatite/calcite mixture	137
5.32 Effect of pH on selective flocculation of apatite from apatite/calcite mixture	137
5.33 Effect of P(MAAA) dosage on selective flocculation of apatite from apatite/silica mixture	139
5.34 Effect of P(MAAA) dosage on selective flocculation of fluorite from fluorite/calcite mixture	139
5.35 Effect of P(MAAA) dosage on selective flocculation of fluorite from fluorite/silica mixture	141
5.36 Effect of dispersants concentrations on zeta potential of fluorite	143

5.37 Effect of dispersants concentrations on zeta potential of apatite	143
5.38 Effect of dispersants concentrations on zeta potential of calcite	144
5.39 Effect of dispersants concentrations on zeta potential of silica	144
5.40 Effect of sodium silicate on flocculation of fluorite, apatite and calcite	145
5.41 Effect of sodium tripolyphosphate on flocculation of fluorite, apatite and calcite	145
5.42 Effect of sodium tripolyphosphate concentration on selective flocculation of apatite from apatite/calcite mixture at two levels of P(MAAA) dosage	146
5.43 Effect of sodium silicate concentration on selective flocculation of apatite from apatite/calcite mixture	146
5.44 Effect of pH on selective flocculation of apatite from apatite/calcite mixture in the presence of sodium tripolyphosphate	148
5.45 Effect of sodium silicate on selective flocculation of apatite from apatite/silica mixture	148
5.46 Effect of sodium tripolyphosphate on selective flocculation of apatite from apatite/silica mixture	149
5.47 Effect of pH on selective flocculation of apatite from apatite/silica mixture in the presence of sodium silicate	151
5.48 Effect of sodium silicate concentration on selective flocculation of fluorite from fluorite/calcite mixture	151
5.49 Effect of sodium silicate concentration on selective flocculation of fluorite from fluorite/silica mixture	153
5.50 Effect of P(MAAA) dosage on selective flocculation of fluorite from fluorite/silica mixture in the presence of sodium tripolyphosphate	153
5.51 Effect of pH on flotation of fluorite at two different concentrations of sodium oleate following 5 minutes conditioning	155
5.52 Effect of pH on flotation of apatite at two different concentrations of sodium oleate following 5 minutes conditioning	155
5.53 Effect of pH on flotation of calcite with sodium oleate following 5 minutes conditioning	156

5.54 Effect of conditioning time on flotation of apatite under acidic and alkaline conditions	156
5.55 Effect of pH on flotation of different sizes apatite with sodium oleate	157
5.56 Effect of pH on flotation of fine apatite in the presence of P(MAAA)	157
5.57 Comparison of effect of addition order of P(MAAA) and oleate on flotation of fine apatite	159
5.58 Flotation of fine apatite with P(MAAA) at natural pH	159
5.59 Effect of pH on flotation of fine apatite in the presence of P(MAAA) and oleate for two different flotation times	160

NOMENCLATURE

ν	Kinetic viscosity, Ns/m^2
ω	Rate of rotation of the disc, rad/sec
%	Mass percentage
κ	Debye-Hückel reciprocal length, m^{-1}
ϵ	Permittivity of suspension, F/m
η	Suspension viscosity, Ns/m^2
ζ	Zeta potential, volt
ψ_8	Potential at Stern layer, volt
ψ_1	Surface potential of particle 1, volt
ψ_2	Surface potential of particle 2, volt
ψ_0	Surface potential, volt
A	Hamaker - London constant, Joule
a	Radius of particle, m
a_1	Radius of particle 1, m
a_2	Radius of particle 2, m
c	Concentration, kmol/m^3
C	Number of centerpoints
D	Brownian diffusion coefficient, m^2/s
ν	Degree of freedom
e	Electronic charge, -1.6×10^{-19} coulomb
μ	Electrophoretic mobility, $\text{m}^2 \text{sec}^{-1} \text{volt}^{-1}$
F	Form factor, $a_1 a_2 / a_1 + a_2$, m
Grade	Mass content of valuable component
H_0	Shortest separation distance between two particles, m
j	Flux, $\text{particle/m}^2 \text{sec}$

k	Boltzmann's constant, 1.38×10^{-23} J/T
N	Number of factorial runs
Pulp density	Mass solid content in the pulp
r	Distance from the rotating axis, m
r	Number of replicate runs
s	Response error estimate with ν degree of freedom
s_G	Standard deviation for grade
s_R	Standard deviation for recovery
t	Absolute temperature, °K
t	Student's t statistic
T_g	Glass transition temperature, °K
V_A	London-van der Waals dispersion energy, Joule
V_R	Electrostatic repulsive energy, Joule
V_S	Structural energy, Joule
V_T	Total potential energy of interaction, Joule
v_z	Velocity normal to the disc, m/sec
z	Distance normal to the disc, m
z	Ionic charge

ACKNOWLEDGEMENTS

First, I would like to express my sincere thanks to my supervisor, Professor Janusz S. Laskowski who introduced me to the field of mineral processing which I have found to be an interesting field of study. I appreciate his invaluable guidance and support in the course of this work. I am also grateful to my supervising committee members, Dr. Chris Brion (Dept. of Chemistry), Professor Colin W. Oloman (Dept. of Chemical and Bio-resource Eng.) and Dr. Bern Klein, for their valuable advice and constructive comments during my thesis work.

My sincere thanks are due to the technicians, Mrs. Sally Finora, Mr. Pius Lo and Mr. Frank Schmiddiger, for their kind and reliable technical assistance. My thanks are also due to Mr. Peter Kempe and Mr. Larry Wong for the chemical analysis of the mineral samples. I would also like to thank our graduate secretary Mrs. Marina Lee for her kind help in general graduate administration work especially during my absence from the department.

I would also like to acknowledge many useful discussions with Dr. Qun Wang who is now a Research Scientist at World Minerals.

The financial support of the Natural Sciences and Engineering Research Council of Canada is gratefully acknowledged.

Finally, I owe an apology to my parents, Tingyu Zhan and Shuru Zhang, for the long time between visits. For their patience and understanding, they deserve a great deal of thanks. I must also thank my two wonderful children, my son, Bing and my daughter, Amy, for the joy they brought to me during the course of this work.

INTRODUCTION

Numerous investigations have confirmed that the best particle size range for mineral flotation is 45-150 μm ; individual minerals possess an optimum size of flotability. Particles which are below this size range may be too fine to be separated efficiently by the flotation and are generally disposed of as waste. As the world is being depleted of its high-grade ore deposits and environmental concerns have become more and more important, new separation techniques are needed to recover mineral values from these fine-sized fractions and to reduce the amount of waste materials.

Selective flocculation has emerged as one of the very promising techniques for beneficiation of the fine mineral particles. The commercial application of selective flocculation was reviewed by Attia (1992). The most cited example of a commercial selective flocculation operation is the Tilden Iron Ore mine in Michigan, USA. At Tilden, corn starch is used to selectively flocculate hematite from silica, followed by the flotation of silica from the flocculated (depressed) hematite. Other commercial examples include the upgrading of sylvinite (potash) ore by flocculation and flotation of insoluble slime, and the selective flocculation of titanium minerals from kaolinite. Countless examples of successful selective flocculation separations conducted on both laboratory and pilot plant scales have been reported in literature (Yarar and Kitchener, 1970; Rubio and Kitchener, 1977; Kitchener, 1978; Moudgil and Somasundaran, 1985; Yu and Attia, 1987; Moudgil et al., 1987a; Pradip and Moudgil, 1991; Moudgil et al., 1993, 1994). However, the industrial application of the selective flocculation is still very limited.

Conventional flocculants, such as polyacrylamide, are usually non-selective and are commonly used in thickening and water clarification. The flocs produced by polyelectrolytes are hydrophilic and can not be recovered by flotation. Oil agglomeration is one of the processes that produces hydrophobic agglomerates. However, the process requires a large quantity of oil and the treated particles should initially be hydrophobic (e.g., bituminous coal). The agglomerates can be separated by screening. Oil is also used in agglomerate flotation. The method involves conditioning the fine particles with an appropriate collector to render the particles hydrophobic, followed by adsorption of oil to bridge the hydrophobic particles together. Conventional froth flotation is utilized to recover the agglomerates. Ralston and Kent (1984, 1985) reported the use of a polymer-stabilized oil emulsion in fine particle processing.

In the past ten years, the use of latex in selective flocculation of fine particles has received considerable attention (Littlefair and Lowe, 1986; Attia and Yu, 1987; Laskowski, Yu and Zhan, 1995). The hydrophobic nature of latices tends to make the flocs hydrophobic and, therefore, able to be separated by flotation. Thus, flocculation and flotation can be carried out together in the same circuit.

Selective adsorption/attachment is a prerequisite for selective flocculation; such adsorption may result from the hydrophobic interaction between latices and mineral surfaces which are either inherently hydrophobic, (e.g., graphite, coal, molybdenite) or which are made hydrophobic by specific adsorption of surfactants. Littlefair and Lowe (1986) reported selective flocculation of coal particles with the use of polystyrene latex prepared by emulsion polymerization with oleic acid. The FR-7A latex used by Attia et al. (1987) in selective flocculation of coal seems to belong to the same type of flocculants. A latex prepared by Laskowski et al. (1995) was shown to be more selective and effective in

flocculation of hydrophobic bituminous coal particles and molybdenite (Castro, Stocker and Laskowski, 1997). The "hairy" surface (van de Ven et al., 1983; Zimehl and Lagaly, 1986; Chow et al., 1988) of the latex particles resulting from the adsorption of the emulsifier utilized in emulsion polymerization plays an important role in the adsorption/attachment of latex particles onto the mineral surface. Moreover, the surface properties of latices can be modified by using emulsifiers containing specific chemical functional groups which specifically interact with a given mineral, thus achieving selectivity. In the example of the use of polymer-stabilized oil emulsion in fine particle recovery (Ralston and Kent, 1984, 1985), the carboxylic group in the copolymer of methacrylic acid and its methyl ester specifically interacted with the treated mineral, calcite, through the formation of calcium carboxylate.

The characteristics of polymer latices are determined by i) the emulsifier adsorbed on the surface of latex particles and ii) the monomer making up the backbone of the polymer molecule.

It seems that selective flocculation-flotation which combines flocculation and flotation is the most promising concept for treating fine particles.

CHAPTER 1 OBJECTIVES AND SCOPE

This dissertation intends to study interactions between several synthesized latices, such as polystyrene (PS), poly(2-ethylhexylmethacrylate)[P(EHMA)] and copoly(methacrylate - acrylic acid) [P(MAAA)], and salt-type minerals such as apatite, fluorite and calcite, by means of flocculation and latex deposition tests; to investigate the effect of latex particle characteristics on latex-mineral interactions; and to develop a latex for use in the selective flocculation of apatite from gangue minerals (e.g., silica and calcite). Such a latex, if hydrophobic enough, should also enhance flotation recovery of fine apatite particles.

To fulfil these research objectives, the selection of latices was chosen as the starting point. The selection of polystyrene and poly(2-ethylhexylmethacrylate) was based on the fact that the PS particles are rigid spheres while the P(EHMA) particles are relatively softer than the PS particles. Thus a comparison can be made based on the differences in physical properties of the latex particles. Oleic acid is commonly used as a collector in the flotation of salt-type minerals. In this study, it is used as an emulsifier in the emulsion polymerization of styrene and 2-ethylhexylmethacrylate. Thus, the prepared PS and P(EHMA) latices are stabilized by the carboxylic groups resulting from the adsorption of the emulsifier and by the sulfate group originating from the potassium persulphate initiator.

P(MAAA) latex was produced by the surfactant-free emulsion polymerization of methyl acrylate and acrylic acid at a molar ratio of 1.4 : 1. Polyacrylic acid has been reported to be a flocculant in the selective flocculation of apatite (Mehta, 1993). By copolymerization of methyl acrylate and acrylic acid at a molar ratio of 1.4 : 1, a polymer

latex can be obtained, which, in contrast to the PS and P(EHMA) latex, has carboxylic groups chemically bound to the surface of the latex. Thus the latex is stabilized by carboxylic groups which come from the acrylic acid monomer and sulfate group originating from the potassium persulphate initiator. Structural formulas of PS, P(EHMA), P(MAAA), and potassium oleate are given in Figure 1.1.

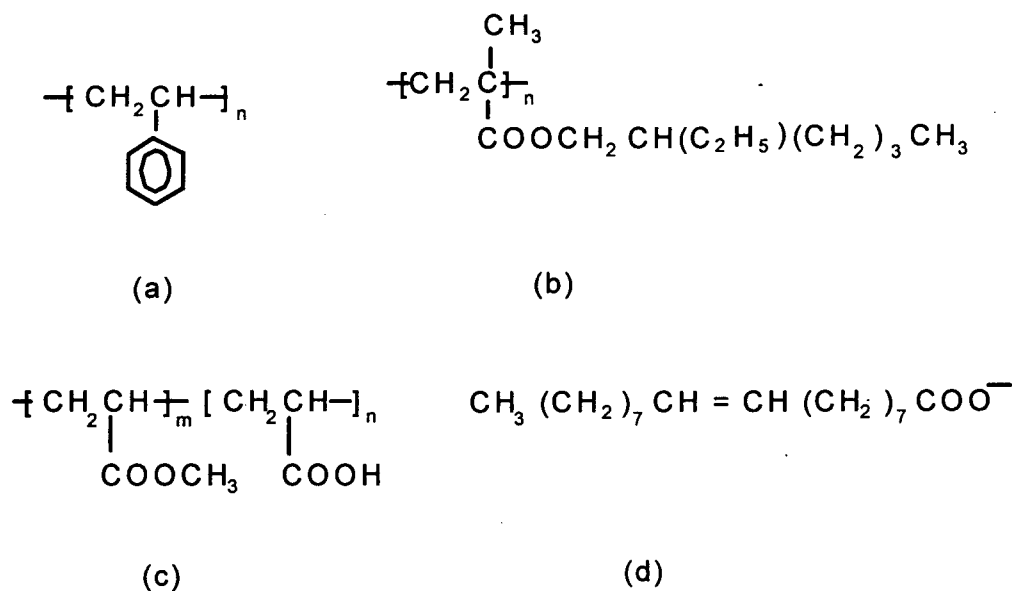


Figure 1.1 Structural formulas of (a) polystyrene (PS), (b) poly(2-ethylhexylmethacrylate) [P(EHMA)], (c) poly(methyl acrylate - acrylic acid) [P(MAAA)], (d) potassium oleate

The scope of this dissertation can be detailed as follows:

1. To prepare polystyrene latex with different concentrations of the potassium oleate emulsifier, to investigate the effect of the proportion of the emulsifier on the properties of latex particles and on the flocculation of salt-type minerals;

2. To prepare the P(EHMA) latex and compare it with polystyrene latex in order to investigate the effect of latex particle characteristics on latex-mineral interaction;
3. To prepare the P(MAAA) latex and compare with PS and P(EHMA) latices in order to evaluate the effectiveness of the P(MAAA) latex used in selective flocculation of apatite/silica, apatite/calcite, fluorite/silica and fluorite/calcite systems;
4. To investigate effects of the P(MAAA) latex dosage, pH and the concentration of dispersant on the selective flocculation of apatite/calcite, apatite/silica, fluorite/silica and fluorite/calcite systems;
5. To carry out a factorial experiment on apatite/calcite and apatite/silica systems in order to examine any interaction between the experimental factors;
6. To investigate the deposition of the P(MAAA) latex particles onto the salt-type minerals and correlate the observation with the flocculation results;
7. To evaluate the P(MAAA) latex in enhancing the flotation recovery of fine apatite mineral particles.

CHAPTER 2 BACKGROUND

Apatite $[\text{Ca}_{10}(\text{PO}_4)_6(\text{F}, \text{Cl}, \text{OH})_2]$ is a carrier mineral of phosphorus and is the valuable mineral in phosphate ores. It is classified as a sparingly soluble salt-type mineral. Its solubility is much lower than those of simple salt minerals, such as halite and sylvite, but higher than those of most oxides and silicates. Fluorite is the simplest mineral in this group, and it is used for comparison in the selective flocculation of apatite. Examples of other salt-type minerals of commercial importance are barite $[\text{BaSO}_4]$, scheelite $[\text{CaWO}_4]$, magnesite $[\text{MgCO}_3]$, calcite $[\text{CaCO}_3]$, dolomite $[(\text{Ca}, \text{Mg})\text{CO}_3]$ and gypsum $[\text{CaSO}_4 \cdot 2\text{H}_2\text{O}]$. Calcite is treated as gangue in the selective flocculation of apatite and fluorite.

About 90% of the phosphate derived from phosphate ores is consumed in agricultural applications, of which 90% is used in phosphate fertilizers and the remainder is used as animal feed. In the process of making fertilizers, phosphate ores are first converted into phosphoric acid and gypsum by sulfuric acid. In order to minimize the consumption of sulfuric acid and the formation of gypsum in this process, it is necessary for the phosphate ore to have P_2O_5 content higher than 32 % and a molar ratio of $\text{CaO}/\text{P}_2\text{O}_5$ that does not exceed 1.6. The quality of phosphate ore is generally expressed not only as $\text{P}_2\text{O}_5\%$ but also as BPL% or TPL% which stands for Bone Phosphate of Lime or Tricalcium Phosphate of Lime. The conversion factor is as follows:

$$\text{P}_2\text{O}_5\% = 0.4576 \text{ BPL}\% \text{ or TPL}\%$$

The grade of phosphate ore is critical to economic mining operations. Normally, a phosphate ore with greater than 32% P_2O_5 can be directly used in the production of

phosphoric acid. Thus rock with more than 32% P_2O_5 is known as acid grade phosphate. In the electric furnace process for the production of elemental phosphorus, silica is required in the furnace to combine with the calcium of apatite, so phosphate ore with a silicate gangue with a grade between 24 and 32% P_2O_5 can be used directly. This is known as furnace grade phosphate rock. Rock of a lower grade, between 18 and 24% P_2O_5 , is not suitable for either the acid or the electric furnace process without beneficiation and is known as beneficiation grade phosphate rock. Finally, rock between 10 and 18% P_2O_5 is generally not used in today's operations but is commonly stockpiled for future use, and is termed low-grade phosphate. Rock with a P_2O_5 content below 10% is regarded as waste.

Although phosphorus has never commanded a price as high as gold and has never been called precious, its availability is much more essential to human existence than that of gold or of any of the precious elements. It is a commodity which is neither substitutable nor recyclable in agricultural applications. Apatite and other carbonates such as calcite and dolomite along with siliceous gangue are often intergrowth in phosphate ores. Currently, high grade siliceous phosphate ores with a low carbonate content are rapidly being depleted. However, vast tonnages of low grade carbonate-containing phosphate ore deposits are present worldwide. This type of phosphate ore is the most common and constitutes more than two thirds of the present day reserves.

Numerous studies have aimed at improvement of the efficiency of the phosphate flotation separation process. However, the traditional flotation technique is extremely inefficient in the processing of the fine mineral particles ($<38\mu\text{m}$), and new separation techniques are necessary to recover mineral values from these fine-size fractions.

CHAPTER 3 SUBJECT OVERVIEW

3.1 Surface Properties of Apatite, Fluorite and Calcite

As was mentioned in the previous section, apatite, fluorite and calcite are classified as salt-type minerals. The chemical composition and crystal structure of these minerals are directly related to their surface properties. Since surface properties of these minerals in an aqueous solution determine their flotation and flocculation properties, understanding their surface properties is the basis for improvement for the beneficiation of these minerals.

3.1.1 Composition and Structure

Among fluorite, apatite and calcite, fluorite has the simplest type of crystal structure which is a face-centered cube. In the cubic unit cell, calcium ions are located at the corners and face centres while fluoride ions reside in the holes of the tetrahedrons of calcium lattice. Each calcium ion, is therefore, coordinated by eight neighboring fluoride ions at the corner of a cube, each of which is, in turn, coordinated by four calcium ions. Thus the structure has an 8:4 coordination. The most probable cleavage is along the (111) plane located between two fluoride layers.

Calcite possesses two forms of structures. In the rhombohedral calcite structure, Ca^{2+} ions locate at the corners and faces of the unit cell and the CO_3^{2-} ions locate at the center of both the edges and the cell itself. Each Ca^{2+} is coordinated by six CO_3^{2-} and each oxygen atom of these anions is coordinated by two Ca^{2+} . In the orthorhombic aragonite

form of CaCO_3 , each Ca^{2+} is coordinated by nine oxygen atoms and each oxygen is coordinated by three Ca^{2+} . The most probable cleavage plane for calcite is the 1011 plane.

The crystal structure of apatite is much more complicated. Apatite belongs to the hexagonal system and is characterized by the chemical formula $\text{M}_{10}(\text{XO}_4)_6\text{Y}_2$, where M is Ca^{2+} , XO_4 is the PO_4^{3-} anion and Y is a univalent anion such as F^- , Cl^- and OH^- . Two major basic apatite minerals are hydroxyapatite and fluorapatite, $\text{Ca}_{10}(\text{PO}_4)_6(\text{OH})_2$ and $\text{Ca}_{10}(\text{PO}_4)_6\text{F}_2$ respectively.

The unit cell contains 10 cations, 6 anions XO_4 and 2 anions Y. Figure 3.1a and b shows the position of these ions in the unit cell. In Figure 3.1a (considering fluorapatite as an example), two of the oxygen atoms in the tetrahedral PO_4^{3-} ions are in a horizontal plane, and the other two lie in the same vertical plane. These ions are divided into two "groups", where they constitute hexagonal arrangements situated in terms of height at 1/4 and 3/4 of the unit cell.

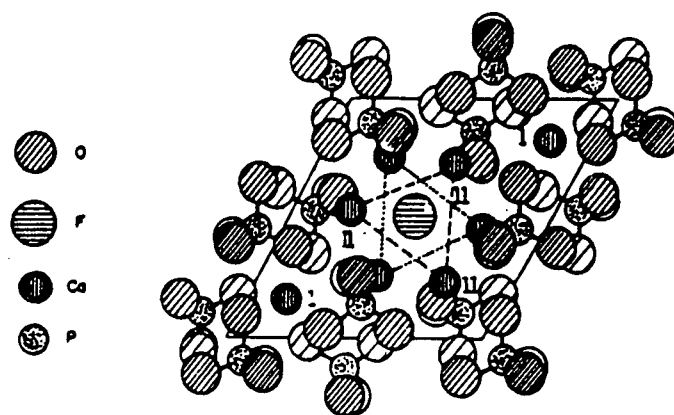
Considering the structure parallel to the "c" axis (vertical), Figure 3.1b shows the PO_4^{3-} ions in the form of "colonies", linked to each other in such a way that each phosphorus is bound to three oxygen ions in one "colony" and to one oxygen in a neighbor "colony".

There are two types of "tunnels" in this structure. One type of tunnel has a mean diameter of 2.5 Å. It is occupied by Ca^{2+} ions, called Ca(1), approximately at levels of 0 and 1/2 of the unit cell (these ions are not shown in Figure 3.1b). The second type of tunnel is wider, with a mean diameter between 3 and 3.5 Å. Its centre is located at the hexad symmetry axis. It is surrounded by Ca^{2+} ions, called Ca(2), arranged as equilateral triangles, situated at levels of 1/4 and 3/4 of the unit cell. This second type of tunnel is also

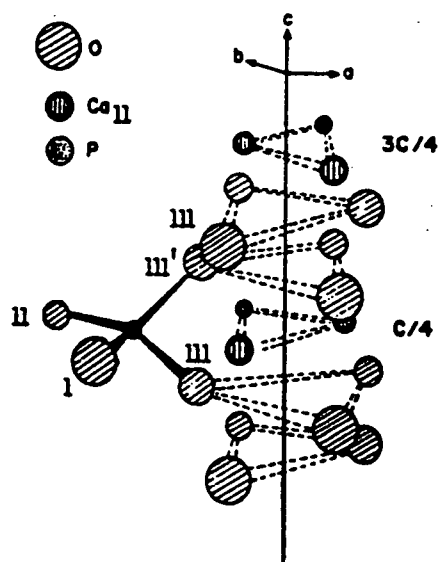
surrounded by 4 other triangles formed by oxygen ions from the neighboring PO_4^{3-} ions. The Y ions (Cl^- , F^- and OH^-) are situated inside the tunnels of the second type. Their positions are indicated in Figure 3.1b. F^- lies at the centre of a triangle of Ca(2) ions, Cl^- lies nearly at the centre of the triangle of oxygen ions, the oxygen O(H) of the hydroxyl ion lies about 0.4 Å out of the plane of the Ca(2) triangle, and the hydrogen lies 1 Å further away, nearly in the plane of the nearest oxygen triangle.

As shown in Figure 3.1a, apatite possesses an "open lattice". This type of lattice is responsible for the large number of substituents found in most natural apatites. Thus, calcium in the apatite lattice is reported to be substituted by Mn, Sr, Mg, rare earth elements, Na, K, H_2O , H_3^+O , Cu, Sn, Pb, C, etc.; phosphate by SO_4^{2-} , SiO_4^{4-} , CO_3^{2-} , $\text{H}_4\text{O}_4^{4-}$, AsO_4^{3-} , VO_4^{3-} and CrO_4^{2-} ; and F^- by OH^- , H_2O , Cl^- . Because of the possibility of extensive substitutions, the chemical composition of apatites and, therefore, their surface properties can be expected to vary markedly from deposit to deposit.

The surface energy of minerals depends strongly on the cleavage plane of the crystals. In the case of fluorite, the surface energy is 543 erg/cm² at the (111) face and 1082 erg/cm² at the (110) face (Adamson, 1967). In addition, variations in surface energy can also result from any perturbation of the periodic pattern of the crystal lattice owing to the presence of lattice defects or impurity species or even from the abrupt ending and rearrangement of the lattice at the surface.



(a)



(b)

Figure 3.1 Structure of Apatite (Mackie and Young, 1973; Montel et al., 1977) (a) Apatite projected on the ab plane (b) Perspective drawing of a Y-ion column

Fluorite, calcite and apatite are classified as semiconductors. In fact, the crystal lattice of a mineral normally deviates from the ideal structure, and the degree of deviation can be estimated from its electrophysical parameters such as the Fermi level or the concentration ratio of the charge carriers, p / n , since these parameters reflect such deviations.

The Fermi level represents the energy level whose probability of being occupied by electrons is 1/2. Carta et al. (1970, 1974) have presented correlations between various electrophysical parameters and the flotation response as well as the electrostatic response of certain minerals. They have observed that fluorite and calcite change from n- to p-type semiconductors upon dry grinding and thereby become more floatable with an anionic collector (e.g., sodium oleate) due to the enhanced electrostatic interaction between the mineral and the collector. Heating of the solid can also be expected to affect the flotation response since upon increasing the temperature, the Fermi level of a n-type material would be lowered thereby enhancing the anionic collector adsorption while the Fermi level of a p-type material rises with temperature so that the anionic collector adsorption on the solid is decreased.

3.1.2 Mineral/Water Interfaces

The salt-type mineral/water interfaces are much more complex than those of oxides and silicates. The potential-determining ions for these minerals are the lattice ions, e.g., Ca^{2+} and F^- for fluorite, Ca^{2+} , PO_4^{3-} and F^- (OH^-) for fluorapatite (hydroxyapatite) and Ca^{2+} and CO_3^{2-} for calcite. However, since these ions undergo hydrolysis which is

controlled by H^+ and OH^- ions (pH), these ions can also be considered as potential-determining ions.

The charge characteristics of a mineral/water interface are determined by the chemical composition of the aqueous phase and the solubility of the mineral. In general, solubility decreases in the presence of electrolytes that contain constituent ions of the mineral and increases when other electrolytes are added. However, it is noteworthy that the responses of the individual species in a mineral to the addition of an electrolyte could be different from each other. For example, in the case of fluorite with an addition of Na_2CO_3 , while the solubility of Ca^{2+} ions from fluorite is decreased by the addition of Na_2CO_3 , that of F^- ions is greatly enhanced (Bahr et al., 1968). Based on the data (Bahr et al., 1968), the presence of carbonates can be expected to enhance the solubility of fluorite. Bilsing (1969) has reported a significant increase in the solubility of CaF_2 and $CaCO_3$ in the presence of each other. Amankonah and Somasundaran (1985) have studied the effect of dissolved mineral species on the electrokinetic behavior of calcite and apatite and found that the isoelectric point of each mineral in the supernatant of the other was similar to that of the other mineral. These effects are of particular relevance in the study of flotation chemistry of salt-type minerals, since extraneous ions can be present depending upon the type of water used and the mineralogical composition of the ore.

3.1.2.1 Fluorite/Water Interface

Fluorite has a solubility product, K_{sp} , of around 9.6×10^{-10} at $25^\circ C$ (Sturm et al., 1981). One of the important features of fluorite in aqueous solution is its surface carbonation, as shown in the following reaction.



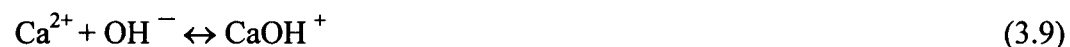
Miller and Hiskey (1972) and Miller et al. (1984) have argued that pure fluorite is always positively charged, and that the fall in electrokinetic potential at pH values above 8 is caused by carbonation of the surface by dissolved carbon dioxide. The isoelectric point (iep) obtained by electrokinetic measurements at room temperature and pressure is around pH 10. The iep shifts to a lower pH when the CO₂ pressure increases.

Surface carbonation is also evident from a doublet in the infrared spectrum with absorption bands at 1400 cm⁻¹ and 1480 cm⁻¹ (Miller et al., 1972).

Although the carbonation phenomenon explains the pH dependence of the zeta potential, some other electrokinetic data are not as easy to explain. In the absence of surface carbonation (pH < 7), the fluoride ion would be considered to be a potential-determining ion. However, it has not been possible to reverse the positive zeta potential exhibited by fluorite at pH 5.0 even at a high concentration of sodium fluoride (Miller et al., 1972; Calara and Miller, 1983). It seems that, in the absence of specific chemical reactions (e.g., surface carbonation), the surface potential of fluorite is determined by the hydration of lattice ions (Miller et al., 1984). Carbonation of the fluorite surface also causes a decrease in oleate adsorption (Lovell et al., 1974).

3.1.2.2 Calcite/Water Interface

Calcite's solubility product, K_{sp}, was estimated to be around 9.6x10⁻⁸ at 25°C (Sturm et al., 1981). When calcite is brought into contact with water, it undergoes the following reactions (Hanna and Somasundaran, 1976):



These reactions produce a number of chemical species including H_2CO_3 , HCO_3^- , CO_3^{2-} , Ca^{2+} , CaHCO_3^+ , CaOH^+ and $\text{Ca(OH)}_{2(aq)}$ (Hanna and Somasundaran, 1976).

Development of a surface charge on calcite is controlled by the presence of various charged complex species resulting from the hydrolysis reactions listed above, in addition to any preferential adsorption of constituent species. By examining these equations, as calcite approaches equilibrium with water at high pH values, an excess of negative HCO_3^- and CO_3^{2-} will exist, whereas at low pH values, an excess of Ca^{2+} , CaHCO_3^+ and CaOH^+ species will occur. These ionic species may be produced at the solid-solution interface or may form in solution and subsequently adsorb onto the mineral surface and, therefore,

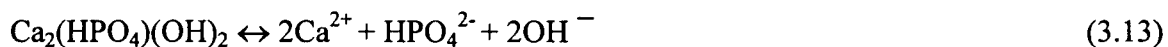
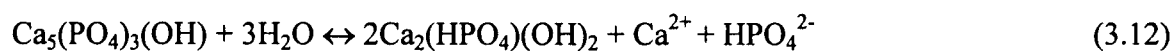
affect the zeta potential of this mineral. In either case, the net result will be a positive charge on the surface at low pH values and a negative charge at high pH values.

The point of zero charge (in terms of pH units) can be obtained by estimating the pH at which the total concentration of negative ions is equal to that of the positive ions. For calcite, a value of 8.2 was obtained (Somasundaran and Agar, 1967). Somasundaran et al. (1985) calculated the point of zero charge (pzc) for calcite by using thermodynamic data for the systems either closed or opened to atmospheric CO₂. They found that the pzc depends on the partial pressure of carbon dioxide in equilibrium with the system. Values of 11.3 and 8.4 were obtained for calcite systems closed and opened to atmospheric CO₂ respectively. Different isoelectric points of calcite have been reported in the literature, ranging from pH 4.5 to 10.8 (Amankonah et al., 1985; Marinakis et al., 1985; Pugh et al., 1985; Somasundaran et al., 1985; Rao, et al., 1988/1989,). This variance can be attributed to differences in mineralogy, sample preparation methods, conditioning time and measuring techniques. The iep (isoelectric point) obtained from zeta potential measurements can differ from the pzc due to specific adsorption of ions like calcium or because of non-equilibrium conditions that exist even after prolonged contact of the mineral with aqueous solution.

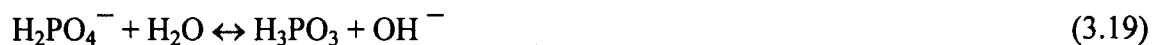
3.1.2.3 Apatite/Water Interface

The mechanism of charge generation for apatite, a tri-ionic crystal, is much more complex. The solubility of this mineral is much lower than fluorite and calcite. The solubility products of fluorapatite and hydroxyapatite were estimated to be around 10^{-118} at ambient temperature (Somasundaran et al., 1985) and 10^{-114} at 25°C (Sturm et al., 1981)

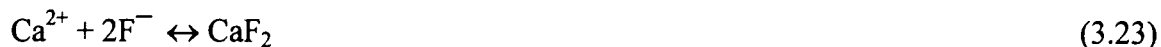
respectively. The mechanism of charge development at the apatite surface involves a number of pH-dependent hydrolysis reactions:



The charged species produced by dissolution of the original $\text{Ca}_5(\text{PO}_4)_3(\text{OH})$ or the complex $\text{Ca}_2(\text{HPO}_4)(\text{OH})_2$ can undergo further hydrolysis and complex formation according to the reactions given below:



The fluoride ions present in the fluorapatite also undergo similar reactions:



Depending upon the solution pH, the concentration of these hydrolysis species will determine the surface charge. The zeta potential of the mineral is greatly affected by lattice ions and the chemical species that result from the hydrolysis reactions (Somasundaran, 1968).

The pzc measurements for apatites are scattered between pH 3 and 7.5 (Somasundaran, 1968; Amankonah et al., 1985; Pugh et al., 1985; Somasundaran et al., 1985; Rao et al., 1988;). This variance can be attributed to the differences in mineralogy, sample preparation methods, conditioning time, atmosphere, and measuring techniques. Somasundaran et al. (1985) found that the pressure of CO_2 in the apatite equilibrium system affects apatite solubility and therefore, the isoelectric point as well.

3.2 Flotation Beneficiation of Phosphate Ores

On the basis of the mineralogy of the phosphate deposits, the industrially processed phosphate ores can be classified into two types: marine sediment ores such as those from the Southeastern U.S. and North Africa, and igneous ores such as those from South Africa, Russia, Finland and Brazil. Separation of carbonates (calcite and dolomite) from igneous phosphate is practised in industrial plants in Brazil, Finland and South Africa. However, the separation of carbonates from sedimentary phosphate has not been realized industrially, with the possible exception of some plants in China. The main problems with sedimentary phosphates are i) the high substitution of CO_3^{2-} and F^- for PO_4^{3-} in the apatite

lattice, ii) the large surface area of the phosphate particles because their surface is porous and irregular and iii) the tendency of sedimentary minerals to produce more slime in conditioning than the crystalline minerals; hence, larger dosages of collectors are required for sedimentary minerals.

The flotation of phosphate ores containing siliceous gangue is successful due to the different surface properties of silicates and apatite. However, separation of carbonates from apatite is extremely difficult owing to the similarity between their physicochemical properties. In addition, interactions of dissolved anions or cations from one mineral with those from other minerals in the pulp, as well as with collector species, also result in poor selectivity.

3.2.1 Flotation of Phosphate Ores Containing Siliceous Gangue

Beneficiation of phosphate ores containing siliceous gangue is achieved by the flotation of apatite with fatty acids around pH 9 which is sometimes followed by a reverse flotation of quartz with amine collectors around pH 7 (Houot et al., 1981). Sodium silicate is used as a depressant for silica in the anionic flotation circuit. The use of fatty acids or their salts as anionic collectors in the mineral industry is popular because of their availability and relatively low cost (Leja, 1982). Research directed towards improving the flotation efficiency of separating silica gangue from apatite has been reviewed by Moudgil and Somasundaran (1986). The fundamental aspects of fatty acids and sodium silicate have been extensively studied and will be discussed later in this chapter. Some of the major developments of reagents in this area are present below.

Synthetic substitutes for fatty acids, such as esters of polycarboxylic acids, sulfosuccinic derivatives, sulfonated derivatives and perfluoroalkyl compounds associated with fatty acids (Wang et al., 1977, 1979), were developed in order to improve collector reliability and efficiency. A new family of silica control agents called the hydrophilic alkanol amine has recently been developed (Klimpel et al., 1990, 1991). The silica control agents were shown to increase the recovery of the valuable mineral at extremely low dosages and improve the product grade at higher dosages. The advantage of these agents over sodium silicate is that a much smaller amount is required (Klimpel et al., 1993). In addition, it appears to be less sensitive to variables such as hydrocarbon addition, water chemistry, pH and different levels of fines in the feed.

3.2.2 Flotation of Phosphate Ores Containing Calcareous Gangue

Many examples of the industrial application of beneficiation of calcareous phosphate ores are given in the review article by Houot (1982). Beneficiation of igneous phosphate ores with calcareous gangue (e.g., dolomite and calcite) is carried out by using tall oil as a collector with sodium silicate as a gangue depressant and dispersing agent. pH is maintained by sodium hydroxide not lower than 8. In addition, nonylphenyltetraglycol ether is used as a depressant for carbonates and as a dispersant of the tall oil collector. When the carbonate content in the ore is higher, a higher amount of ether along with polysaccharides is required to control froth volume (Lovell, 1976). In Brazil, depression of carbonates and iron oxides is achieved at pH 10 using causticized starch in the presence of tall oil collectors (Betz, 1979). Tall oil has since been replaced by a new amphoteric synthetic collector although the use of starch is still prevalent (Filho et al., 1993). Finnish

apatite is floated by using N-substituted sarcosine, an amphoteric collector which acts as an anionic collector for apatite under basic pH, between 8 and 11 (Kiukkola, 1980). A depressant for calcite and dolomite is not needed when this collector is used. Recently a research group from the University of Nevada has reported the use of a bacterium, *Mycobacterium phlei*, to depress dolomite in the anionic flotation of apatite from dolomite (Zheng, Smith et al., 1997). They found that *Mycobacterium phlei* functions as a dolomite depressant especially when it is used with a diphosphonic acid collector.

Although flotation of sedimentary phosphate ores with calcareous gangue has not been commercialized, several reagent schemes have been developed for the system. Flotation of this type of ore often involves a reverse flotation of carbonates with fatty acids as collectors and phosphoric acid, monosodium phosphate and fluorosilicates as phosphate depressants (Henchiri, 1993). Tartaric acids and aluminum sulfate were used as depressants in the reverse flotation of phosphate ores with fatty acid as the collector (Smani et al., 1975). Flotation with phosphoric esters involves floating the carbonate/phosphate mixture in a slightly basic pH followed by depressing the phosphatic components by an acid conditioning and then floating the carbonates (Henchiri et al., 1980). The flotation of Turkish ores was conducted also with sodium oleate as a collector and phosphoric acid as the phosphate depressant (Onal et al., 1975). A no-conditioning process was developed by Mineral Reagents International (MRI) for the selective fatty acid flotation of carbonate under acidic pH without the use of a specific phosphate depressant (Anazia et al., 1987, Hanna et al., 1989). Reverse flotation of carbonates from an oolitic phosphate ore using sodium oleate as the collector and phosphoric acid as the depressant for the phosphate was also reported (Abramov et al., 1993).

The improvement of the efficiency of the beneficiation of phosphate ore is continuing to be an interesting subject for many researchers from both practical and fundamental points of view. Moudgil et al. (1992) have reported that the improvement in the flotation of coarse phosphate particles can be achieved by emulsifying the collector with fuel oil. It has been determined that emulsification causes higher collector adsorption on phosphate particles and thus improves their floatability. More recently, with regard to phosphate flotation, the wetting phenomena at francolite surfaces by the measurement of contact angles have been studied by Lu, Drelich and Miller (1997). They found that, in the absence of fuel oil, significant francolite flotation requires that the fatty acid/sodium oleate concentration to be close to or above the critical micelle concentration. In contrast to quartz francolite is readily wetted by fuel oil. The presence of fatty acids in the solution can significantly facilitate the natural spreading of fuel oil at francolite surfaces but has little effect on the natural spreading of fuel oil at quartz surfaces.

Recovery of phosphate from slime is another interesting and important subject in the beneficiation of phosphate industry. Phosphate mining in Florida generates approximately 100,000 tonnes/day of phosphatic slime. This waste slime contains a significant amount of P_2O_5 . About 20-30% of the phosphate mined ends up in phosphatic clays (Zhang, Snow et al., 1998a). The waste also creates a difficult disposal problem in the mining industry. Zhang and Snow et al. (1998a, 1998b) have reported some research progress on the recovery of phosphate from Florida beneficiation slime. They evaluated different dispersants as the first step to remove clay minerals from phosphatic clays for downstream upgrading of phosphate. They also evaluated the use of a classifying cyclone to maximize phosphate recovery in the underflow product.

3.3 Fundamental Aspects of Flotation with Fatty Acids

Fatty acids and their soaps are the most common collectors in the flotation of salt-type minerals. Oleic acid is the most widely used, and its solution chemistry, adsorption, and flotation properties have been extensively studied.

3.3.1 Oleate Colloid Chemistry

Oleic acid is a weak-electrolyte surfactant. It undergoes dissociation in aqueous solution, as shown by reaction (3.24).



At high pH values, oleic acid exists as ions (RCOO^-) and at low pH values as neutral molecules. The domain diagram of oleic acid is shown in Figure 3.2 (Laskowski, 1988, 1993). This figure shows that, at high concentrations, oleate micelles are formed in the alkaline range, and precipitation of the molecular form takes place in the acidic range. The precipitate appears as emulsion droplets which are electrically charged and exhibit a clear iep around pH 2-2.5 (Vurdela and Laskowski, 1987). Micelles appear in solution when concentration of sodium oleate exceeds its critical micelle concentration (CMC), 2.1×10^{-3} M at 26°C (Zimmels and Lin, 1974).

The existence of pre-micellar association of ions, molecules or ion-molecules such as oleate-oleic acid, has also been suggested and discussed by a number of authors (Mukerjee, 1967; Nikolov et al., 1981; Ananthapadmanabhan et al., 1981, 1988; Castro et

al., 1986). Similar to the case of micellization, the major driving force for the formation of dimers is considered to be the interaction between adjacent hydrocarbon chains. The formation of an acid-soap complex is more favorable than that of a doubly-charged dimer because of the absence of electrostatic repulsion in the former. The acid-soap complex often forms at an intermediate pH and the pre-micellar concentration range which is near critical micelle concentration; the complex is more surface active than acid or soap alone .

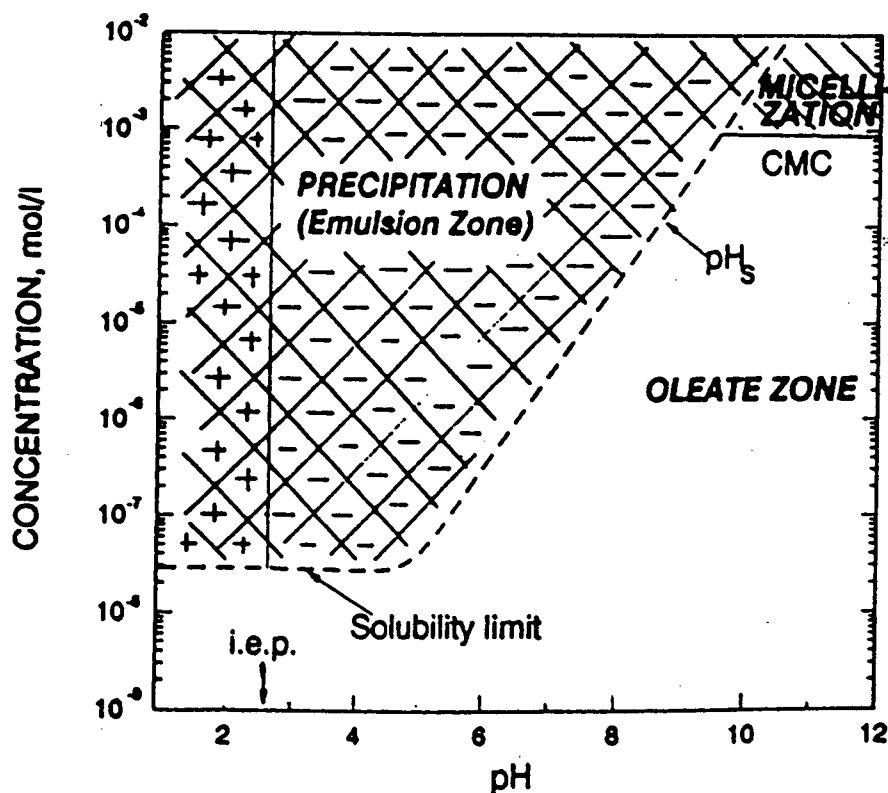


Figure 3. 2 Domain diagram for oleic acid (Laskowski, 1988)

The surface tension decrease in surfactant solution is due to the adsorption of molecules (or ions) at a solution/gas interface. A mechanism in which the surfactant molecule tends to escape from solution can be considered to be the driving force for the adsorption of molecules (or ions) at the interface. The same driving force causes

micellisation. With the orientation of the hydrocarbon chains exposed to the air and polar groups pointing to water, a decrease in the surface free energy results.

It has been observed that the surface tension of oleate solutions begins to decrease above a certain concentration of oleate at pH 11.4 (Ananthapadmanabhan et al., 1981). This decrease has been attributed to the formation of pre-micellar aggregates such as dimers and acid-soap complexes in solution. Surface tension of the oleate aqueous solution reaches a minimum in the intermediate pH range and is correlated with the maximum concentration of the acid-soap complex (Ananthapadmanabhan et al., 1981, 1988).

3.3.2 Flotation with Fatty Acids

Flotation with fatty acids may be quite satisfactory over a very broad pH range. Since fatty acids are weak-electrolyte type surfactants, they may form colloidal systems depending on surfactant concentration and pH. This has a very pronounced effect on the flotation properties (Laskowski et al., 1988, 1994). The flotation-pH curves which exhibit maximum around the neutral pH region have been reported by many researchers. A mechanism of chemical interaction between the carboxylic group on fatty acid and the calcium site on surface of mineral was proposed. Smani et al. (1975) observed two flotation maxima in the acidic and alkaline pH range on the flotation of different apatites with sodium oleate. They, therefore, proposed that flotation above pH 6 was associated with the chemisorption of oleate, resulting in the formation of Ca oleate on the surface. The second flotation maximum occurring close to the iep of the samples is due to the physical adsorption of neutral oleate molecules. Mishra (1982) also studied apatite from Durango (Mexico) with sodium oleate and found only one maximum in the tested pH

range. He proposed that the adsorption was due to a combination of chemical and hydrophobic bonds (formation of hemi-micelles). Brandao and Poling (1982) strongly believed that the adsorption mechanism of fatty acids onto magnesite involves chemisorption over the entire pH range.

Laskowski et al. (1994) have indicated that the observed maximum flotation around neutral pH region holds true only for a given conditioning time. With increased conditioning time, the maximum on the recovery-pH curve shifts towards the acidic pH region. The flotation of fluorite, hematite and magnesite with oleic acid was substantially improved in the acidic pH range by prolonging the conditioning time, as shown in Figure 3.3, while flotation in the alkaline range was not significantly affected by the conditioning time. It is believed that slow diffusion of the colloidal species in the acidic pH range is responsible for this phenomenon. In the alkaline pH range, the collector is ionized. Because of the fast diffusion of such ions, adsorption equilibrium is reached quickly.

The evidence of chemisorption of oleic acid and oleate on fluorite was first provided by French et al. (1954) based on infrared spectroscopic results. Subsequently Peck and Wadsworth (1963) reported chemisorption of oleate on calcite and barite in addition to fluorite. The absorption band at 1724 cm^{-1} is associated with stretching of the C=O double bond of the -COOH group while those at 1562 cm^{-1} and 1470 cm^{-1} are associated with the asymmetric and symmetric stretching modes respectively of the C=O double bond of -COO^- group. The presence of the -COOH and -COO^- groups on the surface of fluorite suggests that two types of adsorption, physical and chemical, are present. Predali (1969) has suggested that, at basic pH, chemisorption is maximum whereas

physical adsorption is nil; at a very acidic pH, only physisorption of neutral molecules occurs on the surface.

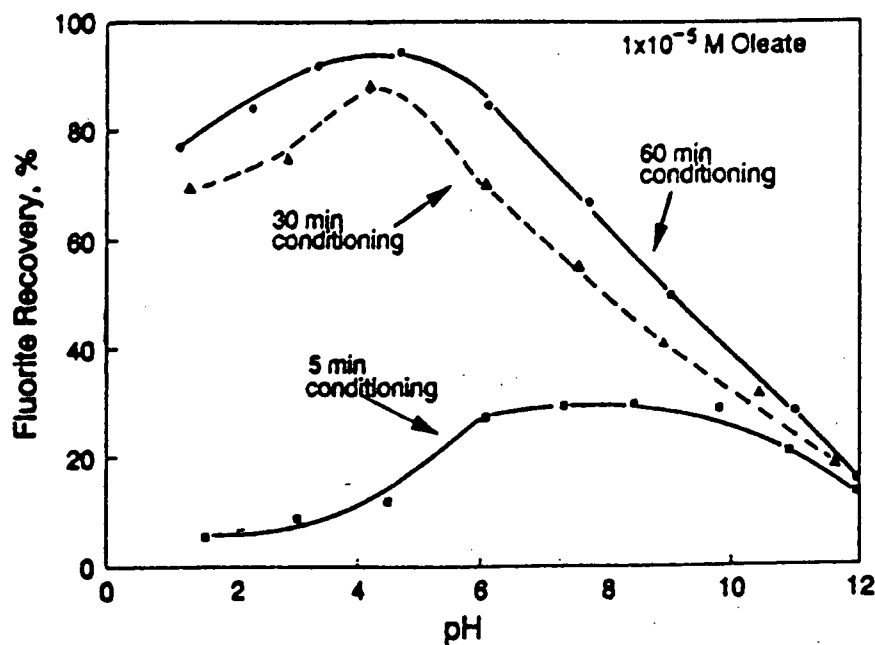


Figure 3.3. The effect of conditioning time and pH on the flotation response of fluorite at a concentration of sodium oleate of 10^{-5} M (Laskowski and Nyamekye 1994).

Chemisorption was proposed by Peck and Wadsworth (1964) to occur by ion exchange in which the oleate anions replace an equivalent amount of the crystal lattice anions such as F^- , CO_3^{2-} and SO_4^{2-} to build a surface layer of an alkaline earth oleate salt whereas physical adsorption of oleic acid or oleate occurs on account of van der Waals and coulombic forces.

The above mechanism explains adsorption of the first layer of fatty acid on a mineral surface. However, a multilayer adsorption of oleic acid has been found to take place on calcium minerals. Several studies regarding oleate and calcium dioleate

precipitate adsorption in the fluorite/oleate, calcite/oleate and apatite/oleate systems have been reported (Giesekke and Harris, 1984; Miller et al., 1984; Marinakis and Shergold, 1985; Pugh and Stenius, 1985; Hu et al., 1986; Finkelstein, 1989; Rao et al., 1988, 1989, 1990, 1991; Kellar et al., 1990). It has been proposed that oleic acid is first adsorbed on a mineral's surface by either physical or chemical interaction or both and is followed by the direct precipitation of calcium oleate or the formation of a bilayer on top of the monolayer before precipitation. Abramov and Magazanik (1998) have recently indicated that the regularities of fluorite flotation cannot be explained by the calcium oleate formation on surface of the fluorite. The optimal conditions for mineral flotation are observed at the pH value corresponding to zero charge of the mineral surface which can be calculated by the use of thermodynamic data for the mineral-water system.

Flotation with oleate is also influenced by ionic strength and temperature (Kulkarni and Somasundaran, 1980; Hu et al., 1986). Kulkarni et al. (1980) observed that increase in ionic strength at lower temperatures improves both the oleate adsorption characteristics and its surface activity at liquid/air interface, as well as the hematite flotation. An increase in temperature under low ionic strength conditions increases oleate adsorption on hematite and leads to an improvement in the hematite flotation response (Kulkarni and Somasundaran, 1980). Chemisorption of oleate on fluorite increases with an increase in temperature while adsorption due to the surface-precipitation decreases (Hu et al., 1986).

3.3.3 FTIR Studies on Adsorption Mechanism

It is interesting to mention that, in the more advanced Fourier Transfer Infrared Spectroscopy (FTIR) techniques such as in-situ and ex-situ FTIR/IRS, the traditional KBr

pellet is substituted by a reactive element (Kellar et al., 1990; Rao et al., 1991; Gong et al., 1992; Young and Miller, 1993; Wensel et al., 1994; Free and Miller, 1995; Lu and Miller, 1998). The in-situ and ex-situ FTIR techniques, using the studied mineral crystals, for instance, fluorite crystals as the reactive FTIR elements, enable the adsorption of oleate onto minerals to be determined without disturbing the surface. This is very different from the traditional KBr pellet preparation. In the in-situ technique, the internal reflection element (IRE) is fixed in the FTIR sample cell, and the adsorption solution is injected onto the element while, in the ex-situ technique, the IRE is removed from the sample cell and suspended in the adsorption solution for adsorption to take place and then put back in the sample cell for spectra collection.

Kellar et al. (1993) have identified the various states of adsorption of surfactants on mineral surfaces by the in-situ FT-IR/IRS technique. They found that, in the fluorite/oleate system, at room temperature, the adsorbed aggregates behave more like a gel or coagel; these aggregates resemble a micelle only at elevated temperatures.

Figure 3.4 shows spectra of chemisorbed oleate and the adsorbed calcium dioleate precipitates at pH around 9.8 (Free and Miller, 1995). The absorption peak located around 1550 cm^{-1} is identified to be chemisorbed oleate rather than physically adsorbed oleate because the absorption peak did not show any change after the sample was subjected to a ultrasonic cleaning in hexane. This unique spectral characteristic of chemisorbed oleate at a fluorite surface was also found for other calcium-bearing sparingly soluble minerals including calcite and apatite (Miller et al., 1994). The peaks at 1575 and 1535 cm^{-1} are the same as those observed for the calcium dioleate salt and have been assigned to weakly adsorbed calcium dioleate precipitates. The interpretation of these peaks was confirmed by

the disappearance of the peaks after the sample was cleaned ultrasonically in hexane for 15 minutes.

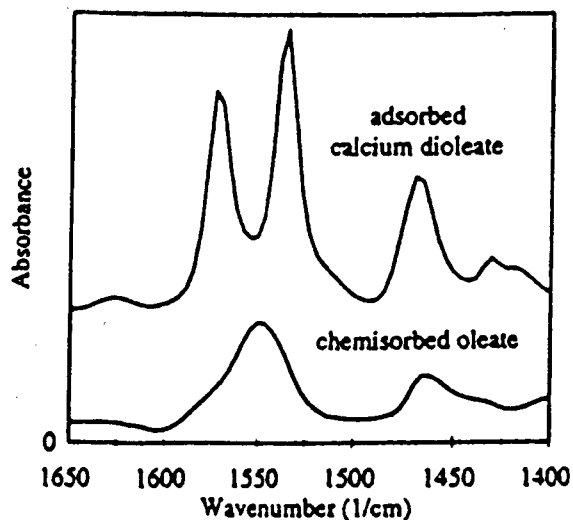


Figure 3.4 Ex-situ FTIR/IRS spectra of chemisorbed oleate and adsorbed calcium dioleate (Free and Miller, 1995)

The adsorption isotherms obtained by in-situ and ex-situ FTIR measurements are shown in Figure 3.5 (Free and Miller, 1995). The plateau region shown in the isotherm corresponds to the chemisorbed oleate monolayer while the region showing a sharp increase in the slope corresponds to the calcium dioleate precipitates.

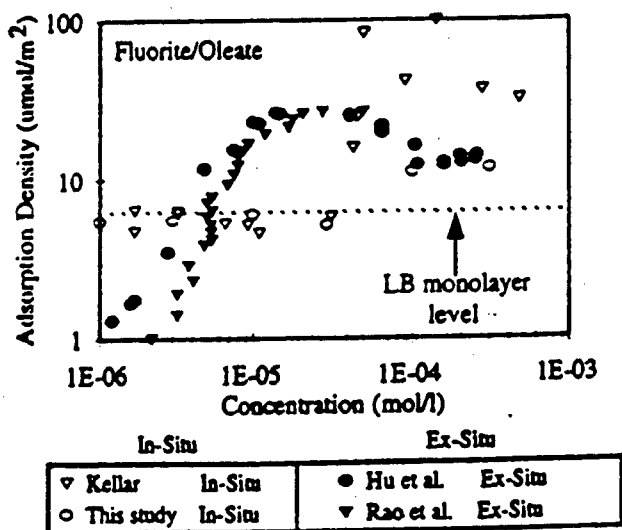


Figure 3.5 Comparison of adsorption density versus oleate concentration for both in-situ and ex-situ FTIR adsorption analyses, pH 9.5 to 10 (Free and Miller, 1995).

3.3.4 Effects of Modifying Reagents

Sodium silicate and sodium tripolyphosphate are the two most commonly used modifying reagents in flotation of the salt-type minerals. These reagents can act as both slime dispersants and depressants. The role of sodium silicate as a depressing reagent has been studied by many investigators; however, it is still not clearly understood due to the complexity of the hydrolysis of sodium silicate in an aqueous solution which, depending upon the solution pH, produces a number of monomeric, polymeric and colloidal species.

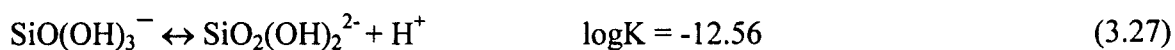
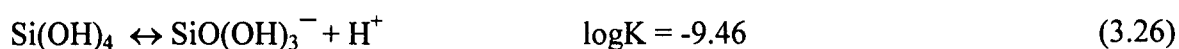
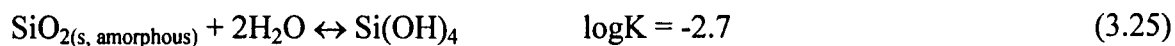
Sodium silicate is characterized by a chemical formula of $m\text{Na}_2\text{O} \cdot n\text{SiO}_2$. The ratio of n/m is referred to as a modulus. Silicate with a low n/m ratio forms a strongly alkaline pulp and depresses silica. As the modulus increases above 3, increased dissolution of silicate produces coarsely dispersed colloidal silica gel. Silicates with the modulus of 2.2 to 3.3 are frequently used in flotation processes. The dissolution of sodium silicate, depending upon the solution pH, produces a great variety of species.

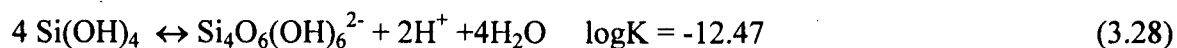
Different mechanisms of the action of sodium silicate in flotation have been proposed. Klassen and Mokrousov (1963) initially concluded that silicic acid was the active species since the depressing action of sodium silicate depends on the concentration of silicic acid in the solution. Eigeles (1964) concluded that HSiO_3^{2-} ionic species were active and that neither SiO_3^{2-} ions nor molecular silicic acid had any effect on flotation. This statement was supported by the finding that fluorite was sharply depressed at $\text{pH} = 9$, a pH at which the HSiO_3^- species was present at much higher concentrations than SiO_3^{2-} or silicic acid. Fuerstenau et al. (1968) proposed that different species had different effects for different minerals. Colloidal silica was responsible for calcite depression whereas

silicate anions were responsible for fluorite depression. Marinakis and Shergold (1985) studied the influence of sodium silicate addition on the adsorption of oleic acid on fluorite, calcite and barite and claimed that sodium silicate depressed these minerals by preventing oleate species from reacting with surface sites. The effect was independent of the total silica concentration. Aged sodium silicate solutions did not produce markedly different results to those obtained with fresh solutions.

Mercade (1981) observed that, the flotation of calcite decreased by combining sodium silicate with a polyvalent metal salt in certain proportions. The depression effect increased in the order of $\text{Na}^+ < \text{Ca}^{2+} < \text{Ni}^{2+} < \text{Al}^{3+} < \text{H}^+ < \text{Fe}^{2+} < \text{Cu}^{2+} < \text{Cr}^{3+}$. Later, Fuerstenau and Fitzgerald (1989) also indicated that the effectiveness of sodium silicate was enhanced by the combination of sodium silicate with polyvalent metal salts. The combination of polyvalent ions and sodium silicates results in the formation of highly-charged polymerized metal-oxy-silicate species which confer an effective negative charge on the depressed mineral surfaces. They found that the addition of aluminosilicate hydrosol to porphyry and oxide copper ores and to a tungsten ore resulted in enhanced flotation recoveries ranging from about 1.5 to 5 percent.

Marinakis and Shergold (1985) calculated the distribution of species in sodium silicate solutions according to the following equilibria:





However, with this model (model 1), polymeric silicate species other than $\text{Si}_4\text{O}_6(\text{OH})_6^{2-}$ are considered negligible. More recently, Gong and Warren (1993) developed a more sophisticated model based on ^{29}Si NMR studies and potentiometric titrations (Sjoberg et al., 1985). This model includes four types of polymeric silicate species: $\text{Si}_2\text{O}_3(\text{OH})_4^{2-}$, $\text{Si}_2\text{O}_2(\text{OH})_5^-$, $\text{Si}_3\text{O}_5(\text{OH})_5^{3-}$ (linear) and a tetramer of chain or branched forms with total silica concentration of 0.01 mol/l in solution. The degree of polymerization of silicate depends on pH. At a pH from 4 to 9, silicate is mainly present as Si(OH)_4 . As pH increases, because of the formation of charged monomeric and polymeric silicates, the concentration of soluble silica increases. At a given pH, the tendency to form polymeric species increases with increasing total SiO_2 concentration. With this model, 15% of silica present as polymeric species in solution, under the conditions close to those in flotation, e.g., $[\text{SiO}_2] = 0.005 \text{ mol/l}$ and $\text{pH} = 10$, while model 1 only indicated 5% of silica present as polymeric species in solution.

Gong and Warren (1993) used the ATR-FTIR (attenuated total reflectance FTIR) technique to identify the polymeric species in a sodium silicate solution. They observed a shifting of the band at about 1000 cm^{-1} to higher frequency with decreasing the silica concentration. As the decrease of the silica concentration causes the solution pH to decrease and the degree of polymerization increases. Furukawa et al. (1981) assigned the infrared bands in the 1000 to 1100 cm^{-1} region to the asymmetric stretchings of Si-O bonds of silicates and indicated that the frequencies of these bands tend to increase as the degree of polymerization increases from the SiO_4 tetrahedra to a three-dimensional framework.

According to Iler (1979), when alkaline metal silicate solution is diluted, a large part of the silicate is converted to higher polymeric species or colloidal particles. Therefore, it is evident that the shifting of the band at about 1000 cm^{-1} in the spectra of sodium silicate solution to higher frequencies is consistent with an increase of the polymerization of silicate species in solution.

The DRIFT (diffuse reflectance infrared Fourier transform) spectra of apatite and hematite, treated first with sodium silicate of different modulus and then with sodium oleate, showed that, after treatment with modulus 3.3 sodium silicate, the adsorption of sodium oleate on both minerals was greatly inhibited, as shown by the reduction of the intensities of the C-H stretching peaks at 3007 , 2959 , 2924 and 2853 cm^{-1} . However, after treatment with modulus 2.06 sodium silicate, the adsorption of sodium oleate on hematite was reduced, but that on apatite was not. This is consistent with the observation on flotation of Mt. Weld phosphate ore with sodium silicate as a hematite depressant (Gong et al., 1992). The depressing effect of sodium silicate increased with the modulus for both apatite and hematite. The highest selectivity was obtained by using sodium silicate of medium modulus 2.06. X-ray photoelectron spectroscopic (XPS) analysis has also provided strong evidence for the adsorption of polymeric silicate species on hematite from a silicate solution with concentrations typical of those used in flotation, i.e., 10^{-3} to 10^{-2} mol/l.

It is evident that the active species in silicate solution for the depression of flotation are polymeric silicate species and small colloidal silica particles. They concluded that polymeric silicate species have a stronger depressing effect than monomeric silicates and colloidal amorphous silica particles. Highly polymerized silicates have a stronger

depressing effect than low-molecular-weight polymers. However, for colloidal amorphous silica, the larger particles have weaker depressing effect than the smaller ones.

The flotation behaviour of apatite and calcite in the presence of oleate and sodium metasilicate was studied by Mishra (1982). He found that, while apatite can be 100% floated at a pH around 10 in the presence of 5×10^{-4} M sodium oleate and 5×10^{-3} M sodium metasilicate, calcite is completely depressed (Mishra, 1982). Selective separation of calcite from apatite can be achieved in this alkaline pH environment.

In addition to a depressing effect, at low concentrations, sodium silicate can act as an activation in flotation of some minerals. Klassen et al. (1959) showed that a small amount of sodium silicate activates the flotation of hematite with a sharp decrease in the negative electrokinetic potential. Further increase in sodium silicate raises the electrokinetic potential. The selective action of sodium silicate can be achieved by reacting sodium silicate with polyvalent cations (Klassen and Mokrousov, 1963).

Sodium tripolyphosphate is another common modifying reagent in the flotation of salt-type minerals. This reagent is effective in conferring a high negative zeta-potential onto the salt-type minerals. Parsonage et al. (1984) studied the effect of sodium tripolyphosphate on the flotation of dolomite, calcite and apatite and observed that sodium tripolyphosphate acts as a depressant for the three minerals at a concentration below about 0.4g/l, but, at a higher concentration, its effectiveness in depressing the carbonates is reduced. So, at high reagent levels (> 5 g/l), calcite and dolomite float well whereas apatite remains depressed.

Comparison of the depressing mechanism of sodium tripolyphosphate with sodium silicate and gum arabic was also made by Parsonage et al. (1984). They concluded that

sodium tripolyphosphate disperses by adsorbing at the cation sites on the mineral surfaces and increasing the negative zeta-potential. In the presence of oleate the dispersant will compete strongly for sites and reduce the adsorption of the collector, thereby causing depression. Gum arabic and polymeric sodium silicate adsorb by multiple weak bonds to form hydrated layers at the mineral surface. Dispersion is produced both by the increase in negative zeta-potential and by the stabilizing effect of the hydrated layers. The hydrophilic nature of the layers causes depression of flotation.

In addition to sodium tripolyphosphate, also hexametaphosphate has been used extensively. Li et al. (1984) have argued that the mechanism of depression of the calcium minerals by phosphates is through the selective complexing and dissolution of the calcium ions from the mineral surfaces by phosphate ions. The crystal structure of the minerals is a primary factor influencing calcium solubility; the shorter the Ca-O bond, the lower the solubility of the calcium cation. The phosphate structure is a primary factor influencing its complexing ability. The mixture of hexametaphosphate and pyrophosphate (Leja, 1982) is a commercially produced dispersant under the trade name Calgon.

Sodium chloride is also known to depress apatite in flotation of apatite/dolomite ore with sodium oleate in acidic solutions (Moudgil and Ince, 1991). It has been observed that, in the presence of sodium chloride, at a pH of 4, apatite is completely depressed while dolomite is floated with sodium oleate (Moudgil and Ince, 1991). It can be explained that, at pH 4, oleic acid exists in the form of emulsion droplets and the increased ionic strength of the solution in the presence of sodium chloride compresses the electrical double layer around the droplet; apparently this affects the interaction between the emulsion droplets and the apatite. In the case of dolomite/oleic acid, the presence of sodium chloride does not affect the interaction. The reason for this phenomenon is that, dolomite's iep is around

pH 12 and the faster diffusion kinetics of negatively charged oleic acid droplets towards dolomite particles resulting from the strong electrostatic attraction apparently leads to the better flotation of dolomite.

3.4 Selective Flocculation

The treatment of fine particles has received special attention in the last 20 years. The reason for such interest results from the fact that exploitation of lower grade ores characterized by fine dissemination requires fine grinding, and this generates a large quantity of fine particles which cannot be efficiently separated by any of the conventional beneficiation processes.

Selective flocculation aims at recovering valuable minerals from fine suspensions and is achieved by selectively aggregating certain mineral particles to sizes that enable their effective separation from the suspension. Selective flocculation by polymers has been a widely studied technique to achieve selective aggregation. Aggregation is used here as a general term. An aggregate formed by the addition of organic polymers is referred to as a 'floc'. The floc possesses loose and open structure. An aggregate formed by the compression of electrical double layers (generally more compact than a floc) is referred to as a 'coagulum'. When aggregation results from the action of an immiscible bridging liquid, such as oil in aqueous dispersion, the process is known as oil agglomeration and the aggregates are referred to as agglomerates.

Selective flocculation of either the valuable components or the gangue components may be employed depending on which route is more technically and economically feasible.

Reverse selective flocculation is also possible; for example, waste clays in a sylvinitic ore are selectively flocculated and floated (Banks, 1979).

3.4.1 Basic Principles

Selective flocculation is based upon the creation of a set of physico-chemical conditions (Yarar and Kitchener, 1970; Friend and Kitchener, 1973) which include (i) dispersion of the suspension (slurry), (ii) selective adsorption of a flocculant onto a desired mineral and (iii) promotion of the growth of the flocs mainly consisting of valuable minerals.

The principle of the method is schematically shown in Figure 3.6. The process basically consists of five sub-processes: (i) dispersion of slurry, (ii) addition of flocculant, (iii) selective adsorption of flocculant, (iv) conditioning and floc formation, and (v) floc separation. The objective of the first sub-process is to achieve a relatively stable and homogeneous suspension of minerals with the individual particles essentially separated from one another. This is achieved by the use of dispersants or by adjusting the suspension pH (Yarar and Kitchener, 1970; Laskowski and Pugh, 1992). Secondly, a high-molecular-weight polymer is added which adsorbs selectively on one of the minerals. Thirdly, collision processes created by gentle stirring result in floc formation. Finally the flocs can be separated from the dispersed phase by different means (e.g. sedimentation).

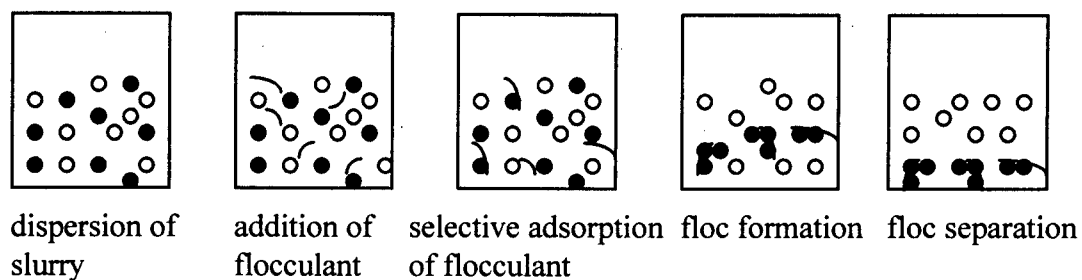


Figure 3.6 Schematic illustration of selective flocculation in a two-component ore

3.4.2 Stability of Mineral Suspensions

Dispersion is the first pre-requisite for selective flocculation. The stability of colloidal dispersion is of special interest in many fields. Colloid chemists have been studying the stability of colloidal systems for over a century. The stability of colloidal systems is controlled by an electrical double layer built on the surface of the particles.

3.4.2.1 Electrical Double Layer

A particle suspended in an aqueous phase acquires a charge. Thus a surface potential, ψ_0 , develops at the interface, and an electrical double layer is formed to maintain the condition of electroneutrality. The electrical double layer consists of two parts, with one layer referred to as the Stern layer and the other layer known as the diffuse layer. An important property of the diffuse part of the double layer is its thickness, which is dependent on the ionic strength of the solution. When the ionic strength of the solution increases, the double layer is compressed and its thickness decreases.

Since surface potential, ψ_0 , at a solid/liquid interface is not attainable experimentally for many systems, it is characterized indirectly by the values of the electrokinetic potential (zeta potential). One of the most common techniques to determine zeta potential of solid particles is by measurement of the electrophoretic mobility, μ , which is related to ζ - potential by the Henry expression:

$$\mu = \frac{\epsilon\zeta}{4\pi\eta} f(\kappa a) \quad (3.28)$$

where η is the viscosity of the medium and $f(\kappa a)$ is a numerical factor which depends on the size of the particle and the thickness of the double layer (Ottewill and Shaw, 1972; Hunter, 1981). Depending on the magnitude of κa , equation (3.28) converts either to Smoluchowski and Hückel's equations or Henry's equation respectively (Overbeek, 1952; Hunter, 1981). Details are explained in Appendix I.

3.4.2.2 Stability of Mineral Suspensions

In an aqueous dispersion system, attractive interactions arise from long-range London-van der Waals dispersion forces. The classical Derjaguin-Landau-Verwey-Overbeek (DLVO) theory of colloid stability relates the stability of lyophobic colloids to the total potential energy of interaction between a pair of particles. The total potential energy of interaction is determined by the sum of the electrostatic repulsive energy (V_R) and the London-van der Waals dispersion interaction energy (V_A), i.e.,

$$V_T = V_R + V_A \quad (3.29)$$

Hamaker (1937) extended London's classical treatment of dispersion forces between atoms to calculate the forces between colloidal particles. The potential energy (V_A) of interaction between two spherical particles of the same materials is then given by the following equation:

$$V_A = -\frac{FA}{6H_o} \quad (3.30)$$

In the case of particles with different surface potentials, the electrostatic repulsion V_R has been formulated by Hogg, Healy and Fuerstenau (1966) as follows:

$$V_R = \frac{F\varepsilon}{4} \left\{ 2\psi_1\psi_2 \ln\left[\frac{1 + \exp(-\kappa H_o)}{1 - \exp(-\kappa H_o)}\right] + (\psi_1^2 + \psi_2^2) \ln[1 - \exp(-2\kappa H_o)] \right\} \quad (3.31)$$

where A is the Hamaker-London constant, for substance 1 and 2 in medium 3 and is given

$$\text{by } A = A_{12} + A_{33} - A_{13} - A_{23},$$

$$A_{12} = \pi^2 q_1 q_2 \lambda_{12}$$

$$A_{33} = \pi^2 q^3 \lambda_{33}$$

$$A_{13} = \pi^2 q_1 q_3 \lambda_{13}$$

$$A_{23} = \pi^2 q_2 q_3 \lambda_{23}$$

q = number of atoms per m^3

λ = London-van der Waals constant, can be expressed by

$$\lambda_{kl} = \frac{3}{2} \alpha_k \alpha_l \frac{I_k I_l}{I_k + I_l}$$

α_k and α_l are the polarisabilities of atoms in substance k and l , I_k and I_l are certain characteristic potentials of the atoms in substance k and l . Detailed calculation can be referred to Hamaker (1937).

$$F = \frac{a_1 a_2}{(a_1 + a_2)}, \quad a_1, a_2 = \text{radii of the respective particles}$$

H_0 = shortest separation distance between two particles

ϵ = permittivity of the suspension medium

ψ_1, ψ_2 = surface potential of the respective particles

κ = Debye - Hückel reciprocal length parameter which is related to the ionic strength of the

medium, given by $\kappa^2 = \frac{8ce z^2}{\epsilon k t}$ where:

c = concentration

e = electronic charge

k = Boltzmann's constant

t = absolute temperature

z = ionic charge

In using the above equations, it is usually assumed that the surface potentials ψ_1 and ψ_2 are relatively low and can be replaced by respective zeta potential values. Hogg, Healy and Fuerstenau (1966) pointed out that relationship (3.31) is a good approximation for $|\psi_1|$ and $|\psi_2|$ smaller than 50 - 60 mv.

The above discussion demonstrates the importance of surface charge on the stability of colloidal dispersions. The colloidal dispersions can also be stabilized by a "physical barrier" around interacting particles which will prevent them from approaching one another to a distance at which there is a significant attraction force (steric stabilization) (Napper, 1983). Practically, the steric stabilization is imparted by adsorption of macromolecules onto the surfaces of particles in good solvents ($\chi < 0.5$). χ is the polymer chain-solvent interaction parameter and is usually referred to as the Flory-Huggins interaction parameter (Tadros, 1996). Simple monomeric compounds, mostly inorganic, are used to increase electrostatic repulsive forces between interacting solid particles while polymeric compounds (both inorganic and organic) are also utilized to impose the steric effect on the system (Laskowski, 1988).

It should be pointed out that the DLVO theory only considered van der Waals and the double layer interactions for an ideal system. Nevertheless, it is difficult to apply the DLVO theory to real systems which are complicated by a number of factors, for example, the variety of the size and shape of particles and the presence of many ionic species introduced by the partial dissolution and hydrolysis of some minerals during the milling operation. The basic principles, however, apply. Heterocoagulation can be avoided by the addition of dispersants. Selective coagulation is possible under very controlled conditions. Parsonage et al. (1982) applied DLVO theory to study the slime coating with considerable success.

As already mentioned, the van der Waals and double layer interactions only were considered in the DLVO theory. For strongly hydrophobic and hydrophilic substances, an additional force should be considered (Churaev and Derjaguin, 1985). This additional force

is generally referred to as a structural force and arises from the re-arrangement of water molecules near the interface. The structural force produces either repulsion between the particles if the liquid is able to wet the substance or attraction if the substance is poorly wetted by the liquid. Thus, an extended form of the classical DLVO theory can be expressed as

$$V_T = V_A + V_R + V_S \quad (3.32)$$

in which V_S is the structural energy. The hydrophobic force is detected experimentally when $\theta_a > 64^\circ$ (θ_a is the advancing water contact angle) while the hydration force is noticeable when $\theta_a < 15^\circ$. For the lyophobic colloids for which $15 < \theta_a < 64^\circ$, V_S may be considered to be negligible (Dergajin and Churaev, 1989). The extended DLVO theory successfully explains the phenomenon of the stability of hydrophilic sols of silica (Xu, Yoon, 1989; Yotsumoto and Yoon, 1993) and rutile (Yotsumoto and Yoon, 1993) and coagulation of coal and methylated silica (Xu and Yoon, 1989, 1990).

3.4.3 Dispersing Agents

The simplest way of controlling dispersion is by controlling pH; most minerals are strongly negatively charged in an alkaline media. By increasing pH, the V_R term in the energy equation is increased because the zeta potential on the particles is increased. However, the presence of different ionic species in pulps is one of the possible reasons that pH control alone is sometimes not sufficient to impart a high degree of dispersion and some dispersing agents have to be used, too.

Dispersing agents used in the mineral processing field can be classified into inorganic compounds, polymeric dispersants derived from natural sources, and synthetic polymeric dispersants. Sodium silicate and sodium tripolyphosphate are the two most commonly used dispersants in the processing of salt-type minerals. They have been discussed in the previous section. Other dispersants were discussed by Laskowski and Pugh (1992).

In addition to the aforementioned inorganic dispersants, also organic polymeric dispersants are utilized. The most commonly used polymeric dispersants derived from natural sources are polysaccharides such as starch and starch derivatives e.g., dextrin.

It is worthy of mention that polymers which can be used as flocculants can also be used as dispersants depending on the molecular weight. While the polymer flocculants are linear and are characterized by high molecular weight (above 10^6), the polymer dispersants are of low molecular weight (in the range of 10^4) and may have a branched structure. One must, however, bear in mind that all polyelectrolytes at high concentration may cause dispersion (Lyklema et al., 1987; Furusawa et al., 1988).

3.4.4 Flocculants and Flocculation

The second stage in the selective flocculation process is the addition of the flocculant to the system and the selective adsorption of polymer macromolecules on the valuable mineral. The aggregation of particles is induced by a variety of mechanism including bridging, charge neutralization (also referred to as coagulation) and depletion flocculation.

The polymers used in flocculation are commonly classified into two types: coagulants which are usually highly charged cationic polyelectrolytes with molecular weight in the 50,000 to 1,000,000 range and flocculants which have a substantially higher molecular weight (up to 20 million) and are usually nonionic or partially anionic. Because of great majority of particles encountered in mineral processing and water treatment are negatively charged, commercial available polymer coagulants are almost invariably cationic.

Bridging mechanism occurs when the adsorbed polymer extends into the solution to span at least the distance over which the electrostatic repulsion between particles is operative. This is the process by which neutral and like-charged polymers flocculate solid particles; in some cases, bridging by oppositely-charged polyelectrolytes may also occur. The efficiency of this mechanism is related to macromolecular size and effects pertaining to molecular weight should be observed. Bridging between particles is favored under conditions in which the particles are not completely coated by the polymer flocculant. According to Healy and La Mer (1964) and as modified by Hogg (1984), maximum flocculation occurs when the fraction of the particle surface covered by polymer molecules is lower than 0.5. Excess coverage can lead to steric stabilization.

It has been found that even non-adsorbing polymers can promote flocculation of suspensions (Sperry, Hopfenberg and Thomas, 1981). The mechanism of this process is fairly well understood (Fleer, Scheutjens and Vincent, 1984). The origin of this effect is thought to be in the exclusion of large polymer molecules from the narrow zone between closely-approaching particles. This exclusion occurs for simple geometric reasons and leads to an osmotic pressure difference between the contact zone and the bulk solution

which tends to pull particles together. The effect is called "depletion flocculation" and may be important in certain systems, especially with concentrated dispersions.

The conventional polyelectrolytes are commonly used for the clarification of process water. These types of flocculants are usually nonselective (Laskowski, 1982). In order to achieve selective adsorption, the polymer's functional groups must have different affinity towards the different mineral particles. The forces involved in the adsorption of polymeric flocculants on mineral surfaces can be either physical or chemical or both. In summary, the following interactions may be involved:

- (a) electrostatic interaction
- (b) hydrophobic association
- (c) chemical bonding
- (d) coordination bonding
- (e) hydrogen bonding
- (f) dipole-dipole interaction

Electrostatic interaction is predominant in the adsorption of polymers with a large number of charged units onto oppositely charged mineral particles. Both anionic and cationic polymers are commonly used in mineral processing. Cationic polymers usually have lower molecular weight and are commonly used as coagulants. Hydrophobic association is characterized by the tendency of nonpolar molecular groups (or molecules) to escape from an aqueous environment. The interaction between the polymer latex and a hydrophobic solid (e.g., coal) is an example of hydrophobic association. Chemical bonding occurs when chemical functional groups of polymer react with metallic sites on solid surfaces. Coordination bonding includes chelating or complex formation. Hydrogen bonding probably presents in almost every case of polymer adsorption on minerals bearing

oxygen and nitrogen. For instance, the hydrogen atom in the -NH_2 group of polyacrylamide is able to accept electrons from the electronegative atoms, such as from the oxygen of -OH groups on the surface of an oxide mineral, resulting in the formation of a hydrogen bond. At interfaces, dipole-dipole interactions play a very significant role, particularly in the adsorption of surfactants onto polar and uncharged surfaces and in the mutual interactions between molecules of different surfactant species.

Numerous selective flocculants have been designed and applied in selective flocculation tests. Examples of selective flocculants having chemical interaction functions towards the desired minerals are given in the literature (Attia and Kitchener, 1975; Clauss et al., 1976; Attia, 1977; Baudet, 1978; Sresty et al., 1978; Attia et al., 1986). The development of polyxanthate flocculants for the selective flocculation of sulfide minerals and oxidized copper minerals was first reported by Attia and Kitchener (1975) and was later confirmed by Sresty et al. (1978) and Baudet et al. (1978). Selective polymers based on hydrophobic effect were developed and found to have the greatest potential for selective flocculation of hydrophobic solids (with natural or induced hydrophobicity) in mixed suspensions with hydrophilic solids. Examples of these flocculants are polymer latices produced by emulsion polymerization. The application of the polymer latices in the selective flocculation of coal has been extensively studied, and positive results have been reported (Attia et al., 1987; Laskowski et al., 1995). However, the mechanism of the adsorption/attachment of such colloidal particles onto mineral surfaces has not yet been elucidated. Conventional analytical methods used to study adsorption of polyelectrolytes that involve measurements of difference of concentration before and after adsorption can not be applied to this system. The use of turbidity to measure latex concentration is impossible in the presence of slime. In the present research, the deposition of the latex

particles onto mineral surfaces was used to study the adsorption/attachment of latex particles.

Polyethylene oxide is known to be partially hydrophobic and was found in selective flocculation of hydrophobized copper minerals (Rubio et al., 1978). In the Rubio et al.'s study, the initially hydrophilic surfaces of oxidized copper minerals were selectively made hydrophobic by selective adsorption of surfactants or by sulfidization with sodium sulfide. Then, by introducing polyethylene oxide, selective flocculation of oxidized copper minerals from associated silicate minerals was achieved.

Of special interest to the present study is the use of a latex as the selective flocculant in the selective flocculation of apatite and fluorite. Although the latex used in this study was not designed to produce flocculation through hydrophobic interaction, the hydrophobicity of the latex seems to be sufficient to impart the hydrophobicity to flocs, thus assisting the flotation.

Rubio and Hoberg (1993) reported a process to concentrate fine mineral particles from aqueous suspensions. The process is unique and interesting. They used hydrophobic polymeric spheres, such as polypropylene with uniform sizes of the order of 3.7 mm and having a density of 0.68 g/cm^3 as carriers to capture hydrophobic mineral particles. The polymeric spheres were pretreated with emulsified oleic acid to increase their hydrophobicity, and the mineral fines were conditioned with a flotation collector to make the surface hydrophobic before mixing with the polymeric spheres. The attachment of the mineral fines to the polymeric spheres is due to the hydrophobic interaction; thus, shear is needed to bring particles into contact. The separation was conducted by collecting floated particles, and the carrier particles were separated by agitation of the "aggregates" with sodium hydroxide solutions. Because the polymeric carrier used had a density lower than

that of water, the actual separation by flotation was very rapid and allowed an easy removal of the polymeric particles from the pulp.

3.4.5 Separation of Apatite from Carbonate and Silica by Selective

Flocculation

Separation of apatite from dolomite by selective flocculation using either high molecular weight polyethylene oxide (PEO) or polyacrylic acid (PAA) has been extensively studied by Moudgil and co-workers (Moudgil et al., 1987a; Moudgil et al., 1987b; Moudgil and Vasudevan, 1989; Behl and Moudgil, 1992; Moudgil et al., 1994; Mathur and Moudgil, 1995). Selective flocculation of apatite from an apatite/silica system with PAA flocculant, and dolomite from a dolomite/silica system with PEO flocculant was observed, but selectivity was not observed in an apatite/dolomite system with either PEO or high molecular weight PAA. Heteroflocculation was suspected to be the major reason for loss of selectivity (Moudgil et al., 1987a). However, the heteroflocculation can be minimized by adding a lower molecular weight fraction of PEO as a site block agent. Thus, selectivity can be achieved with PEO flocculant in an apatite/dolomite system (Moudgil et al., 1994).

Behl et al. (1993) used diffuse reflectance FTIR technique to identify surface groups of dolomite and apatite. They found that some dolomite samples reach an absorption peak at 3621 cm^{-1} which is assigned to be the isolated hydroxyl group (-OH), while, in apatite, there is a broad band at 3400 cm^{-1} which is known to be the result of the adsorption of surface water. The samples with the isolated hydroxyl group or the surface water exhibited flocculation with PEO; otherwise, they did not flocculate. The adsorption

of PEO on dolomite and apatite surfaces took place through hydrogen bonding. The reasons for dolomite having isolated hydroxyl groups on some samples and not on others are not well understood.

PAA is known to flocculate apatite (Pradip and Moudgil, 1991). It was determined from the FTIR studies that polyacrylic acid (PAA) specifically interacts with tribasic calcium phosphate through the formation of calcium carboxylate bonds (Pradip and Moudgil, 1991). Since Ca^{2+} sites are also present on dolomite surfaces, selectivity may not be expected in the dolomite/apatite system. Additionally, it has been shown that flocculation with PAA decreases as the particle size decreases (Mehta, 1993), and selective flocculation of an artificial mixture of dolomite and apatite of different particle size distribution with PAA was also studied (Mathur et al., 1995). A PAA with MW of 4 million was found to flocculate both dolomite and apatite irrespective of the different particle size distribution of the two minerals. However, their flocculation was significantly different when PAA with MW of 450,000 was utilized for the different particle size distributions of two minerals. Thus the selectivity in dolomite-apatite system is possible, provided that particle size distributions of the two minerals are different from each other and an appropriate molecular weight of PAA is used (Mathur et al., 1995). However, it should be realized that, in a real system, it is difficult to control the particle size to be different for the two different mineral components.

The role of active sites in selective flocculation was evaluated by Moudgil and Vasudevan (1988). It is very common to observe that selectivity predicted on the basis of single component tests is lost when mixed component flocculation is attempted.

3.5 Polymer Latices

Polymer latices can be produced by either conventional emulsion or inverse emulsion polymerization. Both processes comprise of emulsification of a monomer in a continuous medium followed by polymerization with a free radical initiator. The monomer is immiscible with the continuous medium. In the conventional emulsion polymerization, the water- immiscible monomer is emulsified in a continuous water medium using an oil-in-water emulsifier and a water-soluble or oil-soluble initiator to produce a polymer latex of average particle size of 0.1- 1 μ m. In the inverse emulsion polymerization, a water-miscible monomer is emulsified in a continuous oil medium using a water-in-oil emulsifier and an oil-soluble or water-soluble initiator to give a colloidal dispersion of water-swollen polymer particles in oil. The average particle size of the latex is usually 0.05-1 μ m. Some other polymerization techniques, such as dispersion polymerization also produce polymer latex. However, the polymer latex produced by the dispersion polymerization has a broad range of particle size distribution and the technique has been far less investigated than the conventional emulsion polymerization. Among the polymerization techniques, the conventional emulsion polymerization is the most extensively studied and widely used to produce polymer latex.

3.5.1 Emulsion Polymerization

The process of emulsion polymerization can be divided into two stages: particle nucleation and particle growth. A number of nucleation mechanisms have been proposed, for example, monomer solubilized in micelles for the micellar nucleation mechanism

(Harkins, 1947; Smith and Ewart, 1948; Smith, 1949), monomer dissolved in the continuous phase for the homogeneous nucleation (Preist, 1952; Patsiga, Litt and Stannett, 1960) and the coagulative nucleation mechanisms (Napper and Gilbert, 1988). The surfactant used in the emulsification plays an important role in the process of emulsion polymerization. The specific characteristics of polymer latices are mainly determined by the properties of the monomers and by the surfactant used in the emulsification.

3.5.2 The Role of Surfactants

Surfactant molecules comprise a hydrophobic "tail" and a hydrophilic "head". The hydrophobic "tail" contains a number of hydrocarbon units, and the hydrophilic "head" contains either an ionic or a nonionic polar group but may also contain both anionic and cationic groups. According to the type of the "head" group, the surfactant can be classified into four categories: (i) anionic surfactants, such as those containing carboxylates, sulfates and sulfonates, alkylaryl sulfonates, alkyl phosphates; (ii) cationic surfactants, such as those containing alkyl quaternary ammonium salt, amines and nitriles; (iii) nonionic surfactants, including poly-oxy adducts; (iv) amphoteric surfactants, such as those containing both amino and carboxylic groups. The balance of hydrophile and lipophile (HLB) is defined as

$$\text{HLB} = \text{Sum (values for hydrophilic groups)} - \text{Sum (values for hydrophobic groups)} + 7$$

The value of HLB is usually used as a reference in the selection of a surfactant for a given application. Surfactants with low HLB values are good stabilizers for water-in-oil emulsions; surfactants with high HLB values are good stabilizers for oil-in-water emulsions. Polymerization rate, latex stability, viscosity and particle size of the latices were found to vary strongly with the surfactant HLB and the composition of the surfactant

mixture used to reach a given HLB (Jagodic et al., 1976). However, Rosen (1978) pointed out that selection of the surfactant using the HLB value is useful only as a rough guide since it indicates neither the efficiency of the surfactant nor its effectiveness as a stabilizer in a particular system. Selection of surfactants based on more fundamental surfactant/substrate properties is more appropriate. However, such selection methods are usually more tedious since they require determination of the surfactant adsorption isotherms.

Surfactants play major roles in the formulation and application of latices. The role of surfactants in emulsion polymerization is numerous and can be summarized as (i) stabilization of the monomer emulsion, (ii) solubilization of monomer in micelles, (iii) determination of the mechanism of particle nucleation, (iv) determination the number of particles nucleated and thus the rate of polymerization, (v) maintenance of the colloidal stability during the particle growth stage, (vi) control of the average particle size and size distribution of the final latex system. In a latex system, most of the surfactant molecules are adsorbed at the particle/water interface and only small fraction is available for the air/water interface (some remain in the bulk aqueous phase).

The role of surfactant in emulsion polymerization is different for different nucleation mechanisms. In the case of a micellar nucleation mechanism, the number of monomer-swollen micelles increases as the concentration of emulsifier increases. Thus, the number of particles increases and the particle size decreases with increasing concentration of emulsifier at a constant concentration of monomer. In the homogeneous and coagulative nucleation mechanisms, the surfactant mainly acts as the stabilizer for maintaining colloidal stability during the particle growth stage. As the concentration of emulsifier increases, the surface charge of the polymer particle increases. The increasing repulsion

forces between particles slow the rate of particle growth so that the size of the particles decreases but their number increases. In any one of the mechanisms, the particle size decreases with increasing concentration of emulsifier at constant concentration of monomer.

3.5.3 The Stability of Polymer Latices

A latex particle is built from a large number of polymer macromolecules and the surfactant molecules adsorbed on its surface. The physical state of the latex particle is important in close-range interactions and in drying. For example, if the particles are soft, coalescence of the particles can occur to give a continuous film whereas with hard particles individual characteristics are retained in the dry state.

The stability of a latex is determined by the balance between the electrostatic and steric repulsion forces and the London-van der Waals attraction forces. The electrostatic repulsion forces arise from adsorbed or chemically bound surface ions; the adsorbed groups can be conventional emulsifiers, e.g., sodium lauryl sulfate, or a polymeric emulsifier, such as methylcellulose. The chemically bound surface ions come from the initiator applied in the polymerization. The electrostatic repulsion forces are strongly affected by the concentration and valence of the counterions. The steric repulsion forces arise from adsorbed or chemically bound hydrated uncharged surface groups. Such a layer, if hydrated, will prevent the particles from approaching one another to a distance where the attractive forces prevail. London-van der Waals attraction force exists in all types of intermolecular interaction. It is generated by the rapidly fluctuating dipoles which created

by the continuous motion of electrons in molecules. Considering only spherical particles, the latex particles can be visualized as shown in Figure 3.7.

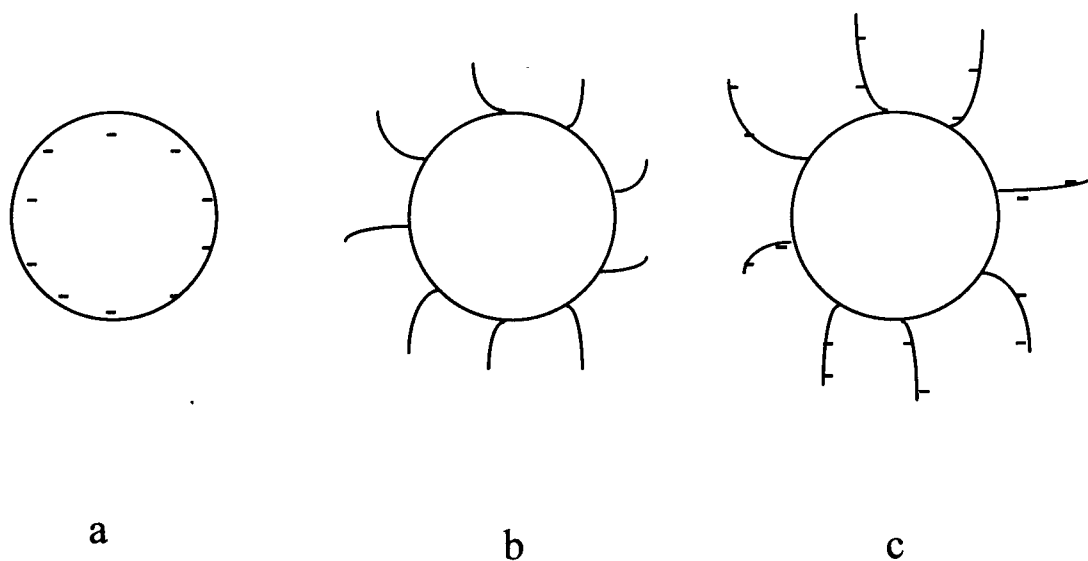


Figure 3.7. Schematic illustration of various types of latex particle surfaces: a) smooth; b) with nonionic chains; c) with ionic chains

3.5.4 The Glass Transition Temperature, T_g , of a Polymer

The glass transition temperature is one of the fundamental properties of polymer latices. If the melt of a non-crystalline (amorphous) polymer is cooled, it becomes more viscous. If the temperature is reduced further, it becomes rubbery, and then it becomes relatively hard and elastic. The temperature at which polymer undergoes the transformation from a rubber to a glass is known as the glass transition temperature, T_g . This dictates the temperature conditions under which they form continuous films and the degree of softness or flexibility imparted to the item containing the latex polymer. The glass transition temperature is characterized by the monomer making up the backbone of the polymer

molecule and depends upon the physical and chemical nature of the polymer macromolecules.

The characteristic of the polymer chain which affects T_g is chain flexibility (Young and Lovell, 1991). In other words, the T_g is determined by the chain flexibility. The chain flexibility is governed by the nature of the chemical groups that constitute the main chain. Polymers, such as polyethylene $(-\text{CH}_2-\text{CH}_2-)_n$ and polyoxyethylene $(-\text{CH}_2-\text{CH}_2-\text{O}-)_n$, tend to have low values of T_g due to the relatively flexible chains resulting from the easy rotation around the main bond. However, the incorporation of side units to the main chain impedes rotation and stiffens the chain, resulting in a large increase in T_g . For example, the presence of a p-phenylene ring in the polyethylene chain causes poly(p-xylylene) to have a T_g 200°C higher than that of polyethylene.

In vinyl polymers of the type $(-\text{CH}_2-\text{CHX}-)_n$, the nature of the side group has a profound effect upon T_g . The presence of side groups on the main chain has the effect of increasing T_g through a restriction of bond rotation. Large and bulky side groups tend to cause the greatest stiffening. However, if the side group itself is flexible, the effect is not so profound. The presence of polar groups, such as $-\text{Cl}$, $-\text{OH}$ or $-\text{CN}$, tends to raise T_g more than non-polar groups of equivalent size. This is because the polar interactions restrict rotations further, so poly(vinyl chloride) $(-\text{CH}_2-\text{CHCl}-)_n$ has a higher T_g than polypropylene $(-\text{CH}_2-\text{CHCH}_3-)_n$ (Table 3.1) (Brandrup and Immergut, 1975).

It is also known that the physical characteristics of the molecules, such as molar mass, branching and crosslinking, affect the temperature of the glass transition (Young and Lovell, 1991). The value of T_g is found to increase as the molar mass of the polymer is

increased. A small number of branches on a polymer chain are found to reduce the value of T_g . A high density of branching has the same effect as side groups in restricting chain mobility and hence in raising T_g . Polymers that have the lower glass transition temperature would make up the lattices that are softer.

Table 3.1. Approximate values of glass transition temperature, T_g , for various polymers

Repeat unit	T_g/K
-CH ₂ -CH ₂ -	148
-CH ₂ -CH ₂ -O-	232
 -O-	358
-CH ₂ -  -CH ₂ -	353
	side group (X)
-CH ₂ -CHX-	-CH ₃ 260
	-CH ₂ -CH ₃ 249
	-CH ₂ -CH ₂ -CH ₃ 233
	-COOCH ₃ 283
	-COOCH ₂ CH ₃ 249
	-COOCH ₂ CH(C ₂ H ₅)(CH ₂) ₃ CH ₃ 223
	 373
	-Cl 354
	-OH 358
	-CN 370
-CH ₂ -CXCH ₃ -	-COOCH ₂ CH(C ₂ H ₅)(CH ₂) ₃ CH ₃ 263

3.5.5 Surface Characterization of Latices

Latices have been of great interest to colloid chemists over the last two decades. This interest has centered around their use as model dispersion for testing theories of colloid stability. Monodisperse latices have also found a wide variety of applications as calibration standards in different methods of particle size determination and particle counting. As a result, it is important to understand their surface characteristics; also the size of the latex particles is of a paramount importance.

Methods for the characterization of surface groups of latices include potentiometric titration, conductometric titration and electrophoresis. Several review articles dealing with theoretical and experimental aspects of the potentiometric and conductometric titrations of latices have been published (Hearn et al., 1981; Vanderhoff, 1981; James et al., 1982).

Conductometric titration is by far the most commonly used method for the characterization of charged groups on latices. The measurements are easy and sensitive to both strong and weak acids. The total conductivity is given by the sum of the contributions from each individual ionic species in the solution. Because conductance is nonspecific, conductometric titration is not a very useful qualitative method. However, it is quantitative for a single known electrolyte in solution or for one ionic species in a multicomponent solution provided that its concentration is changed without extensive change in the other concentration.

Potentiometric titration is of interest as a method of characterization since it is capable of providing a direct measure of the surface charge and of the dissociation constants of the different surface groups. Potentiometric titrations can be carried out conveniently and with high precision if precautions are taken to calibrate the electrodes

properly. Although a potentiometric titration experiment can be very precisely controlled, its interpretation is rather difficult. If the difference between the dissociation constants of the weak and strong acid groups is sufficiently large, two inflection points appear in the titration curve, but this may be quite sensitive to the electrolyte concentration as well (Laaksonen et al., 1975; Bagchi et al., 1979; Everett et al., 1979).

The titration method gives a detailed evaluation of the actual acid or base groups on the surface. The electrophoretic mobility usually makes it possible to obtain information rapidly on the electrokinetic charge and often requires quite small quantities of the involved material. The limitation of the method is that it measures the potential net charge in the surface of shear between the surrounding liquid and the particle. The distance of this plane from the surface may depend on the solution conditions, such as ionic strength, especially in the case of specifically adsorbing surfactants.

The aforementioned methods can be used to characterize the surface properties, such as surface acid or base groups and electrical charge of latices. They can be interpreted satisfactorily in terms of the well-known Gouy-Chapman-Stern-Grahame electrical double layer model. The main problems associated with the characterization of these surfaces are experimental. Minute quantities of impurities and small changes in experimental conditions and cleaning procedures considerably affect the relative amounts of the studied surface groups.

The scanning electron microscope and transmission electron microscope are usually used to characterize the surface structure of latex particle including the particle size and shape.

3.5.6 Methods of Latex Cleaning

Latices are comprised of colloidal particles of submicron dimension in a continuous media. The latex may also contain a number of other ingredients, such as electrolytes resulting from a residual initiator and its decomposition products, emulsifier molecules which are soluble in the aqueous phase and adsorb at the particle surface; oligomers and/or water soluble polymers which are soluble in aqueous phase and adsorb at the particles surface; and ionic or nonionic end-groups which are chemically bound to the surface of the particles or buried inside the latex particles as a result of the initiator fragments, and/or of functional groups-containing monomers used in the polymerization process. Some of these ingredients are added in the polymerization recipe (e.g., initiator and emulsifier); others, such as oligomers, are generated during the course of the polymerization process. "Cleaning" or "purification" of a latex system is a process which is used to remove part or all of the unreacted ingredients. Cleaning of a latex is usually carried out before characterization.

The following methods have been developed and used to "clean" latex systems. Dialysis (Edelhauser, 1969; Everett et al., 1979) and hollow-fiber dialysis (McCarvill et al., 1978); ion-exchange (van den Hul et al., 1968; Vanderhoff et al., 1970; Vanderhoff et al., 1981); gel filtration (Muroi et al., 1976); activated charcoal adsorption (Wilkinson et al., 1981); centrifugation (Garvey et al., 1974; Norde et al., 1978; Vijayendran et al., 1981); and serum replacement (Ahmed et al., 1980; El-Aasser et al., 1980; Daniels et al., 1981).

3.6 Deposition of Colloidal Particles on Planar Surfaces

Deposition of colloidal particles onto much larger particles is of great importance in many industrial processes. In froth flotation, the fine gangue mineral particles often form so-called slime coatings on the valuable mineral surfaces and depress their flotation. Selective aggregation (heterocoagulation or flocculation) in mixed mineral suspensions is an example of another process which is based on the differences in the deposition rates between dissimilar particles. The study of particle deposition is also of intrinsic interest to the field of colloid science. By comparing the behavior of model latex particles near solid surfaces with theoretical predictions, important information can be obtained regarding the nature of colloidal forces operating at short particle-solid surface distances.

Deposition of colloidal particles on solid surfaces is mainly determined by the hydrodynamic conditions in the vicinity of the solid surface (usually referred to as the collector), and the energy of interaction between particles and the collector. In addition, there are a variety of other important factors affecting deposition, such as surface heterogeneity and roughness, and particle detachment. In Adamczyk et al.'s review (1983), several theories for predicting deposition rates of flowing colloidal particles onto various collector surfaces were studied and compared. Several experimental procedures for measuring deposition rates were discussed. The comparison of the experimental data (Marshall and Kitchener, 1966; Hull and Kitchener, 1969; Clint et al., 1973) with theoretical predictions reveals discrepancies especially in the case when the interaction energy vs. distance curves exhibit large energy barriers. This is mainly because the theory neglects such factors as surface heterogeneity and roughness. Various types of collectors, such as rotating disc, plate in uniform flow, cylindrical collector in uniform flow,

stagnation point flow collector and so on have been studied. Of them, the rotating disc is the one most widely used and extensively studied.

The rotating disc is commonly used in electrochemical measurements. The theory of the rotating disc system was developed by Levich (1962). The basic hydrodynamics and construction of the rotating disc electrodes have been discussed by Riddiford (1966).

3.6.1 The Rotating Disc System

Spinning a disc in solution imposes a pattern of flow on the solution which is illustrated in Figure 3.8. The spinning disc acts as a pump, sucking the solution towards the disc and flinging it out centrifugally close to the disc. The angular velocity of the fluid increases as the surface of the disc is approached until the angular velocity of the rotating disc is attained. Furthermore, the fluid also acquires a radial velocity under the influence of the centrifugal force. The disc is assumed to be sufficiently large so that edge effects are negligible. F, G and H shown in Figure 3.8 denote the functions describing radial velocity, angular velocity and normal velocity, respectively. Those functions depend only on z (the normal distance to the disc) and do not depend on r (the distance from the rotating axis which is on the centre of the disc); in particular, the flow towards the disc, v_z (the normal velocity of the disc), is a function of z only and is independent of r . The stirring of the solution keeps the concentrations of species equal to their bulk values except for the thin layer (the diffusion layer) near the disc. The flow pattern shown in Figure 3.8 is established over a distance where $z \sim 0.1\text{mm}$. The thickness of the diffusion layer is smaller than this distance.

The maximum mass flux to the rotating disc surface is described by Levich's equation:

$$j = D \left(\frac{\partial c}{\partial z} \right)_{z=0} = 0.62 D^{2/3} \nu^{-1/6} \omega^{1/2} c_0 \quad (3.33)$$

where D is the Brownian diffusion coefficient, ν is the kinetic viscosity, ω is the rate of rotation of the disc (in radians per second) and c_0 is the bulk concentration of the solution.

A significant characteristic of the rotating disc is that the thickness of the diffusion boundary layer is not a function of the distance from the rotation axis but is constant over the entire disc surface. This means that, regardless of the distance from the axis of rotation, the conditions for transport of matter to any point on the surface of the disc are identical. This is one of the advantages of the rotating disc system. Such a surface may be termed uniformly accessible.

It should be mentioned that the Levich equation was developed based on an assumption of the infinitely small dimensions of the transported particles. This assumption is fulfilled well by ions in electrochemical systems, but it is usually not justified in the case of colloidal particles. Dabros and Czarnecki (1975) have described the transport of particles with finite dimensions to a rotating disc surface. Their equations show that, as the radius of the particles becomes comparable with the thickness of the diffusion layer, the actual flux becomes progressively greater than that calculated using Levich's expression. In addition, particles at the plane parallel to the disc would be subjected to different velocities

at different distances from the rotating axis except at the centre area which is in the effective range of the stagnation point (Czarnecki, 1995).

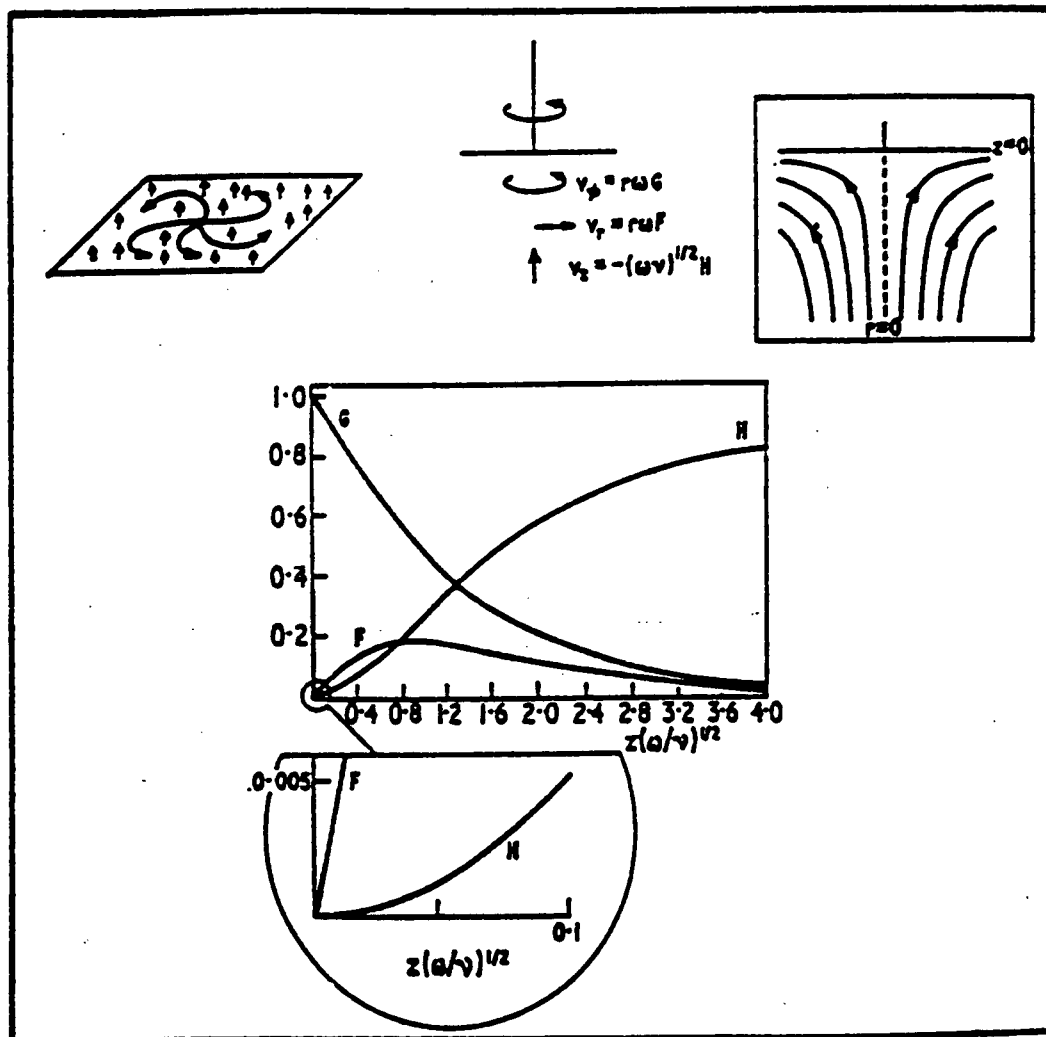


Figure 3.8 The flow pattern imposed by a rotating disc. The right-hand inset shows the stream lines below the disc. The left-hand inset shows the stream lines in an x, y plane and emphasises that v_z does not depend on the radial distance. The bottom inset shows the values of F (radial velocity) and H (velocity towards the disc) that are found in the diffusion layer.

3.6.2 Deposition of Colloidal Particles on Planar Surface

The first experimental data on the deposition of colloidal particles on a surface of disc with a well-defined geometry under well-defined hydrodynamic conditions were reported by Marshall and Kitchener (1966) and Hull and Kitchener (1969). In their study of the deposition process, they used the rotating disc technique. In the first reference, the deposition of graphitized carbon black particles with an average diameter of $0.45 \mu\text{m}$ and a concentration of about $6 \times 10^8/\text{cm}^3$ was studied on various collectors, such as glass, polystyrene, polyvinyl formaldehyde, polyvinyl pyridine and cellulose. The angular velocity of the disc was usually 200 r.p.m., and all the experiments were made under laminar flow conditions. An optical microscope at 480x magnification with dark-field illumination was used to determine the coating density. The results of their experiments were interpreted in terms of Levich's formula. When the particles were negatively charged and the film positively charged (no energy barriers), the value of the flux to the collector surface was close to what can be expected theoretically, i.e., the deposition rate was solely controlled by diffusion. However, when the charges of particles and the surface of the plate were the same, the double-layer repulsion reduced the deposition rate by interposing an energy barrier. High electrolyte concentrations were required to produce a measurable deposition. The forces determining the adhesion or non-adhesion, considered in these studies were the long-range London-van der Waals forces of attraction and electrical double-layer interaction, which was repulsive for like sign and attractive for unlike sign.

A better quantitative agreement with results calculated using Levich's formula was obtained by Hull and Kitchener (1969) for the deposition of $0.308 \mu\text{m}$ polystyrene latex

particles on a cationic polymer [copoly(vinylpyridine styrene)] and an anionic polymer (polyvinylformaldehyde) surfaces.

Adamczyk and Pomianowski (1980) modified the conventional rotating disc apparatus to study the effect of the particle gravity on the deposition rate. The differential equations describing quantitatively transport of spherical particles to the rotating disc surface were solved. The solved numerical solution permitted the determination of the particle flux at the disc surface as a function of the liquid viscosity and density, temperature, particle dimensions and density, Hamaker constants, zeta potentials and disc angular velocity. The measurements of the particle deposition rate from CaCO_3 and BaSO_4 suspensions (average particle sizes were 1.25 and 0.86 μm , respectively) onto glass and Cu_2S disc surfaces, under various physicochemical conditions, were studied. The distribution of particles on the surface of the disc, taking the blocking effects into account, was also discussed by Adamczyk and Pomianowski. Analysis of the data revealed that a particle was able to block an area which was much larger than its geometrical cross-section.

As mentioned previously, the colloid stability has a direct impact on the deposition process. Deposition of aggregates and particles from unstable dispersions was studied by Clint et al. (1973). The deposition of 0.43 μm negatively charged latex particles onto a negatively charged polystyrene surface was studied using the rotating disc technique, for a variety of electrolyte concentrations. For high values of the salt concentration, the deposition of aggregates was observed. By assuming that coagulation did only influence the diffusion coefficient and that the aggregates were sufficiently spherical so that one value of the diffusion coefficient sufficed for the description of diffusion, and by adopting

Smoluchowski's theory of coagulation to describe the concentration of i -fold aggregates, the observed deposition could be described reasonably well.

A direct method of studying deposition is to observe the solid surface under a microscope when the coating is being formed in a well-defined flow field. This allows one to observe the dynamic nature of the processes connected with the escape of deposited particles from the solid surface, the distribution of particles on the surface and the behavior of particles in the vicinity of the solid surface (Dabros and van de Ven, 1983). In this method, particle deposition takes place in a stagnation point flow which is generated by an impinging jet cell, and the disc surface is stationary and must be transparent to enable the direct observation of the particles deposition. Figure 3.9a shows a schematic picture of the experimental setup used in the direct observation. It should be mentioned that the thickness of the diffusion boundary layer is also constant for a stagnation point flow. Figure 3.9b shows the pattern of the flow around the stagnation point.

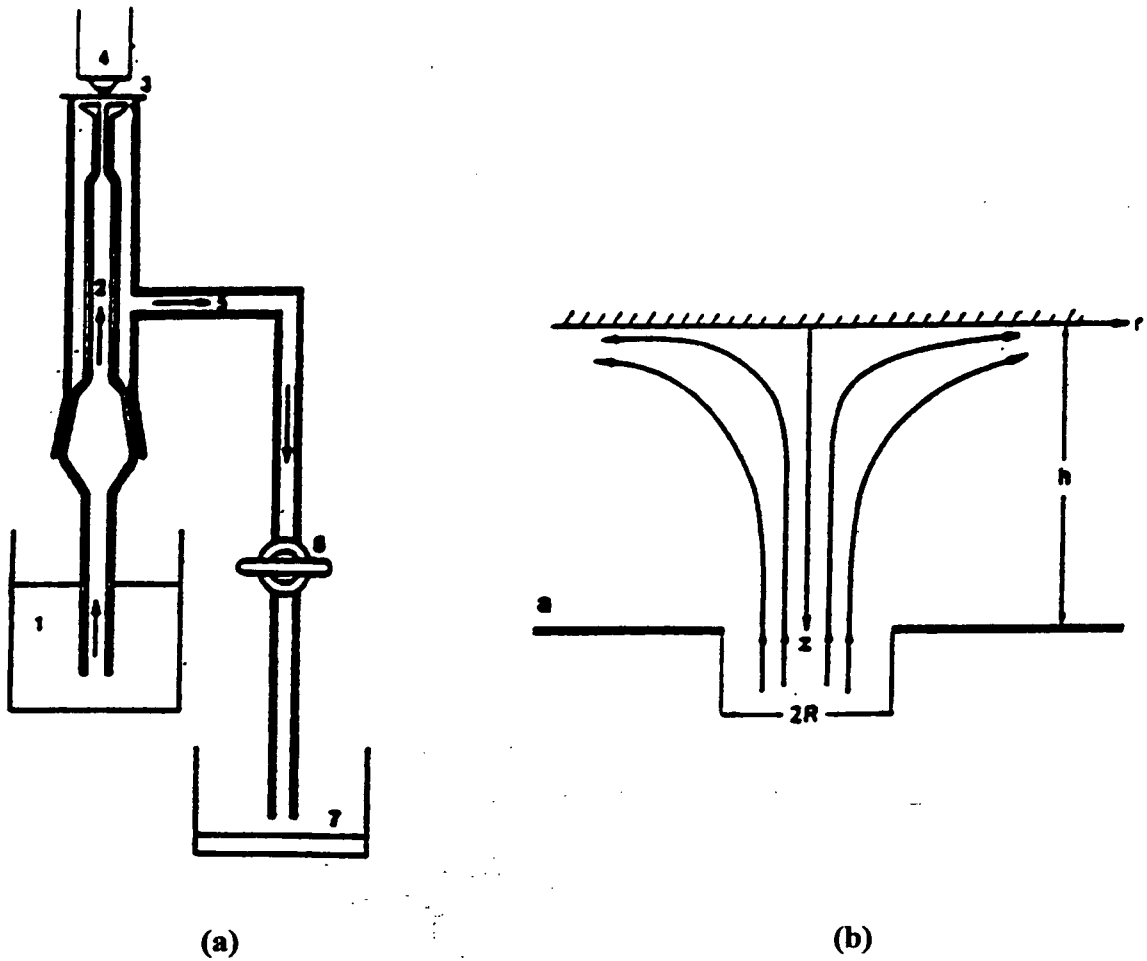


Figure 3.9 (a) Stagnation point flow disc. 1. colloidal dispersion; 2. entrance tube; 3. collecting surface; 4. microscope; 5. outflow tube; 6. flow speed control valve; 7. reservoir (b) stagnation point flow, two-dimensional schematic representation of fluid streamlines and coordinates system.

CHAPTER 4 EXPERIMENTAL

This chapter describes experimental approach followed by experimental techniques, including the experimental procedure and setups for the preparation and characterization of mineral samples, preparation and characterization of latices, flocculation tests, deposition tests and flotation tests involved in this research work.

4.1 Definition

There are two fundamental operations in mineral processing, namely liberation of the valuable minerals from their waste gangue minerals, and separation of these values from the gangue. This latter process is known as *concentration*. This thesis primarily deals with the latter process.

For separation of a two-component (one valuable mineral and gangue) ore, if the masses of the feed, concentrate and tailings are F , C and T respectively, and their corresponding contents of valuable component (grade) are f , c and t , then

$$F = C + T \quad (4.1)$$

$$\text{or on percent basis, } 100 = \gamma_c + \gamma_T \quad (4.2)$$

where γ_c and γ_T are percent yields of concentrate and tailings.

$$\text{Since } Ff = Cc + Tt \quad (4.3)$$

$$\text{The recovery (in concentrate) is given by } R_c = \frac{Cc}{Ff} \times 100\% \quad (4.4)$$

Since $\frac{C}{F} \times 100\% = \gamma_c$, yield of concentrate,

$$R_c = \gamma_c \frac{c}{f} \quad (4.5)$$

The recovery (in tailings) is $R_t = \frac{Tt}{Ff} \times 100\% = \gamma_t \frac{t}{f}$ (4.6)

In selective flocculation, C is the mass of the flocs, F and T are the masses of feed and tailings. f , c and t are their corresponding contents of valuable component.

For single mineral flotation or flocculation, $c=f=t$, thus recovery is given by

$$R = \frac{C}{F} \times 100\% = \text{yield} \quad (4.7)$$

The valuable component in phosphate ore is P_2O_5 . The percentage of mass content of P_2O_5 is also referred to as grade. In separation of fluorite from gangue, the valuable component is fluorine.

There is an approximately inverse relationship between recovery and grade of concentrate in all concentrating processes. If a high recovery of valuable mineral is aimed for, there will be more gangue in the concentrate and the grade of concentrate will decrease. If an attempt is made to attain a very high-grade concentrate, the recovery will be low.

In the concentration plant, the importance of the recovery-grade relationship is in determining the most economic combination of recovery and grade which will produce the greatest financial return per tonne of ore treated in the plant. For metallic ores, this will depend primarily on the current price of the valuable product, transportation costs to the smelter, refinery, or other further treatment plant, and the cost of such further treatment, the latter being very dependent on the grade of concentrate supplied. For phosphate ore, this

will depend primarily on the current price of phosphorus fertilizer and transportation costs to the manufacture of phosphorus fertilizer.

In the selective flocculation of apatite from apatite-calcite and apatite-silica, the separation is evaluated by the parameters of apatite recovery, P_2O_5 grade of flocs and selectivity index (SI) (Andersen and Somasundarian, 1993). In the selective flocculation of fluorite from fluorite-calcite and fluorite-silica, the separation is evaluated by the parameters of fluorite recovery, fluorine grade and the selectivity index.

The selectivity index used in this thesis is defined as the grade increase expressed as a fraction of the maximum possible grade, i.e., $SI=0$ means no separation and $SI=1$ indicates complete separation. SI can be expressed as

$$SI = \frac{c - f}{G - f} \quad (4.6)$$

where c is the grade of flocs, f is the grade of feed, G is the grade of pure mineral (maximum grade).

4.2 Experimental Approach

Once the mineral samples were prepared and analyzed, and the latices were prepared and characterized, flocculation tests were conducted. Numerous studies on selective flocculation have confirmed that three variables such as flocculant dosage, pH and the concentration of dispersant are the most important factors affecting the selective flocculation. Since the tested latices were newly developed in the present work, their effects on selective flocculation were considered the most important. The pulp pH and the concentrations of dispersants determine the mineral/water interfacial properties and thus

the interaction between the latex particles and the mineral surfaces. Therefore, univariant experiments were first conducted focusing on latex dosage, pH and the concentrations of dispersants.

It is well established that a low pulp density is required in selective flocculation. Thus a 2% pulp density (solid content in the pulp) was kept constant in all flocculation tests. Because of the large pulp volumes and economic considerations, all mineral concentration processes are practically carried out at ambient temperature. All the flocculation and flotation tests present in this dissertation were conducted at room temperature and pressure.

It is known that a given amount of energy (power input) is required to initiate a flocculation. This energy can be introduced by applying a shear force which is characterized by the degree of agitation and the geometry of stirring paddle and the flocculation vessel, the material and the solid content of the pulp. Since all the flocculation tests were carried out in the same device and the solid content of the pulp was kept constant and relative low, i.e. 2%, it has been decided to characterize the power input by a stirring speed. Some preliminary flocculation tests with the flocculation device (shown later in this chapter) with the tested latices showed that a stirring speed of 350 rpm to initiate the flocculation followed by a lower stirring speed, 150 rpm for the conditioning, produced the best flocculation results. This is also supported by Yu's findings (Yu, 1998). Thus, all flocculation tests were conducted under these conditions. Therefore, the effects of pulp density, temperature and mixing conditions were not examined and these factors were held constant in all the flocculation tests.

The univariant experiments explored a large range of magnitude of each variable. However it might neglect the possible interactions between the experimental variables.

Therefore, a factorial experiment on selective flocculation of the apatite-calcite and apatite-silica systems was designed. The levels of the factors were selected based on the results of the univariant experiments and were confined in a relative small range in which the selective flocculation produced a relative higher apatite recovery and P_2O_5 grade.

Deposition tests were conducted aiming at studying the interaction of the latex particles with the mineral surfaces and comparing with the flocculation results. Finally the flotation of fine apatite with and without the addition of the selected latex was conducted to evaluate the latex in enhancing the flotation recovery of fine apatite.

4.3 Preparation of Mineral Samples

The mineral samples used in the present work include fluorite and fluorapatite from Cave-in-rock, Illinois, and calcite from Santa Eulalia, Chihuahua, Mexico. These samples were purchased from Ward's Natural Science Establishment Inc. One phosphate ore sample used in the flotation study was obtained from IMC Agrico Company; the sample was from Florida in the USA. Silica containing 99.7% of SiO_2 was obtained from the Mines Branch in Ottawa. The results of the chemical analyses of these mineral samples are summarized in Table 4.1. The phosphate ore sample was analyzed for contents of P_2O_5 , CaO, MgO and insoluble material for two size fractions, -420+106 μm and -38 μm , which were used in flotation tests. The assay results are given in Table 4.2.

Table 4.1 Chemical Characterization of Mineral Samples (wt%)

	Ca(1)	Mg(1)	Fe(1)	Al(1)	F(2)	P ₂ O ₅ (1)	C(1)	SiO ₂ (1)
Fluorite	51	0.01	0.06	0.01	47.6	-	0.09	1.13
Fluorapatite	39.4	0.17	0.08	0.01	2.60	39.00	0.86	1.30
Calcite	39.0	0.17	0.07	0.02	-	-	4.68	0.53
Silica	-	-	-	-	-	-	-	99.7

Notes: (1) UBC, Department of Mining and Mineral Process Engineering, Assay Laboratory. Ca, Mg, Fe and Al were assayed by atomic absorption; P₂O₅, C and SiO₂ were assayed by wet analytical methods.
 (2) ACME Analytical Lab, Vancouver, by ionic selective electrode.

Table 4.2 Compositions of the Phosphate Sample

Size, μm	Analysis, wt%			
	P ₂ O ₅	MgO	CaO	Insol
-420+106	4.79	0.076	4.20	85.46
-38	5.16	0.068	5.89	84.76

The assay was conducted on -38 μm samples using the same methods as above. The theoretical P₂O₅ content in fluorapatite is 42%. Thus the purity of the fluorapatite sample is 93%. The theoretical fluorine content in fluorite is 49%. Thus the purity of the fluorite sample is 97%. As expected, the sample of fluorapatite had more contaminants than the other samples. However the purity of the fluorite and fluorapatite samples was considered high enough for the purpose of this work, and no additional chemical treatment was applied.

The sample of phosphate ore was a low grade siliceous ore (see Table 4.2). A -420+106 μm fraction was obtained by wet screening from the as-received sample. The

-38 μm fraction was obtained by wet grinding in a ceramic ball mill followed by screening, settling, decanting and drying. These fractions were used in the batch flotation tests.

The mineral samples were first crushed by a hammer to below 10mm, and then crushed in a jaw crusher and sized by screening in an automatic "Ro Tap" screen shaker. The -210 + 150 μm fraction was wet ground in a ceramic ball mill (the ceramic ball mill was cleaned by grinding with a small portion of sand several times and rinsed copiously with water several times) at 50% solid content using distilled water. After two hours of grinding, the -150+75 μm fraction was wet screened and then dried at room temperature overnight. This sample was used in the microflotation tests. The -75 + 38 μm fraction was returned to the ball mill for another 2-3 hours of grinding. The -38 μm fraction was separated by wet screening, and the suspension was decanted and then dried overnight at room temperature. This fraction was kept for the flocculation tests. The material suspended in the supernatant after the overnight settling period was kept for microelectrophoresis. Part of the -38 μm fraction of the fluorapatite sample was subjected to further sizing by decanting to yield a -10 μm material that was also used in the microflotation tests.

4.4 Chemicals

Table 4.3 lists the chemicals used in the present work. These reagents include chemicals used in the emulsion polymerization of latices, simple inorganic chemicals for pH regulation and ionic strength control, sodium silicate (meta) used in the flotation as a gangue depressant, and a surfactant used in the flotation as a collector. All reagents in this category are reagent grade.

Dispersants used in the flocculation tests include sodium tripolyphosphate and sodium silicate. These were technical grade reagents.

Some materials (e.g., ion-exchange resins) used in the purification of latices are also listed in Table 4.3.

Table 4.3 Chemicals

Compound	Formula (M.W.)	Supplier (Grade)	Usage
Styrene	C_8H_8 (104.08)	Aldrich, (99%)	To prepare polystyrene latex
2-Ethylhexyl methacrylate	$C_{12}H_{22}O_2$ (198.31)	Aldrich, (98%)	To prepare P(EHMA) latex
Methyl acrylate	$C_4H_6O_2$ (86.09)	Aldrich, (99%)	To prepare P(MAAA) latex
Acrylic acid	$C_3H_4O_2$ (72.06)	Aldrich, (99%)	To prepare P(MAAA) latex
Ethylene glycol	$C_2H_6O_2$ (62.07)	Anachemia (A.C.S)	To prepare P(EHMA) latex
Sodium EDTA powder	$Na_4C_{10}H_{12}N_2O_{16}$ (416.23)	Anachemia (A.C.S)	To prepare P(EHMA) latex
Potassium persulphate	$K_2S_2O_8$ (270.31)	BDH (Analytical)	Initiator in polymerization
Oleic acid, potassium salt	$C_{18}H_{33}O_2K$ (320.57)	Aldrich, 40% paste in water	Emulsifier in polymerization
Potassium hydroxide	KOH (56.10)	BDH (A.C.S.)	Neutralization of acrylic acid
Sodium hydroxide	NaOH (40.00)	BDH (A.C.S.)	pH modifier
Hydrochloric acid	HCl (36.5)	Fisher (A.C.S.)	pH modifier

Table 4.3 - continued

Compounds	Formula (M. W.)	Supplier (Grade)	Usage
Sodium tripolyphosphate	$\text{Na}_5\text{P}_3\text{O}_{10}$ (367.93)	VWR Waters and Rogers Ltd (technical)	Dispersant
Sodium silicate	$m\text{Na}_2\text{O} \cdot n\text{SiO}_2$ (n/m=3.2)	Fisher (technical)	Dispersant
Sodium silicate (meta)	Na_2SiO_3 (122.07)	Fisher (A.C.S.)	Depressant
Oleic acid, sodium salt	$\text{C}_{18}\text{H}_{33}\text{O}_2\text{Na}$ (304.47)	Sigma (99%)	Flotation collector
Ethanol	$\text{C}_2\text{H}_6\text{O}$ (46.02)	Fisher (A.C.S.)	Ethanol and nitric acid together were
Nitric acid	HNO_3 (63.01)	Fisher (A.C.S.)	used in cleaning glass-wares
Methanol	CH_4O (32.01)	Fisher (A.C.S.)	Resin purification
Potassium nitrate	KNO_3 (101.10)	BDH (A.C.S.)	Ionic strength control
Dowex 1 - X4 (OH ⁻)	-	Sigma	Anion exchanger resin
Dowex-50 w - X4 (H ⁺)	-	Sigma	Cation exchanger resin

4.5 Experimental Setups and Methods

4.5.1 Preparation of Latices

The setup for the preparation of the latices is shown in Figure 4.1. The reaction vessel is a 500ml three-neck round-bottom flask which was immersed in a thermostated water bath in a fume hood. The flask was stirred with a mechanical stirrer with a glass paddle to ensure sufficient agitation for emulsification and heat transfer during the reaction. The reaction temperature was monitored by a mercury thermometer which was placed in one of the necks of the flask. The system was purged with nitrogen to displace oxygen thus to prevent the production of a free radical scavenger. After the reaction took place and the temperature reached a stable value, the thermometer was replaced by a refluxing condenser.

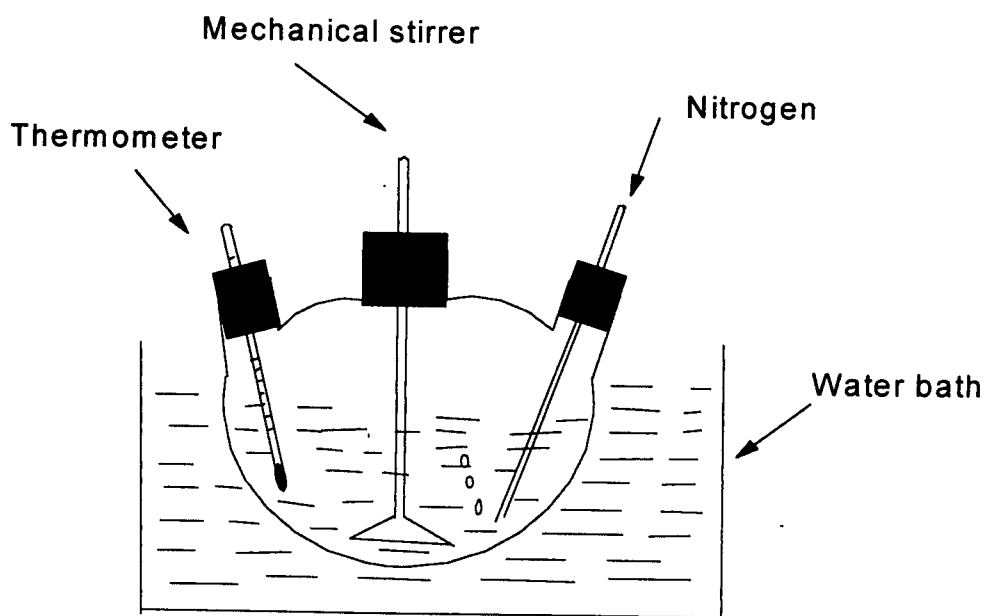


Figure 4.1 - A sketch of the experimental apparatus used to produce latices

The recipes and the polymerization conditions for the preparation of the polystyrene (PS), Poly(2-ethylhexylmethacrylate) [P(EHMA)] and Poly(methylacrylate-acrylic acid) [P(MAAA)] latices are given in Table 4.4.

All glassware was thoroughly cleaned with an EtOH/HNO₃ mixture before the experimentation began. The general procedure for emulsion polymerization was as follows.

The potassium oleate emulsifier was first dissolved in distilled water at an elevated temperature around 70°C and then transferred to the three-neck round-bottom flask. The monomer was added to the flask with the emulsifier solution under intense stirring. The temperature of the water bath was set at the required value (see Table 4.4). When the temperature reached the set temperature, the potassium persulphate initiator, dissolved in a small amount of water, was injected into the reaction vessel. The temperature went up approximately 2-3°C as soon as polymerization was initiated since this is an exothermic reaction.

For preparation of the P(EHMA) latex, the pH of the emulsifier solution was adjusted to approximately 7 by the addition of hydrochloric acid. In addition, ethylene glycol was added to assist the dispersion of the emulsion and a small amount of sodium EDTA was employed to chelate the trace metallic ions which may be present in the solution. Nitrogen was bubbled through the emulsion for 10 minutes before the addition of the initiator to expel oxygen.

For preparation of the P(MAAA) latex, acrylic acid was neutralized to a pH of 7 by the addition of 1N KOH before mixing with methyl acrylate. Co-polymers of the two monomers with various ratios were synthesized. However, only at a ratio of 1.4:1 of methyl acrylate to acrylic acid, a latex obtained was stable and displayed properties of a selective

Table 4.4 Recipes and Conditions of Latices Preparation

Latices	Monomer	Initiator	Emulsifier	Temperature	Time, hours	Distilled water	Remarks
PS	Styrene, 60 ml	Potassium persulphate, 0.1 g	40% Potassium oleate, varied	70 °C	4.5	150 ml	No N ₂
P(EHMA)	2-Ethylhexylmeth acrylate, 100 ml	Potassium persulphate, 0.2 g	40% Potassium oleate, 15.74 g	70 °C	5	100 ml	Ethylene glycol, 50 ml, Sodium EDTA, 0.050g Apply N ₂ .
P(MAAA)	Methyl acrylate, 22 ml, acrylic acid, 11.9 ml	Potassium persulphate, 0.08g	not applied	75 °C	4.5		1N potassium hydroxide for neutralizing acrylic acid to pH around 7, no addition water needed. No N ₂

flocculant. Both monomers were then stirred under intense agitation for 10 minutes, and the initiator was added at the set temperature.

A series of polystyrene latex with different concentrations of potassium oleate were prepared and listed in Table 4.5.

Table 4.5 Preparation of Polystyrene with Various Concentrations of Emulsifier

Polystyrene Latex	40% Potassium Oleate, g
PS1	3.0
PS2	2.5
PS3	1.3
PS4	0.6
PS5	0

4.5.2 Purification of the Latices

The P(MAAA) latex was purified by a serum replacement technique to remove the unreacted monomers. The feed dispersion was diluted with double-distilled water to 5%. The technique and the setup is described in section 4.3.2.1. An ion-exchange resin treatment was applied to the PS and P(EHMA) latices to remove the adsorbed emulsifier. Both techniques, the serum replacement and the ion-exchange resin treatment are effective methods for latex purification by removing adsorbed emulsifier, excess emulsifier, unreacted monomer and electrolyte in the latex suspension (Ahmed, El-Aasser et al., 1980; Kamel, El-Aasser et al., 1981). The techniques have their own advantages and drawbacks that will be discussed later.

4.5.2.1 Serum Replacement Technique

Figure 4.2 diagrammatically shows the cell for serum replacement.

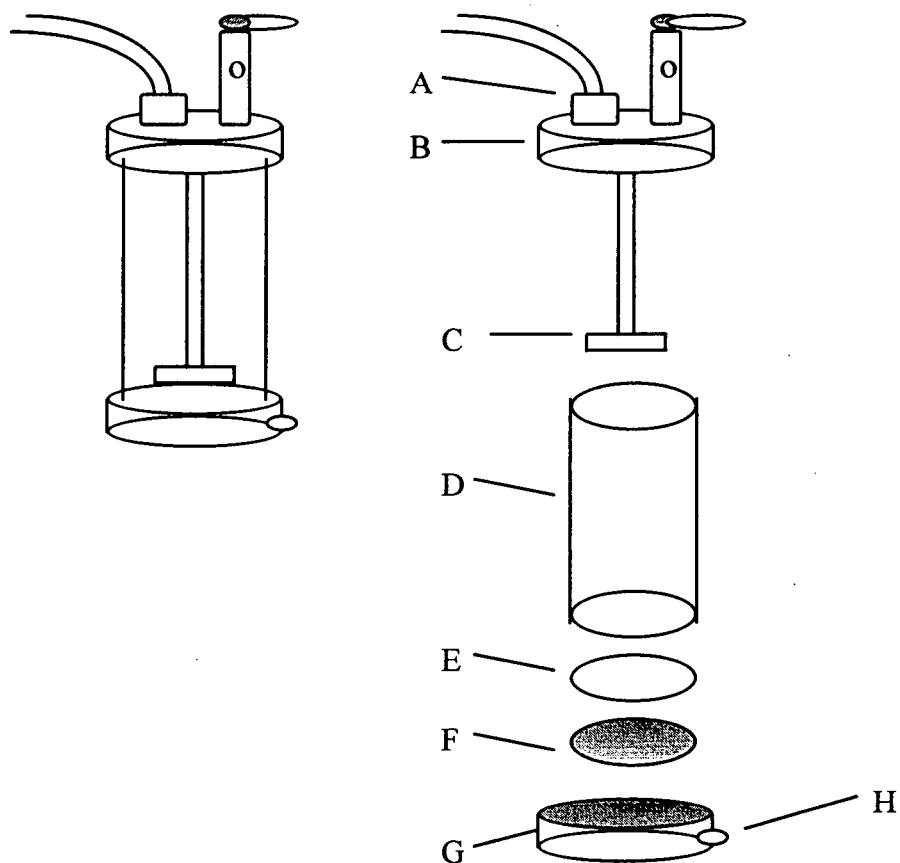


Figure 4.2 - A sketch of the filtration cell used for serum replacement of latices. (A) feed stream inlet; (B) polyacetal top plate; (C) Teflon-coated magnetic stirring bar; (D) polycarbonate reservoir; (E) ethyl-propylene copolymer O-ring; (F) polyethylene porous disc; (G) polyacetal bottom plate; (H) filtrate outlet

The cell consists of a cylindrical glass reservoir held between two polyacetal plates. A Nuclepore filtration membrane of the desired pore size is supported by a porous polyethylene disk at the bottom of the cell. Two pore sizes of filtration membranes, 0.15

and $0.05\mu\text{m}$, were used. A Teflon-coated stirring bar rotates close to the membrane surface to prevent clogging of the membrane by the latex particles and to give a steady flow rate over long periods of time. Water is fed from a reservoir into the top of the cell to replace the serum by flushing it out through the Nuclepore filtration membrane. A plastic tube, connected to the bottom of the funnel in the bottom plate, is connected to a suction pump to collect the filtrate. Pressure is applied to increase the filtration rate. In the serum replacement technique, the latices with 5% solid content were used in the purification process. The latices were washed with double-distilled water until the conductance of the filtrate was about the same as that of the feed water.

4.5.2.2 Ion-Exchange Resin

Ion-exchange resin treatment is another method for the purification of latex. When ion-exchange resin is used, the resin has to be purified first since the commercial ion-exchange resins contain leachable polyelectrolytes which could adsorb on the surface of the latex particles. The resin was washed with 3N NaOH, hot water, methanol, cold water, then 3N HCl, hot water, methanol and cold water in a five-fold excess amount by volume. This cycle was repeated 3-4 times until the final filtration water from the mixed resin showed no UV absorption at 224 nm. The cationic and anionic resins were rinsed copiously with double distilled water and mixed in a 1:1 ratio by weight under stirring. Once the resin was purified, the latices were cleaned for two hours by agitation with a five-fold excess of mixed resins, and then filtered on a Buchner funnel through a #1 Whatman filter paper to remove the resin.

Comparing the two techniques, the ion-exchange resin treatment is a more time-effective process for removing impurities present in the latex emulsion, especially in removing the adsorbed emulsifier on the surface of the latex particles, than the serum replacement technique. However, the ion-exchange resin treatment may introduce other impurities which are contained in the resin. In contrast to the ion-exchange resin treatment, the serum replacement technique is a time-consuming process, but it has the advantage of preventing the introduction of new contaminants (Ahmed, El-Aasser et al., 1980; Kamel, El-Aasser et al., 1981).

4.5.3 Characterization of Latices

The prepared latices were characterized by the microelectrophoretic mobility measurement and scanning electron microscope analysis. The contact angles were measured on the films made of latices to characterize their hydrophobicity.

4.5.3.1 Microelectrophoretic Mobility Measurements

The surface charge of latex particles was characterized by measuring the microelectrophoretic mobility. A Rank Brothers Mark II Particle Micro-Electrophoresis apparatus was used in the measurements. The apparatus consists of a transparent cell with electrodes for applying a electrical potential within the suspension, and a microscope for observing the resulting motion of the particles. The average electrophoretic mobility ($\mu\text{m}/\text{sec}/\text{volt}/\text{cm}$) is obtained by measuring the time taken for a number of individual particles to cover a given distance (as determined by a calibrated grid in the microscope

eyepiece) in a known potential gradient. The calculation for mobility is given in Appendix I. An average of at least 20 measurements was made in each test, and the mean and standard deviation of the electrophoretic mobilities of the particles were computed. Only the results showing a standard deviation from the mean of less than or equal to 0.30 ($\mu\text{m}/\text{sec}/\text{volt}/\text{cm}$) were accepted.

The measurements were conducted in a 10^{-3}N KNO_3 solution, varying pH.

4.5.3.2. Scanning Electron Microscope Analysis

The Scanning Electron Microscope (SEM) was used to examine the latex particles for the size, shape, porosity and fine surface structure. The samples for the SEM analysis were coated with a sputtered gold layer to provide a conductive path to reduce charging effects in the specimen.

A Hitachi S-2300 scanning electron microscope and an SEM with an image analysis system were utilized. In these observations, a fine beam of electrons of medium energy (5-50 keV) was caused to scan across the sample in a series of parallel tracks. These electrons interact with the sample, producing a secondary electron emission which can be detected and displayed on the screen of a cathode ray tube.

4.5.3.3 Contact Angle Measurement

Water contact angles were measured on films made of latices to characterize their hydrophobicity. Latex films were prepared by evenly spreading 10 ml of latex dispersion on a cleaned glass plate and then drying the films in an oven at 50°C for 4 hours. A sessile drop method was used. A fixed volume of water drop was gently placed on

the film, and the angle formed was measured with a Rame-Hart contact angle goniometer microscope. Each drop was measured on both sides and ten drops were made and measured on one latex film.

4.5.4 Characterization of Minerals Samples

The mineral samples were characterized by infrared spectroscopy, in addition to the chemical analysis, to determine any chemical functional groups contained on the surface of the mineral samples. The specific surface area of the mineral samples were determined and the charge on the electrokinetic surface in the aqueous solution vs. pH was measured.

4.5.4.1 Infrared Spectroscopy

Traditional transmission infrared spectroscopy in which KBr discs are utilized have recently been replaced by other methods. The method referred to as DRIFT (diffuse reflectance FTIR) is often used to characterize mineral samples. In this work, fluorite, apatite and calcite samples were characterized by infrared spectroscopy using a Bio-Rad Century Series Model FTS 175C with a Bio-Rad Diffuse Reflectance Accessory. The samples were kindly run by Mr. Roger Gervais of Bio-Rad Laboratories (Canada)Ltd. A total of 256 scans were co-added at a spectral resolution of 8 cm^{-1} . The DRIFT spectra of pure KBr powder was collected and used as a background. The fluorite samples were diluted with pure KBr to approximately 50% to obtain a reasonable spectrum. The sizes of the samples provided for the IR work were $\sim 38\mu\text{m}$; further grinding may be conducted

during the mixing with KBr. The samples were also analyzed without dilution for comparison purposes. The apatite sample was diluted with KBr to approximately 5% in apatite content. All diffuse reflectance spectra were recorded in Kubelka-Munk units.

4.5.4.2 Surface Area Measurements

Surface areas of mineral samples were estimated by a multipoint BET technique. A Quantasorb (Quantachrome Corporation) BET unit was employed. Nitrogen and helium were used as adsorbate and carrier gases, respectively. To obtain a multipoint BET isotherm, N₂ and He are mixed in various proportions, and the amount of adsorption and desorption of N₂ is measured at each ratio. Details can be found elsewhere (for operational details see Anonymous, 1970; for BET theory and applications in the determination of surface area see, for example, Hiemenz, 1977, and Leja, 1982).

4.5.4.3 Electrokinetic Measurements

Electrophoretic mobilities of mineral samples were determined with the Rank Brother Mark II Particle Micro-Electrophoresis apparatus. Finely ground, pure mineral samples in very dilute aqueous suspensions were subjected to electrophoresis. The mobilities were converted into zeta potentials by applying the Smoluchowski's equation (for detailed calculation, see Appendix I). The zeta potential values were plotted vs. pH.

4.5.5 Microflotation Tests

Microflotation using fluorite, apatite and calcite with sodium oleate as the collector,

was carried out in a Hallimond flotation tube, modified so that the vertical part of the bottom tube was longer than the original Hallimond tube. The effects of pH and conditioning time on flotation recovery were studied. The flotation of fine apatite in the presence of P(MAAA) latex and with sodium oleate in the presence of P(MAAA) was also examined. These tests were carried out to investigate the effect of latex on flotation of fine apatite.

The flotation procedure consisted of weighing a 1.5 g sample into a beaker and conditioning it for 5 minutes with 170 ml of aqueous solution of the collector of known concentration at a predetermined pH. The suspension was then transferred into the modified Hallimond tube and floated for 2 minutes. A nitrogen flow rate was maintained at a 150 ml/min to generate stable bubbles. The flotation pH shifted a little bit (about ± 0.3) from the initial value during the flotation and the pH at the end of the flotation was recorded to be the flotation pH. The flotation recovery was expressed as the percentage of mass of mineral floated to that of the total sample mass. In the experiment with P(MAAA) latex, 4 minutes of conditioning time was applied following addition of the latex.

4.5.6 Univariant Flocculation Tests

Flocculation was carried out in a 1L beaker in which four glass baffles had been glued on the beaker wall. A standard six-paddle stirrer (from Phipps & Bird, Richmond, VA) with speed control and paddle height adjustment was used to generate the agitation for the flocculation experiment. A sketch of the flocculation device with the dimensions indicated is shown in Figure 4.3.

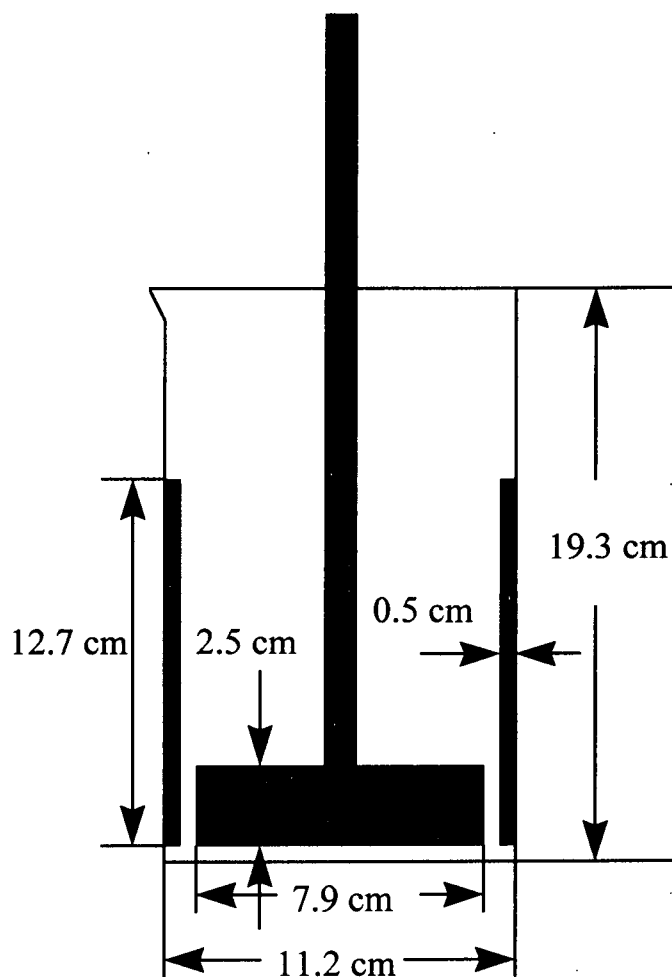


Figure 4.3 - A sketch of the flocculation device

Flocculation tests were first conducted with each single mineral to examine the response of flocculation to the latices at their natural pulp pH. Once 80% of flocculation recovery can be achieved, the effect of pH on the flocculation was examined. By comparison of the flocculation of fluorite, apatite and calcite with the latices, the P(MAAA) latex exhibited a higher flocculation on fluorite and apatite than calcite. Thus the P(MAAA) latex was selected to be tested in the selective flocculation of fluorite/calcite, fluorite/silica, apatite/calcite and apatite/silica systems.

An 18 g of mineral sample was mixed with a small portion of distilled water in a blender at high speed for two minutes, and then transferred to the 1 L beaker. Water was added to the beaker to the 900 ml mark to make a 2% solid content suspension. For experiments with a dispersant, the dispersant was mixed with the sample in the blender. The suspension was stirred at 350 rpm for two minutes, and then a known amount of latex was added to the suspension by a syringe at the point of greatest agitation; the stirring rate was maintained at 350 rpm for two minutes and then reduced to 150 rpm for another two minutes.

The flocs were separated from the suspension by sieving on a 53 μm screen. The flocs recovered by screening were dried in an oven at 100°C overnight. The flocs recovered on the screen are strong enough to withstand the hydrodynamic conditions. A blank test was also carried out and no flocs were collected on the screen.

Selective flocculation tests were conducted using 1:1 suspension of fluorite/silica, fluorite/calcite, apatite/silica, apatite/calcite. The effect of the P(MAAA) latex dosage on the apatite flocculation recovery and P_2O_5 grade, fluorite flocculation recovery and fluorine grade at their natural pulp pH was examined. It was observed that the selective flocculation was poor in terms of apatite or fluorite flocculation recovery and P_2O_5 or fluorine grade without a dispersant. Thus the effect of concentrations of dispersants on selective flocculation of these systems was examined.

The flocs recovered on the screen were dried, weighed and then analyzed for P_2O_5 or fluorine content. The fluorine content was analyzed by an ion-selective electrode; the P_2O_5 was analyzed by a method in which phosphorus is precipitated as ammonium phosphomolybdate. The detailed procedure of the analytical method can be seen by

referring to "Chemical Analysis in Extractive Metallurgy" (Young, 1971). Each experimental point was repeated at least once and only those data with the deviation of the flocculation recovery from the mean value within 5% were accepted.

4.5.7 Batch Flotation Tests

Flotation of phosphate ore was carried out in an Agitar flotation machine. Two size fractions, $-420+106\ \mu\text{m}$ and $-38\ \mu\text{m}$, were used in the flotation tests to compare the effect of P(MAAA) latex on flotation. A sample of 300 grams was conditioned in 1 liter of tap water in a 1-liter flotation cell at 1000 rpm for 5 minutes while adjusting pulp pH to the required value. After the depressant, collector and latex were added and conditioned for 5 minutes for each reagent, 200 ml of water were added to make a 20% pulp density. The pH slightly shifted from the required pH after adding the reagents and water. The adjustment of pH was made after all the reagents were added. The air came from the compressed air was controlled by a flow meter at a flow rate of 100 ml/min and the flotation was carried out for two minutes at this flow rate. The standard deviation of flotation recovery is within 5%.

4.5.8 Deposition of Latex Particles on Mineral Surfaces

Deposition studies were conducted in a rotating disc apparatus similar to that of Marshall and Kitchener (1965) (Figure 4.4). The apparatus consists of a constant-speed electric motor with a speed controller and a Teflon disc of 5 cm diameter with a recess 2.5

cm in diameter and 0.7 cm in depth in the base of the disc. The drive and shaft are built to avoid vibrations. The suspension (250ml) was contained in a dish 10.5 cm in diameter.

The deposition tests were carried out on smooth surfaces of fluorite, apatite, calcite and quartz. The pure mineral crystals of fluorite, apatite, calcite and quartz were obtained from the Department of Geology at UBC. They were carefully split along their cleavage planes into small pieces, then these small pieces were embedded in epoxy resin. The surfaces of the mineral-containing epoxy plates were ground on a wheel with emery paper of successively fine grades, followed by polishing on a polisher, using $0.03\mu\text{m}$ alumina. A smooth surface of calcite was difficult to obtain since calcite is relatively soft. Extra careful polishing was applied to the calcite sample. The samples were washed first with a hot mixture of water and alcohol and then with water alone to remove all the substrate used in the polishing process. The surface should be as smooth as possible to avoid deposition due to surface roughness. The mineral-containing plates were placed in the disc and spun in a latex suspension under set conditions which include latex concentration, suspension pH, and disc spinning time. The superficial density of the particles was determined by counting over 10 randomly selected disc areas (of about $5 \times 10^3 \mu\text{m}^2$) with an SEM associated with an image analysis system. Results were expressed by the number of particles N_d deposited per $1000 \mu\text{m}^2$ of the disc surface. The standard deviation of the counts of N_d was the deviation from the mean value taken from the 10 selected disc area. The standard deviation was within the order of 5%.

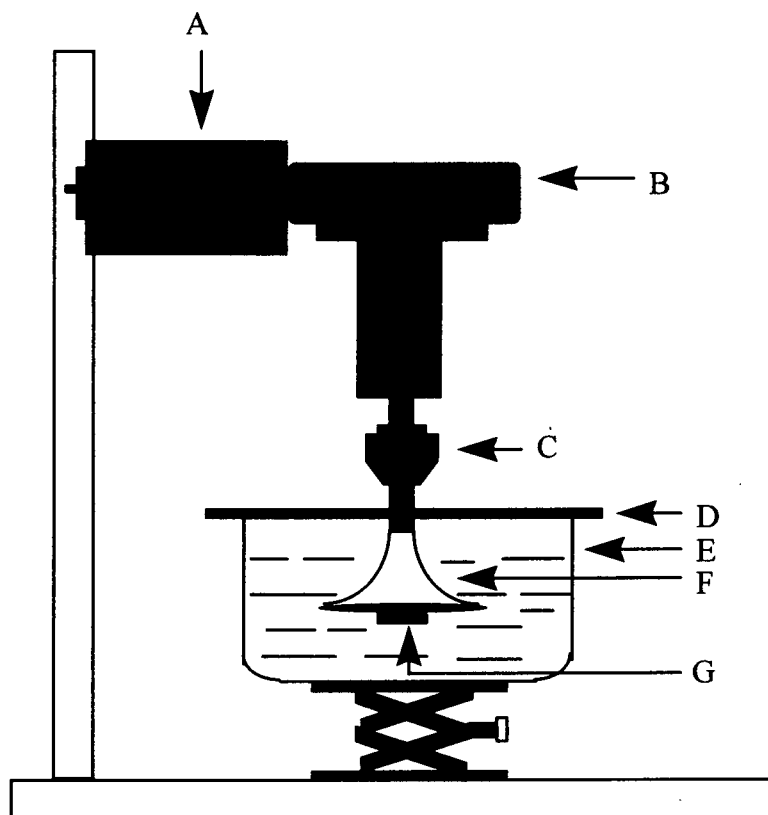


Figure 4.4 Diagram of the rotating disc apparatus. (A) constant speed motor with reduction gears; (B) roller bearing; (C) collect chuck; (D) cover; (E) glass dish containing the dispersion; (F) Teflon disc; (G) deposition surface.

4.5.9 2^3 Factorial Design Flocculation Experiments

In order to investigate the effects of interactions among the experimental factors used in the previous flocculation tests, to estimate the experimental errors and to examine the reliability of the experimental data, a two-levels and three-factor full factorial design was applied in the apatite/calcite and apatite/silica systems. The values of levels of factors were assigned based on the results of previous univariant flocculation tests which show the relative higher apatite flocculation recovery and P_2O_5 grade. Since the selective

flocculation of apatite/calcite mixture required a higher dosage of P(MAAA) latex than that of apatite/silica mixture, a higher dosage of P(MAAA) latex was assigned in the apatite/calcite system than in apatite/silica system. The experimental design is shown as follows:

Apatite : Calcite = 1 : 1 mixture

The three factors together with their factor-level ranges are

P(MAAA) Latex dosage, kg/t	X_1	2 - 3
pH	X_2	9.0 - 10.0
Sodium tripolyphosphate, mg/l	X_3	2 - 6

The extremes of these ranges were picked as the low- and high-factor levels. With three factors, an eight-run design was required. A decision was made to run three centerpoints to estimate the response error. The centerpoints (cp) of the factor levels X_1 through X_3 are

P(MAAA) Latex dosage, kg/t	2.5
pH	9.5
Sodium tripolyphosphate, mg/l	4

The design matrix is

	+	-	0
X_1	3.0	2.0	2.5
X_2	10.0	9.0	9.5
X_3	6	2	4

Apatite : silica = 1: 1 mixture

Three factors together with their factor-level ranges are

P(MAAA) latex dosage, kg/t	X_1	1.0 - 2.0
pH	X_2	8.8 - 10.0
Sodium silicate, mg/l	X_3	10 -30

The three centerpoints are

P(MAAA) latex dosage, kg/t	1.5
pH	9.4
Sodium silicate, mg/l	20

The design matrix is

	+	-	0
X_1	2.0	1.0	1.5
X_2	10.0	8.8	9.4
X_3	30	10	20

The overall design appears as follows:

<u>Run</u>	X_1	X_2	X_3
1	+	+	+
2	+	-	-
3	+	-	+
4	-	+	+
5	+	+	-
6	-	-	-
7	-	+	-
8	-	-	+
cp1	0	0	0
cp2	0	0	0
cp3	0	0	0

In order to prevent the systematic errors during the experiment, the eight factorial runs were randomized by drawing run numbers 1-8 from a container and running them in the order of the draw. The three centrepoints (cp1, cp2 and cp3) were run at the first, middle and last run of the designed experiment. The same flocculation device and experimental procedure as used in the previous univariant experiment were used for all runs of the tests.

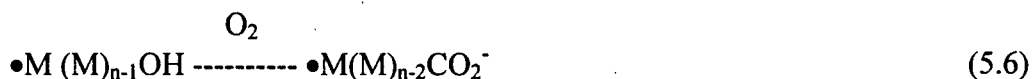
CHAPTER 5 RESULTS AND DISCUSSION

5.1 Latex Characterization

Polystyrene latices with different concentrations of emulsifier, poly(2-ethylhexylmethacrylate) and poly(methyl acrylate-acrylic acid) latices prepared by emulsion polymerization were opaque and white in color. The results of characterization of the latices by the electrophoretic mobility measurement, scanning electron microscope analysis and contact angle measurement are present and discussed below.

5.1.1 Electrophoretic Mobility

In order to help understand the type of the surface charge on the latex particles, the polymerization process in the absence of the emulsifier is illustrated in the following equations:



where M represents the monomer. The first step of the polymerization is the decomposition of the persulfate initiator under the heat condition to generate the sulfate free radical (5.1). The free radical then initiates the polymerization of the monomer (as shown in equation 5.2) followed by the chain growing (as shown in equation 5.3). The sulfate free radical could also react with the water molecule to generate the hydroxyl free radical which could initiate the monomer to produce the polymer chain with the hydroxyl endgroup (5.4, 5.5). This hydroxyl endgroup will undergo oxidation in the presence of oxygen and become carboxylic group (5.6). The polymer chain could be terminated by reacting with any free radicals in the system (5.7).

The mobility curve for PS5, which was prepared without potassium oleate, appears to be parallel to the pH axis over the region 7.5 to 11 as indicated in Figure 5.1(a). This suggests that ionization of the ionogenic surface groups is nearly complete around pH 8. An inflection point on the curve suggests that two types of acidic groups are present on the surface of the latex particles. The mobility behavior at the lower pH values indicates the presence of strong acidic groups, sulfate groups, which arise from the decomposition of the persulfate initiator. The mobility behavior at the higher pH values indicates the presence of carboxylic groups. It is well known that the presence of oxygen causes polymer oxidation during the polymerization process. Oxygen is assumed to have been present in the initial system since no attempt was made in the preparation of the polystyrene latex to displace it from the solutions by flushing with nitrogen, and oxygen could have been introduced by the decomposition of hydrogen peroxide resulting from the decomposition of potassium persulphate in an alkaline aqueous medium. Thus, the presence of carboxylic groups is likely caused by the oxidation of the polymer in an alkaline aqueous media.

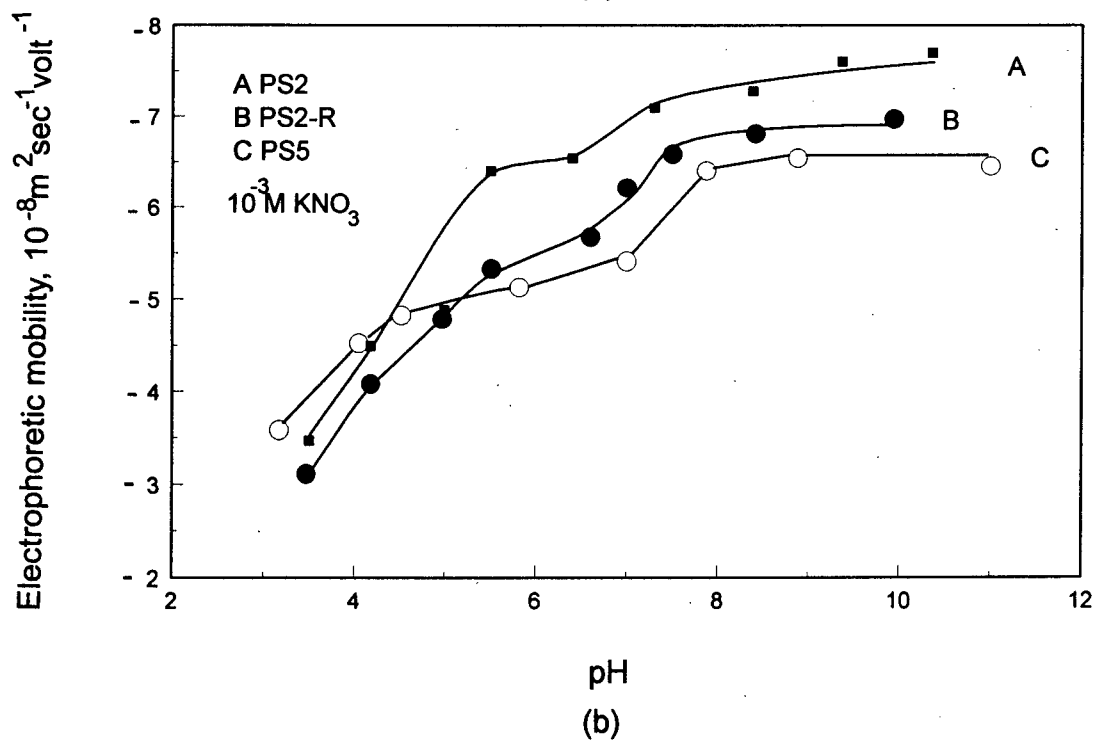
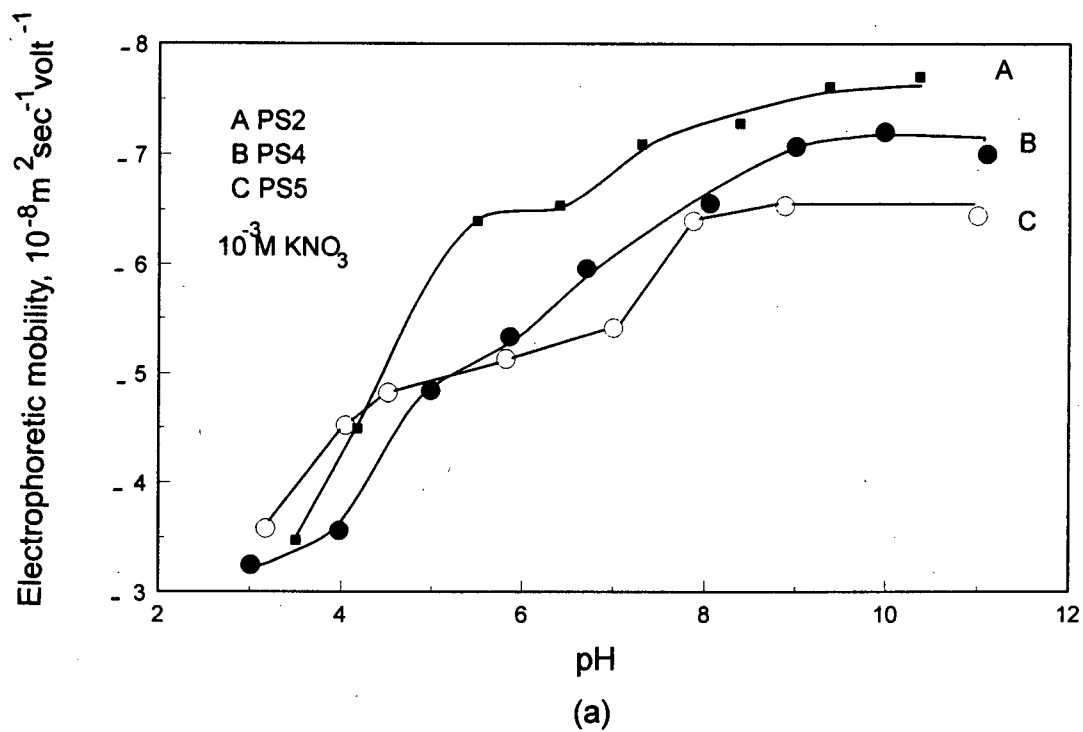


Figure 5.1 - Electrophoretic mobility of polystyrene latex particles

- (a) effect of emulsifier concentration on mobility of latex particles
 (b) effect of ion-exchange resin treatment on mobility of latex particles

Hence, a latex prepared in this way has a 'mixed-charge' surface. Both groups are considered to be an integral part of the latex particles.

The mobility of polystyrene latex prepared with potassium oleate as an emulsifier is higher than that of polystyrene latex prepared without potassium oleate, and it increases with the concentration of potassium oleate as indicated in curves in Figure 5.1(a). The inflection points on curves PS2 and PS4 are not so apparent in comparison with curve PS5. This can be explained by sulfate endgroups becoming buried inside the particle once the emulsifier has been adsorbed to the surface of the particle. In the lower pH range, below pH=5, the mobility of polystyrene latex without potassium oleate is higher than with potassium oleate because the mobility in the lower pH range is determined mainly by the presence of sulphate groups on the surface of the latex particles. The pH for complete ionization is higher (around 9) in the case of polystyrene latex emulsified with potassium oleate than without emulsifier (around 8) as shown in Figure 5.1a. The mobility of PS2R (after ion-exchange resin treatment) is lower than that of PS2 (no ion-exchange resin treatment) (Figure 5.1b). The lower electrokinetic potential clearly indicates the loss of surface groups owing to the desorption of the surfactant. This explains the inflection point on the curve PS2R and the similarity in shape to the curve for PS5.

To produce a stable P(EHMA) latex, a higher ratio of emulsifier to monomer was needed in contrast to PS latex. As a result, the mobility of P(EHMA) is much higher than the PS latex (Figure 5.2). The P(EHMA)-R latex is the P(EHMA) with the surface emulsifier completely removed. The mobility of the latex after treatment with ion-exchange resin is substantially decreased as a result of the loss of surface oleate. Electrophoretic mobility measurements were used to monitor the emulsifier removal until no further decrease in the mobility was observed. There is no apparent inflection point on

the electrophoretic mobility curve even after treatment with the ion-exchange resin. This may be explained by the fact that no chemically bound carboxyl group is present on latex particles since oxidation has been minimized by carrying out the polymerization under nitrogen.

The P(MAAA) latex was produced without emulsifier. The mobility curve as shown in Figure 5.3 indicates an apparent inflection point in a pH ranging from 5 to 7. This indicates two types of acidic groups: sulfate groups which arise from the decomposition of the persulphate initiator, and carboxylic groups which arise from one of the acrylic acid monomers. Both acidic groups are chemically bound to the surface of the latex particles.

5.1.2 Scanning Electron Microscope

The SEM micrograph (Figure 5.4) which shows that the polystyrene latex contains spherical and nonporous rigid particles of approximately equal size and indicates a good monodispersity. The variation of each particle size is less than 5% from the mean particle diameter and may be considered to be monodisperse. A slight coagulation is visible. The size of latex particles decreases with the increasing concentration of potassium oleate as given in Table 5.1. The P(EHMA) latex particles are spherical (Figure 5.5). The monodispersity is not as good as that of PS latex. The average particle size is about 0.65 μm . It should be pointed out that a lower voltage was used in scanning the P(EHMA) latex. As a result, the P(EHMA) latex particles look three dimensional on the SEM micrograph.

The surface structure and the shape of the P(MAAA) latex particles are quite different from the PS and P(EHMA) latex particles. The surfaces of the P(MAAA) latex particles are rougher than those of PS and P(EHMA) latices and show a hairy structure

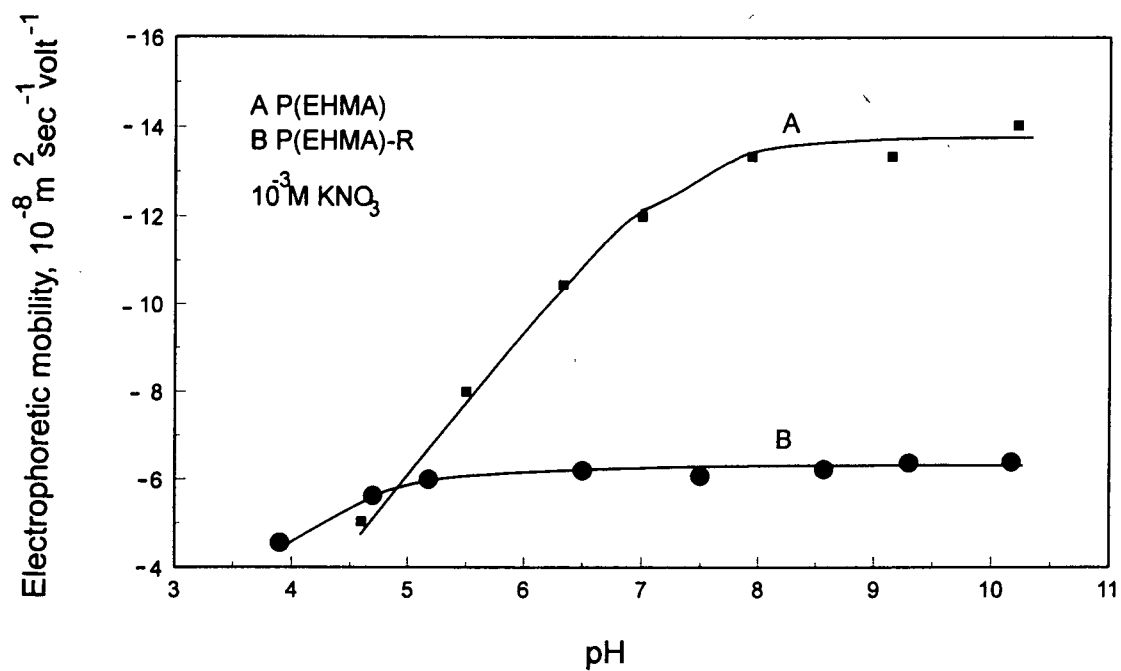


Figure 5.2 - Comparison of electrophoretic mobility of P(EHMA) and P(EHMA)-R latex particles

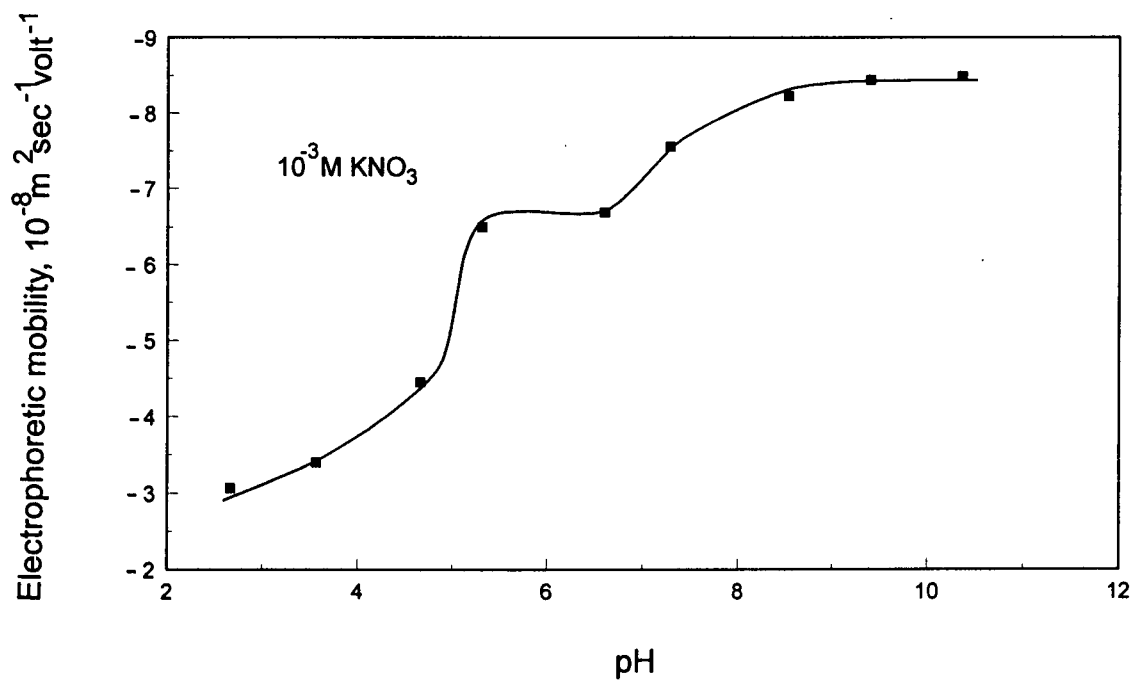


Figure 5.3 - Electrophoretic mobility of P(MAAA) latex

(Figure 5.6). The particles look loose and swollen. This may be attributed to the lower hydrophobicity of the latex in contrast to PS and P(EHMA) as shown by their contact angles which will be discussed in the following section. The average size of the latex particles is about 0.70 μm .

Table 5.1 Effect of Emulsifier Concentration on the Size of Polystyrene Latex Particles

Polystyrene Latices	K Oleate, mol/l	Particle Diameter, μm
PS1	17.8×10^{-3}	0.04 ± 0.003
PS2	14.9×10^{-3}	0.08 ± 0.005
PS3	7.43×10^{-3}	0.09 ± 0.004
PS4	3.56×10^{-3}	0.13 ± 0.006
PS5	0	0.14 ± 0.006

5.1.3 Contact Angle Measurements

The results of contact angle measurements for the PS, P(EHMA), P(EHMA)-R and P(MAAA) latices are given in Table 5.2.

The contact angle values indicate that polystyrene is the most hydrophobic while P(MAAA) is the least hydrophobic among the latices. The latex with the potassium oleate emulsifier seems to be more hydrophobic than the same latex from which the emulsifier had been removed.

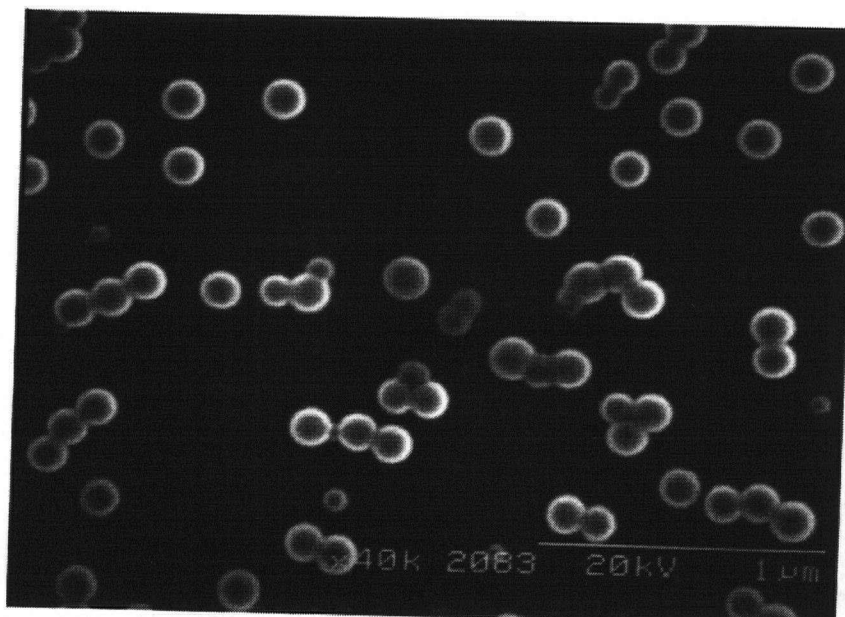


Figure 5.4 - SEM micrograph of PS latex (PS4)

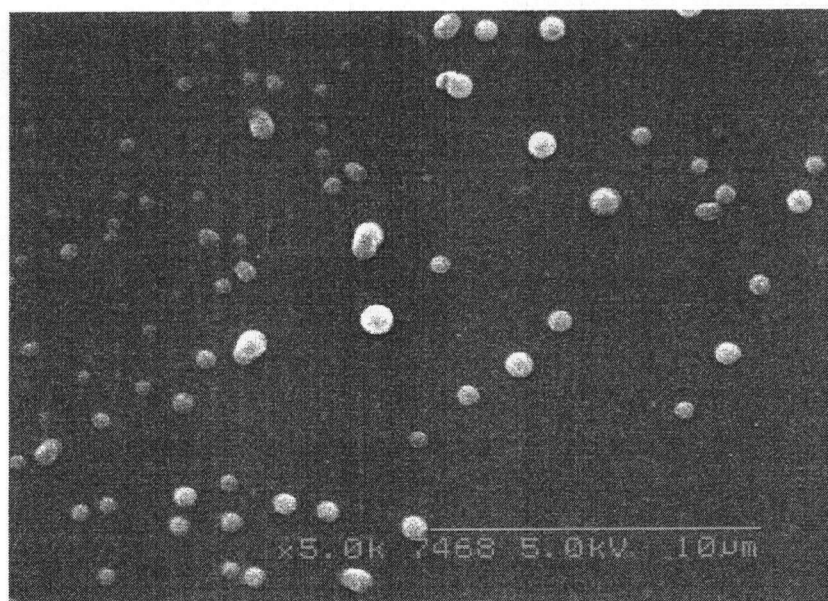


Figure 5.5 - SEM micrograph of P(EHMA) latex

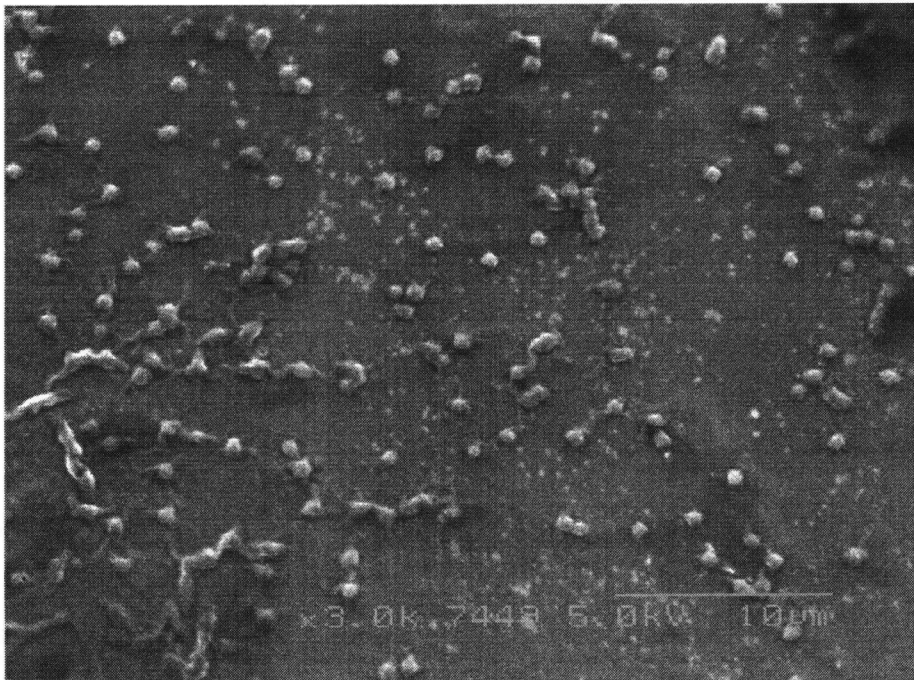


Figure 5.6 - SEM micrograph of P(MAAA) latex

Table 5.2 Water Sessile Drop Contact Angles on the Latex Films

Latices	Contact Angle, °
PS	84±4
P(EHMA)	65±3
P(EHMA)-R	58±3
P(MAAA)	38±4

5.2. Characterization of Mineral Samples

The results of characterization of the mineral samples by the FTIR, specific surface area measurement and electrokinetic measurement are presented and discussed as follows.

5.2.1 FTIR Spectroscopy

The mineral samples were characterized by IR spectroscopy. Diffus reflectance FT-IR spectra were collected on four fluorite samples which were prepared in different ways. Fluorite A was prepared by wet grinding and wet screening to obtain particle size 100% below 38 μm ; fluorite B was purchased at a different time, and it was prepared by dry grinding and wet screening to separate a -38 μm fraction; fluorite C was from the same batch as of fluorite B but was prepared by hand grinding in an agate mortar without contacting with water; fluorite D was a fraction of fluorite B but was exposed in water for a longer time.

The DRIFT spectra on fluorite A, fluorite B and fluorite D all show absorption

bands at 1645, 1516, 1435 and 887 cm^{-1} (Figure 5.7). In addition, fluorite A has a doublet at 1068 and 1102 cm^{-1} . Fluorite C spectrum reveals only bands at 1460 cm^{-1} and 887 cm^{-1} as shown in Figure 5.7. These bands are assigned to surface carbonates that were formed either with dissolved carbon dioxide while wet grinding or wet screening, or with atmospheric carbon dioxide during air-drying, or both. Comparing fluorite B and fluorite D, indicates that fluorite D, which was exposed to water for a longer time, had a higher surface carbonate content than fluorite B (see higher peaks at 1435 cm^{-1} and 1516 cm^{-1}). Fluorite C was not in contact with water during the sample preparation, and the DRIFT spectrum shows only a single peak at 1460 cm^{-1} . The calcium carbonate is characterized by a strong absorption peak around 1435 cm^{-1} and a medium-intensity peak around 887 cm^{-1} . The peak heights on the spectra for the four fluorite samples were distinguishable when the spectra were collected on fluorite without dilution with potassium bromide (KBr) (Figure 5.7). The comparison of spectra for these samples shows that fluorite D has higher surface carbonation than fluorite B and fluorite A. Fluorite A has the lowest surface carbonation. When the IR samples were diluted with KBr to 50%, the peak intensity decreased and the peak heights of the surface carbonate for the four fluorite samples became similar (Figure 5.8). However, the spectra collected on the diluted fluorite samples show better resolution, especially in the wavenumber below 800 cm^{-1} . Except for surface carbonate impurity, no other bands can be seen in the spectrum, indicating the sample is very pure. Fluorite A was used in the flocculation tests.

The DRIFT spectra collected for apatite (Figure 5.9) show absorption bands at 3540 and 1000 cm^{-1} which correspond to the isolated hydroxyl group and Si-O bond. These very strong peaks are characteristic of silicate materials but have been shifted to a lower wavenumber as has been suggested by Grim (1968). The peaks at 1050, 1100, 580, 600

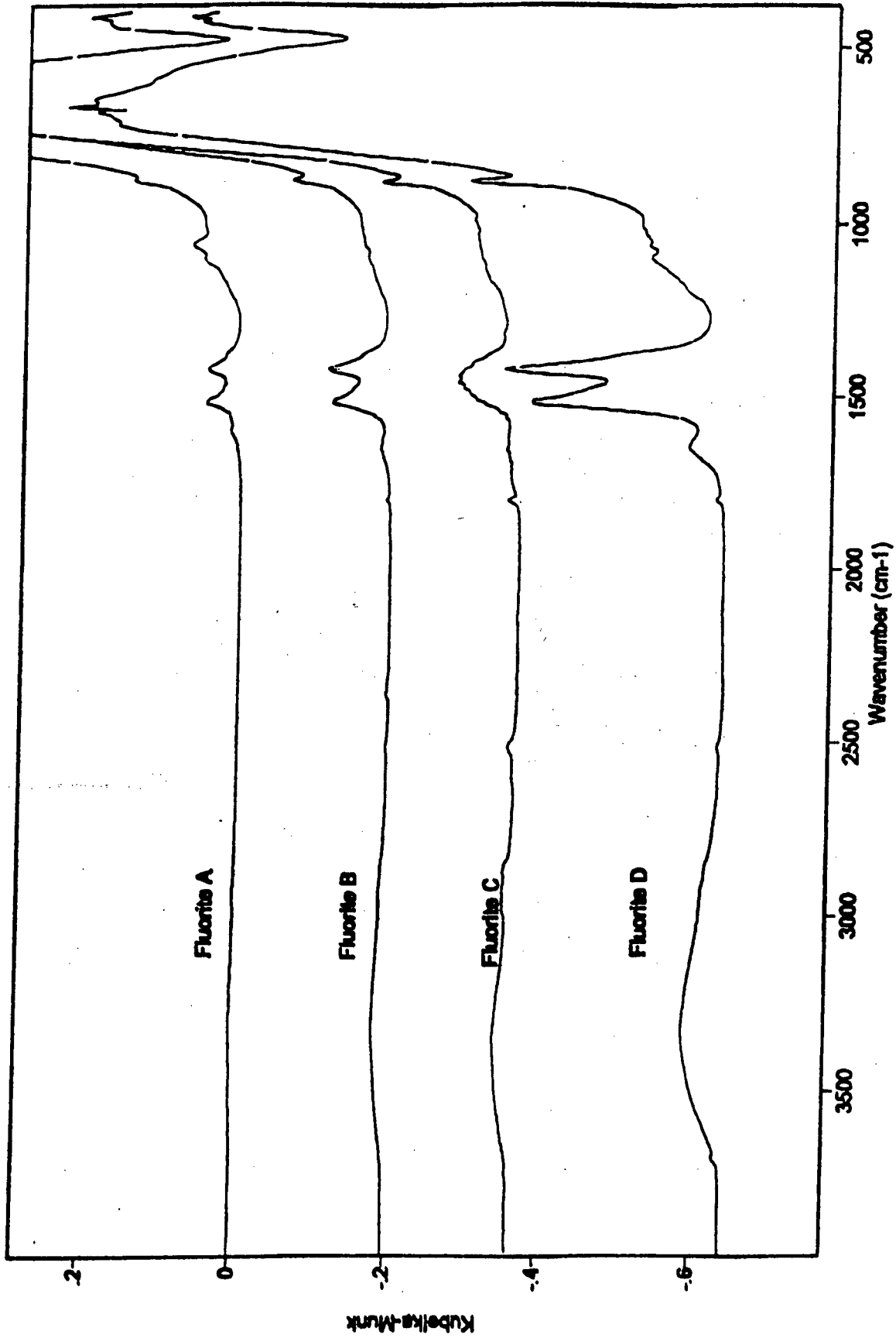


Figure 5.7 - Diffuse reflectance FTIR spectra of the fluorite sample (sample without mixing with KBr)

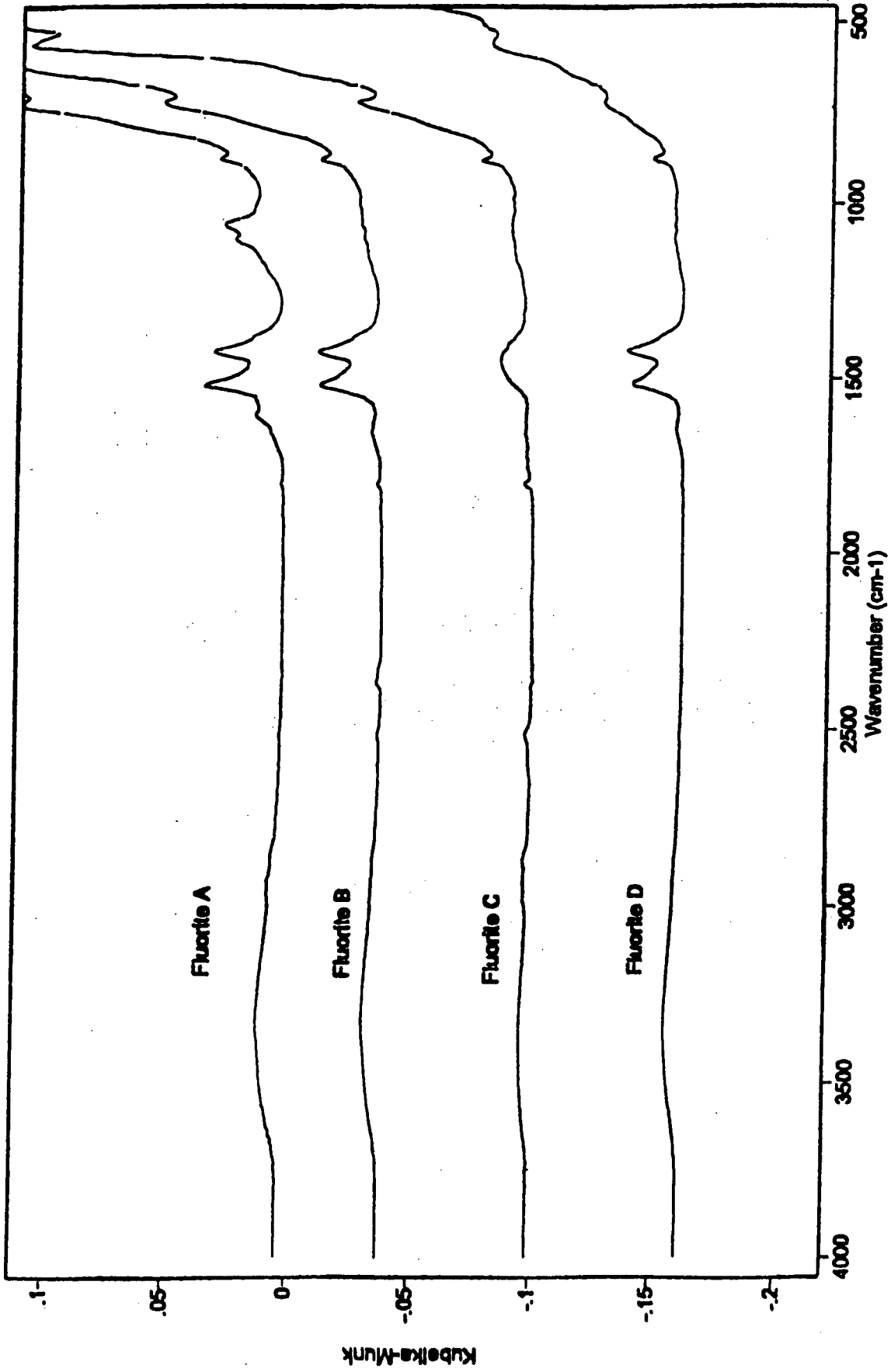


Figure 5.8 - Diffuse reflectance FTIR spectra of fluorite (sample mixed with 50% of KBr)

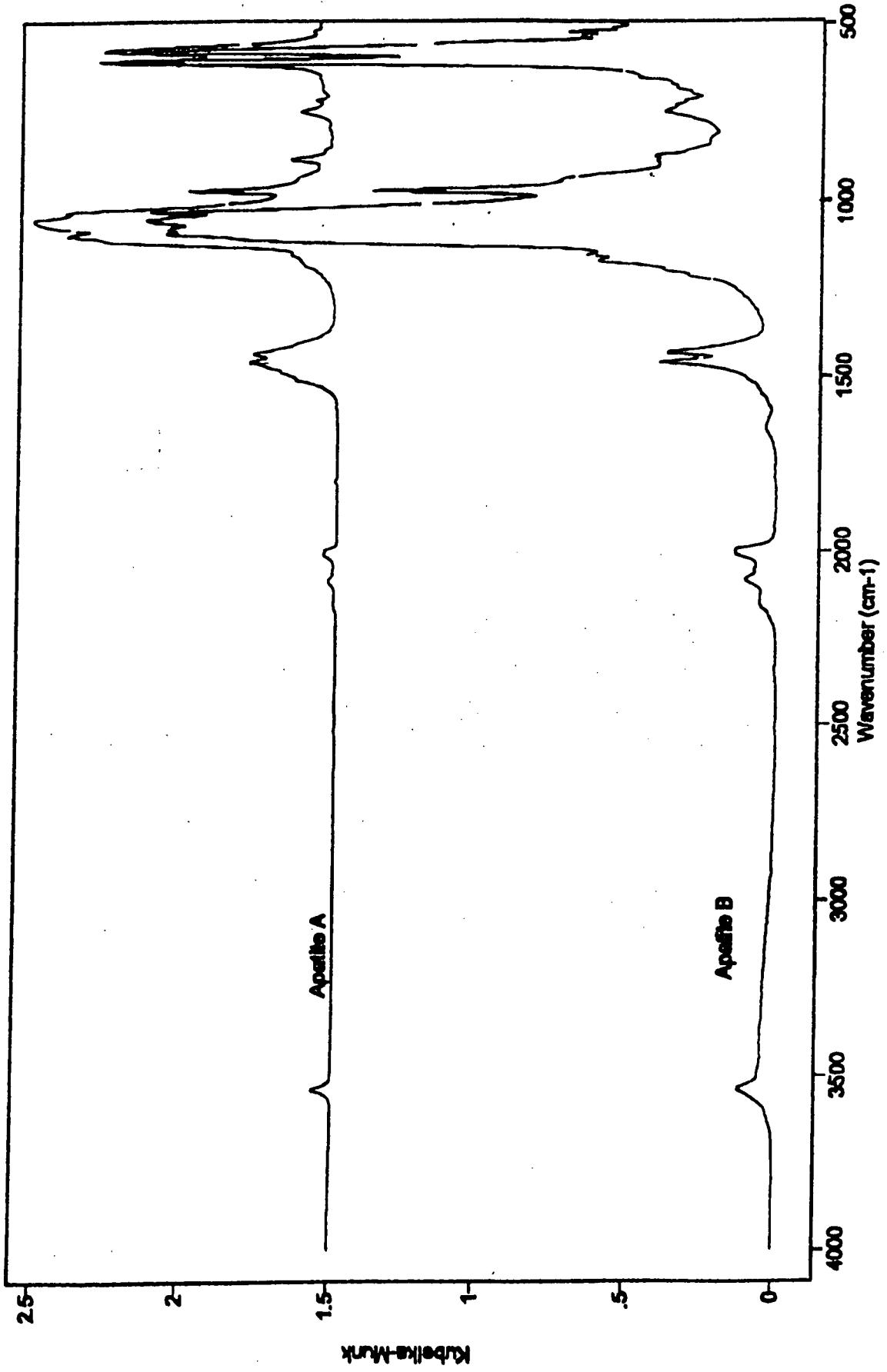


Figure 5.9 - Diffuse reflectance FTIR spectra of apatite (sample mixed with 50% of KBr)

cm^{-1} are P-O fundamental vibrations. The peaks at 1460, 1427 and 871cm^{-1} are assigned to surface carbonates. Apparently the apatite samples contain carbonated and silicates impurities. Apatite B seemed to have a higher content of silicates than apatite A as reflected in the higher peak at 1000cm^{-1} . Apatite A and apatite B were purchased separately, but both were wet ground and wet screened to obtain 100% $-38\ \mu\text{m}$. Apatite A was used in the flocculation test.

The DRIFT spectrum (Figure 5.10) of calcite shows typical carbonate peaks at 1461, 1433 and 876cm^{-1} . Since calcite was used as a gangue mineral in the selective flocculation, a detailed examination of the other peaks was not attempted.

5.2.2 Surface Area Measurements

The specific surface area of the apatite, fluorite, calcite and silica samples used in the selective flocculation tests are given in Table 5.3. The specific surface areas of the four samples were quite different despite similar size range ($-38\ \mu\text{m}$). The high specific surface area of apatite indicates that this mineral is porous.

Table 5.3 BET Surface Area Determination

Mineral	Specific Surface Area, m^2/g
Apatite	18.34
Fluorite	0.28
Calcite	3.13
Silica	0.90

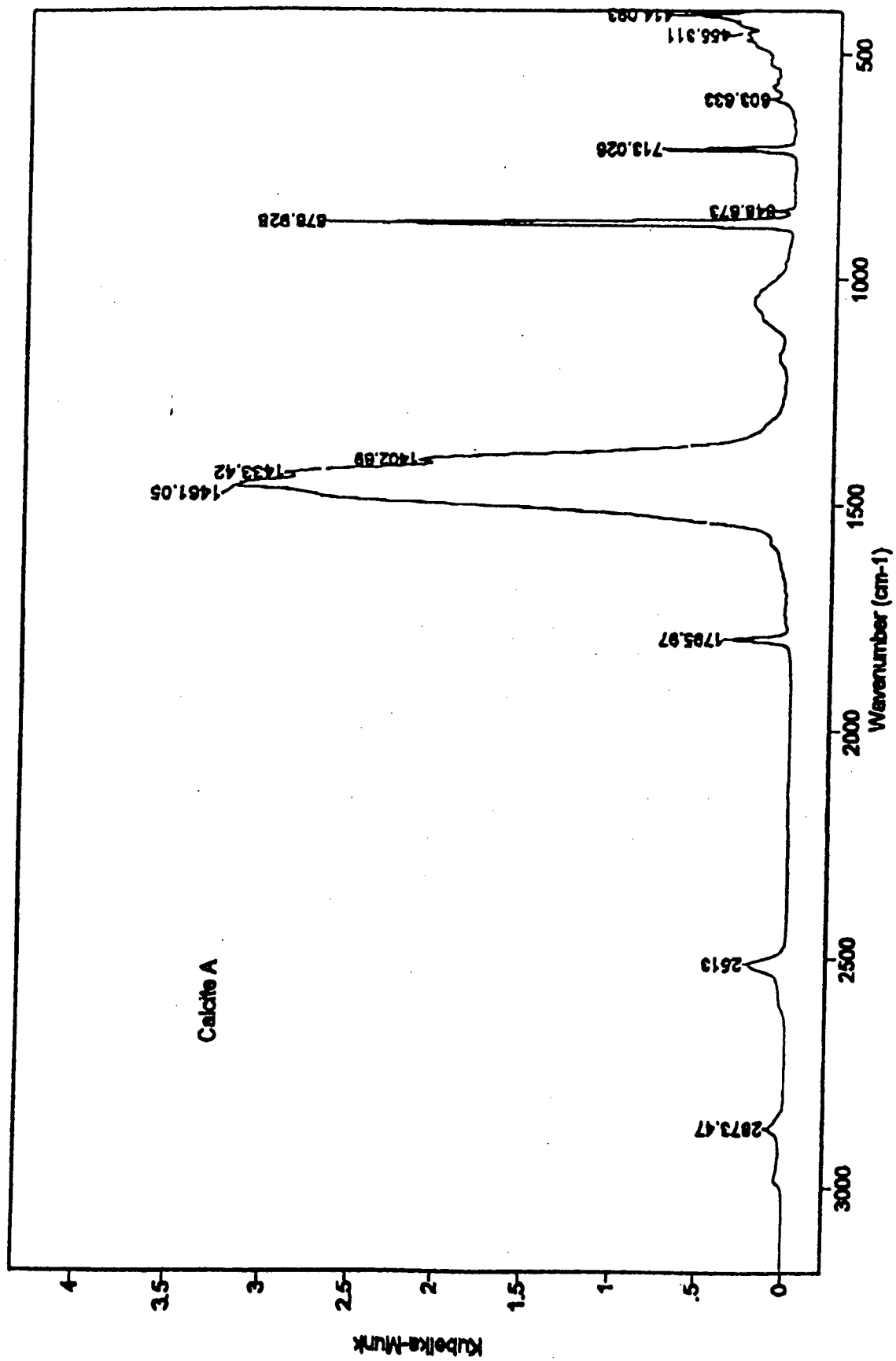


Figure 5.10 - Diffuse reflectance FTIR spectra of calcite (sample mixed with 50% of KBr)

5.2.3 Electrokinetic Measurements

The zeta potential of fluorite, apatite, calcite and silica as a function of pH is shown in Figure 5.11. As this figure indicates, fluorite has an isoelectric point around 6 while apatite has an isoelectric point around 5 which is in close agreement with those reported earlier (iep varies from 6 to 9 for fluorite and 4 to 5 for apatite) (Somasundaran, 1968; Smani et al., 1975; Mishra, 1982). Calcite and silica were characterized by negative values of zeta potential over the entire tested pH range. The dissolution of calcite was observed when pH was decreased below 5.5.

It is known that in the case of sparingly soluble minerals, dissolved species have a marked effect on the electrokinetic properties of these minerals. Amankonah and Somasundaran (1985) reported a shift of the apatite zeta potential to that of calcite when apatite was contacted with calcite supernatant. This phenomenon was also observed in this study as shown in Figure 5.12. The zeta potential - pH curve for apatite in the supernatant of calcite almost overlaps the zeta potential of calcite and is not that different from the zeta potential of calcite in the supernatant of apatite. These results also indicate that, in the pH range of 9-10, apatite and calcite should be fairly easy to disperse since their negative zeta potentials exceed 20×10^{-3} V. Therefore, the primary requirement of selective flocculation that all the constituents be in a dispersed state seems to be satisfied in a pH range of 9 -10.

5.3 Single Mineral Flocculation with Latices

5.3.1 Effect of P(EHMA) and PS Latex Dosages

PS2 and PS4 polystyrene latices were tested in the flocculation of fluorite at the

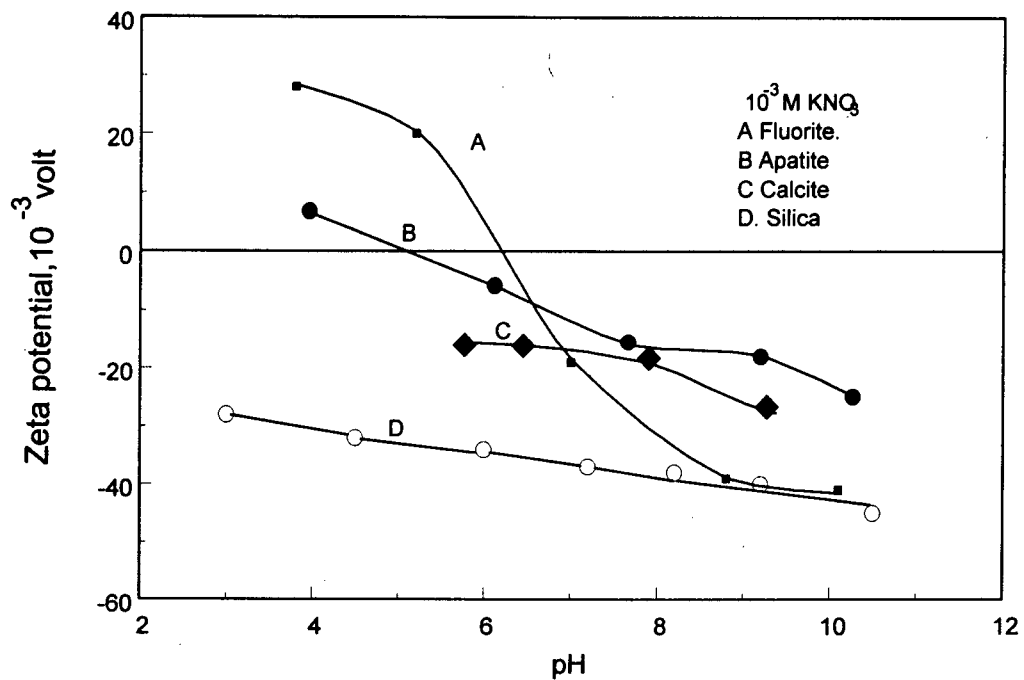


Figure 5.11- Zeta potential of fluorite, apatite, calcite and silica as function of pH

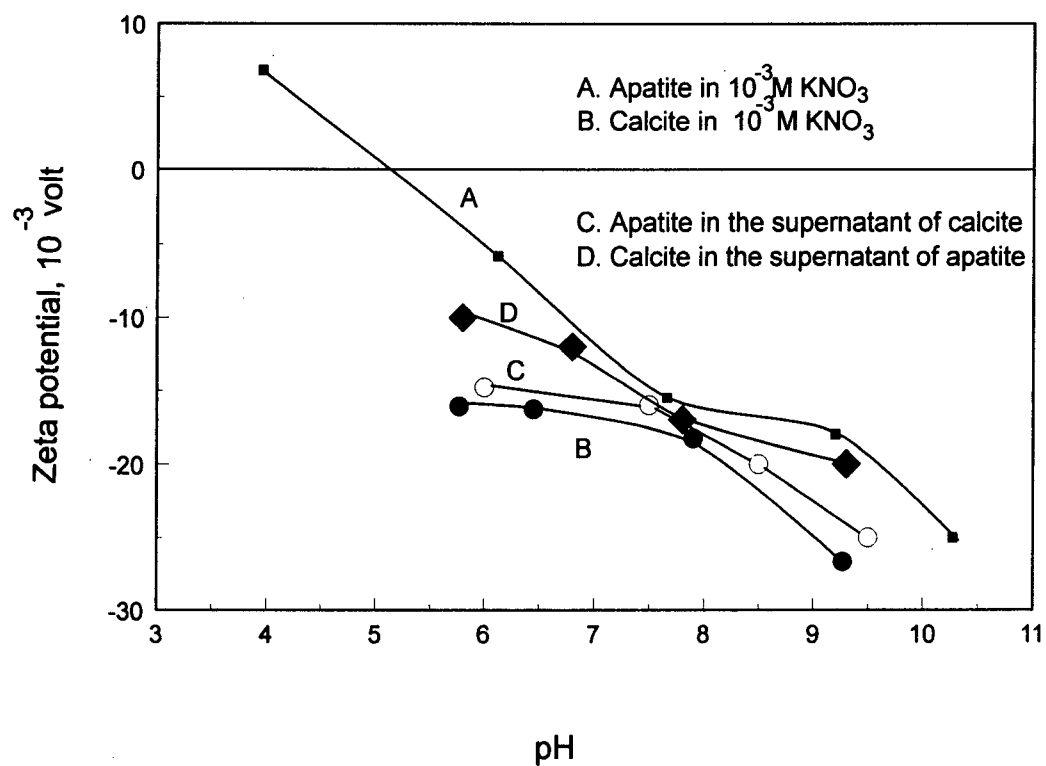


Figure 5.12 -Effect of calcite supernatant on the zeta potential of apatite and apatite supernatant on the zeta potential of calcite

natural pulp pH . The results, shown in Figure 5.13, demonstrate that the latex prepared with a higher concentration of oleic acid produces a higher flocculation recovery. The flocculation reached a plateau at 75% recovery with a dosage of 1kg/t of PS2 and 70% recovery with a dosage of 1.5 kg/t of PS4. This phenomenon was also observed when testing flocculation with P(EHMA) latex. Figure 5.14 shows that a dosage of about 0.3 kg/t of P(EHMA) latex can produce 90% of fluorite flocculation recovery while a dosage of 1 kg/t of P(EHMA)-R latex is required to achieve the same degree of flocculation recovery. Comparing the flocculation of fluorite with PS and P(EHMA) latices, shown that flocculation with PS reaches a plateau at 75% recovery with a dosage of 1kg/t while with P(EHMA) a plateau of 90% recovery can be obtained with a dosage of 0.3 kg/t. This is attributed to a higher content of carboxylic groups on the surfaces of P(EHMA) latex particles in comparison to PS latex particles. A higher content of carboxylic groups on the surfaces of latex particles provides more reactive sites. The chemical interaction seems to dominate the process of adsorption/attachment of the latex particles onto the mineral surfaces. In addition, the soft characteristics of P(EHMA) latex apparently facilitates the adhesion of these particles to the mineral surfaces.

Flocculation of apatite and calcite with P(EHMA) and P(EHMA)-R was also tested at their natural pulp pH, and the results are shown in Figures 5.15 and 5.16. The results reveal that 90% of apatite flocculation recovery can be obtained at a dosage of 0.8 kg/t of P(EHMA) while the same flocculation recovery needs about 1.6 kg/t of P(EHMA)-R. Flocculation with P(EHMA)-R is due to the interaction between sulfate groups on the surface of the latex particles and the calcium sites on the mineral surfaces. In the case of calcite, a dosage as high as 1.6 kg/t of P(EHMA) is required to produce 60% flocculation

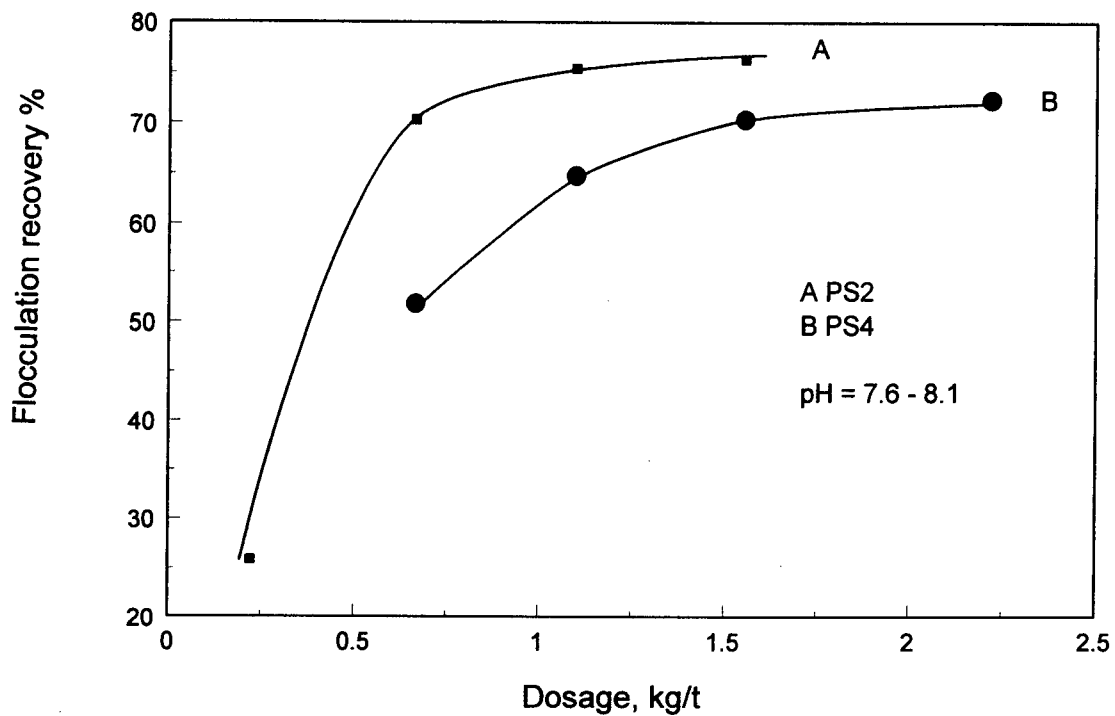


Figure 5.13 - Effect of PS dosage on flocculation of fluorite

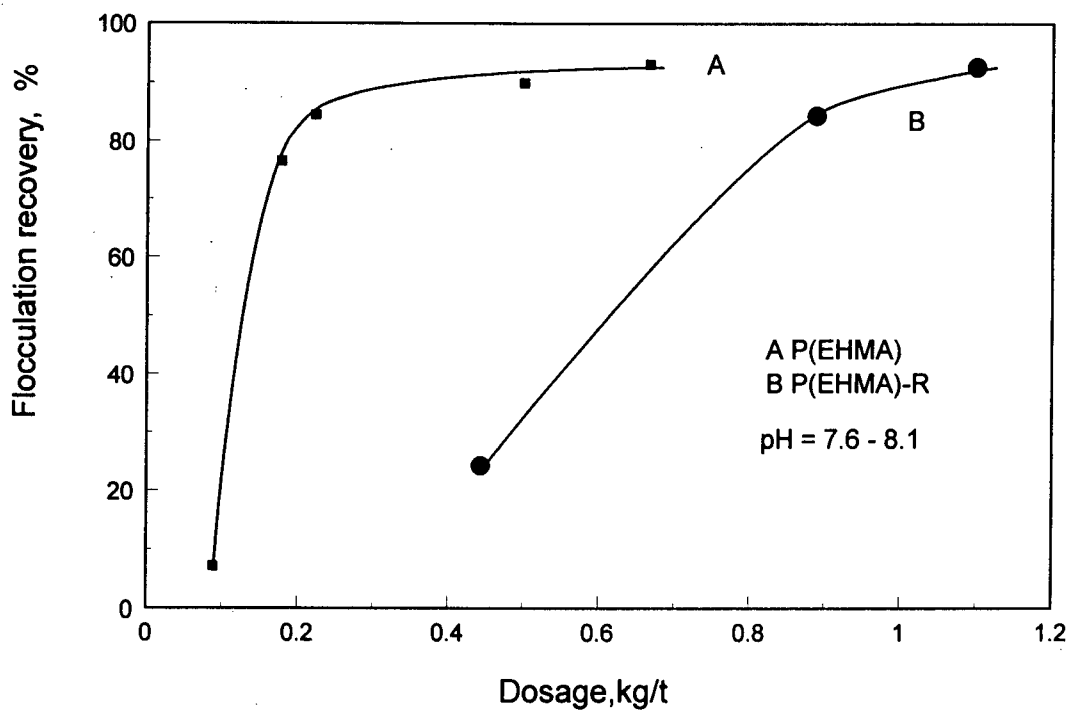


Figure 5.14 - Effect of P(EHMA) dosage on flocculation of fluorite

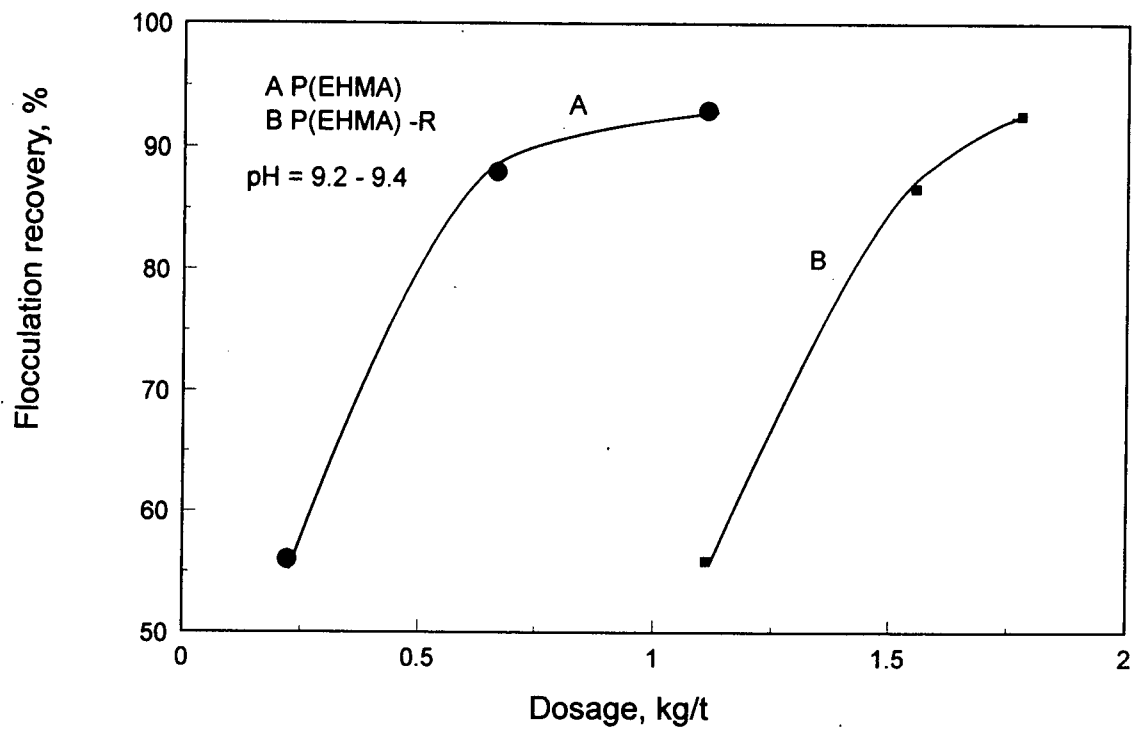


Figure 5.15 - Effect of P(EHMA) dosage on flocculation of apatite

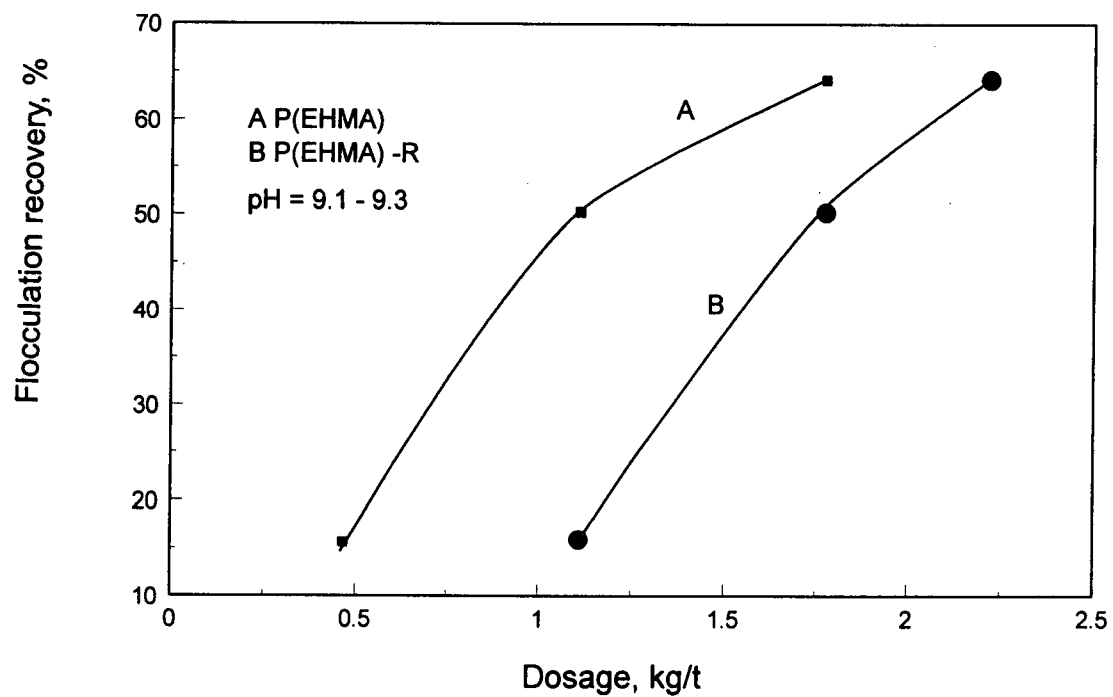


Figure 5.16 - Effect of P(EHMA) dosage on flocculation of calcite

recovery and with P(EHMA)-R even higher dosages are needed to flocculate similar amounts. The curves show an increase flocculation tendency with increasing latex dosage, and a plateau is not reached within the tested range.

5.3.2 Effect of pH on Flocculation Using P(EHMA) Latex

The effect of pH on the flocculation of fluorite, apatite and calcite with P(EHMA) and P(EHMA)-R latices is shown in Figures 5.17, 5.18 and 5.19. pH was varied from around 4 to 11 while the values of latex dosage for P(EHMA) and P(EHMA)-R were chosen based on the results from the tests on the effect of the latex dosages on the flocculation and held constant. The dosages for P(EHMA) and P(EHMA)-R were chosen to enable the flocculation response to pH would have a maximum around 80% and the response for the two latices can be distinguished.

Patterns of fluorite flocculation with P(EHMA) and P(EHMA)-R versus pH are similar, but again, a higher dosage of P(EHMA)-R is needed to obtain a similar flocculation recovery (Figure 5.17). The curves show a decreasing tendency of flocculation from 70% to 63% with increased pH from 4 to 6, and a minimum at around pH 6. This indicates that flocculation below pH 6 is mainly due to an electrostatic interaction between the negatively charged latex and the positively charged fluorite particles (fluorite's iep is situated around pH 6). The chemical interaction between the latex surface carboxylic groups and the calcium sites on fluorite surfaces also takes place in the acidic range. Improved flocculation above pH 6 and a maximum of flocculation of 82% around pH 7 suggests that chemical interaction is likely dominant over the electrostatic repulsive force in this pH range. A small drop from 82% to 72% of flocculation between pH 7 and 8.2 is

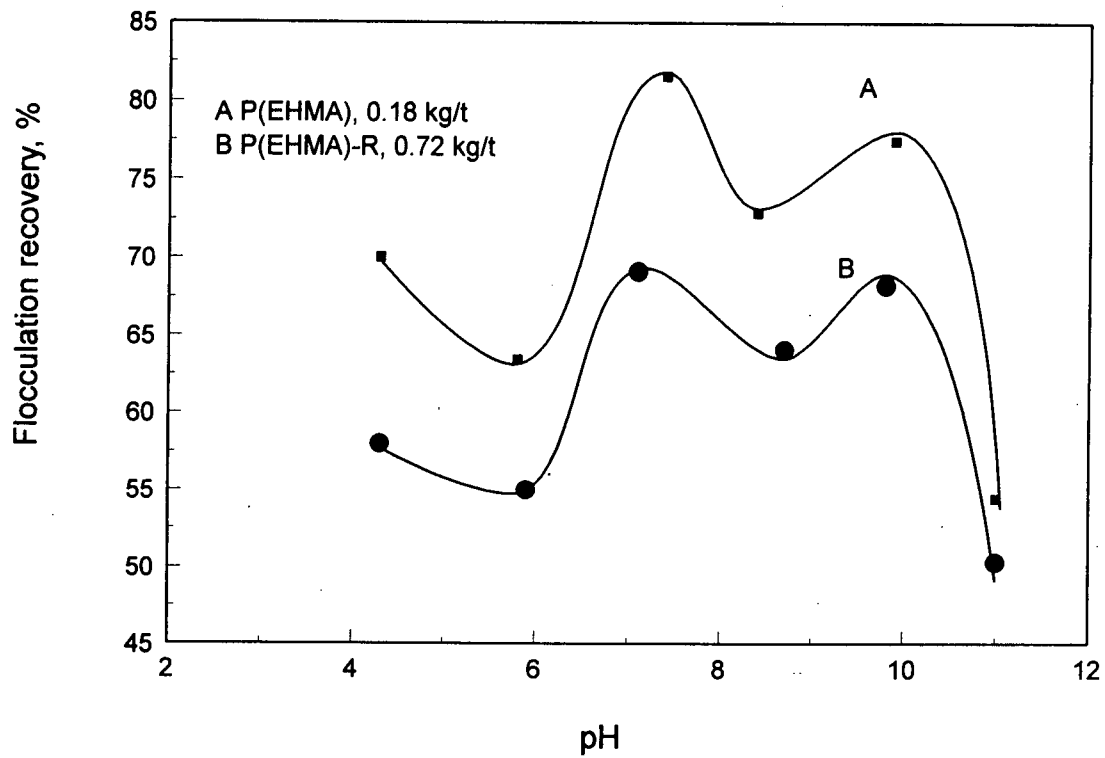


Figure 5.17 - Effect of pH on flocculation of fluorite with P(EHMA) latices

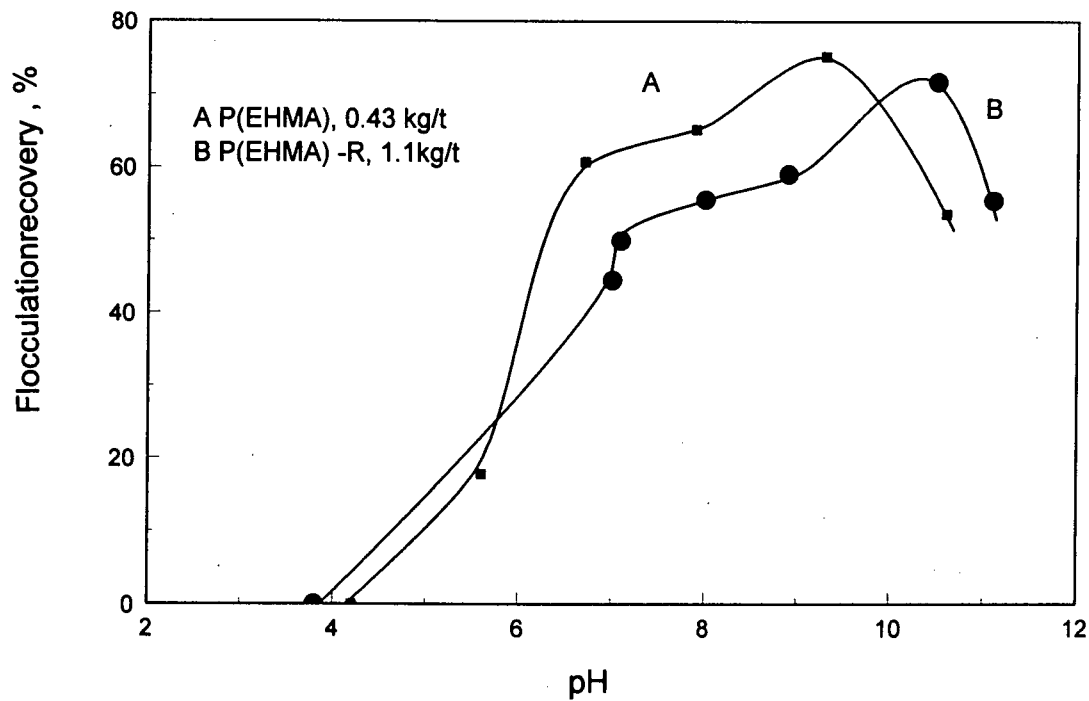


Figure 5.18 - Effect of pH on flocculation of apatite with P(EHMA) latices

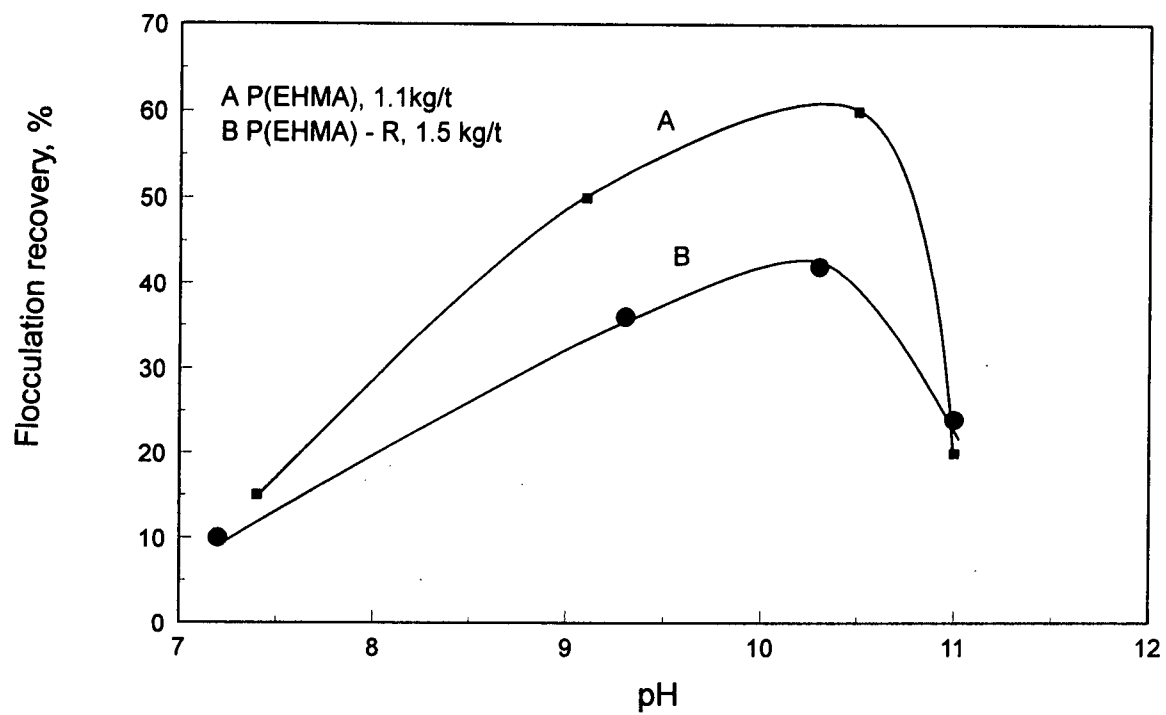


Figure 5.19 - Effect of pH on flocculation of calcite with P(EHMA) latices

attributed to an increased electrostatic repulsion force between latices and fluorite with both substances becoming more negative as pH increased. Flocculation increased a little bit (from 72% to 78%) as pH was further raised since the latex P(EHMA) is completely ionized at pH around 8.5 (Figure 5.2) and resulted in a strong chemical interaction. The strong chemical interaction seems dominant over the electrostatic repulsion over the pH ranging from 8.5 to 10. The sharp decrease in flocculation after pH 10 is again attributed to the strong electrostatic repulsion forces between the latex and fluorite. In the case of the flocculation of apatite with P(EHMA), the flocculation maximum of 75% at the given latex dosage shifted to pH around 9 for P(EHMA) and pH around 10 for P(EHMA)-R (Figure 5.18) in contrast to the case of fluorite which had two maxima around pH 7 and 9.5. The flocculation increased with pH which indicates that the flocculation was mainly due to the chemical interaction between carboxylic groups on surfaces of latex particles and calcium sites on apatite surface.

In contrast to the flocculation of apatite and fluorite, the flocculation of calcite needs a much higher dose of the latex. The flocculation maximum of 60% at the given latex dosage occurs around pH 10.2 (Figure 5.19). In order to analyze the possibility of separation of fluorite and apatite from calcite by selective flocculation, the flocculation of fluorite, apatite and calcite with P(EHMA) is compared in Figures 5.20, 5.21. Separation of fluorite from calcite seems possible with a P(EHMA) dosage of about 0.25 kg/t and pH around 7; under such conditions, calcite does not flocculate (flocculation recovery is zero) while fluorite flocculates very well. However, separation of apatite from calcite is more difficult. At a P(EHMA) dosage of 0.7 kg/t and pH around 9.2, 85% of apatite and 30% of calcite flocculate. Increasing the latex dosage higher than 1.1 kg/t would not increase the flocculation of apatite but would increase the flocculation of calcite. The flocculation

maxima for apatite and calcite falls in the same pH range from 9 to 10. The flocculation of fluorite, apatite and calcite with P(EHMA)-R is compared in Figures 5.22 and 5.23. It is similar to the case of P(EHMA) that the separation of fluorite from calcite is possible at a dosage of 1.1 kg/t and pH around 7. However, separation of apatite from calcite seems more difficult.

5.3.3 Single Mineral Flocculation with the P(MAAA) Latex

The flocculations of fluorite, apatite and calcite using P(MAAA) latex are shown in Figures 5.24 and 5.25. Selective separation of fluorite and apatite from calcite by using P(MAAA) seems to be possible because the degree of calcite flocculation with the P(MAAA) latex is very low over the range tested. The maximum flocculation of calcite is about 10% while apatite flocculation shows an increasing tendency with the P(MAAA) dosage.

The effect of surface carbonate on flocculation with P(MAAA) is also shown in the case of fluorite. The fluorite sample which has the lowest surface carbonate content requires a smaller amount of P(MAAA) latex to produce flocculation. It was observed that 5 ml of 0.4% P(MAAA) can produce 94% of flocculation on fluorite A, 80% of flocculation on fluorite B and none on fluorite D. Flocculation of fluorite with P(MAAA) is similar to that with P(EHMA), but the second maximum was not observed. Flocculation of apatite and calcite with P(MAAA) is different from that with P(EHMA), especially in the acidic pH range. In the case of apatite, flocculation is high around pH 4, decreases with increasing pH until a minimum at around 8.5 is reached, then substantially increases until a

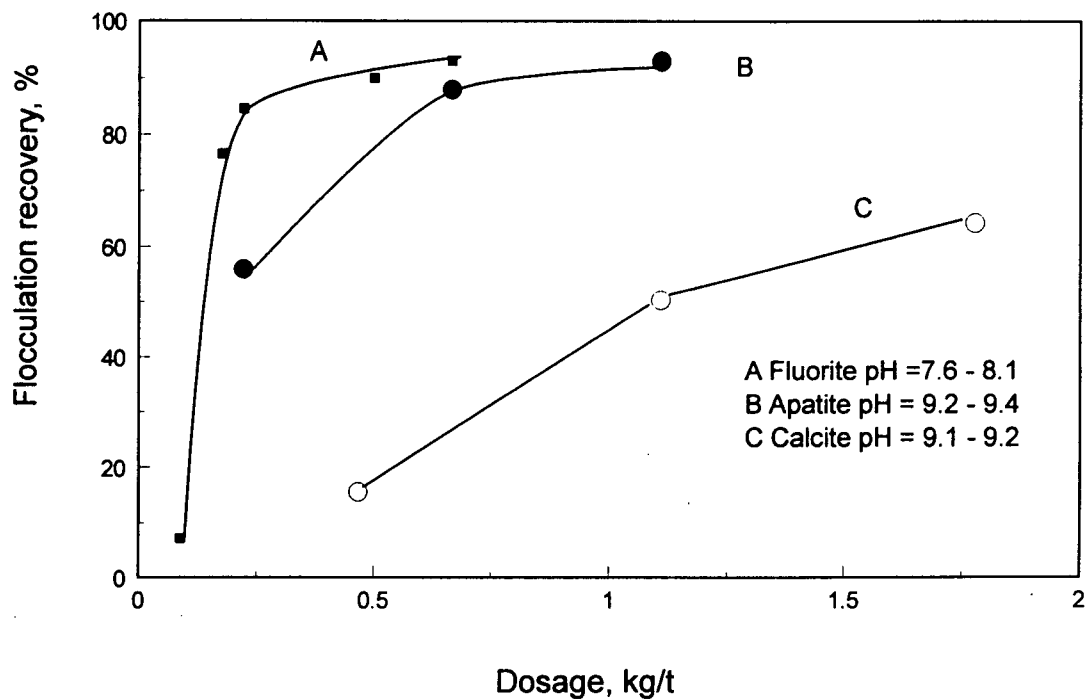


Figure 5.20 - Effect of P(EHMA) latex dosage on flocculation of fluorite, apatite and calcite at their natural pH

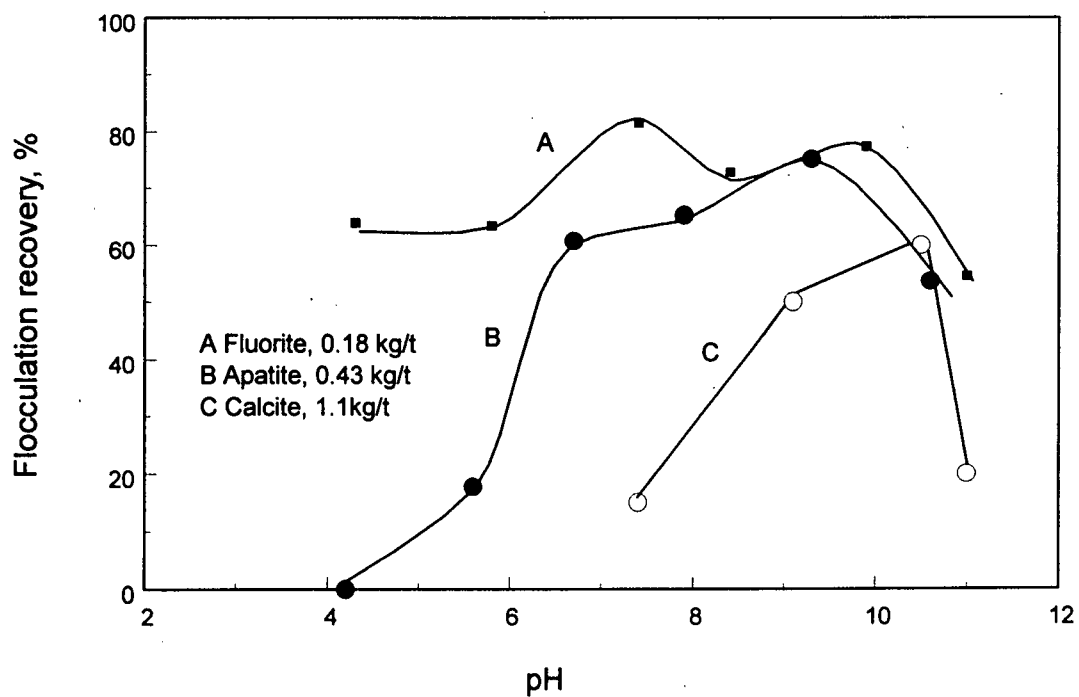


Figure 5.21 - Effect of pH on flocculation of fluorite, apatite and calcite with P(EHMA) latex

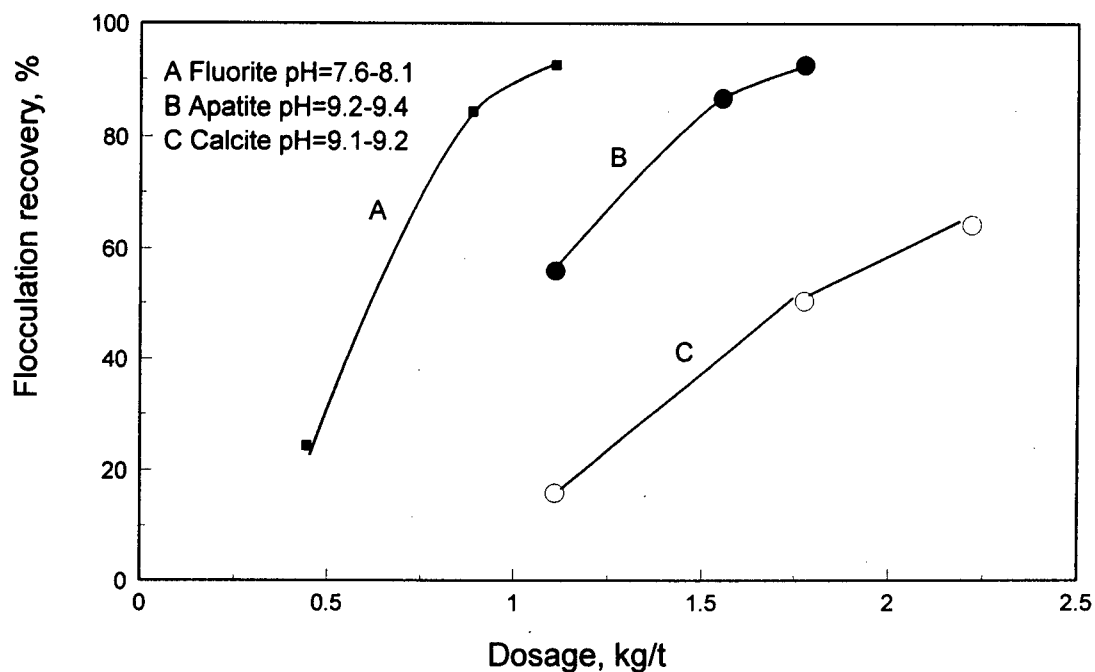


Figure 5.22 - Effect of P(EHMA)-R dosage on flocculation of fluorite, apatite and calcite at their natural pH

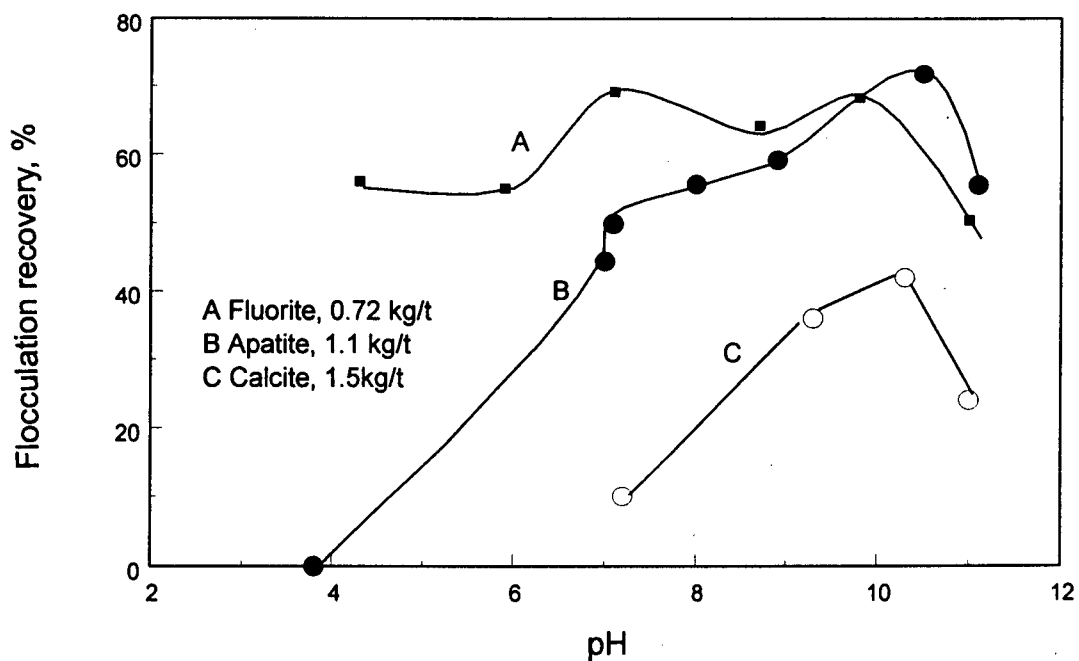


Figure 5.23 - Effect of pH on flocculation of apatite, fluorite and calcite with P(EHMA)-R latex

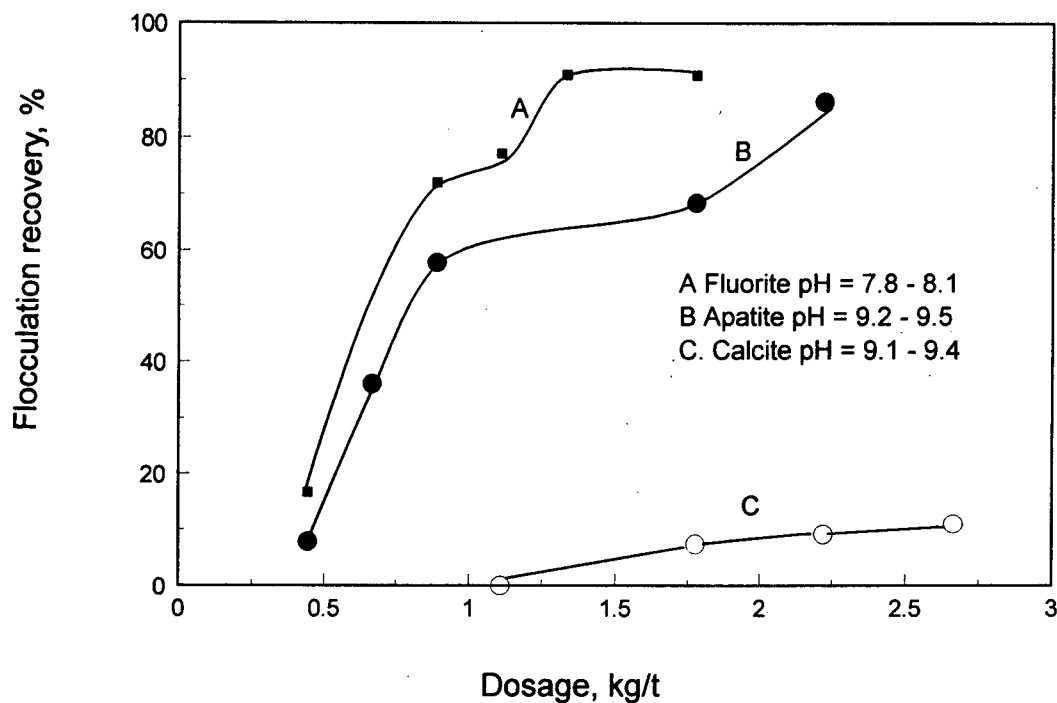


Figure 5.24 - Effect of P(MAAA) dosage on flocculation of fluorite, apatite and calcite

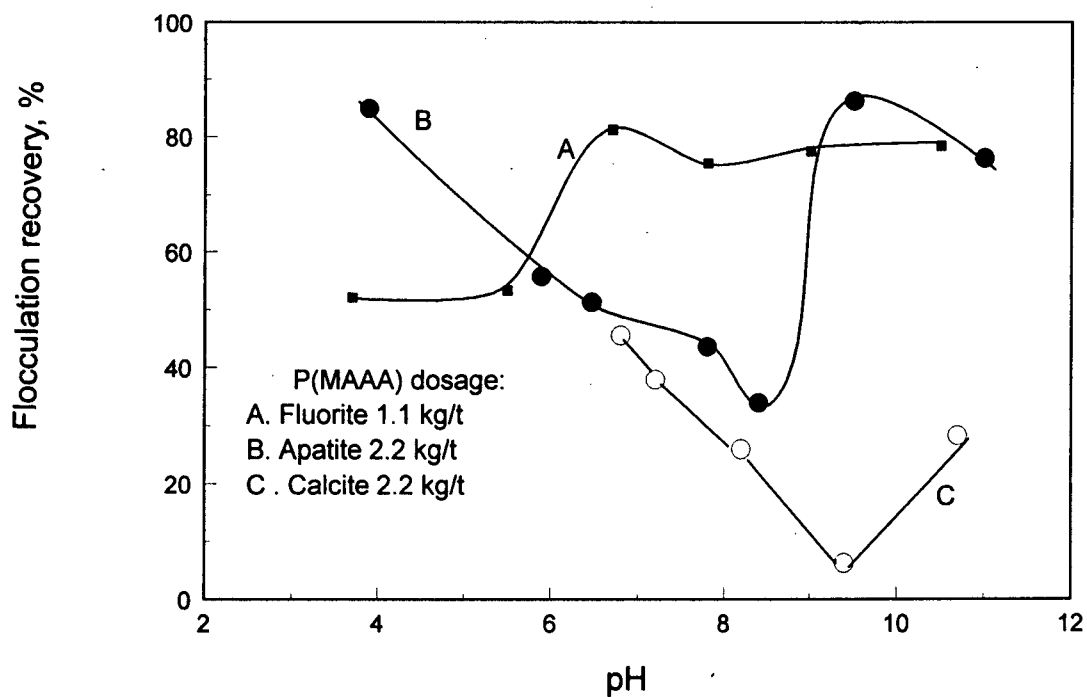


Figure 5.25 - Effect of pH on flocculation of apatite, fluorite and calcite with P(MAAA) latex

maximum at around pH 9.2 is reached. In the case of calcite, the minimum flocculation occurs around pH 9.5. This indicates that selective flocculation is possible by controlling the pH. The decrease in apatite flocculation within the pH range of 4 to 8.5 is mainly due to the increase of electrostatic repulsion force between the latex and apatite. The lowest pH tested during calcite flocculation was 6.5 as dissolution was observed when pH was further decreased. It is interesting that a different flocculation behavior was observed around pH 4 when using P(MAAA) and P(EHMA) latices on apatite. It is believed that the electrophoretic mobility of the latices around pH 4 is mainly determined by the surface sulfate group. The sulfate group on the surface of P(EHMA) latex particles may be coated by the adsorbed emulsifier and not available for interaction with mineral surfaces while the sulfate group on the surface of P(MAAA) latex particles remains exposed and provides an active site for chemical interaction.

Flocculation of silica with all the latices were also tested, but none of the latices flocculated silica.

Flocculation of fluorite, apatite and calcite with all the latices showed that P(MAAA) is the best flocculant of those tested in terms of the selectivity towards fluorite, apatite and calcite.

5.4 Deposition of the Latices onto Mineral Surfaces

Previous deposition experiments (Marshall and Kitchener, 1966; Hull and Kitchener, 1969; Clint et al., 1972) have shown that, when the deposition particles were negatively charged and the deposition surfaces were positively charged, the deposition rate was solely controlled by diffusion. With negative particles and negative surfaces, because

of the presence of an energy barrier, high electrolyte concentrations were required to produce measurable deposition. In the latter case, the deposition was anomalous and was not proportional to time or to the concentration of the dispersion. In their experiments, the chemical forces determining the adhesion or non-adhesion of particles were assumed to be the long-range London-van der Waals forces of attraction and electrical double-layer interaction.

In the present study, the role played by the chemical interaction between carboxylic groups on latex particle surfaces and calcium sites on mineral surfaces in the deposition was evaluated.

Deposition of P(EHMA) latex onto fluorite surfaces was not observed at conditions of 10^{-3} M KNO_3 , 10^9 particles/ml, pH=7.2, 100 rpm and 15 minutes. The use of 10^{-3} M KNO_3 was to keep the ionic strength of the dispersion constant. The deposition was still not observed when the concentration of the dispersion was increased to 30×10^8 particles/ml while the other conditions were kept the same. This absence of deposition was mainly due to a large energy barrier that exists at this pH between the highly negatively charged P(EHMA) latex particles and the negatively charged fluorite surfaces. The electrostatic repulsive force played the major role in the deposition of P(EHMA) latex particles onto fluorite surface. P(EHMA)-R latex was then tried in the deposition test. Although the surface negative charge on the P(EHMA)-R latex particles was substantially reduced by removing the surface emulsifier, the deposition was not observed under the aforementioned conditions used with P(EHMA) latex. However, in the flocculation system, the applied shear apparently provided sufficient energy to overcome the energy barrier between the latex and the mineral surface, explaining why flocculation was observed. This is probably similar to what was referred to as "shear flocculation" in which

a high shear rate is required to produce the flocculation of a negatively charged hydrophobic fine particles system (Warren, 1974).

It was surprising to observe a deposition of P(MAAA) latex on the fluorite surface under the same conditions. The latex was uniformly deposited around the stagnation point of the rotating disc as shown in Figure 5.26. This indicates that the deposition is mainly due to the chemical interaction between carboxylic groups on the surfaces of latex particles and calcium sites on fluorite surfaces. Although P(MAAA) latex is also negatively charged, the magnitude of the charge is much lower than that of the P(EHMA) latex. At pH 7.2, the electrophoretic mobility of P(MAAA) is around $-7.5 \times 10^{-8} \text{ m}^2 \text{ sec}^{-1} \text{ volt}^{-1}$ while the mobility of P(EHMA) is around $-12.5 \times 10^{-8} \text{ m}^2 \text{ sec}^{-1} \text{ volt}^{-1}$. Deposition tests were also carried out on apatite and calcite surfaces. The results are shown in Figure 5.27. The deposition density is proportional to the particle concentration (for 10×10^8 - 30×10^8 particles/ml). Fluorite exhibits a higher deposition density than apatite and calcite. Although fluorite has a higher negative charge than apatite and calcite at this pH, chemical interaction apparently dominates the deposition process. The higher deposition density could be due to a higher packing density of calcium on fluorite surfaces than on apatite and calcite surfaces. Due to the small size of fluorite's anion F^- , the distance between calcium ions on a fluorite surface should be smaller than apatite or calcite surfaces.

The deposition kinetics of the P(MAAA) latex was tested as well. The results show that deposition density is proportional to the deposition time (for 0 - 20 minutes). Fluorite and apatite are characterized by higher deposition rates than calcite, as shown in Figure 5.28. The rate of deposition is controlled by mass transfer through the solution up to the interface region, then controlled by adhesion or non-adhesion as determined by the surface

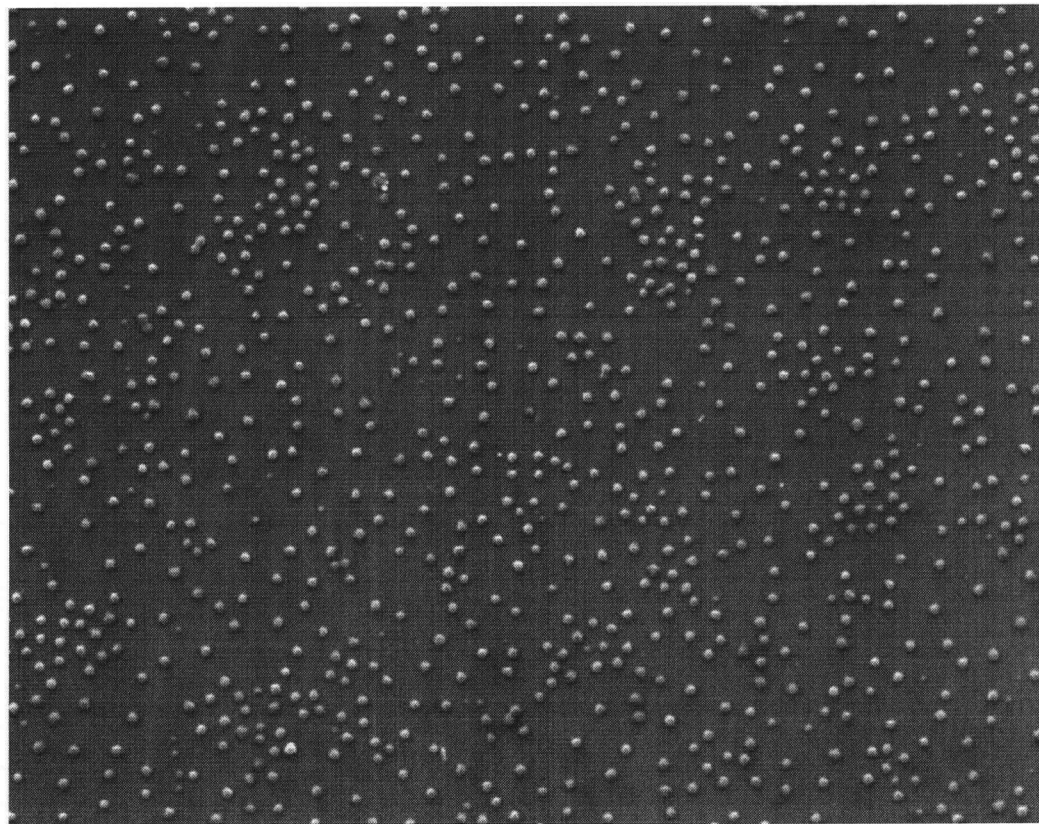


Figure 5.26 - Deposition of P(MAAA) latex onto fluorite surface at conditions of 10^{-3} M KNO_3 , 10×10^8 particles/ml, pH=7.2, 100rpm 15 minutes

chemical forces. The results indicate that the chemical forces existing between the latex and the fluorite and apatite surfaces are stronger than between the latex and calcite.

Deposition of P(MAAA) latex on fluorite, apatite and calcite versus pH were carried out to examine the effect of pH on deposition. The results, as shown in Figure 5.29, resemble the flocculation curve (Figure 5.25). Deposition on fluorite reaches a maximum around pH 7; on apatite a maximum is observed around pH 9 while calcite is characterized by a very low degree of deposition.

The effect of pH on deposition onto apatite and calcite was also confirmed at two different pH levels as shown in Figure 5.30. This Figure reveals that apatite has a higher deposition density at pH 9.2 than at pH 7.2 while calcite has a higher deposition density at pH 7.2 than at pH 9.2.

The deposition of negatively charged P(MAAA) latex particles onto the salt-type minerals may be occurring on the areas with less negative potential than the average value, such as on the calcium surface sites. The deposition results may also be affected by the degree of surface smoothness and electrostatic uniformity.

Deposition was not found on quartz surfaces. This was expected because there is no chemical interaction or electrostatic attraction between the latex particles and the quartz surface. A high electrolyte concentration would be required to produce the deposition of the negatively charged latex onto a negatively charged solid surface.

5.5 Selective Flocculation Using P(MAAA) Latex

The selective flocculation using the P(MAAA) latex was studied on the 1:1 apatite-

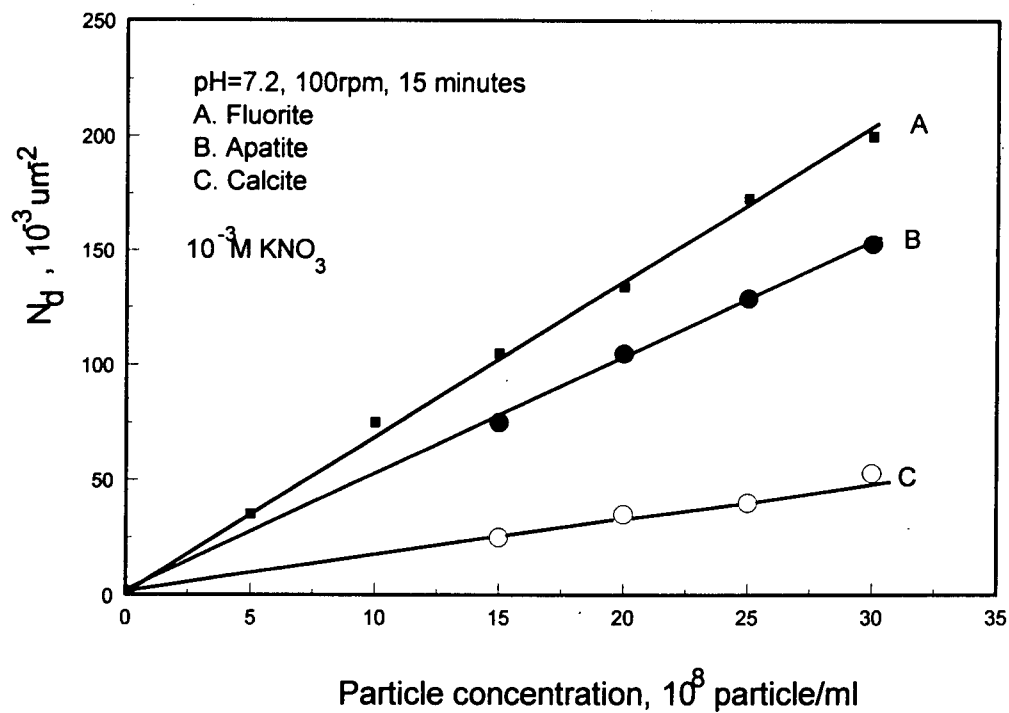


Figure 5.27 - Comparison of deposition of P(MAAA) latex onto fluorite, apatite and calcite surfaces

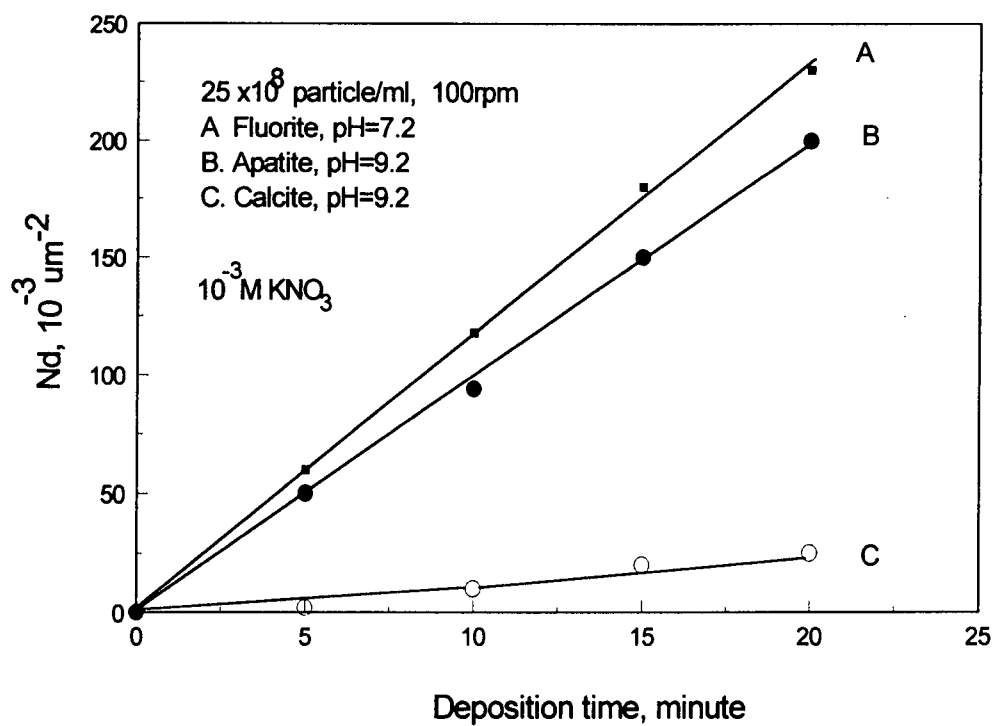


Figure 5.28 - Deposition of P(MAAA) latex onto fluorite, apatite and calcite surfaces vs. the deposition time

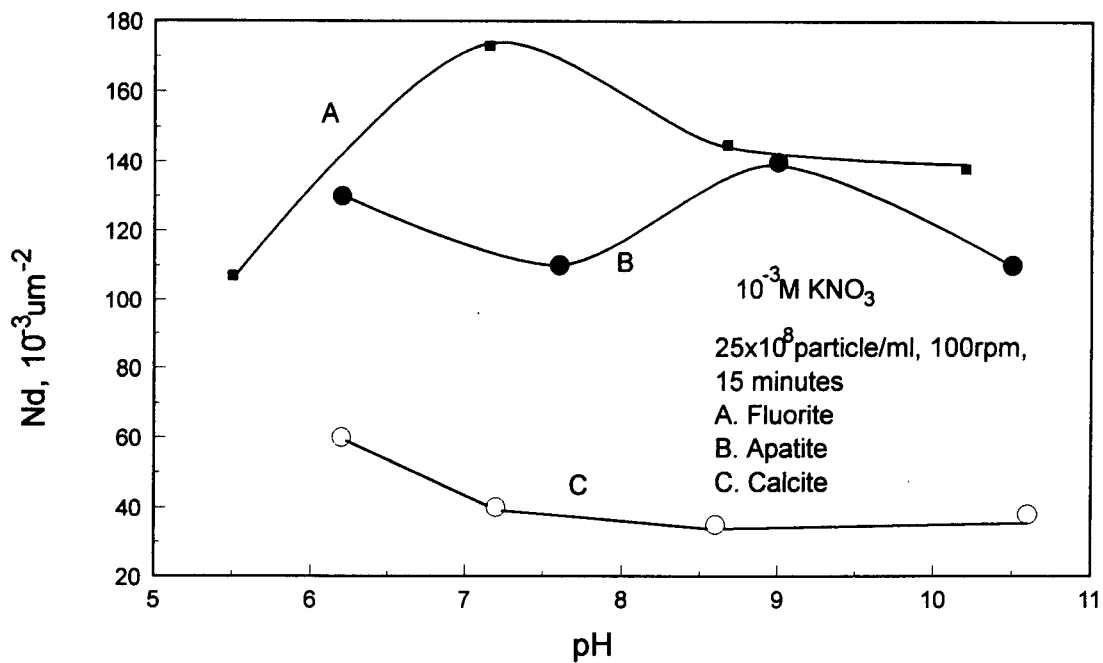


Figure 5.29 - Deposition of P(MAAA) latex onto fluorite, apatite and calcite surfaces vs. pH

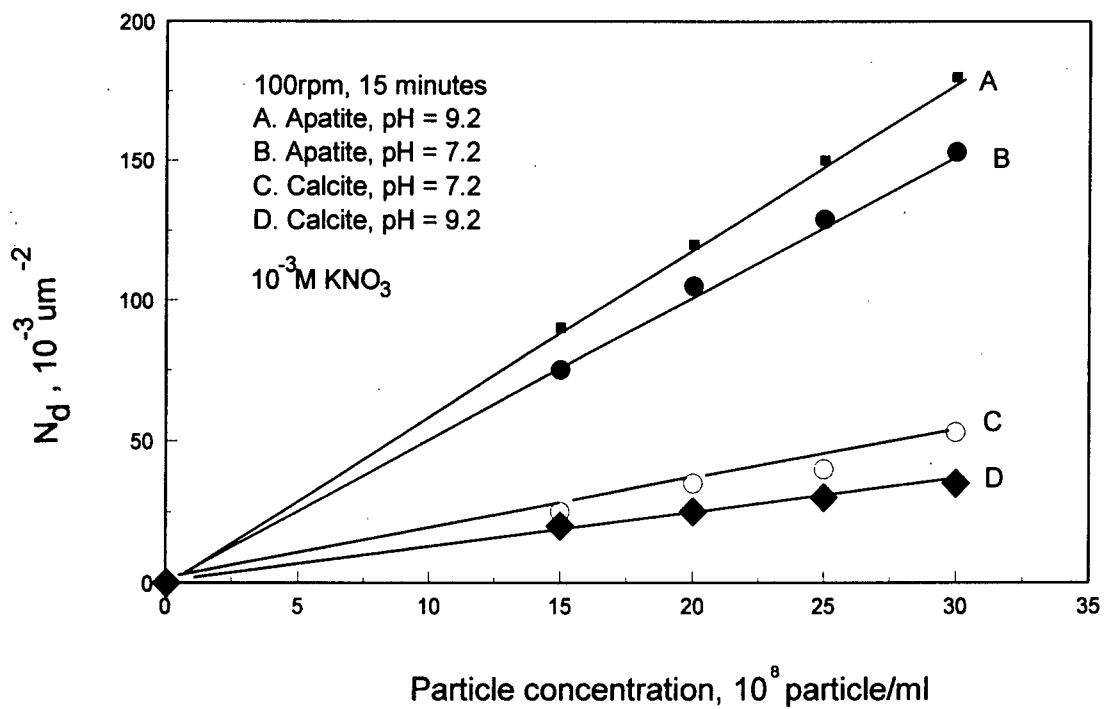


Figure 5.30 - Deposition of P(MAAA) latex onto apatite and calcite surfaces at two different pH level

calcite, apatite-silica, fluorite-calcite and fluorite-silica mixtures to examine the effectiveness of the latex as a selective flocculant in the separation of these minerals.

Apatite - Calcite Mixture

As pointed out in the previous section, selective flocculation of fluorite and apatite with P(MAAA) latex should be possible. The selective flocculation was carried out using a 1:1 apatite-calcite mixture at a pH ranging from 9.3 to 10.3. The results, as shown in Figure 5.31, reveal that apatite flocculation recovery increases with P(MAAA) dosage while the P_2O_5 content (grade) in the flocs initially increases with P(MAAA) dosage but then decreases after reaching a maximum. The highest P_2O_5 content (about 32%) corresponds to an apatite flocculation recovery of 40% (at 1.3 kg/t of latex). A higher flocculation recovery of 85% corresponds to a P_2O_5 grade of 25% (SI=0.3). With further increase in latex dosage and apatite flocculation recovery, the grade dropped significantly. Since the apatite surface contains carbonate, as revealed by the FTIR spectra, a higher latex dosage is required to produce a significant flocculation. Consequently, calcite in the bi-mineral system was also flocculated with the high dosage of P(MAAA). The poor selectivity as indicated by the selectivity index may also be due to the interaction between ions in the system and/or the entrapment resulting from larger flocs (Yu and Attia, 1987).

The effect of pH on the selective flocculation of an apatite/calcite system is shown in Figure 5.32. Apatite flocculation recovery increased with pH and reaches a maximum around pH 10 while the P_2O_5 grade increased progressively with pH. The highest apatite flocculation recovery of 90% around pH 10 was obtained at a 23% grade (SI=0.22).

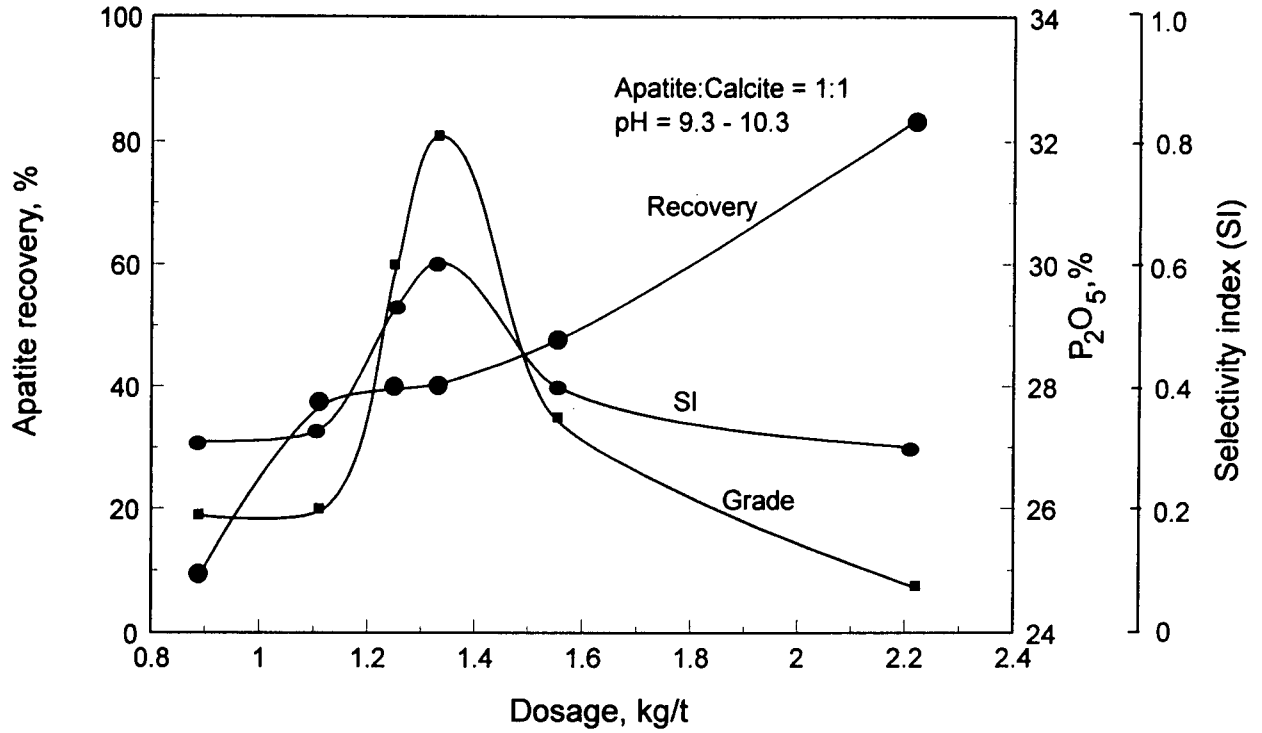


Figure 5.31 - Effect of P(MAAA) dosage on the selective flocculation of apatite from apatite/calcite mixture

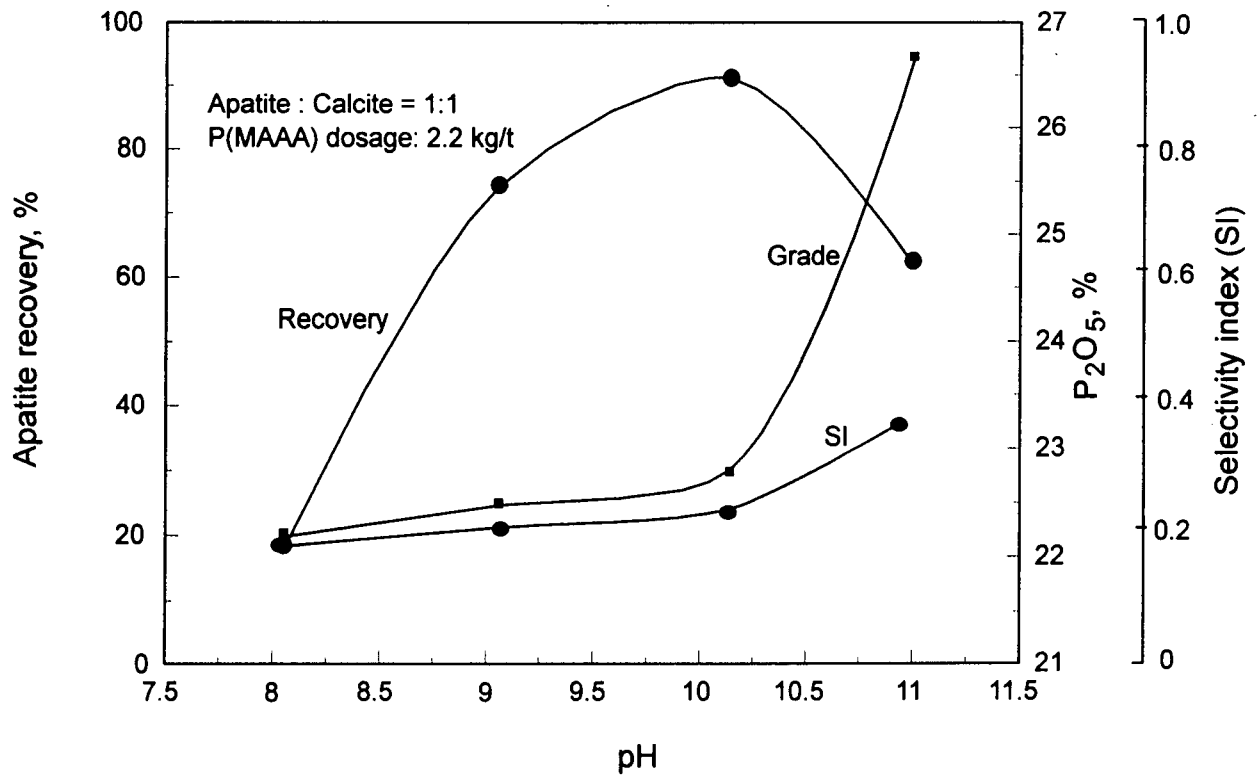


Figure 5.32 - Effect of pH on selective flocculation of apatite from apatite/calcite mixture

Selectivity increased a little bit when pH increased to 11 (SI=0.35) and this may be attributed to a better dispersion of the particles in alkaline conditions.

Apatite - Silica Mixture

The results of selective flocculation of a 1:1 mixture of apatite-silica around pH 9.1 - 9.3 is shown in Figure 5.33. Apatite flocculation recovery and the P_2O_5 grade continuously increased with the latex dosage over the entire tested range. The curves show that, at a latex dosage of 1.75 kg/t, 90% of the apatite can be recovered into the flocculated product at its grade of 27.5% (SI=0.4). As the curves suggest, the grade will probably increase further at higher latex dosages.

Fluorite - Calcite Mixture

The results of selective flocculation of a 1:1 mixture of fluorite-calcite around pH 8.9 - 9.3 is shown in Figure 5.34. Increasing the latex dosage caused the fluorite flocculation recovery to increase and the fluorine grade to decrease over the entire tested range. Neither the recovery nor the grade curves showed any maxima. However, the fluorine grade curve appears to have reached a bottom while fluorite flocculation recovery shows an increase tendency with increasing latex dosage. The selectivity is poor as indicated by the selectivity index varying from 0.3 to 0.2. It is believed that the presence of trace amounts of carbonate on fluorite surfaces as identified by the FTIR has resulted in the poor selectivity. This also indicates calcite was flocculated.

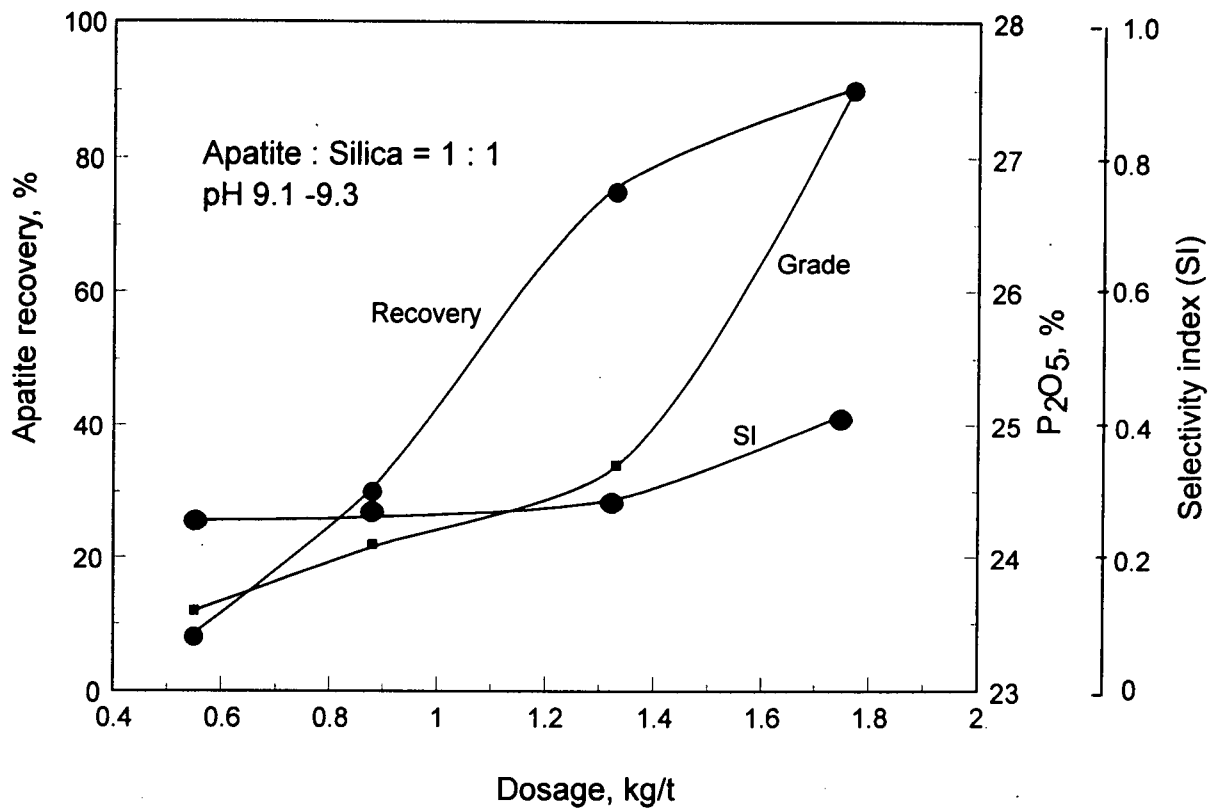


Figure 5.33 - Effect of P(MAAA) dosage on selective flocculation of apatite from apatite/silica mixture

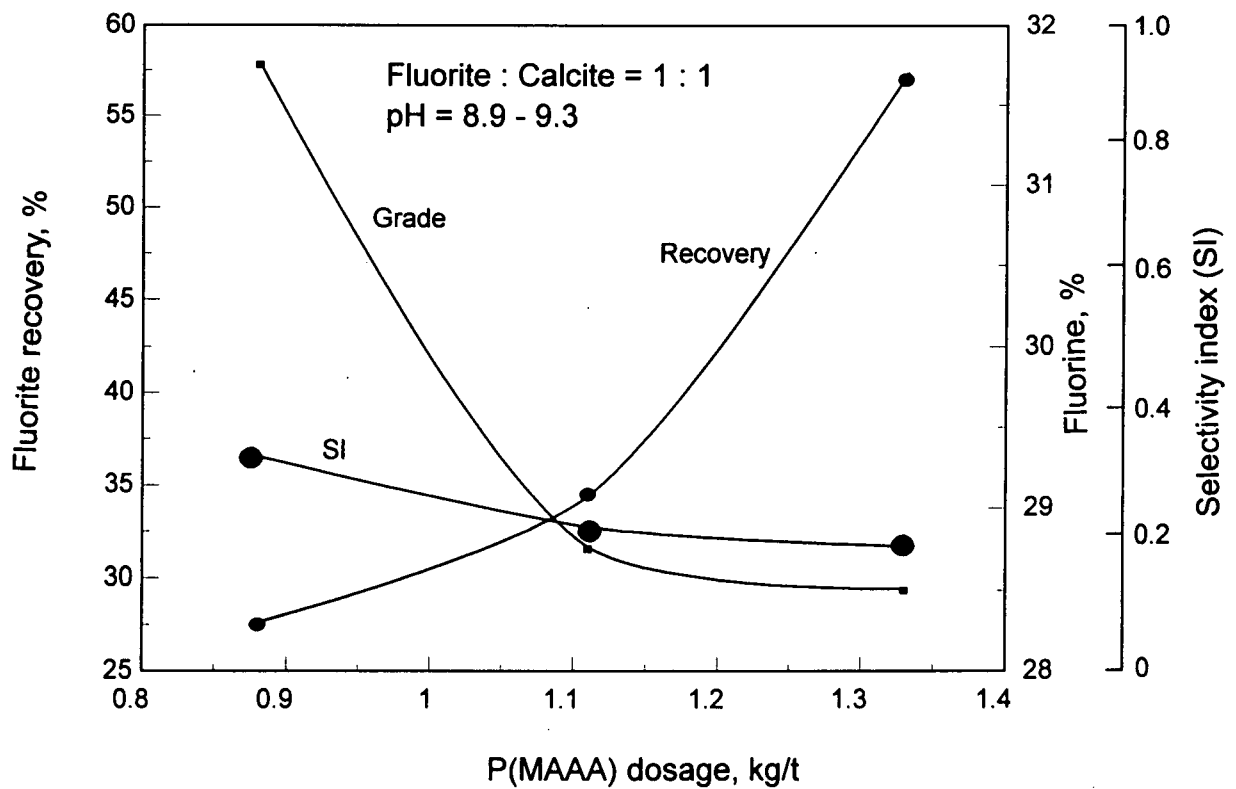


Figure 5.34 - Effect of P(MAAA) dosage on selective flocculation of fluorite from fluorite/calcite mixture

Fluorite - Silica Mixture

The results of selective flocculation of a 1: 1 mixture of fluorite-silica around pH 8.7 to 8.9 is shown in Figure 5.35. Fluorite recovery increased with the latex dosage and reached a maximum of 82% at a dosage of 1.1 kg/t. The fluorine grade stayed high around 45%. Since the effect of the latex dosage on fluorine grade was not significant over the range tested, the variation of fluorine grade was not shown on the figure. The separation is better in this case compared to the cases of separation of apatite-calcite, apatite-silica and fluorite-calcite as indicated by the selectivity index of 0.9 although silica is possible to be activated by the calcium ions.

5.6 Effect of Dispersing Agents

Although alkaline pH produced better selectivity, as has been shown in the previous section, the selectivity was not very good without dispersing agents. Therefore, sodium tripolyphosphate and sodium silicate ($m\text{Na}_2\text{O}\cdot n\text{SiO}_2$) were included as dispersing agents in the tests as follows.

Single Minerals

As Figures 5.36, 5.37 and 5.38 demonstrate, both dispersing agents moved the zeta potential values of fluorite, apatite and calcite to a more negative range, but the required dosage for sodium tripolyphosphate was significantly less than that required for sodium silicate. Sodium tripolyphosphate was very effective in conferring a high negative charge

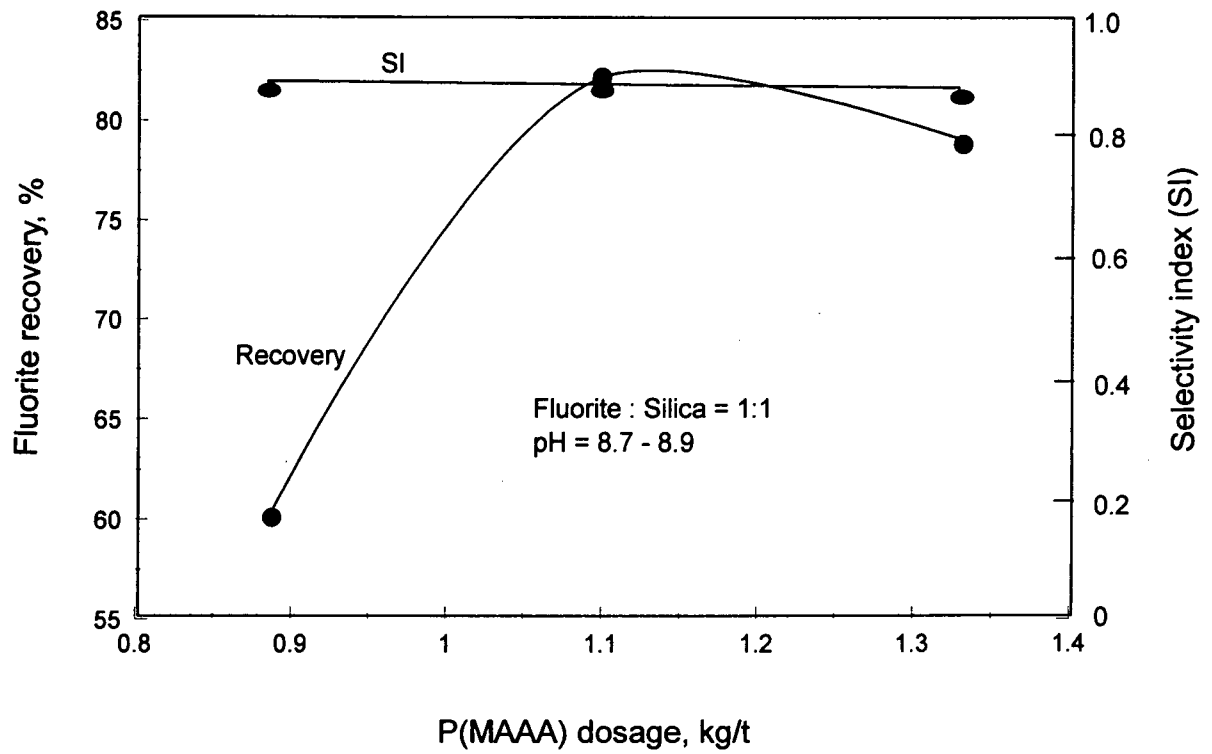


Figure 5.35 - Effect of P(MAAA) dosage on selective flocculation of fluorite from fluorite/silica mixture

onto the minerals. The zeta potential of silica was not affected by either sodium tripolyphosphate or sodium silicate as shown in Figure 5.39.

The effect of sodium silicate and sodium tripolyphosphate on a single mineral flocculation at their natural pHs is shown in Figures 5.40 and 5.41. Fluorite is activated at low concentrations of the tested dispersants then is depressed as the concentrations increase. The flocculation of apatite was insensitive to both tested dispersants over a broad range of dispersant concentrations while calcite flocculation was strongly depressed, even at very low concentrations of both dispersants.

Selective Flocculation - (Apatite - Calcite Mixture)

The effect of sodium tripolyphosphate and sodium silicate on selective flocculation of an apatite/calcite mixture is shown in Figures 5.42 and 5.43. For the apatite/calcite system at pH of 9.1 - 9.4, apatite recovery increased with concentration of sodium tripolyphosphate and reached a maximum at a given concentration of this dispersant. While the apatite recovery depended remarkably on the latex dosage, the grade of the flocculated product did not depend on the latex dosage and remained high. As a result, a grade of 34% could also be obtained at 90% recovery when the dosage of latex was increased to 2.2 kg/t. The selectivity was improved in the presence of sodium tripolyphosphate as indicated by the increased selectivity index (SI increased from 0.3 to 0.8) over the range tested. With sodium silicate, the highest grade of 29% with the recovery of 75% could be obtained at a latex dosage of 1.1 kg/t (Fig. 5.43). The recovery could be increased further using a higher latex dosage, but the grade would not be expected to increase. The selectivity index

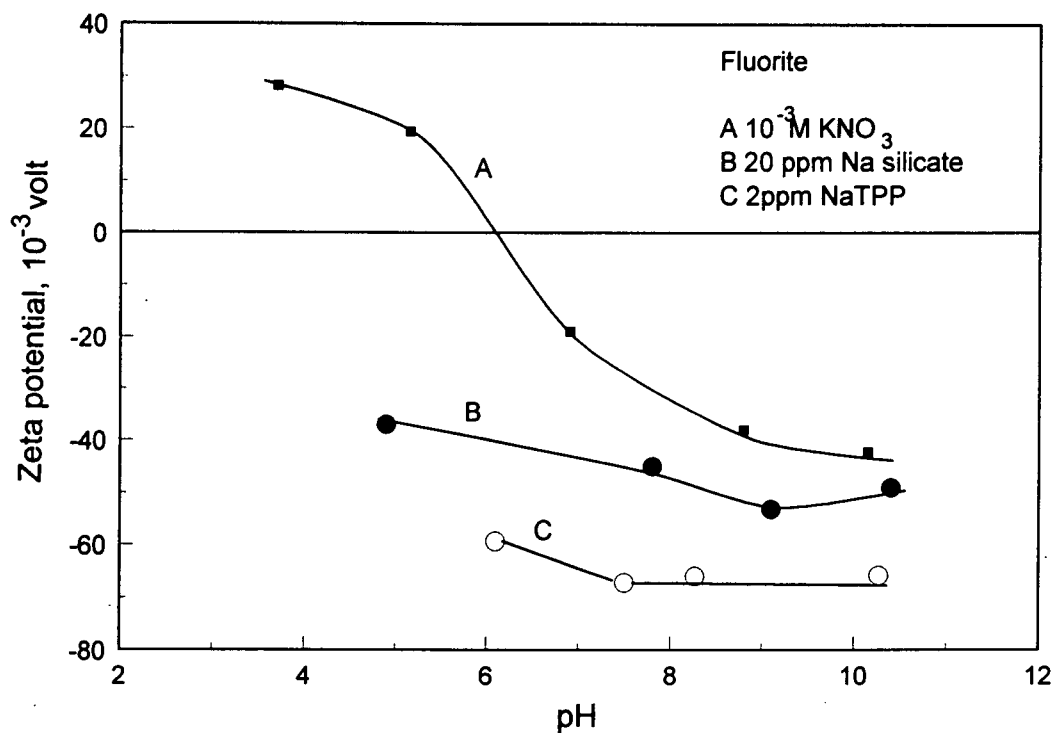


Figure 5.36 - Effect of dispersants concentrations on zeta potential of fluorite

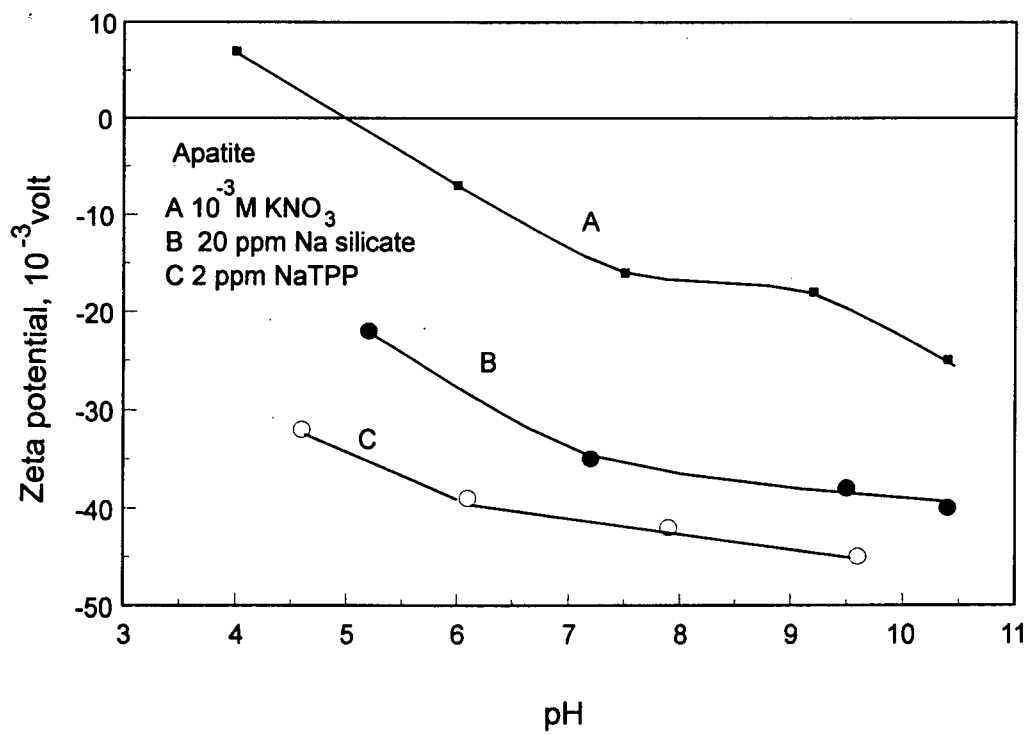


Figure 5.37 - Effect of dispersants concentrations on zeta potential of apatite

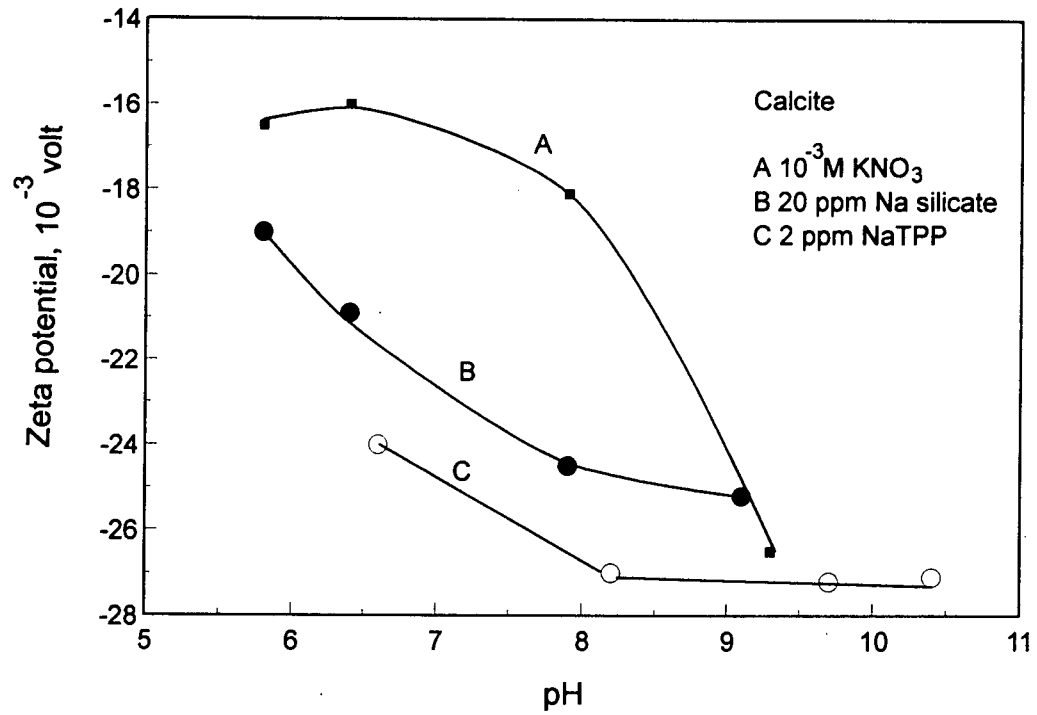


Figure 5.38 - Effect of dispersants concentrations on zeta potential of calcite

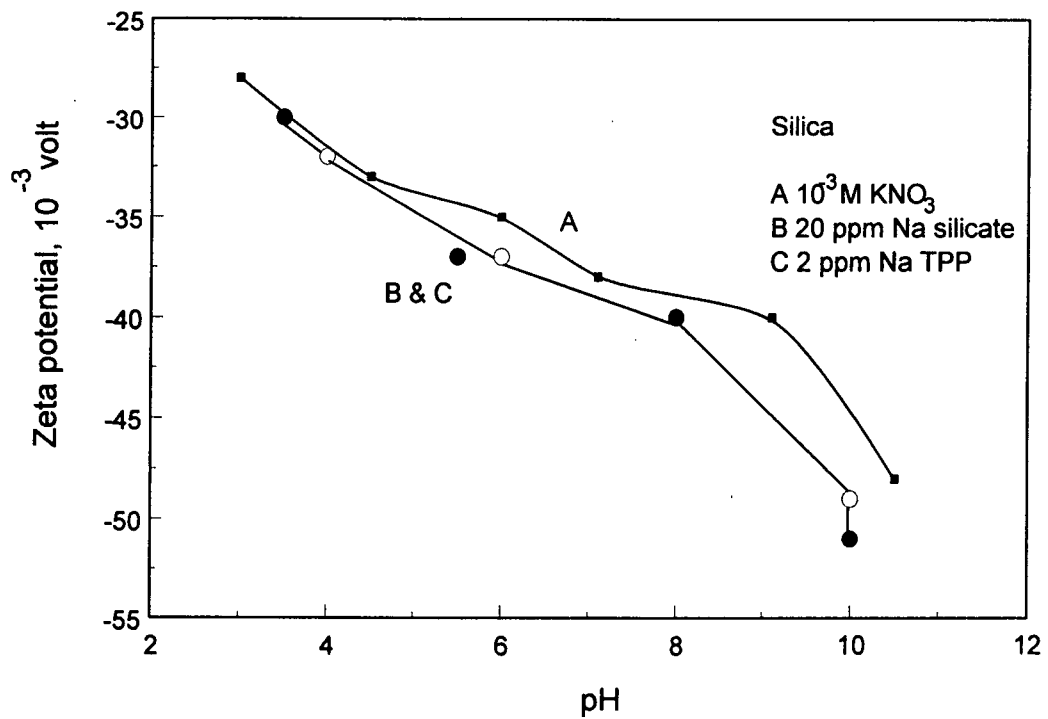


Figure 5.39 - Effect of dispersants concentrations on zeta potential of silica

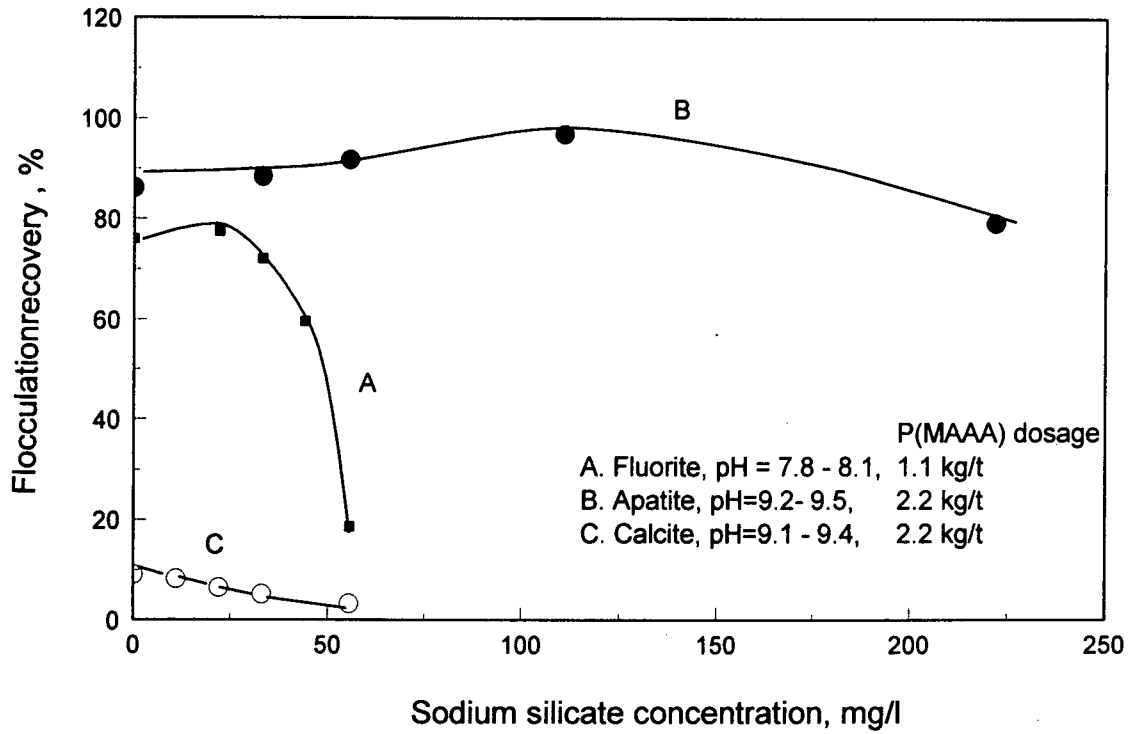


Figure 5.40 - Effect of sodium silicate on flocculation of fluorite, apatite and calcite with P(MAAA) latex

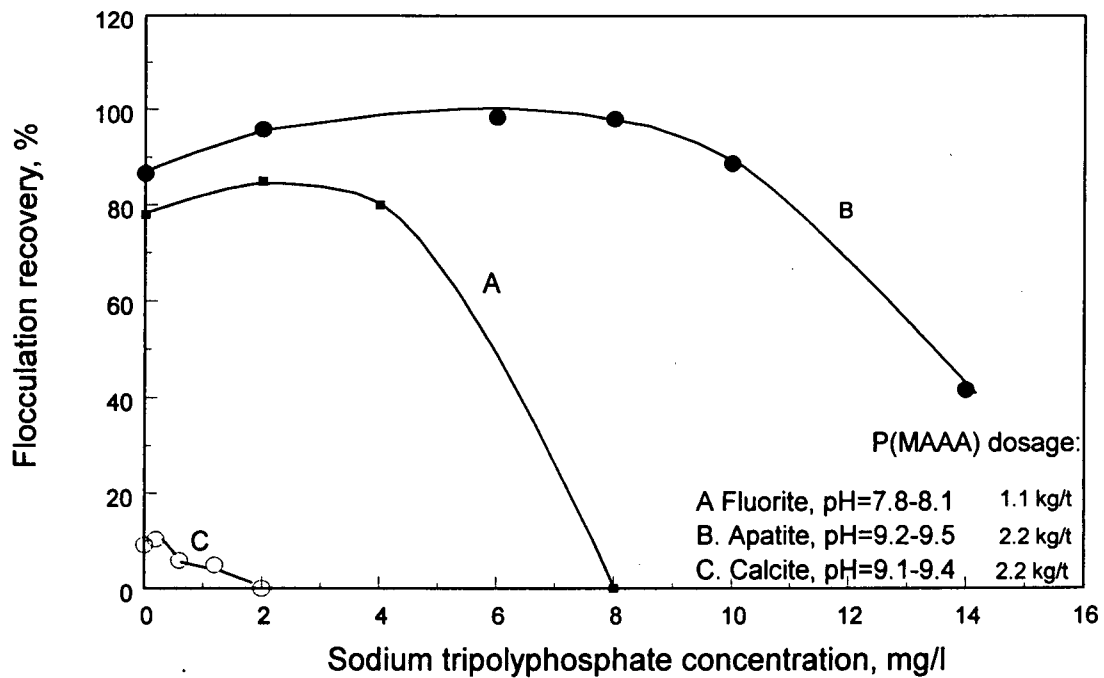


Figure 5.41 - Effect of sodium triphosphate on flocculation of fluorite, apatite and calcite with P(MAAA) latex

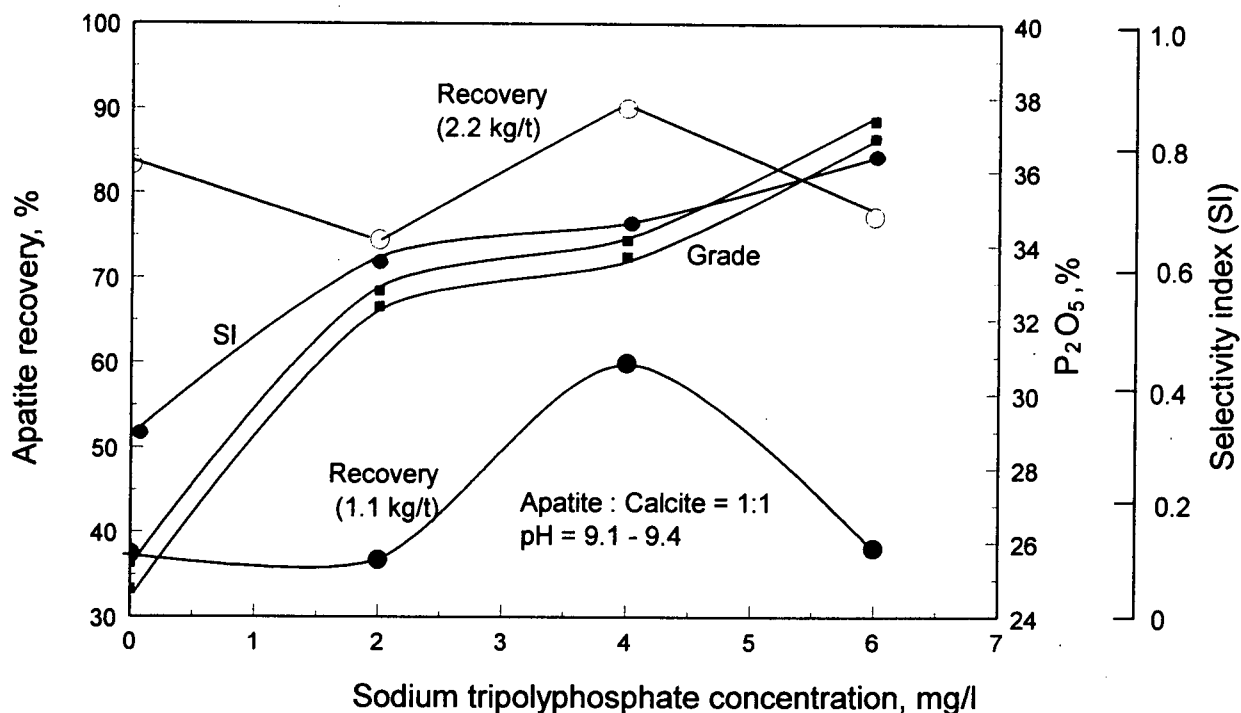


Figure 5.42 - Effect of sodium tripolyphosphate concentration on selective flocculation of apatite from apatite/calcite mixture at two levels of P(MAAA) dosage

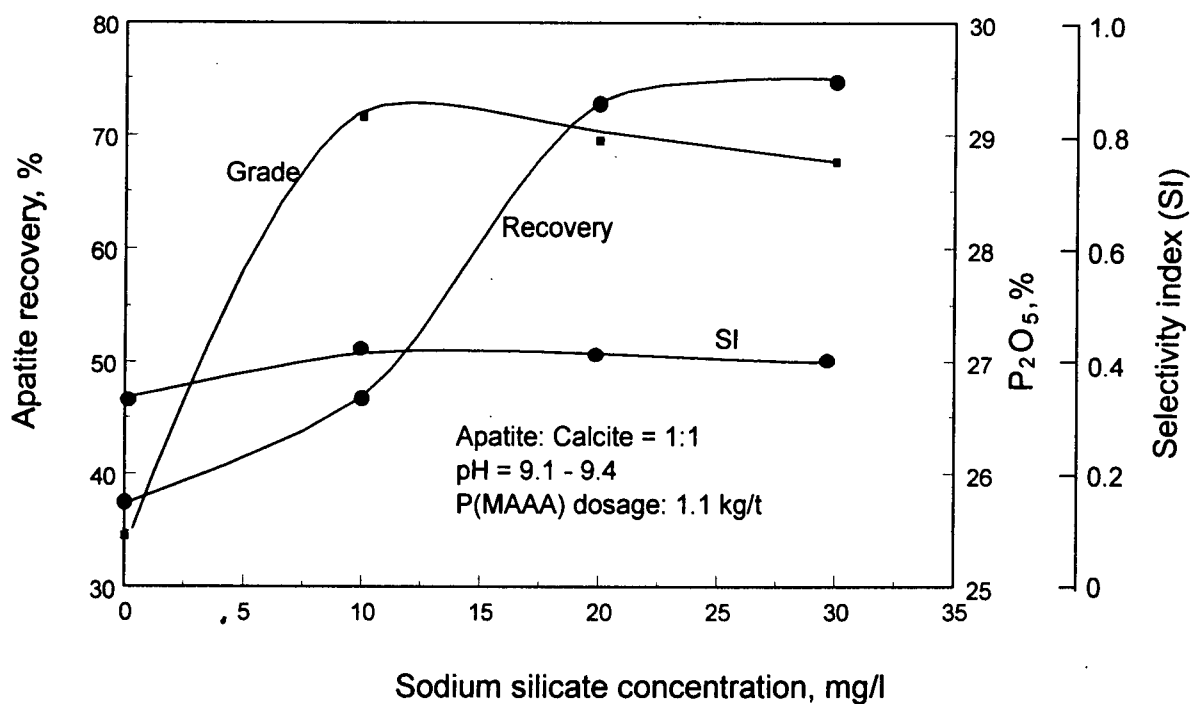


Figure 5.43 - Effect of sodium silicate concentration on selective flocculation of apatite from apatite/calcite mixture

was not significantly changed and stayed around 0.4. The results show that sodium tripolyphosphate works better with the apatite-calcite mixture than sodium silicate.

The effect of pH in the presence of sodium tripolyphosphate is shown in Figure 5.44. The pH of maximum apatite recovery has shifted from 10 in the absence of sodium tripolyphosphate to 9.2 in the presence of this dispersant. A maximum apatite recovery of 80% was obtained at 37% grade (SI=0.7) of the flocculated product at pH of 9.5.

Selective Flocculation - (Apatite - Silica Mixture)

The effect of sodium silicate and sodium tripolyphosphate on selective flocculation of apatite-silica at a pH of 9.1 - 9.3 is shown in Figures 5.45 and 5.46. Apatite recovery increased and reached a maximum (80%) when the dosage of sodium silicate was raised to 20 mg/l; the grade of the flocculated product was observed to increase continuously up to 35% P₂O₅ (SI=0.7) (Fig. 5.45). With sodium tripolyphosphate, clear maxima are present on recovery and grade curves at the same concentration of the dispersant (Fig. 5.46). Further increasing the concentration of sodium tripolyphosphate, both recovery and grade were depressed. The curves suggest that sodium silicate works better for an apatite - silica mixture than sodium tripolyphosphate.

The effect of pH on selective flocculation of the apatite - silica mixture in the presence of sodium silicate is shown in Figure 5.47. The highest recovery of 85% was obtained at pH of 9-9.2 at a grade of 33% (SI=0.6); as pH increased, the selectivity increased.

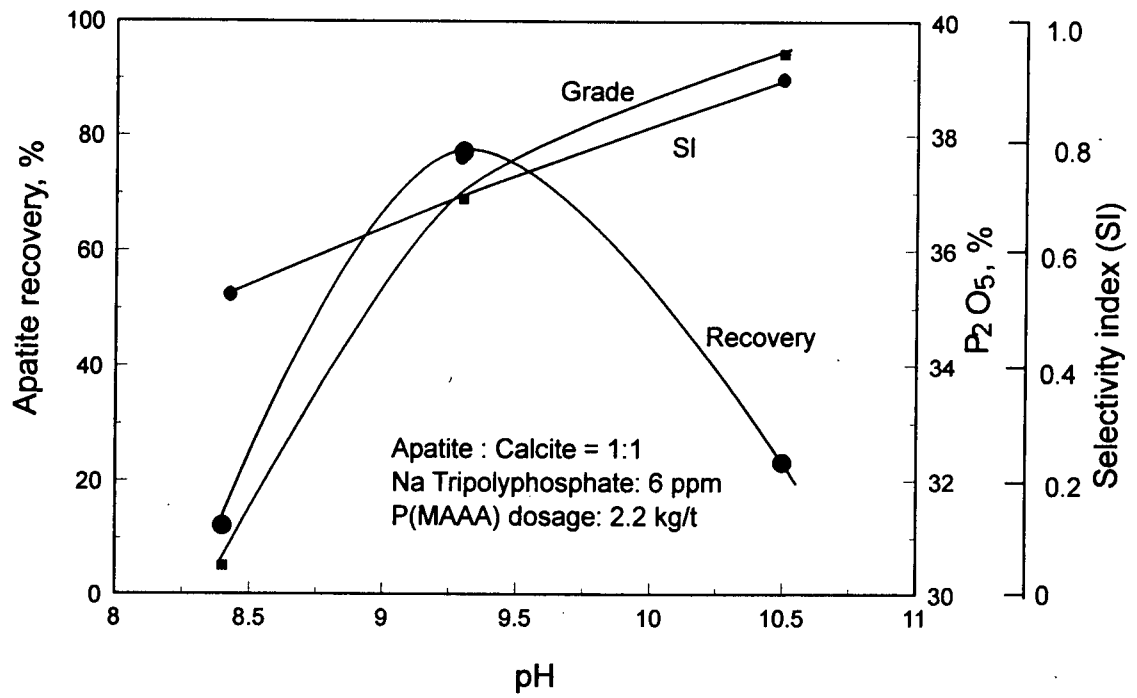


Figure 5.44 - Effect of pH on selective flocculation of apatite from apatite/calcite mixture in the presence of sodium tripolyphosphate

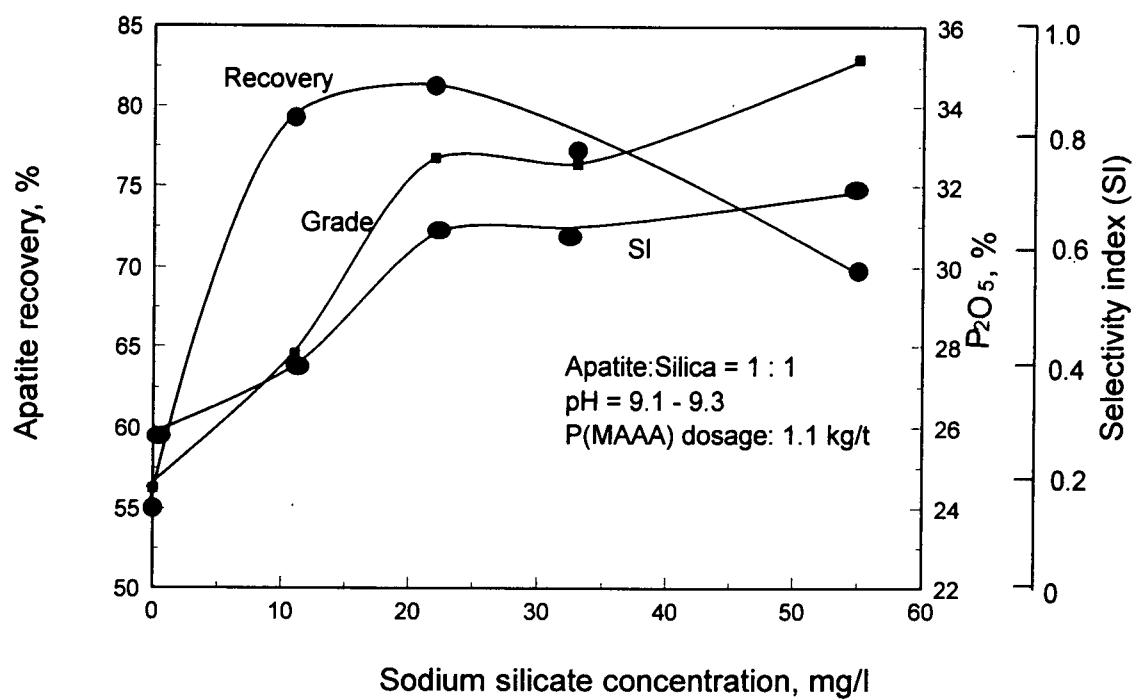


Figure 5.45 - Effect of sodium silicate on selective flocculation of apatite from apatite/silica mixture

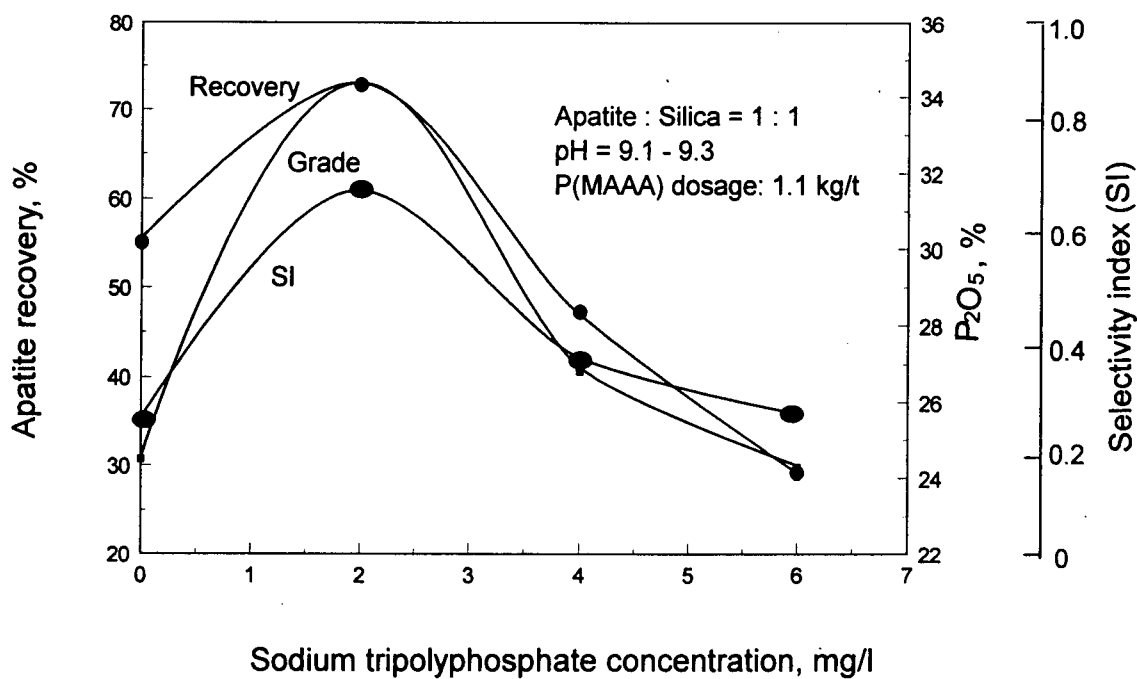


Figure 5.46 - Effect of sodium tripolyphosphate on selective flocculation of apatite from apatite/silica mixture

Selective Flocculation - (Fluorite - Calcite Mixture)

The effect of sodium silicate on selective flocculation of fluorite-calcite mixture at a pH of 8.9 - 9.3 is shown in Figure 5.48. Fluorite recovery increased and reached 75% with sodium silicate concentration raised to about 15 mg/l; the fluorine content was observed to increase continuously with sodium silicate concentration. The addition of sodium silicate improves the selectivity as indicated by the increased selectivity index (SI increased from 0.2 to 0.45). However, the separation remained limited, as shown in Figure 5.48, with the highest recovery observed being 75% and corresponding to a grade of 33% (SI=0.38). The recovery may be increased using a greater latex dosage, but the grade is not expected to increase as the heteroflocculation may be encountered at a higher dosage of the latex.

Flocculation was not observed in the presence of sodium tripolyphosphate even at a very low concentration (i.e., 2 ppm). This is attributed to the high negative charge on the fluorite surface in the presence of sodium tripolyphosphate. As shown in Figure 5.36, the fluorite surface acquired a negative zeta potential of -70×10^{-3} V in the presence of 2 ppm sodium tripolyphosphate.

Fluorite - Silica Mixture

The effect of sodium silicate on selective flocculation of fluorite-silica mixture at a pH of 8.7 - 8.9 is shown in Figure 5.49. While fluorite recovery increased with sodium silicate concentration and reached a maximum of 95%, fluorine content in the flocculated

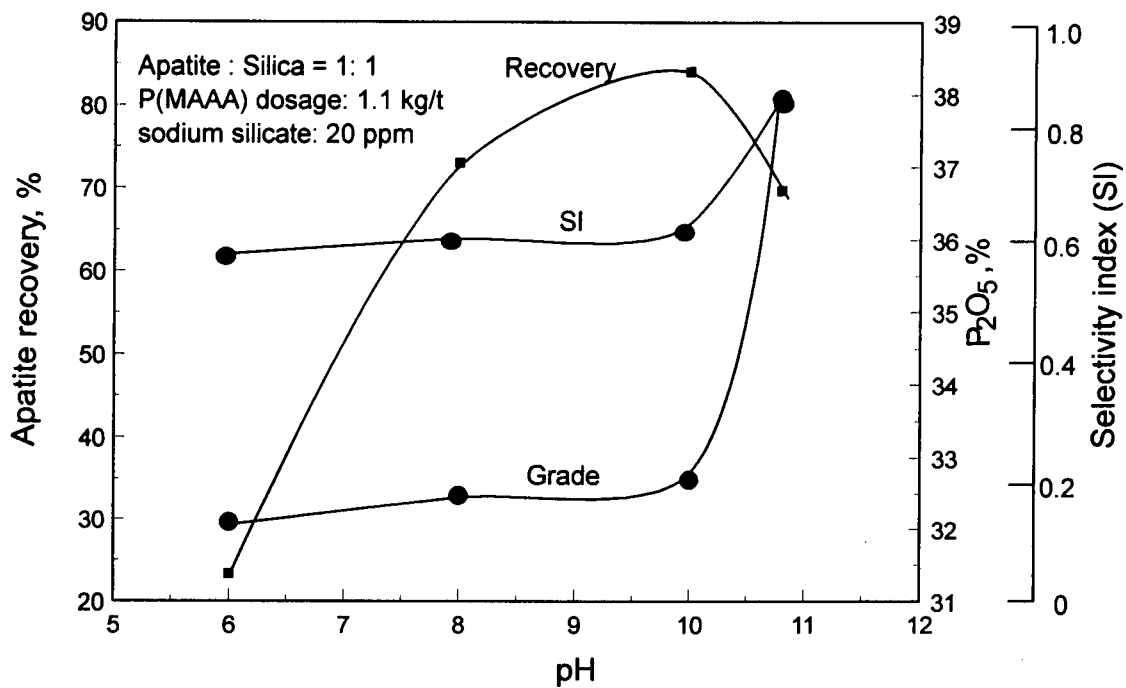


Figure 5.47 - Effect of pH on selective flocculation of apatite from apatite/silica mixture in the presence of sodium silicate

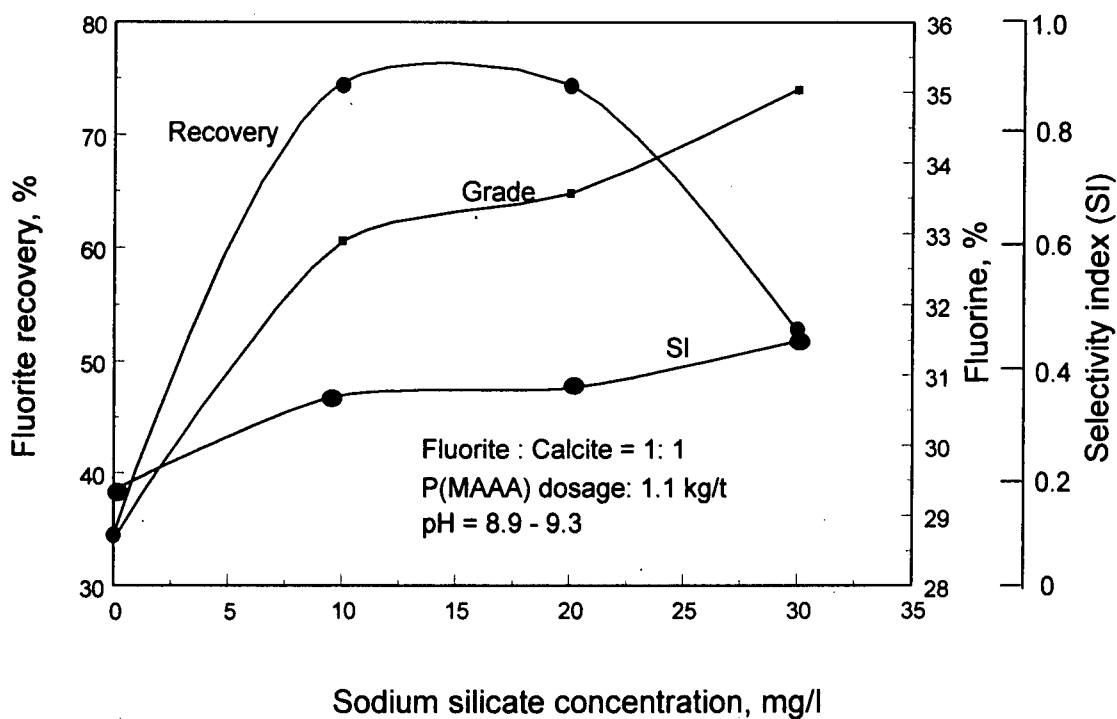


Figure 5.48 - Effect of sodium silicate concentration on selective flocculation of fluorite from fluorite/calcite mixture

product showed a decrease tendency but may not be significant. The selectivity index stayed high around 0.95 to 0.85 over the range tested.

The effect of sodium tripolyphosphate on the selective flocculation of fluorite-silica mixture at a pH of 8.7-8.9 is shown in Figure 5.50. The presence of sodium tripolyphosphate depresses the fluorite flocculation compared to the system without sodium tripolyphosphate. A maximum fluorite recovery of 90% was obtained with a maximum of fluorine content of only 30.5% (SI=0.25).

Apparently sodium tripolyphosphate does not meet all the requirements for the fluorite-calcite and fluorite-silica mixtures because it imparts a high negative charge to the fluorite surface, and this, in turn, prevents the fluorite-latex interaction. Sodium silicate does improve the separation of fluorite-calcite and fluorite-silica mixtures. It is surprising to observe the poorer separation for the fluorite-calcite mixture in comparison with the apatite-calcite mixture as this is different from what could be predicted from a single mineral flocculation test. Various factors may be responsible for this behavior. Bilsing (1969) reported a significant increase in the solubility of CaF_2 and CaCO_3 in each other's presence. This implies that the mineral surfaces would be contaminated with ions from the other minerals. The increased solubility of calcium minerals would increase the calcium concentration and, in turn, reduce the number of active sites on the surface of the latex.

5.7 Microflotation

The flocs produced by the P(MAAA) latex are expected to have some degree of hydrophobicity and may be floatable. The flotation properties of these minerals with oleic

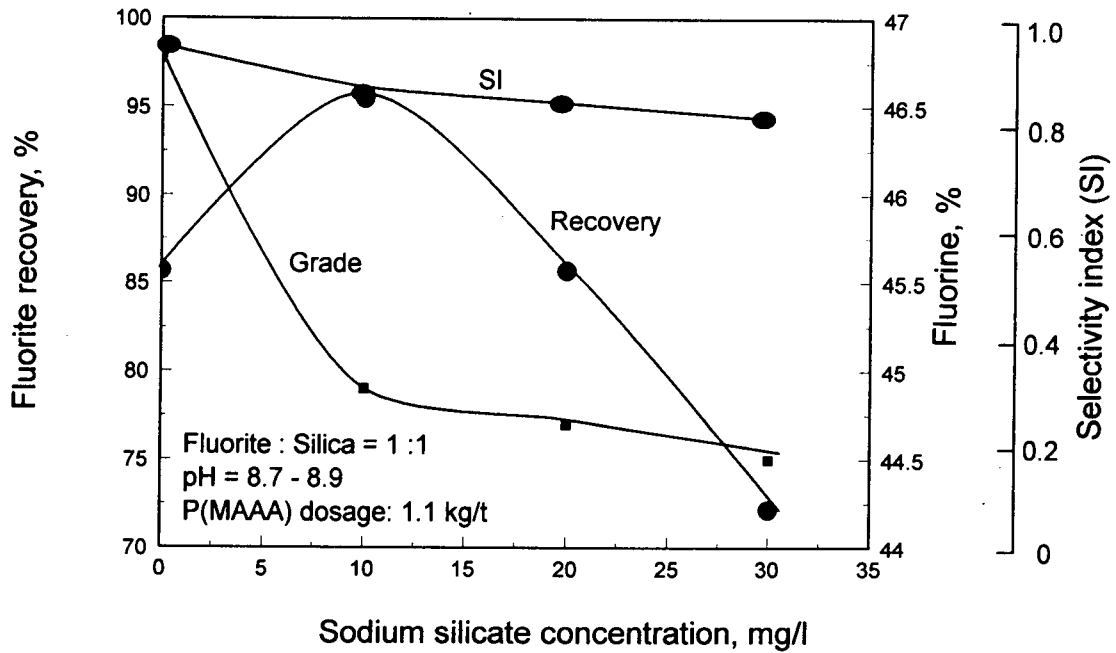


Figure 5.49 - Effect of sodium silicate concentration on selective flocculation of fluorite from fluorite/silica mixture

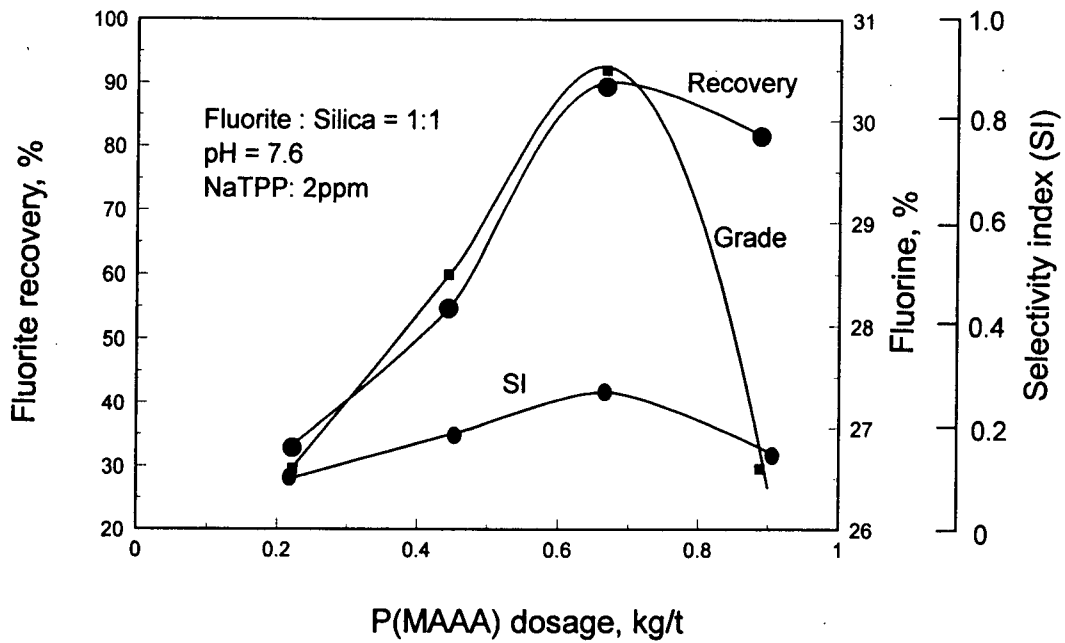


Figure 5.50 - Effect of P(MAAA) dosage on selective flocculation of fluorite from fluorite/silica mixture in the presence of sodium tripolyphosphate

acid, which is a common flotation collector for this type of mineral, were examined in a Hallimond tube. Flotation tests with the fine minerals and oleic acid in the presence of P(MAAA) latex were conducted to examine the effect of P(MAAA) latex on flotation of fine mineral particles.

The results of the flotation of fluorite, apatite and calcite with oleic acid are shown in Figures 5.51 to 5.53. The flotation spectrum of fluorite is similar to the one reported earlier (Laskowski and Nyamekye, 1994) and was carried out under similar conditions. The flotation of apatite and calcite shows two maxima in the tested pH range. The effect of the conditioning time with the reagent prior to flotation is quite different in acidic and in alkaline pH ranges (Laskowski and Nyamekye, 1994), and the results shown here were obtained after a short conditioning time with reagents prior to flotation. As shown in Figure 5.54, the flotation of apatite with oleic acid improved remarkably with conditioning time around pH 4, while in an alkaline pH of 10, flotation after 5 and 60 minutes of conditioning were not very different. It is obvious that oleic acid is present as emulsion droplets in the acidic pH range and as oleate ions in the alkaline pH range. In the emulsion zone, flotation is controlled by a slow diffusion of the colloidal oleic acid droplets toward mineral surfaces; therefore, longer conditioning times improve flotation results. On the other hand, an adsorption equilibrium is established fairly quickly for an ionized collector; therefore, in the oleate zone, the effect of conditioning time is negligible.

The effect of the particle size of apatite on flotation with oleic acid is shown in Figure 5.55. It is obvious that the flotation of fine apatite is not as efficient as the flotation of intermediate sizes, especially in neutral and alkaline pH ranges. Since poor flotation of fine particles results from the low collision probability, the addition of latex P(MAAA) should improve the flotation of fine apatite. Figure 5.56 shows the effect of P(MAAA) on

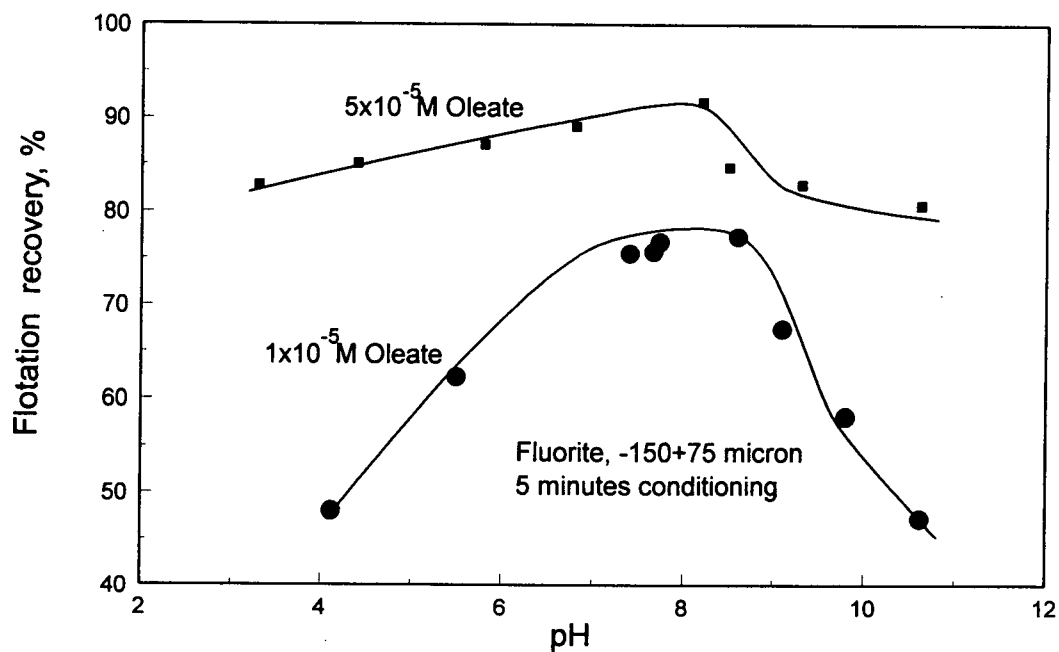


Figure 5.51 - Effect of pH on flotation of fluorite at two different concentrations of sodium oleate following 5 minutes conditioning

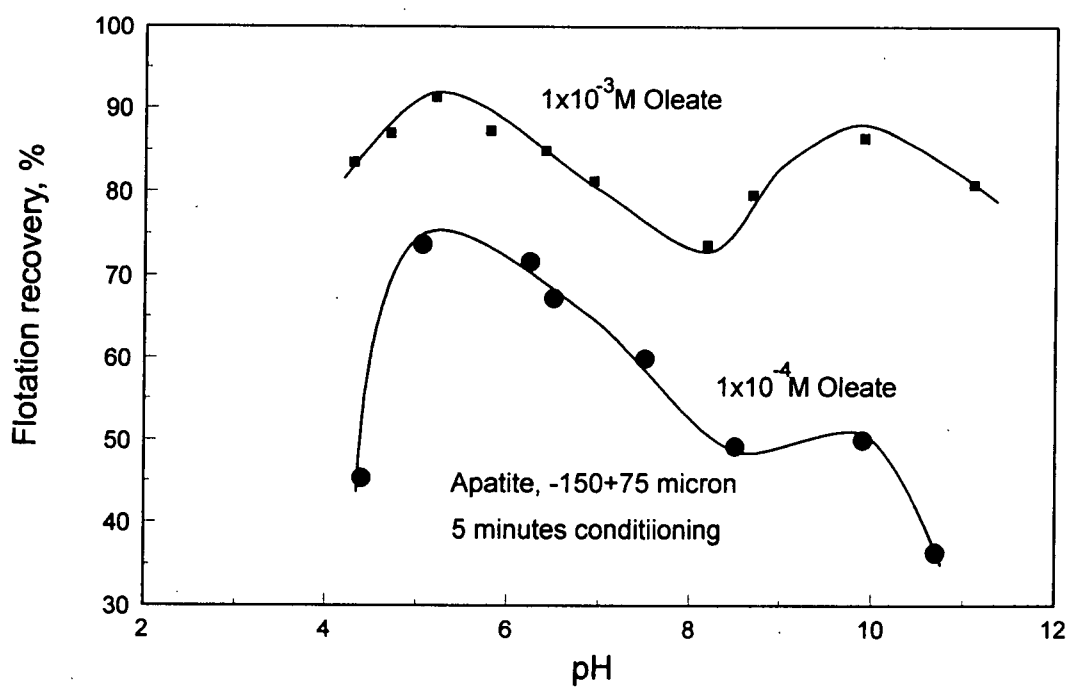


Figure 5.52 - Effect of pH on flotation of apatite at two different concentrations of sodium oleate following 5 minutes conditioning

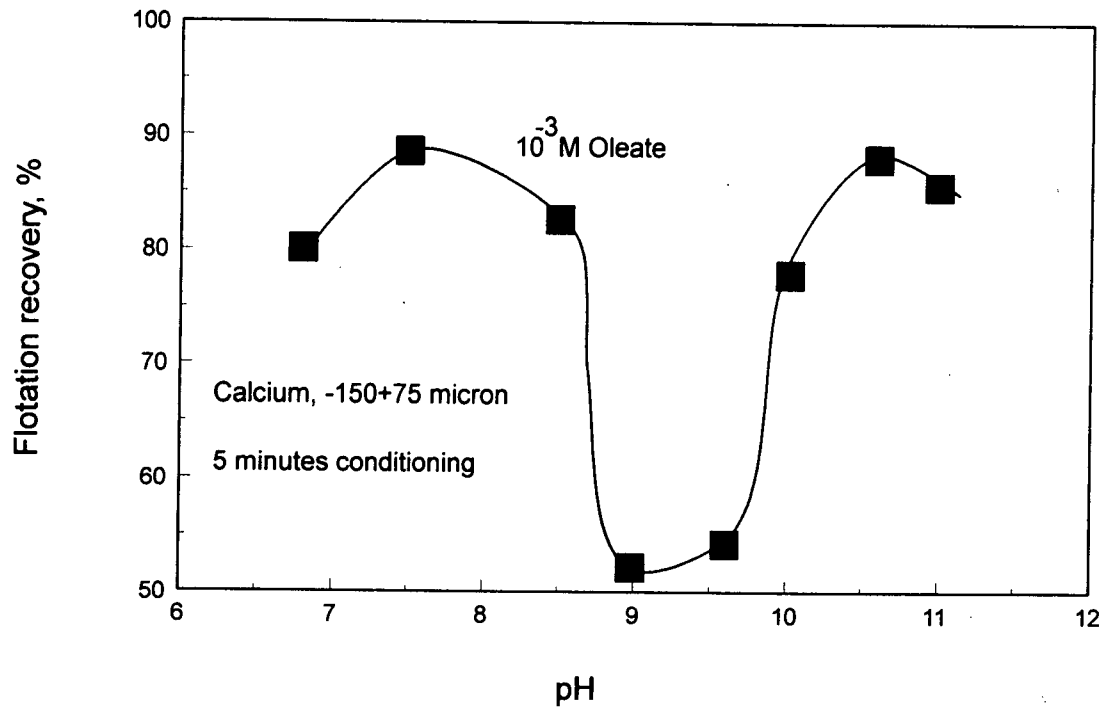


Figure 5.53 - Effect of pH on flotation of calcite with sodium oleate following 5 minutes conditioning

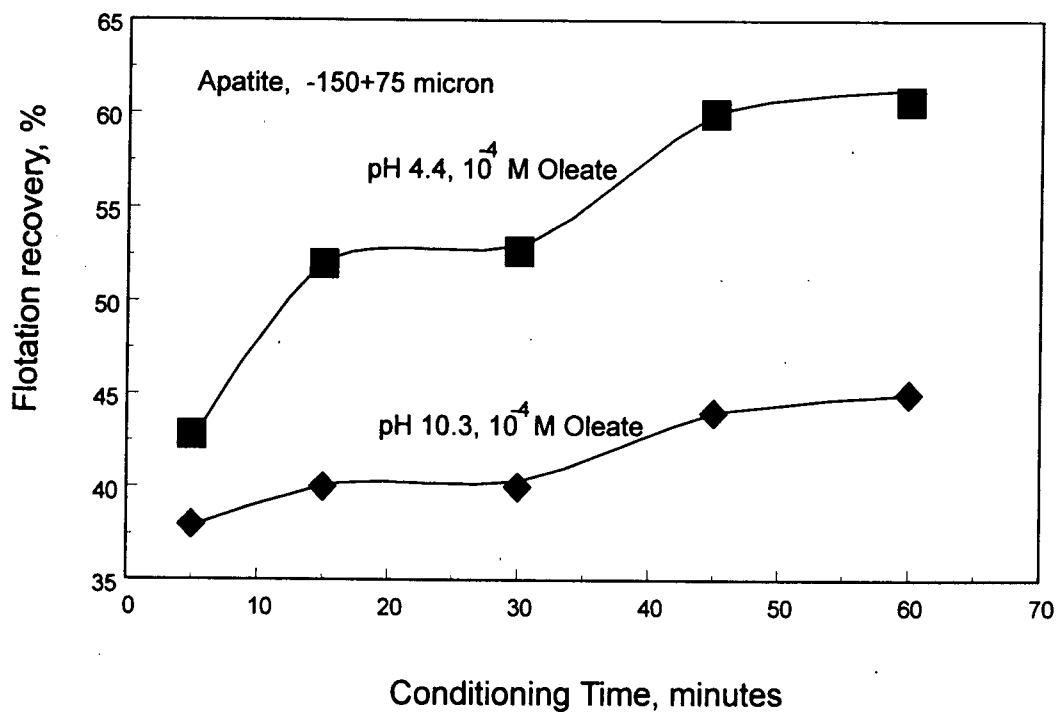


Figure 5.54 - Effect of conditioning time on flotation of apatite under acidic and alkaline conditions

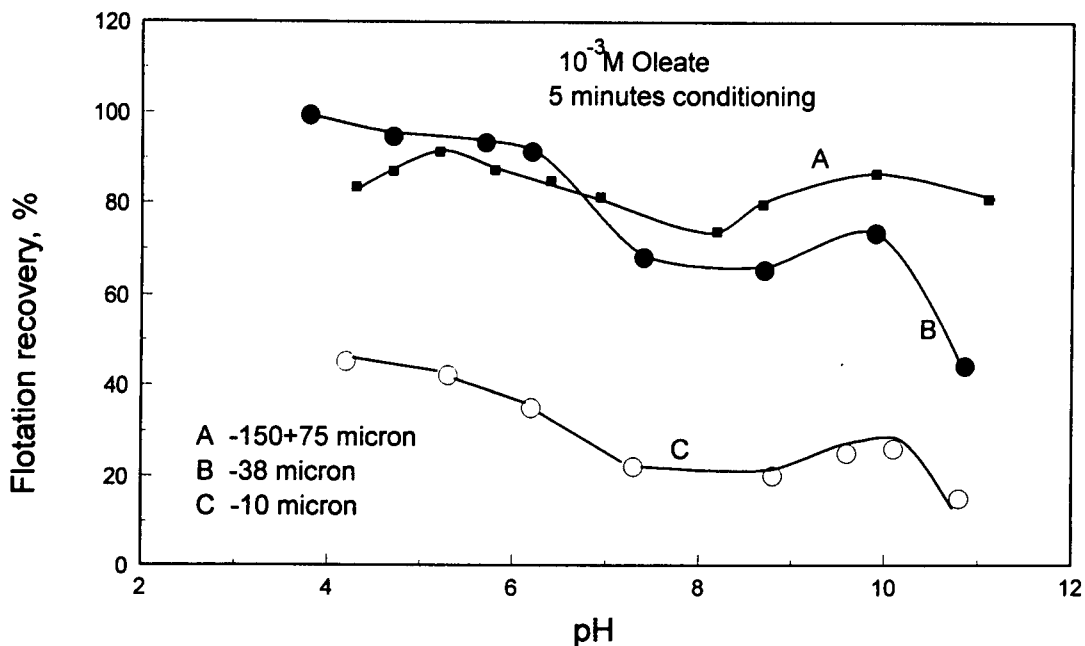


Figure 5.55 - Effect of pH on flotation of different sizes of apatite with sodium oleate

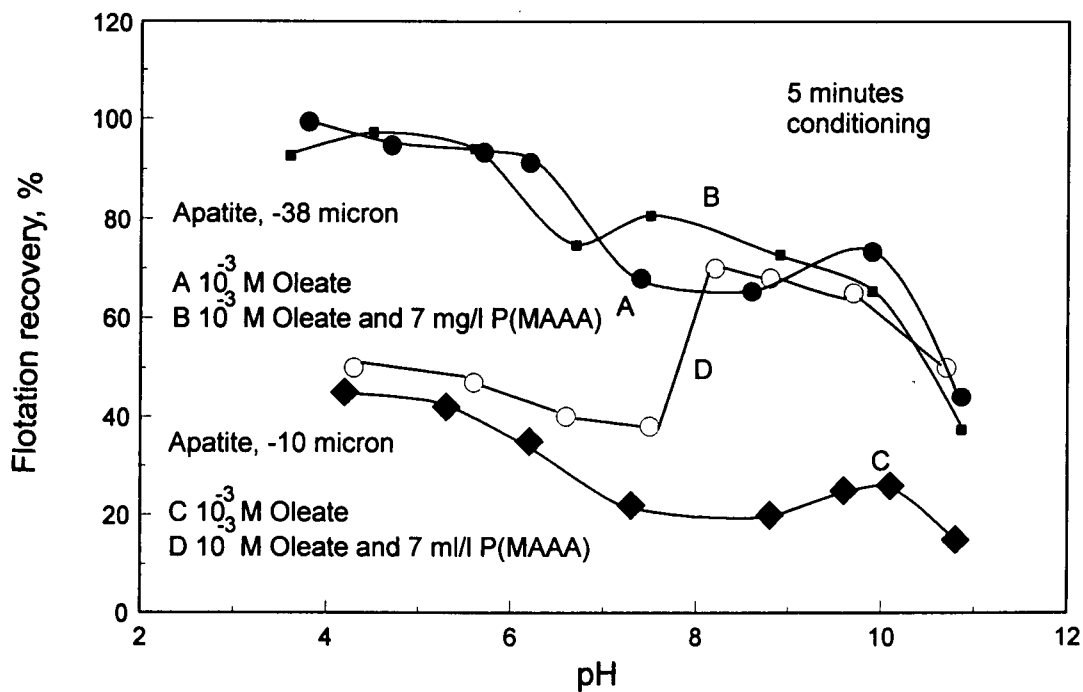


Figure 5.56 - Effect of pH on flotation of fine apatite in the presence of P(MAAA)

the flotation of fine apatite with oleate. While the improvement of the flotation of a -38 μm apatite fraction by the addition of 7 mg/l of P(MAAA) is not pronounced, the improvement in the flotation of a -10 μm apatite fraction is quite substantial. The effect of the addition order of the oleate collector and P(MAAA) latex was also examined, and the results did not reveal any specific effects (Figure 5.57).

Flotation of a -38 μm apatite fraction with P(MAAA) latex was also examined. The results (Figure 5.58) reveal that the flotability of the fine apatite improved with the increasing concentration of P(MAAA) and reached a plateau at a recovery of 40%. This may imply that P(MAAA) latex has some degree of hydrophobicity but, cannot be used alone as a flotation collector. However, it can be used as an extender in the flotation of fine apatite.

The effect of flotation time on the flotation of fine apatite with P(MAAA) latex and an oleate collector was also examined. The results (Figure 5.59) show that a longer flotation time (from 2 minutes to 4 minutes) provides better results, especially in a neutral pH range.

The improvement of the flotation of fine apatite by the addition of P(MAAA) latex must be attributed to the flocculation effect which increased the size of the floated particles and thus enhanced their collision probability with air bubbles.

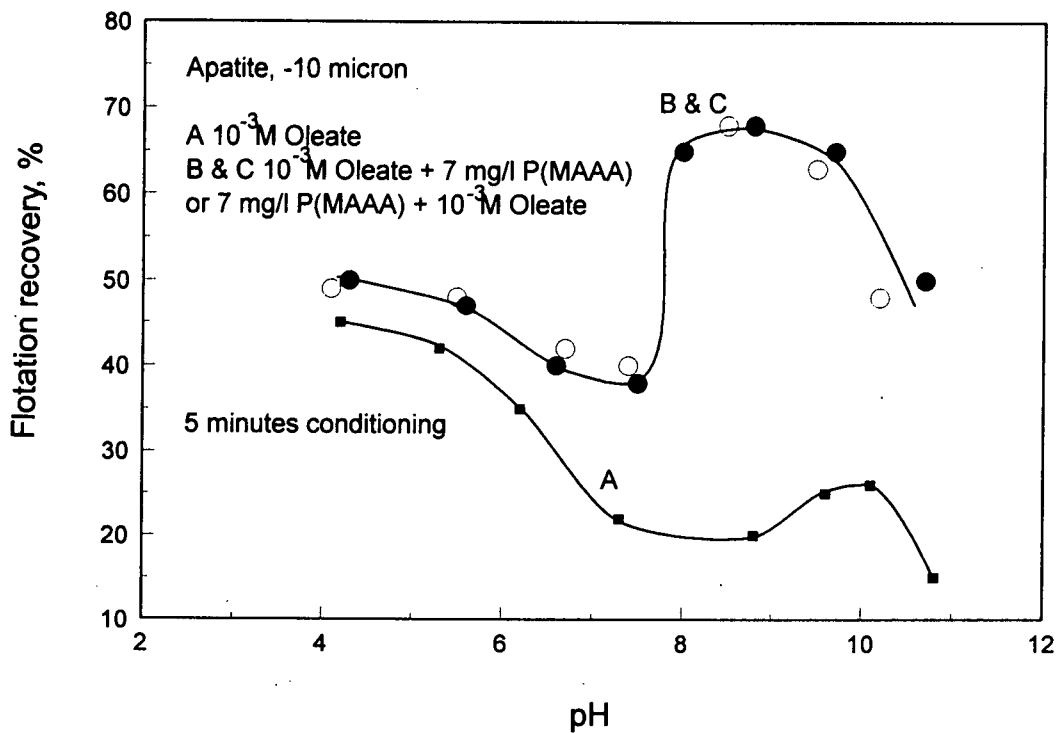


Figure 5.57 - Comparison of effect of addition order of P(MAAA) and oleate on flotation of fine apatite

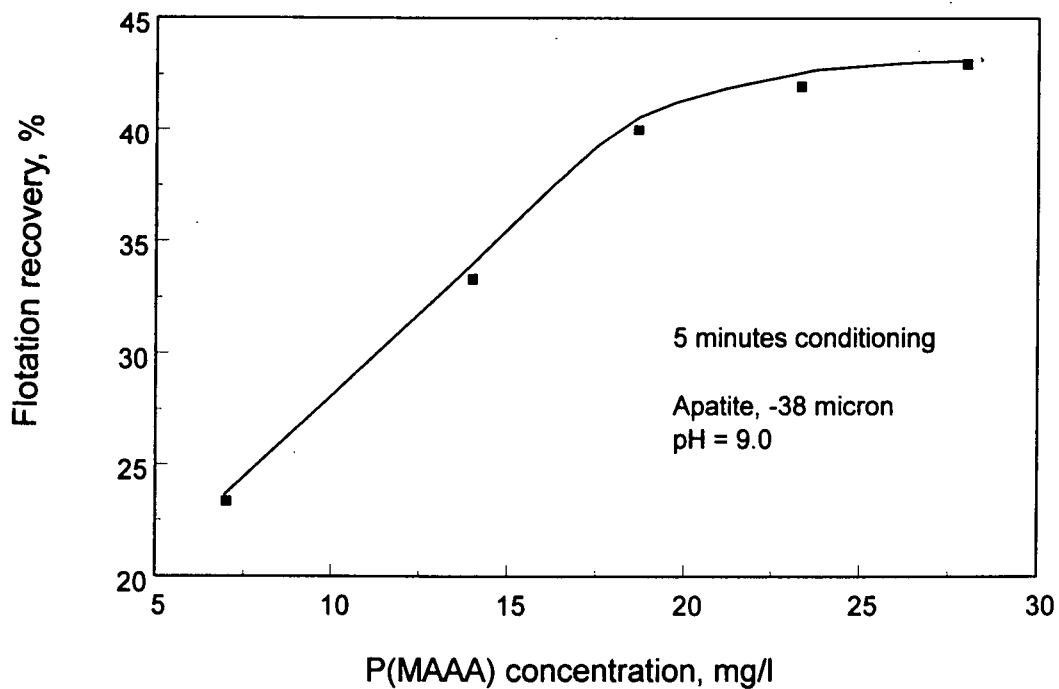


Figure 5.58 - Flotation of fine apatite with P(MAAA) at natural pH

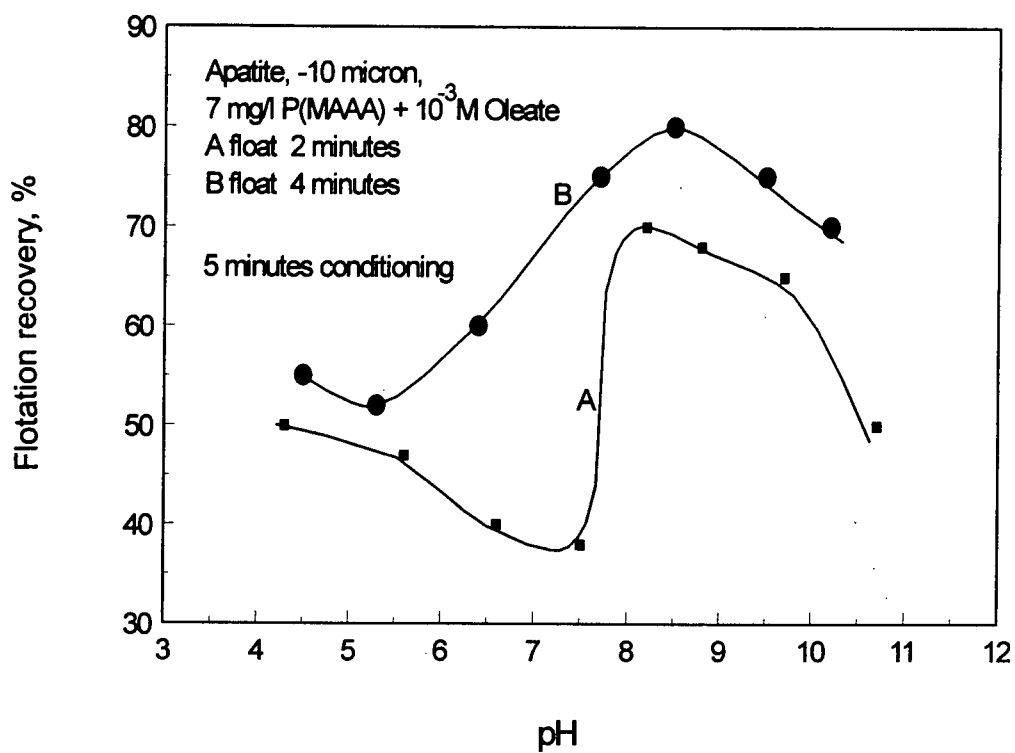


Figure 5.59 - Effect of pH on flotation of fine apatite in the presence of P(MAAA) and oleate for two different flotation times

5.8 Batch Flotation

Flotation of coarse and fine Florida phosphate was tested, and the results are compared in Table 5.4.

Table 5.4 Results of the Flotation of Coarse and Fine Florida Phosphate

Size μm	Oleate kg/t	pH	Product	wt,%	Grade, %		Recovery, %	
					P ₂ O ₅	Insol	P ₂ O ₅	Insol
-420+106	0.6	9.6-9.7	Conc.	8.8	24.1	30.8	43.7	3.1
			Tails	91.2	3.0	90.6	56.3	96.9
	0.8	9.6-9.7	Conc.	14.4	23.8	21.9	71.3	3.7
			Tails	85.6	1.6	96.1	28.7	96.3
	1.0	9.6-9.7	Conc.	24.8	16.1	53.9	83.5	15.6
			Tails	75.2	1.1	95.8	16.5	84.4
		Feed	100	4.8	85.5	100.0	100.0	
-38	0.6	9.6-9.7	Conc.	12.8	10.1	71.1	25.2	10.7
			Tails	87.2	4.4	86.7	74.9	89.3
	0.8	9.6-9.7	Conc.	13.6	12.0	65.4	31.8	10.5
			Tails	86.4	4.1	87.8	68.3	89.5
	1.0	9.6-9.7	Conc.	18.6	8.4	70.5	30.4	15.5
			Tails	81.4	4.4	88.0	69.6	84.5
		Feed	100.0	5.2	84.8	100.0	100.0	
-38	0.6	9.1-9.2	Conc.	3.7	13.5	66.1	9.7	2.9
			Tails	96.3	4.8	85.5	90.3	97.1
	0.8	9.1-9.2	Conc.	7.4	22.1	37.7	31.6	3.3
			Tails	92.6	3.8	88.5	68.4	96.7
	1.0	9.1-9.2	Conc.	12.2	15.6	53.6	36.9	7.7
			Tails	87.8	3.7	89.1	63.1	92.3
		Feed	100.0	5.2	84.8	100.0	100.0	

As indicated in the table, the flotation of the coarse fraction of the phosphate can upgrade the phosphate ore from 5% of P_2O_5 grade to 24% at a recovery of 70% at an oleate dosage of 0.8 kg/t, pH 9.6-9.7 in the absence of a depressant. However, flotation recovery was very poor (32%) with the fine fraction under similar flotation conditions. Apparently P_2O_5 grade (12%) in the flotation concentrate has substantially decreased. The reduction in grade was mainly caused by the small mass and momentum of fine silica particles. These particles were carried into the froth after either becoming entrained in the liquid or mechanically entrapped with particles being floated. When flotation was carried out at pH 9.1-9.2, the grade of flotation concentrate was improved, e.g., 22%, but the fraction of material that transported to the froth was very small, e.g., 7%. Sodium silicate was added to improve the flotation selectivity. The results, as indicated in Table 5.4, show that the P_2O_5 grade in the flotation concentrate increased to 24% at a recovery of 45%. The P_2O_5 recovery is still very low. This is mainly due to the fine particle size. The addition of P(MAAA) latex has increased the P_2O_5 recovery to 85% with a 21% P_2O_5 grade, as indicated in Table 5.5.

Apparently, the fraction of material that was transported to the concentrate increased by the addition of P(MAAA) latex. This suggests that the flocs produced by P(MAAA) latex are strong enough to withstand the hydrodynamic conditions in the flotation cell. Increasing the P(MAAA) dosage to 0.3 kg/t, caused the grade in the concentrate to drop to 10% P_2O_5 . It is believed that silica in the phosphate suspension was activated by calcium ions and that a high dosage of P(MAAA) latex caused the silica to flocculate.

Table 5.5 Results of the Flotation of Fine (-38 μm) Florida Phosphate in the Presence of Sodium Silicate (meta) and P(MAAA) Latex

Oleate kg/t	Na silicate kg/t	P(MAAA) kg/t	pH	Product	wt,%	Grade,%		Recovery,%	
						P ₂ O ₅	Insol	P ₂ O ₅	Insol
1	1.0	0	9.1-9.2	Conc.	10.4	22.4	37.4	44.8	4.6
				Tails	89.6	3.2	90.2	55.2	95.4
1	1.2	0	9.1-9.2	Conc.	9.6	24.2	34.6	44.6	3.9
				Tails	90.4	3.2	90.1	55.4	96.1
1	1.0	0.1	9.1-9.2	Conc.	16.8	22.1	37.7	72.1	7.5
				Tails	83.2	1.7	94.3	27.9	92.5
1	1.0	0.2	9.1-9.2	Conc.	20.7	21.2	39.4	85.1	9.6
				Tails	79.3	1.0	96.6	15.0	90.4
1	1.0	0.3	9.1-9.2	Conc.	31.5	10.8	77.4	65.8	28.7
				Tails	68.5	2.6	88.2	34.2	71.3
				Feed	100.0	5.2	84.8	100.0	100.0

5.9 2³ Factorial Design Experiments

The results of the factorial design experiments on the apatite-calcite and apatite-silica flocculation with P(MAAA) latex and the results of the calculation of main and interaction effects among factors on the recovery and grade are summarized below.

Apatite - Calcite system

Table 5.6 Results and Calculations of Factorial Experiments for the Apatite-Calcite System

Run	Recovery	Grade	X_1	X_2	X_3	$X_1 X_2$	$X_2 X_3$	$X_1 X_3$	$X_1 X_2 X_3$
1	94.0	30.4	+	+	+	+	+	+	+
2	69.1	31.0	+	-	-	-	+	-	+
3	66.5	32.1	+	-	+	-	-	+	+
4	67.8	33.9	-	+	+	-	+	-	-
5	94.7	30.1	+	+	-	+	-	-	-
6	38.4	30.1	-	-	-	+	+	+	-
7	71.0	31.2	-	+	-	-	-	+	+
8	31.4	29.2	-	-	+	+	-	-	+
Effect on apatite recovery			28.9	30.5	-3.4	-4.0	1.4	1.7	-0.4
Effect on grade of apatite concentrate			-0.2	0.8	0.8	-2.1	0.7	-0.1	-1.1

Columns of X_1 , X_2 and X_3 stand for the latex dosage, pH and concentration of sodium tripolyphosphate; and columns of $X_1 X_2$, $X_2 X_3$, $X_1 X_3$ and $X_1 X_2 X_3$ represent the interaction effects among the factors. Detailed calculations of the main and interaction effects and an assessment of the significance of these effects are given in Appendix II.

Standard deviation estimated on the three replicate centrepoints is

Recovery, % 85.4 87.5 89.6 $s_R^2 = 4.3$

Grade, % 30.0 31.3 31.5 $s_G^2 = 0.7$

s_R represents standard deviation for recovery, s_G represents standard deviation for grade.

The standard deviation on the two previous points is

Recovery, % 64.1 67.2 $s_R^2 = 4.8$

Grade, % 22.5 23.6 $s_G^2 = 0.6$

The pooled variance s which combines the error estimates from the above two different sources gives 2.1 for the apatite recovery and 0.8 for the grade of apatite concentrate. The detailed calculation of the standard deviation and pooled variance is given in Appendix II.

The precision of the estimated effects is generally stated in the form of a confidence interval, which is an interval to include the "true" effect at a stated confidence level. A 95% confidence interval is 4.7 for the apatite recovery and 1.8 for the grade of the apatite concentrate (the detailed calculation is given in Appendix II). Therefore, the estimated main and interaction effects on the recovery and grade at the 95% confidence intervals are:

	Effect on Recovery, %	Effect on Grade, %
X_1 P(MAAA) latex dosage (2 - 3 kg/t)	28.9 ± 4.7	-0.2 ± 1.8
X_2 pH (9 - 10)	30.5 ± 4.7	0.8 ± 1.8
X_3 NaTPP (2 - 6 ppm)	-3.4 ± 4.7	0.8 ± 1.8
X_1X_2	-4.0 ± 4.7	-2.1 ± 1.8
X_2X_3	1.4 ± 4.7	0.7 ± 1.8
X_1X_3	1.7 ± 4.7	-0.1 ± 1.8
$X_1X_2X_3$	-0.4 ± 4.7	-1.1 ± 1.8

The above results show that the effects of latex dosage and pH within the tested range are significant on the recovery at the 95% confidence level. The increase of the latex dosage from 2.0 kg/t to 3.0 kg/t increases the recovery by 29%; and the increase of pH from 9.0 to 10.0 increases the recovery by 30%, averaged over all levels of other factors. However, the increase of sodium tripolyphosphate from 2 ppm to 6 ppm does not have a significant effect on the recovery. The previous flocculation result (Figure 5.42) showed that the apatite recovery increased when the concentration of sodium tripolyphosphate increased from 2 ppm to 4 ppm then decreased when the concentration of sodium tripolyphosphate further increased to 6 ppm, at a constant dosage of the P(MAAA) latex. This may explain the result of the factorial experiment and imply a curvature effect. The overall curvature effect is defined as the difference between the experimental centerpoint response and the centerpoint value (average value) from a designed experimental run. The estimated overall curvature effect is 20.9 ± 3.4 for the recovery and 0.1 ± 1.3 for the grade (for the detailed calculation see Appendix II). This effect is significant for the recovery but is not significant for the grade as also can be seen from the results of the previous varying-single-factor experiment (Figures 5.42, 5.44).

In Figure 5.42, the curve of the recovery vs. the concentration of sodium tripolyphosphate reaches a maximum at 4 ppm of the sodium tripolyphosphate concentration while the grade curve shows an increase tendency as the concentration of sodium tripolyphosphate. A similar phenomenon was observed in Figure 5.44. The recovery curve reaches a maximum at around pH 9.3 while the grade curve shows an increase tendency as the pH.

The effects of the latex dosage, pH and concentration of sodium triphosphate within the tested range are not significant on the grade at the 95% confidence level. The X_1X_2 effect on the grade is significant and is not significant on the recovery. The negative value of X_1X_2 implies a negative effect which means that an increase of the latex dosage may increase the grade at a constant value of pH but at another constant value of pH the increase of the latex dosage may decrease the grade within the range tested. The remaining interaction effects are not significant at the 95% confidence level because these effects include zero in the confidence interval. In general, the results of the factorial experiment agree well with the results obtained from the previous flocculation tests.

Apatite - Silica System

The results of the factorial experiments of the flocculation tests for the apatite-silica system including main effects and interaction effects among factors are given in Table 5.7.

Table 5.7 Results and Calculations of Factorial Experiment for the Apatite-Silica System

<u>Run</u>	<u>Recovery</u>	<u>Grade</u>	X_1	X_2	X_3	$X_1 X_2$	$X_2 X_3$	$X_1 X_3$	$X_1 X_2 X_3$
1	90.4	33.6	+	+	+	+	+	+	+
2	89.7	30.5	+	-	-	-	+	-	+
3	93.3	32.6	+	-	+	-	-	+	+
4	81.8	32.1	-	+	+	-	+	-	-
5	91.3	32.6	+	+	-	+	-	-	-
6	65.6	27.4	-	-	-	+	+	+	-
7	76.0	27.9	-	+	-	-	-	+	+
8	73.3	29.3	-	-	+	+	-	-	+
Effect on apatite recovery			17.0	4.4	4.1	-5.1	-1.6	-2.1	-0.7
Effect on grade of concentrate			3.2	1.6	2.3	-0.0	0.3	-0.8	-0.9

Standard deviation was estimated on three centerpoints:

Recovery, %	88.4	90.7	88.3	$s_R = 1.4$
Grade, %	30.7	31.8	32.4	$s_G = 0.9$

The 95% confidence interval is 4.0 for the recovery and 2.7 for the grade (the detailed calculation is given in Appendix II). Therefore, the estimated main and interaction effects on the recovery and grade at the 95% confidence intervals are:

	Effect on Recovery, %	Effect on Grade, %
X_1 P(MAAA) latex dosage (1-2 kg/t)	17.0 ± 4.3	3.2 ± 2.7
X_2 pH (8.8-10)	4.4 ± 4.3	1.6 ± 2.7
X_3 Na silicate (10-30 ppm)	4.1 ± 4.3	2.3 ± 2.7
X_1X_2	-5.1 ± 4.3	-0.0 ± 2.7
X_2X_3	-1.6 ± 4.3	0.3 ± 2.7
X_1X_3	-2.1 ± 4.3	-0.8 ± 2.7
$X_1X_2X_3$	-0.7 ± 4.3	-0.9 ± 2.7

The above results show that the effect of the latex dosage on the recovery and grade is significant at the 95% confidence level. The increase of latex dosage from 1.0 kg/t to 2.0 kg/t averaged over all levels of other factors increases the recovery by 17% and the grade by 3%. The effect of pH is significant on recovery but not on grade within the tested range. The effect of concentration of sodium silicate is not significant within the tested range. The previous univariant experiments show that the recovery reaches a maximum at 20 ppm of sodium silicate (Fig. 5.45) and then decreases as the concentration of sodium silicate further increases to 30 ppm. The recovery reaches a maximum at around pH 10 then

decreases as pH further increases (Fig. 5.47). The Figure 5.47 also shows that the effect of pH on the grade is not significant in the pH range of 6 to 10.

The estimated overall curvature effect which is 6.4 ± 2.2 for the recovery and 0.8 ± 1.4 for the grade also confirms the existence of a maximum on the recovery curve. The interaction effect of X_1X_2 is significant on the recovery. The negative value means a negative effect which implies that an increase of the latex dosage may increase the recovery at a constant value of pH but at another constant value of pH the increase of the latex dosage may decrease the recovery. The remaining interaction effects are not significant at the 95% confidence level. The results of the factorial experiments agree well, in general with the results obtained from the varying-single-factor experiment except that the single-factor experiment explored a larger range of magnitude of each variable but did not observe interactions between factors.

CHAPTER 6 GENERAL DISCUSSION

6.1 Effect of the Characteristics of Latex Particles on Interaction with Mineral Surfaces

Latex particles are known to be flexible and possess a hair-like structure on the surface. These unique characteristics are reflected in their deposition process and interaction with solid surfaces. Van de Ven et al. (1983) observed that latex particles deposited on solid surfaces execute a type of oscillatory or "dancing" motion. This motion of the particles over the surface suggests that they are bound to the surface by a long invisible flexible connection leading van de Ven et al. (1983) to conclude that long chain-like structures exist in latex systems. Additional evidence in support of a hairy structure for latex particles is the fast deposition and adherence of latex particles to solid surfaces even in the presence of large energy barriers (Dabros and van de Ven, 1984). It is possible that the large "tails" either lie very loosely on the particle surface creating a roughness or dangle from the sphere forming flexible bonds. The surface roughness of latex particles reduces the zeta potential and thus the energy barrier between the latex particles and the solid surface (Chow and Takamura, 1988).

Although polystyrene latex is considered to be flexible, it is relatively rigid when compared to other latices because of its high glass transition temperature. The monodisperse polystyrene latex is easily prepared and has been used as a model colloidal system. The P(EHMA) latex is relatively soft as characterized by its low glass transition temperature. Its flexibility is higher than that of polystyrene latex; thus, the adhesion force to the solid surface is likely to be stronger. The adsorption of potassium oleate on latex

particles not only introduces the carboxylic groups and C=C bonds on the surface of latex particles but also imparts the latex flexibility. Although the electrokinetic potential becomes more negative with the adsorption of potassium oleate on latex surfaces, the interaction process appears to be dominated by the chemical functional groups and physical characteristics of the latex. Thus, the latex with the higher oleate concentration has the higher affinity towards mineral surfaces. Since an increase in oleate concentration in the emulsion polymerization decreases the latex particle size at a constant concentration of monomers, the small size of latex particles may also affect the interaction process.

The P(MAAA) latex is quite different from the PS and P(EHMA) latices. It is a copolymer of methyl acrylate and acrylic acid in a molar ratio of 1.4:1. The polymerization of acrylic acid alone produces the water soluble polyacrylic acid. This polymer has been known to flocculate apatite (Pradip and Moudgil, 1991; Mehta, 1993). The copolymerization of methyl acrylate and acrylic acid in the molar ratio of 1.4:1 produces a latex by introducing hydrophobic units (methyl acrylate) into the polymer chain. The hydrophobicity of the resulting P(MAAA) latex is lower than that of the PS and P(EHMA) latices because it contains more hydrophilic units (acrylic acid) in the polymer chain. As a result, the latex particles look loose as revealed by the electron micrograph. The hydrophobicity of the latices does not seem to have a direct effect on the interaction of the latex particles with the tested minerals.

The P(EHMA) latex is considered to be a better flocculant of fluorite, apatite and calcite than P(MAAA) because of its soft and flexible characteristics. The flocculation of the three minerals is sensitive to the dosage of the P(EHMA) latex. Carboxylic groups are physically adsorbed on the surface of this latex as indicated by the decrease of the electrophoretic mobility measured on this latex which was treated with ion exchange resin

(Figure 5.2). This latex still exhibited a high flocculation power even after removing the surface oleate. The attachment of the emulsifier-free latex particles to the mineral surfaces may also be due to the interaction between sulfate groups on the surface of the latex particles and calcium sites on the mineral surfaces. As a result, the selectivity of the P(EHMA) latex is not very good.

6.2 The Role of P(MAAA) Latex in the Selective Flocculation of Apatite, Calcite and Silica

P(MAAA) latex shows better selectivity towards fluorite and apatite than P(EHMA) latex. The chemically bound carboxylic group on the surface of P(MAAA) latex seems to play a major role in the interaction with the minerals. The carboxylic groups on the latex surface completely ionize at pH 9.2 - 9.5, as shown in Figure 5.3. At this pH and a dosage of 2.2 kg/t, 90% of apatite and only about 5% of calcite flocculated. At a lower dosage of 1.1kg/t, 60% of apatite flocculated while calcite did not flocculate at all. Thus, the selectivity of P(MAAA) latex towards apatite and calcite is determined by its dosage and pH. The interaction between the carboxylic groups on the latex particles and calcium sites on the mineral surfaces seems to be a dominant factor. This probably results from good coincidence between the surface stereo-chemistry of the carboxylic groups on the latex and Ca-sites on the surface of fluorite and apatite. This may also explain why the deposition density of P(MAAA) latex particles is lower on calcite than on fluorite and apatite. The P(MAAA) latex particles are not interacting with silica because of the absence of calcium sites on a silica surface. In addition, the electrostatic repulsion between the highly negative silica and P(MAAA) latex particles imposes a large energy barrier on

collision. However, when silica was mixed with apatite, the calcium ions apparently leached out from the apatite adsorbed onto the silica and reduced flocculation selectivity.

6.3 Loss of Selectivity in the Mixed Component Systems

The reasons for loss of selectivity in the mixed component systems have been discussed in many papers (Yarar and Kitchener, 1970; Rubio and Goldfarb, 1975; Attia and Fuerstenau, 1978; Somasundaran, 1980; Bagster, 1985; Krishnan, Attia, 1986; Moudgil et al., 1987(a), 1987(b); Singh, Adler, Moudgil et al., 1998). These include dissolved ion activation, heterocoagulation, physical entrapment or entrainment in the flocs, polymer-induced entrapment (also referred to as "heteroflocculation"), and surface contamination during grinding. Heterocoagulation involves Coulombic interaction between oppositely charged components. Generally, heterocoagulation can be minimized by adding a dispersant to modify surface charge. In dealing with salt-type minerals, activation of the gangue components (e.g., silica) by dissolved ions from other minerals (e.g., calcium minerals) in the suspension can occur. The use of suitable additives to complex the interfering dissolved ions can minimize the loss of selectivity.

The entrapment of gangue in flocs or the entrainment of gangue during the settling or flotation of flocs primarily depends on the pulp density, the relative number and size of particles of various minerals, and the nature of the flocs. Additional influences may include agitation during flocculation and the separation technique utilized to separate the aggregated fraction from the dispersed material. The entrainment of gangue particles can be significantly reduced by washing the flocs since gangue particles are carried with the

flocs while settling or floating. However, to minimize the entrapment of gangue species within flocs, the aggregates will have to be dispersed again.

Heteroflocculation (entrapment) is caused by the adsorption of flocculant onto the gangue component which then is included in the flocs of the valuable component. In such a case, the gangue material cannot be removed from the flocs by washing or other physical methods. The entrapment of the gangue component has been attributed to the formation of bridges between polymer coated sites on the gangue constituent and vacant "active" sites on another particle and vice versa. The role of active sites in selective flocculation has been discussed by Moudgil and Vasudevan (1988) and Moudgil, Shah and Soto (1987). The separation of dolomite and silica from apatite by using lower molecular weight PEO as a site blocking agent has been demonstrated to be an effective method to minimize heteroflocculation (Behl and Moudgil, 1993; Moudgil et al., 1994).

In this study, the addition of a small amount of sodium tripolyphosphate and sodium silicate improved the selectivity of the P(MAAA) latex in apatite-calcite and apatite-silica systems. Sodium tripolyphosphate works better than sodium silicate in the apatite/calcite system. The zeta potentials of apatite and calcite were negative (-20 ~ -30 mV) and very close in the alkaline pH range before the addition of the dispersant. The addition of sodium tripolyphosphate increased the negative charge of both minerals; this is likely due to the adsorption of phosphate anions at the calcium sites on the mineral surfaces. In the presence of 2 ppm sodium tripolyphosphate, apatite became much more negative (-45 mV) than calcite (-28 mV). Although an increase of sodium tripolyphosphate concentration slightly increased the negative potential of calcite, the insignificant increase in zeta potential indicates a limited number of available calcium sites on this mineral. This also explains the poor flocculation of calcite with latices. In fact,

calcite flocculation was completely depressed in the presence of 2 ppm of sodium tripolyphosphate.

Sodium silicate is superior to sodium tripolyphosphate at improving the selectivity of P(MAAA) latex in the apatite-silica system. It is well known that sodium silicate depresses silica. Sodium silicate forms various colloidal species in aqueous solution, and it is known to adsorb by multiple weak bonds to form hydrated layers at the mineral surface. Dispersion is stabilized by both an increased negative charge and the hydrated layers. In comparison to sodium tripolyphosphate, sodium silicate does not confer an effective negative zeta potential on calcite in a pH range of 9 - 10, but it increases the negative zeta potential of silica. Both sodium tripolyphosphate and sodium silicate make the zeta potential of apatite more negative. The same increment of the negative zeta potential can be achieved at a lower concentration of sodium tripolyphosphate than of sodium silicate.

6.4 The Role of Latex P(MAAA) in Flotation of Fine Apatite

Flotation recoveries are significantly lower for fine particles. When a system contains fine and coarse particles, various factors reduce the efficiency of the flotation process. The primary factors for poor flotation recovery of fines include: (1) The small mass and momentum of fine particles which may be carried into the froth by either entrainment in the liquid or entrapment with particles being floated. If these fine particles are gangue, that will reduce the concentrate grade. The entrainment is different from "true" flotation. A detailed discussion of entrainment of particles into flotation froths has been given by Smith and Warren (1989). Based on the available work on the entrainment in conventional flotation systems, they observed a strong correlation between the recovery of gangue and

the recovery of water, in both batch and continuous flotations. In general, it has been found that the higher the "recovery" of water, that is the "wetter" the froth, the higher the proportion of gangue and the lower the concentrate grade. The proportionality between water and gangue in the concentrate has been observed to depend on pulp density as well as on particle size. The higher the pulp density and the finer the particles the higher the amount of gangue entrained in the froths at a given recovery rate. The higher entrainment of fines is associated with the fact that they tend to move with the water due to their low sedimentation velocities. (2) The large specific surface area of fine particles increases the adsorption capacity of the reagents. If a significant proportion of the reagent is consumed by small particles, there may not be sufficient reagent available for the flotation of larger particles with a resultant decrease in recovery. (3) Surface and electrochemical properties of fine particles tend to be different from those of coarse particles of the same material. Fine mineral particles have higher specific surface energy because of the increased number of edges, corners and crystallographic imperfections, and this may influence flotation in a number of ways. For example, increased dissolution from the surface of fine particles may introduce undesirable impurities into the solution and affect the collector/mineral interactions. The high surface energy of particles also increases the tendency of collectors to adsorb nonspecifically. Flotation rate studies have confirmed that fine particles float more slowly than those of intermediate sizes (Trahar, 1981).

The P(MAAA) latex improves the flotation of fine apatite mainly through increasing the size by flocculation of the fine particles thereby increasing the collision probability between particles and air bubbles. Since the tested latices are hydrophobic as found from the contact angle measurement, the floc hydrophobicity is apparently not affected by the latex. Microflotation results have shown that the highest flotation recovery

with the P(MAAAA) latex is about 40%. However, the combination of the latex together with oleate was found to increase the flotation of fine apatite substantially. This was shown in the Hallimond tube flotation on pure apatite, as well as in batch flotation on Florida phosphate. It should be noted that the dosage of P(MAAA) latex is critical since an excess amount of the latex also flocculates gangue minerals and results in decreases of concentrate grade. In the system with oleate and flocs, oleate may adsorb on the surface of the latex through the hydrophobic interaction.

CHAPTER 7 CONCLUSIONS

1. Oleic acid emulsifier is physically adsorbed on surfaces of P(EHMA) and PS latex particles in emulsion polymerization. The adsorption of the emulsifier on the latex particles introduces the carboxylic groups onto the surface of the latex particles, increases the electrophoretic mobility of the latex particles, and also imparts flexibility to the latex particles. The P(MAAA) latex is produced by an surfactant-free emulsion copolymerization of methyl acrylate and acrylic acid in a molar ratio of 1.4:1, thus the carboxylic group is chemically bound to the surface of the latex particles.
2. An increase of the emulsifier concentration in the emulsion polymerization increases the content of carboxylic groups on the surface of latex particles as reflected by the increased electrophoretic mobility. The size of latex particles decreases with increasing concentration of emulsifier at a constant concentration of monomer.
3. The hydrophobicity of latices has been characterized by contact angle measurements for water on the dried films. The contact angles for PS, P(EHMA) and P(MAAA) are $84\pm 4^\circ$, $65\pm 3^\circ$ and $38\pm 4^\circ$ respectively.
4. Apatite and fluorite samples were found to contain carbonates on their surfaces as indicated by the FTIR spectra. The surface carbonates may be intergrown with the minerals or may have formed during the sample preparation. Silica is very pure as characterized by the chemical analysis. The measured isoelectric points of apatite and fluorite of 5 and 6, respectively, closely agree with the reported values. The calcite and silica samples did not have measurable iep. The BET specific surface areas for size range of 100% -38 μm of apatite, fluorite, calcite and silica are 18.34, 0.28, 3.13 and

0.90 m²/g respectively. The large specific surface area of apatite indicates porosity of the mineral.

5. The P(EHMA) and P(MAAA) latices were found to flocculate apatite, fluorite and calcite but not silica. They showed higher affinity towards apatite and fluorite than calcite. The P(EHMA) latex exhibited higher flocculation power but less selectivity than the P(MAAA) latex. The selectivity of P(MAAA) towards apatite, fluorite and calcite depends on its dosage and pH at the constant values of other factors, e.g., temperature, mixing conditions and pulp density.
6. The separation of apatite-calcite and apatite-silica mixtures with the P(MAAA) latex can be improved by the addition of dispersing agents, sodium tripolyphosphate or sodium silicate. The addition of sodium tripolyphosphate in the apatite-calcite mixture produces a higher selectivity increase than sodium silicate does while in the apatite-silica mixture sodium silicate produces a higher selectivity increase. At a P(MAAA) dosage of 2.2 kg/t, pH around 9.1-9.5, and 4 ppm of sodium tripolyphosphate, 90% of apatite can be recovered from a 1:1 apatite-calcite mixture with a 33% P₂O₅ grade (SI=0.7) in the concentrate. For the apatite-silica mixture, at a P(MAAA) dosage of 1.1 kg/t, pH around 9.1 - 9.3 and 20 ppm of sodium silicate, 80% of apatite can be recovered with a 33% P₂O₅ grade (SI=0.7) in the concentrate.
7. Deposition of the P(EHMA) latex on fluorite surfaces was not observed. The highly negative electrokinetic potential of the latex particles and a large resulting energy barrier between the latex particles and the mineral surface are probably responsible for this phenomenon. Deposition of the P(EHMA)-R latex was not observed on fluorite surfaces either, and this is attributed to the insignificant number of carboxylic groups on the surface of latex particles. Deposition was observed with P(MAAA) latex which

indicates that chemical interaction plays a major role in the deposition process. The deposition density observed under similar conditions as flocculation tests agrees well with the flocculation results.

8. The P(MAAA) latex can be used as a flotation aid in the flotation of fine apatite as observed in a Hallimond tube flotation on pure apatite mineral, as well as in a batch flotation on phosphate ore. The flocs produced by the P(MAAA) latex are apparently strong enough to withstand hydrodynamic conditions in the flotation cell. The hydrophobic nature of this flocculant seems to be compatible with the flotation collector, and, this characteristic favors its use in flotation.
9. The affinity of the latices to the mineral surfaces is mainly due to the short range chemical interaction between the carboxylic groups on the surface of latex particles and the calcium sites on mineral surfaces. This has been proved by the strong attractive interaction between the highly negative charge latex particles and the negative charge mineral particles in the alkaline pH range. The classical DLVO theory can not be used to explain the interaction. The soft and flexible characteristics of latex particles enhance the adhesion between latex particles and mineral surfaces.
10. The results of the factorial design flocculation experiment show that, for an apatite-calcite mixture, the increase of the latex dosage from 2.0 kg/t to 3.0 kg/t increases the recovery by 29% and that an increase of pH from 9.0 to 10.0 increases the recovery by 30% averaged over all levels of other factors. The effect of concentration of sodium tripolyphosphate is not significant within the range tested. The effect of the interaction of the latex dosage and pH on the grade is significant and is not significant on the recovery indicating a possible interaction between these two factors. The other interaction effects are not significant. The overall curvature effect is significant on the

recovery but is not significant on the grade. For an apatite-silica mixture, the increase of latex dosage from 1.0 kg/t to 2.0 kg/t averaged over all levels of other factors increases the recovery by 17% and grade by 3%. The effect of pH is significant while the effect of concentration of sodium silicate is not significant within the range tested. The effect of the interaction of the latex dosage and pH on the recovery is significant and the other interactions are not significant at the 95% confidence level. The curvature effect is significant on the recovery but not on the grade. In general, the results agree well with the results obtained from the varying-single-factor experiment.

CHAPTER 8 SUGGESTIONS FOR FUTURE WORK

Many of the findings in the present thesis warrant further research. Some suggestions are as follows.

1. The effectiveness of the P(MAAA) latex in the flocculation of fine natural phosphate ore should further be tested. The effect of various factors, such as the latex dosage, pH, type and dosage of dispersing agents, pulp density, temperature and mixing conditions on the selective flocculation of apatite from the phosphate ore should be examined. Different types of phosphate ores, such as siliceous gangue-containing, or calcareous gangue-containing phosphate ores should be tested with the P(MAAA) latex.
2. The effect of P(MAAA) latex on flotation of various types of phosphate ores requires further tests which should also include the tests of effect of hydrodynamic conditions and flotation collector in the presence of the P(MAAA) latex .
3. The deposition process used as a method of studying mineral-latex interaction should be evaluated further and the effect of the ionic strength and the disc rotation speed on the deposition should also be included in the test.
4. Optimization experiment

If the process is to be commercialized, the parametric optimization is necessary to find the best settings of the variables in order to produce the best product at the lowest cost.

The optimization experiment can be conducted at ambient temperature as in most conventional mineral concentration processes. Five factors, P(MAAA) latex dosage, pH,

concentration of dispersant, pulp density and mixing conditions should be included in the first step of optimization - rough optimization.

The five factors together with their factor-level ranges:

P(MAAA) latex dosage, kg/t,	X_1	0.5 - 2
pH	X_2	6 - 10
Sodium tripolyphosphate, mg/l	X_3	1 - 6
(or Sodium silicate, mg/l)		10 - 60
Pulp density, wt%	X_4	1 - 10
Mixing condition, rpm	X_5	100 - 500

The primary emphasis of the rough optimization is to identify the most important factors. Secondary goals will be rough detection of second-order effects (curvature and interaction), and obtaining a better estimate of response error for use in later investigation.

The relationship of response and variables can be described by the following equation:

$$Y = b_0 + b_1X_1 + \dots + b_nX_n + b_{12}X_1X_2 + \dots + b_{mn}X_mX_n + (\text{overall curvature})$$

The final optimization will require a full quadratic model as shown in the following equation to accurately predict the point of optimal response.

$$Y = b_0 + b_1X_1 + \dots + b_nX_n + b_{11}X_1^2 + \dots + b_{nn}X_n^2 + b_{12}X_1X_2 + \dots + b_{mn}X_mX_n$$

All the terms in the model should be estimated. Computer softwares are available to calculate these terms. Once the experimental factors and their ranges are chosen, the proper softwares (e.g., Graphics) can be chosen to calculate the terms and to optimize the factor response.

CHAPTER 9 REFERENCES

- Abramov, A. A., Abramov, Al. Al., et al, 1993, "Mechanism of Reverse Flotation of Calcareous Phosphate Ores", **Beneficiation of Phosphate: Theory and Practice**, Eds. H. El-Shall, B. M. Moudgil et al, SME, Littleton, Colorado, USA, pp. 281-288.
- Abramov, A. A. and Magazanik, D. V., 1998, "Regularities of Hydrophobisation and Floation of Fluorite", **Fizykochemiczne Problemy Metallurgii**, 32, pp. 183-193.
- Adamczyk, Z. and Pomianowski, A., 1980, "Investigation on Fine Particle Deposition from Flowing Suspensions onto Planar Surfaces", **Powder Technology**, Vol. 27, pp. 125-136.
- Adamczyk, Z., Dabros, T., Czarniecki, J. and van de Ven, T. G. M., 1983, "Particle Transfer to Solid Surface", **Advances in Colloid and Interface Sci.**, Vol. 19, pp. 183-252.
- Adamson, A. W., 1967, **Physical Chemistry of Surfaces**, 2nd ed., Interscience Pub., New York.
- Adersen, B and Somasundaran, P., 1993, "Mechanisms Determining Separation of Phosphatic Clay Waste by Selective Flocculation", **Min. Met. Process.**, pp. 200-205.
- Ahmed, S. M., El-Aasser, M. S., Pauli, G. H., Poehlein, G. W. and Vanderhoff, J. W., 1980, "Cleaning Latexes for Surface Characterization by Serum Replacement" **J. Colloid Interface Sci.** 73, pp. 388- 405.
- Amankonah, J. and Somasundaran, P., 1985, "Effects of Dissolved Mineral Species on the Electrokinetic Behavior of Calcite and Apatite", **Colloids and Surfaces**, Vol. 15, pp. 335-353.
- Ananthapadmanabhan, K. P. and Somasundaran, P., 1981, "Oleate Chemistry and Hematite Flotation", **Interfacial Phenomena in Mineral Processing**, Proceedings of the Engineering Foundation Conference Franklin Pierce College Rindge, Eds. B. Yarar and D. J. Spottiswood, New Hampshire, pp. 207-227.
- Ananthapadmanabhan, K. P. and Somasundaran, P., 1988, "Acid-Soap Formation in Aqueous Oleate Solution", **J. Colloid Int. Sci.**, Vol. 122, pp. 104-109.
- Anazia, I. and Hanna, J., 1987, "New Flotation Approach for Carbonate Phosphate Separation", **Min. Met. Process.**, pp. 196-202.
- Anonymous, 1970, **Quantasorb Manual**, Quantachrome Incorp., New York.
- Attia, Y. A. and Fuerstenau, C. W., 1978, "Principles of Separation of Ore Minerals by Selective Flocculation", in: **Recent Developments in Separation Science**, Ed. N. Li, Vol IV, Ch5, CRC Press, London, pp. 52-69.

Attia, Y. A. and Kitchener, J. A., 1975, **Proc. XIth International Mineral Processing Congress**, University of Cagliari Press, Cagliari, pp. 1232-1248.

Attia, Y. A., Sinclair, R. G., Markle, R. A., Cousin, M., Krishnan, S. V. and Keys, R. O., 1987, "Preparation of Poly(methyl Vinyl Oxime) and other Polyoximes for the Selective Flocculation of Cassiterite from Tourmaline and Quartz", in: **Flocculation in Biotechnology and Separation Systems**, Ed. Y. A. Attia, Elsevier, Amsterdam, pp. 263-276.

Attia, Y. A., Yu, S. and Vecchi, S., 1987, "Selective Flocculation Cleaning of Upper Freeport Coal with a Totally Hydrophobic Polymeric Flocculant", **Flocculation in Biotechnology and Separation Systems**, Eds. Y. A. Attia, Elsevier, Amsterdam, pp. 547-564.

Attia, Y. A., 1977, "Synthesis of PAMG Chelating Polymers for the Selective Flocculation of Copper Minerals", **Int. J. Miner. Process.**, 4, pp.191-208.

Attia, Y. A., 1977, "Development of A Selective Flocculation Process for A Complex Copper Ore", **Int. J. Miner. Process.**, 4, pp. 209-225.

Attia, Y. A., 1992, "Flocculation", **Colloid Chemistry in Mineral Processing**, Eds. J. S. Laskowski and J. Ralston, Elsevier, Amsterdam, pp. 291-308.

Bagchi, P., Gray, B., Birnbaum, S. M., 1979, "Preparation of Model Poly(vinyl toluene) Latices and Characterization of their Surface Charge by Titration and Electrophoresis", **J. Colloid Interface Sci.**, 69, pp. 502-528.

Bagster, D. F., 1985, "Studies in the Selective Flocculation of Hematite from Gangue Using High Molecular Weight Polymers", **Int. J. Miner. Process.**, Vol. 14, pp. 1-32.

Bahr, A., Clement, M. and Surmatz, H., 1968, "On the Effect of Inorganic and Organic Substances on the Flotation of Some Non-sulfide Minerals by Using Fatty-Acid-Type Collectors", **Proceedings 8th International Mineral Processing Congress**, Leningrad, pp1-12.

Banks, A. F., 1979, "Selective Flocculation-Flotation of Slimes from a Sylvinitic Ore", **Beneficiation of Mineral Fines**, Eds. P. Somasundaran & N. Arbitter, National Science Foundation-AIME, New York, pp. 277-280.

Baudet, G., Morio, M., Rinaudo, M. and Nematollahi, H., 1978, "Synthesis and Characterization of Selective Flocculants Based on Xanthate Derivatives of Cellulose and Amylose", **Ind. Miner. Mineralurgie**, 1, pp. 19-35.

Behl, S. and Moudgil, B. M., 1992, "Enhanced Selectivity of Polymer Adsorption in Selective Flocculation", **Minerals and Metallurgical Processing**, 5, pp. 92-94.

Behl. S. and Moudgil, B. M., 1993, "Mechanisms of Polyethylene Oxide Interaction with Apatite and Dolomite", **Journal of Colloid and Interface Science**, 161, pp. 443-449.

Betz, E. W., 1979, "Beneficiation of Brazilian Phosphates", **Proc. XIIIth Int. Miner. Process. Congr.**, Vol. II, Part B, Elsevier, Amsterdam, pp. 1846-1877.

Bilsing, U., 1969, "The Mutual Interaction of the Minerals during Flotation for Example the Flotation of CaF_2 and BaSO_4 ", **Dissertation**, Bergakademie Freiberg.

Brandao, P. R. G. and Poling, G. W., 1982, "Anionic Flotation of Magnesite", **Canadian Metallurgical Quarterly**, Vol. 21, No. 3, pp. 211-220.

Brandrup, J. and Immergut, E. H., 1975, **Polymer Handbook**, Wiley-Interscience, New York.

Calara, J. V. and Miller, J. D., 1983, "The Electrokinetic Behavior of Fluorite in the Absence of Surface Carbonation", **Colloid and Surfaces**,

Carta, M., Ciccu, R., Del Fa, C., Ferrara, G., Ghiani, M. and Massacci, P., 1970, "The Influence of the Surface Energy Structure of Minerals on Electric Separation and Flotation", **Proceedings 9th International Mineral Processing Congress**, Prague, Ustav Pro Vy'zkhum Rud, Vol. 1, pp. 47-57.

Carta, M., Ciccu, R., Del Fa, C., Ferrara, G., Ghiani, M. and Massacci, P., 1974, "Improvement in Electric Separation and Flotation by Modification of Energy Levels in Surface Layers", **Proceedings 10th International Mineral Processing Congress**, London, Instn. Min. Metall., pub. pp. 349-376.

Castro, S. H., Stocker, R. and Laskowski, J. S., 1997, "The Effect of Hydrophobic Agglomerant on the Flotation of Fine Molybdenite Particles", **Proceedings of the XX International Mineral Processing Congress**, Aachen, Germany, Vol 3, pp. 559-569.

Castro, S. H., Vurdela, R. M. and Laskowski, J. S., 1986, "The Surface Association and Precipitation of Surfactant Species in Alkaline Dodecylamine Hydrochloride Solution", **Colloids and Surfaces**, Vol. 21, pp. 87-100.

Chow, R. S. and Takamura, K., 1988, "Effect of Surface Roughness (Hairiness) of Latex Particles on Their Electrokinetic Potentials", **J. Colloid Interface Sci.**, Vol. 125, No. 1, pp. 226-236.

Churaev, N. V. and Derjaguin, B. V., 1985, "Inclusion of Structural Forces in the Theory of Stability of Colloids and Films", **J. Colloid Interface Sci.**, Vol. 103, pp. 542-553.

Clauss, C. R. A., Appleton, E. A. and Vink, J. J., 1976, "Selective Flocculation of Cassiterite in Mixtures with Quartz Using A Modified Polyacrylamide Flocculant", **Int. J. Miner. Process.**, 3, pp. 27-34.

Clint, G. E., Clint, J. H., Corkill, J. M. and Walker, T., 1973, "Deposition of Latex Particles on to a Planar Surface", **J. Colloid Interface Sci.**, Vol. 44, No. 1, pp. 121-132.

Czarnecki, J. 1995, **Personal Communication.**

Dabros, T. and Czarnecki, J., 1975, "Transport of Particles with Finite Dimensions to a Rotating Disc Surface", **J. Colloid Interface Sci.**, Vol. 53, No. 2, pp. 335-336.

Dabros, T. and van de Ven, T. G. M., 1983, "A Direct Method for Studying Particle Deposition onto Solid Surfaces", **Colloid and Polymer Science**, Vol. 261, pp. 694-707.

Daniels, W. E., Vanderhoff, J. W., Enos, C. T., Iacoviello, J. G., Ahmed, S. M. and Frost, J., 1981, "The Stabilization of Poly(vinyl acetate) Latexes by Polymethacrylic Acid" **Emulsion Polymerization of Vinyl Acetate**, Eds. M. S. El-Aasser and J. W. Vanderhoff, Applied Science, London, pp. 191-202.

Derjaguin, B. V. and Chureav, N. V., 1989, "The Current State of the Theory of Long-Range surface Forces", **Colloids and Surfaces**, Vol. 41, pp. 223-237.

Derjaguin, B. V. and Dukhin, S. S., 1981, "Kinetic Theory of the Flotation of Fine Particles", **Proceedings of XIII International Mineral Processing Congress**, Elsevier, Amsterdam.

Edelhauser, H. A., 1969, "Investigation of the Dispersion of Surfactant in a Latex by the 'Rate of Dialysis Methods' Mechanism of Detergent Dialysis", **J. Polymer Sci., Part C**, 27, pp. 291-309.

Eigeles, M. A., 1964, **Fundamentals of Flotation of Non-Sulfide Minerals**, Nedra, Moscow.

El-Aasser, M. S., Ahmed, S. M., Poehlein, G. W. and Vanderhoff, J. W., 1980, "Application of the Serum Replacement Technique in the Characterization of An Ethyl Acrylate-Methyl Methacrylate Copolymer Latex", **Polymer Colloids II**, Ed. R. M. Fitch, Plenum Press, New York, pp. 361-377.

Elgilani, D. A. and Abouzeid, A. Z. M., 1993, "Flotation of Carbonates from Phosphates Ores in Acidic Media", **Int. J. Miner. Process.**, 38, pp. 235-256.

Everett, D. H., Gultepe, M. E. and Wilkinson, M. C. 1979, "Problems Associated with the Surface Characterization of Polystyrene Latices", **J. Colloid Interface Sci.**, 71, pp. 336-349.

Filho, L. de Salles Leal and Chaves, A. P., 1993, "The Influence of Corn Starch on the Separation of Apatite from Gangue Minerals via Froth Flotation", **Beneficiation of Phosphate: Theory and Practice**, Eds. H. El-Shall, B. M. Moudgil et al, SME, Littleton, Colorado, USA, pp. 147-156,

Finkelstein, N. P., 1989, "Review of Interactions in Flotation of Sparingly Soluble Calcium Minerals with Anionic Collectors", **Trans. AIME**, Vol. 98, C. pp. 157-177.

Fleer, G. J., Scheutjens, H.H.M.M. and Vincent, B., 1984, "The Stability of Dispersion of Hard Spherical Particles in the Presence of Non-adsorbing Polymer", in: **Polymer Adsorption and Dispersion Stability**, Eds. E.D. Goddard and B. Vincent, ACS Symposium Series No. 240, pp. 245-263.

Free, M. L. and Miller, J. D., 1995, "The Role of Calcium in the Fluorite/Oleate Flotation System", **SME Preprint 95-57**.

French, R. O., et al, 1954, "Applications of Infrared Spectroscopy to Studies in Surface Chemistry", **J. Phys. Chem.**, Vol. 58, pp. 805-810.

Friend, J. P. and Kitchener, J. A., 1972, "Separation of Minerals from Mixtures by Selective Flocculation", **Filtration and Separation**, 9(1), 25-28.

Fuerstenau, D. W., Chander, S. and Abouzeid, A. M., 1979, "The Recovery of the Fine Particles by Physical Separation Methods", In: **Beneficiation of Mineral Fines**, Eds. P. Somasundaran and N. Arbitter, AIME, New York, pp. 3-59.

Fuerstenau, M. C., Gutierrez, G. and Elgillani, D. A., 1968, "The Influence of Sodium Silicate in Nonmetallic Flotation Systems", **Transactions, AIME**, Vol. 241, pp. 319-323.

Fuerstenau, M. C. and Fitzgerald, J. J., 1989, "Dispersion with Aluminum Silicate Hydrosol in Fine Particles Flotation", in: **Advances in Coal and Mineral Processing Using Flotation**, Proceedings of an Engineering Foundation Conference, Eds. S. Chander and R. R. Klimpel, SME, Littleton, Colorado.

Furusawa, K., Tezuka, Y. and Watanabe, N., 1980, "Adsorbed Polymer Layers on the Platelet Particles and Their Effect on Colloidal Stability", **J. Colloid Interface Sci.**, 73, pp. 21-26.

Garvey, M. J., Tadros, Th. F. and Vincent, B., 1974, "A Comparison of the Volume Occupied by Macromolecules in the Adsorbed State and in Bulk Solution - Adsorption of Narrow Molecular Weight Fractions of Poly(vinyl alcohol) at the Polystyrene Water Interface", **J. Colloid and Interface Sci.**, 49, pp. 57-68.

Giesekke, E. W. and Harris, P. J., 1984, "A Study of the Selective Flotation of Fluorite from Calcite by the Use of a Single Bubble-Stream Microflotation Cell", **Mintek 50: International Conference on Mineral Science and Technology. Council for Mineral**

Science and Technology. Eds. L. F. Houghton, Randburg, South Africa, Vol. 1, pp. 267-269.

Gong, W. Q., Parentich, A., Little, L. H. and Warren, L. J., 1992, "Adsorption of Oleate on Apatite Studied by Diffuse Reflectance Infrared Fourier Transform Spectroscopy", **Langmuir**, Vol. 8, No. 1, pp. 118-124.

Gong, W. Q., Parentich, A., Little, L. H. and Warren, L. J., 1992, "Selective Flotation of Apatite from Iron Oxides", **Int. J. Miner. Process.**, 34, pp. 83-102.

Gong, W. Q., Klauber, C. and Warren, L. J., 1993, "Mechanism of Action of Sodium Silicate in the Flotation of Apatite from Hematite", **Int. J. Miner. Process.**, Vol. 39, pp. 251-273.

Grim, R. E., 1968, **Clay Mineralogy**, McGraw-Hill, New York.

Hamaker, H. C., 1937, "The London-Van Der Waals Attraction Between Spherical Particles", **Physica (Utrecht)**, 4, 1058-1072.

Hanna, H. S. and Somasundaran, P., 1976, "Flotation of Salt-Type Minerals", **Flotation**, A. M. Gaudin Memorial Volume, Ed. M. C. Fuerstenau, AIME, New York, pp. 197-272.

Hanna, J. and Anazia, I., 1989, "Carbonate/Phosphate Flotation by the MRI No-Conditioning Process", **SME Preprint** 89-144.

Harkins, W. D., 1947, "A General Theory of the Mechanism of Emulsion Polymerization", **J. Am. Chem. Soc.**, Vol. 69, No. 5, pp. 1428-1444.

Healy, T. W. and La Mer, V. K., 1964, "The Energetics of Flocculation and Dispersion by Polymers", **J. Colloid Interface Sci.**, 19, pp. 323-330.

Hearn, J., Wilkinson, M. C. and Goodall, A. R., 1981, "Polymer Latices as Model Colloids", **Adv. Colloid Interface Sci.**, 14, pp. 173-236.

Henchiri, A., 1993, "A Contribution to Carbonates-Phosphates Separation by Flotation Technique", **Beneficiation of Phosphate: Theory and Practice**, Eds. H. El-Shall, B. M. Moudgil, R. Wiegel, SME, Littleton, Colorado, USA, pp. 225-230.

Henchiri, A., Cecile, J. L., Baudet, G., Barbery, G. and Bloise, R., 1980, "Treatment of Phosphate Minerals with Silica-Carbonate Gangue", **French Patent No. 80.19366**.

Hiemenz, P. C., 1977, **Principles of Colloid Surface Chemistry**, Marcel Dekker, New York.

Hogg, R., 1984, "Collision Efficiency Factors for Polymer Flocculation", **J. Colloid Interface Sci.**, 102, pp. 232-236.

Hogg, R., Healy, T. W. and Fuerstenau, D. W., 1966, "Mutual Coagulation of Colloidal Dispersions", **Trans. Faraday Soc.** 62, No. 522, Part 6, pp. 1638-1651.

Houot, R., 1982, "Beneficiation of Phosphate Ores Through Flotation: Review of Industrial Application and Potential Developments", **Int. J. Mine. Process.**, 9, pp. 353-384.

Houot, R., Polgaire, J. L., Pirette, P. and Van't Hoff, J 1981, "Reverse Cationic Flotation of Sedimentary Siliceous Phosphates", **Trans. Inst. Min. Metall**, 10, C142-C146.

Hu, J. S., Misra, M. and Miller, J. D., 1986, "Effect of Temperature and Oxygen on Oleate Adsorption by Fluorite", **Int. J. Miner. Process.**, Vol. 18, pp. 57-72.

Hu, J. S., Misra, M. and Miller, J. D., 1986, "Effect of Temperature and Oxygen on Oleate Adsorption by Fluorite", **Int. J. Miner. Process.**, Vol. 18, pp. 57-72.

Hull, M. and Kitchener, J. A., 1969, "Interaction of Spherical Colloidal Particles with Planar Surfaces", **Trans. Faraday Soc.**, Vol. 65, pp. 3093-3104.

Hunter, R. J., 1981, **Zeta-Potential in Colloid Science**, Academic Press, London.

Jagodic, F. and Abe, M. and Ogrizek, N., 1976, "Use of the HLB System in Emulsion Polymerization. II. Copolymerization of MMA/EA, MMA/ST and EA/ST", **Chem. Abstr.**, Vol. 85, 63365y.

Jagodic, F. and Abe, M. and Ogrizek, N., 1976, "Use of the HLB System in Emulsion Polymerization. I. Homopolymerization of Methyl Methacrylate, Ethyl Acrylate, and Acrylonitrile", **Chem. Abstr.**, Vol. 85, 33406h.

James, R. O. and Parks, G. A., 1982, "Characterization of Aqueous Colloids by Their Electrical Double-Layer and Intrinsic Surface Chemical Properties" in: **Surface and Colloid Science**, Vol. 12, Ed. E. Matijevic, Plenum Press, New York, pp.119-216.

Jang, W., Drelich, J. and Miller, J. D., 1995, "Wetting Characteristics and Stability of Langmuir-Blodgett Carboxylate Monolayers at the Surfaces of Calcite and Fluorite", **Langmuir**, 11, pp. 3491-3499.

Kamel, A. A., El-Aasser, M. S. and Vanderhoff, J. W., 1981, "The Preparation and Surface Characterization of an Ideal Model Colloid", **J. Dispersion Science and Technology**, 2(2&3), pp. 183-214.

Kellar, J. J., Cross, W. M. and Miller, J. D., 1990, "In-Situ Internal Reflection Spectroscopy for the Study of Surfactant Adsorption Reactions Using Reactive Internal Reflection Elements", **Separation Sci. and Tech.**, Vol. 25, No. 13-15, pp. 2133-2155.

Kellar, J. J., Cross, W. M., Yalamanchili, M. R., Young, C. A. and Miller, J. D., 1993, "Surface Phase Transitions of Adsorbed Collector Molecules as Revealed by In-Situ FT-IR/IRS Spectroscopy", **Minerals and Metallurgical Processing**, Vol. 10, pp. 75-80.

Kitchener, J. A., 1978, "Flocculation in Mineral Processing", **The Scientific Basis of Flocculation**, Ed. K. J. Ives, Sijthoff and Noordhoff, Alphen aan den Rijn, pp. 283-328.

Kiukkola, K., 1980, "Selective Flocculation of Apatite from Low-Grade Phosphorus Ore Containing Calcite, Dolomite and Phlogopite", **Proc. 2nd Int. Congr. Phosphorus Compounds**, Boston, April, pp. 219-229.

Klassen, V. I. and Mao, T. F., 1959, "Action Mechanism of Sodium Silicate in Flotation of Non-Sulphide Minerals", **Tsvetnye Metally**, 32, No. 9, pp.11-14.

Klassen, V. I. and Mokrousov, V. A., 1963, **An Introduction to the Theory of Flotation**, Butterworths, London.

Klimpel, R. R., Fee, B. S. and Smith, R. A., 1993, "Some New Chemical Reagents for Improved Phosphate Ore Flotation", **Beneficiation of Phosphate: Theory and Practice**, Eds. H. Ei-Shall, B. M. Moudgil and R. Wiegel, SME, Littleton, Colorado, pp. 3-10.

Klimpel, R. R., Hansen, R. D., Leonard, D. E. and Fee, B. S., 1990, "Froth Flotation of Ores Containing Silica Gangue Using Organic Compounds Containing Hydroxyl Groups", **Braz. Pedido PI BR 9002232**.

Klimpel, R. R., Hansen, R. D., Leonard, D. E. and Fee, B. S., 1991, "Depressants for Silica or Silicious Gangue in Ore Flotation", **EUR. Pat. Appl. EP 453677**.

Krishnan, S. V. and Attia, Y. A., 1985, "Floc Characteristics in Selective Flocculation of Fine Particles", in: **Flocculation, Sedimentation & Consolidation**, Eds. B. M. Moudgil and P. Somasundaran, Proceedings of the Engineering Foundation Conference, The Cloister, Sea Island, Georgia, U.S.A., pp. 229-248.

Kulkarni, R. D. and Somasundaran, P., 1980, "Flotation Chemistry of Hematite/Oleate System", **Colloid Surf.**, Vol. 1, pp. 387-405.

Laaksonen, J. Le Bell, J. C. and Stenius, P., 1975, "Potentiometric Titration of Monodisperse Polystyrene Latexes", **J. Electroanal. Chem. Interfacial Electrochem.** 64, pp. 207-218.

Laskowski, J. S., 1982, "Interfacial Chemistry of Mineral Processing Separations" in: **Surface and Colloid Science**, Eds. E. Matijevic, Vol. 12, Plenum Press, New York, pp. 315-357.

- Laskowski, J. S., 1988, "Weak-Electrolyte Type Collectors", **Copper-87 Int. Conf. Vol. 2-Mineral Processing and Process Control**, Eds. A. Mular, G. Gonzales et al, University of Chile, Santiago, pp. 137-154.
- Laskowski, J. S., 1988, "Dispersing Agents in Mineral Processing", in: **Froth Flotation**, Eds. S. H. Castro and J. A. Alvarez, Elsevier, Amsterdam, pp. 1-16.
- Laskowski, J. S., 1993, "Electrokinetic Measurements in Aqueous Solutions of Weak-Electrolyte Type Surfactants", **J. Colloid Interface Sci.**, Vol. 159, pp. 349-353.
- Laskowski, J. S. and Nyamekye, G. A., 1994, "Colloid Chemistry of Weak Electrolyte Collectors: The Effect of Conditioning on Flotation with Fatty Acids", **Int. J. Miner. Process.**, 40, pp. 245-256.
- Laskowski, J. S. and Pugh, R. J., 1992, "Dispersion Stability and Dispersing Agents", in: **Colloid Chemistry in Mineral Processing**, Eds. J. S. Laskowski and J. Ralston, Elsevier, Amsterdam, pp. 115-166.
- Laskowski, J. S., Yu, Z. and Zhan, Y. H., 1995, "Hydrophobic Agglomeration of Fine Coal", **Proceedings of the 1ST UBC-McGill Bi-annual International Symposiums**, Eds. J. S. Laskowski, CIM, pp. 245-258.
- Leja, J., 1982, **Surface Chemistry of Froth Flotation**, Plenum Press, New York.
- Levich, V. G., 1962, **Physicochemical Hydrodynamics**, Prentice-Hall, Englewood Cliffs, New Jersey.
- Li, Changgen and Lu, Yongxin, 1983, "Selective Flotation of Scheelite from Calcite Minerals with Sodium Oleate as a Collector and Phosphates as Modifiers. II. The Mechanism of the Interaction between Phosphate Modifiers and Minerals", **Int. J. Miner. Process.**, Vol. 10, pp. 219-235.
- Littlefair, M. J. and Lowe, N. R. S., 1986, "On the Selective Flocculation of Coal Using Polystyrene Latex", **Int. J. Miner. Process.**, Vol. 17, pp. 187-203.
- Lovell, V. M., 1976, "Froth Characteristics in Phosphate Flotation", **Flotation, A. M. Gaudin Memorial Volume**, Ed. M. C. Fuerstenau, SME-AIME, Littleton, Co. USA, pp. 597-621.
- Lovell, V. M., Goold, L. A. and Finkelstein, N. P., 1974, "Infrared Studies of the Adsorption of Oleate Species on Calcium Fluoride", **Int. J. Miner. Process.**, Vol. 1, pp. 183-192.
- Lu, Y., Drelich, J. and Miller, J. D., 1997, "Wetting of Francolite and Quartz and its Significance in the Flotation of Phosphate Rock", **SME Preprint** 97-123.

Lu, Y. and Miller, J. D., 1998, "Carboxyl Stretching Vibrations of Spontaneously Adsorbed and Lb Transferred Calcium Carboxylates as Determined by FTIR Internal Reflection Spectroscopy", **SME Preprint** 98-127.

Lyklema, J. and Fleer, G. J., 1987, "Electrical Contributions to the Effect of Macromolecules on Colloid Stability", **Colloids and Surfaces.**, 25, pp. 357-385.

Mackie, P. E. and Young, R. A., 1973, "Location of Nd Dopant in Fluorapatite, $\text{Ca}_5(\text{PO}_4)_3\text{F:Nd}$ ", **J. Appl. Cryst.**, Vol. 6, pp. 26-31.

Marinakos, K. I. And Shergold, H. L., 1985, "The Mechanism of Fatty Acid Adsorption in the Presence of Fluorite, Calcite and Barite", **Int. J. Miner. Process.**, 14, pp. 161-176.

Marshall, J. K. and Kitchener, J. A., 1966, "The Deposition of Colloidal Particles on Smooth Solids", **J. Colloid Interface Sci.**, Vol. 22, pp. 342-351.

Mathur, S. and Moudgil, B. M., 1995, "Selective Floc Formation in Apatite-Dolomite System Using Polyacrylic Acid", **SME Annual Meeting**, Denver, Colorado, Preprint No 95-202.

McCarvill, W. T. and Fitch, R. M., 1978, "The Preparation and Surface Chemistry of Polystyrene Colloids Stabilized by Sulfonate Surface Groups", **J. Colloid Interface Sci.**, 64, pp. 403-411.

Mehta, N., 1993, "Flocculation Behavior of Apatite with Polyacrylic Acid", **M.S. Thesis**, University of Florida, Gainesville, Florida.

Mercade, V., 1981, "Effect of Polyvalent Metal-Silicate Hydrosols on the Flotation of Calcite", **Trans. SME/AIME**, Vol. 268, pp. 1842-1846.

Michaels, A. S. and Morelos, O., 1955, **Industrial Engineering Chemistry**, 47, pp. 1801-1807.

Miller, J. D. and Hiskey, J. B., 1972, "Electrokinetic Behavior of Fluorite as Influenced by Surface Carbonation", **J. Colloid and Interface Sci.**, Vol. 41, No. 3, pp. 567-573.

Miller, J. D., Wadsworth, M. E., Mistra, M. and Hu, J. S., 1984, "Flotation Chemistry of the Fluorite/Oleate System", **Principles of Mineral Flotation: The Wark Symposium**, Eds. M. H. Jones and J. T. Woodcock, Parkville, Victoria: Australasian Institute of Mining and Metallurgy, Symp. Series 40, pp. 31-41.

Mishra, S. K., 1982, "Electrokinetic Properties and Flotation Behavior of Apatite and Calcite in the Presence of Sodium Oleate and Sodium Metasilicate", **Int. J. Miner. Process**, Vol. 9, pp. 59-73.

Montel, G., Bonel, G., Trombe, J. C., Heughebaert, J. C. and Rey, C., 1977, "Relations Between Apatite Physico-Chemistry and Their Behavior in Biological Media and Different Industrial Treatments", **Actes Congr. Int. Composes Phosphores, 1st**, Rabbat, pp. 321-346.

Moudgil, B. M. and Ince, D., 1991, "Effect of Sodium Chloride on Flotation of Dolomite from Apatite", **Mineral & Metallurgical Processing**, pp. 139-143.

Moudgil, B. M. and Somasundaran, P., 1985, "Research Needs in Flocculation", **Flocculation, Sedimentation and Consolidation**, Eds. B. M. Moudgil and P. Somasundaran, Engineering Foundation, New York, pp. 591-598.

Moudgil, B. M. and Somasundaran, P., 1986, "Advances in Phosphate Flotation" in **Advances in Mineral Processing**, Ed. P. Somasundaran, SME, Littleton, Colorado, pp. 426-441.

Moudgil, B. M. and spedden, D., 1992, "Plant Test of Coarse Phosphate Flotation with Emulsified Collector", **SME Preprint** 92-158.

Moudgil, B. M. and Vasudevan, T. V., 1989, "Role of Active Sites in Selective Flocculation", **Journal of Colloid Interface Science**, 127(1), pp. 239-243.

Moudgil, B. M., Mathur, S. and Behl, S., 1995, "Flocculation Behavior of Dolomite with Poly(ethylene-oxide)", **Minerals and Metallurgical Processing**, 12(4), pp. 219-224.

Moudgil, B. M., Mathur, S. and Behl, S., 1994, "Removal of Dolomite and Silica from Apatite by Selective Flocculation", **Minerals and Metallurgical Processing**, 11(4), pp. 217-222.

Moudgil, B. M., Shah, B. D. and Soto, H. S., 1987a, "Loss of Selectivity in Apatite-Dolomite Flocculation", **Minerals and Metallurgical Processing**, 4(2), pp. 27-31.

Moudgil, B. M., Shah, B. D. and Soto, H. S., 1987b, "Collision Efficiency Factors in Polymer Flocculation of Fine Particles", **Journal of Colloid Interface Science**, 119(2), pp. 466-473.

Mukerjee, P., 1967, "The Nature of the Association Equilibria and Hydrophobic Bonding in Aqueous Solutions of Association Colloids", **Adv. Colloid Interface Sci.**, Vol. 1, pp. 241-275.

Muroi, S. and Hosoi, K., 1967, "Separation of Water-Soluble Polymer from Emulsion by Gel Filtration", **J. Applied Polymer Sci.**, 11, pp. 2331-2341.

Murphy, T. D., 1977, "Design and Analysis of Industrial Experiments", **Chemical Engineering**, June 6, pp. 168-182.

Napper, D. H. and Gilbert, R. G., 1988, "Emulsion Polymerization: The Mechanism of Latex Particle Formation and Growth", **Scientific Method for the Study of Polymer Colloids and their Applications**, Eds. F. Candau and R. H. Ottewill, Klumer Academic Publishers, The Natherlands, pp. 159-185.

Napper, D. H., 1983, **Polymeric Stabilization of Colloidal Dispersions**, Academic Press, London.

Nikolov, A., Martynov, G. and Exerowa, D., 1981, "Association Interactions and Surface Tension in Ionic Surfactant Solutions at Concentrations Much Lower than the CMC", **J. Colloid Interface Sci.**, Vol. 81, pp. 116-124.

Norde, W. and Lyklema, J., 1978, "The Adsorption of Human Albumin and Bovine Pancreas Ribonuclease at Negatively Charged Polystyrene Surface, I - Adsorption Isotherms. Effect of Charge, Ionic Strength, and Temperature", **J. Colloid and Interface Sci.**, 66, pp. 257-265.

Onal, G., 1973, "Mazidag Low-Grade Calcarous Phosphate Ores Flotation", **Proc. Cento Symposium on the Mining and Beneficiation of Fertilizer Minerals**, Istanbul, pp. 171-180.

Overbeek, J. Th. G., 1952, "Electrochemistry of the Double Layer", in: **Colloid Science**, Vol. 1, Ed. H. R. Kruyt, Elsevier, Amsterdam, pp. 115-190.

Parsonage, P., Melven, D., Healey, A. F. and Watson, D., 1984, "Depressant Function in Flotation of Calcite, Apatite and Dolomite" **Reagents in the Minerals Industry**, Eds. J. Jones and R. Oblatt, pp. 33 - 40.

Parsonage, P., Watson, D. and Hickey, T. J., 1982, "Surface Texture, Slime Coatings and Flotation of Slime Industrial Minerals", **Proc. XIVth International Mineral Processing Congress**, Toronto, pp. V5.1-V5.22.

Patsiga, R., Litt, M. and Stannett, V., 1960, "The Emulsion Polymerization of Vinyl Acetate Part I", **J. Phys. Chem.**, Vol. 64, pp. 801-804.

Peck, A. S. and Wadsworth, M. E., 1964, "I.R. Studies of the Effect of F^- , SO_4^{2-} , and Cl^- Ions on Chemisorption of Oleate on Fluorite and Barite", **Proceedings 7th Int'l Mineral Processing Congress**, New York, Eds. Gordon and Beach, pp. 259-267.

Peck, A. S., and Wadsworth, M. E., 1963, "Infrared Studies of Oleic Acid and Sodium Oleate Adsorption on Fluorite, Barite and Calcite", **U.S. Bureau of Mines, Report of Investigation No. 6202**, pp. 188-190.

Pradip, Y. and Moudgil, B. M., 1991, "Selective Flocculation of Tribasic Calcium Phosphate from Mixture with Quartz Using Polyacrylic Acid Flocculant", **International Journal of Mineral Processing**, 32, pp. 271-281.

Predali, J. J., 1969, "Flotation of Carbonates with Salts of Fatty Acids: Role of pH and the Alkyl Chain", **Trans. Imm. Sec. C**, Vol. 78, pp. 140-147.

Preist, W. J., 1952, "Particle Growth in the Aqueous Polymerization of Vinyl Acetate", **J. Phys. Chem.**, Vol. 56, pp. 1077-1082.

Pugh, R. and Stenius, P., 1985, "Solution Chemistry Studies and Flotation Behavior of Apatite, Calcite and Fluorite Minerals with Sodium Oleate Collector", **Int. J. Miner. Process.**, 15, pp. 193-218.

Ralston, J., Kent, W. and Newcombe, G., 1984, "Polymer-Stabilized Emulsions and Fine Particle Recovery, I. The Calcite-Quartz System", **Int. J. Miner. Process.**, 13, pp. 167-186.

Ralston, J., Kent, W. and Newcombe, G., 1985, "Polymer-Stabilized Emulsions and Fine Particle Recovery, II. The Chalcopyrite-Quartz System", **Int. J. Miner. Process.**, 14, pp. 217-232.

Rao, K. H., Antti, B. and Forssberg, E., 1988/1989, "Mechanism of Oleate Interaction on Salt-type Minerals Part I. Adsorption and Electrokinetic Studies of Calcite in the Presence of Sodium Oleate and Sodium Metasilicate", **Colloids and Surfaces**, 34, pp. 227-239.

Rao, K. H., Antti, B. and Forssberg, K. S. E., 1990, "Mechanism of Oleate Interaction on Salt-Type Minerals, Part II. Adsorption and Electrokinetic Studies of Apatite in the Presence of Sodium Oleate and Sodium Metasilicate", **Int. J. Miner. Process.**, Vol. 28, pp. 59-79.

Rao, K. H., Cases, J. M., DeDonato, P. and Forssberg, K. S. E., 1991, "Mechanism of Oleate Interaction on Salt-Type Minerals, IV. Adsorption, Electrokinetic, and Diffuse Reflectance FT-IR Studies of Natural Fluorite in the Presence of Sodium Oleate", **J. Colloid Interface Sci.**, Vol. 145, No. 2, pp. 314-329.

Rao, K. H., Cases, J. M. and Forssberg, K. S. E., 1991, "Mechanism of Oleate Interaction on Salt-Type Minerals, V. Adsorption and Precipitation Reaction in Relation to the Solid/Liquid Ratio in the Synthetic Fluorite-Sodium Oleate System", **J. Colloid Interface Sci.**, Vol. 145, No. 2, pp. 330-348.

Riddiford, A. C., 1966, "The Rotating Disk System", **Adv. Electrochem. and Electrochem. Eng.**, Vol. 4, pp. 47-116.

Rosen, M. J., 1978, **Surfactant and Interfacial Phenomena**, Wiley, New York.

Rubio, J. and Hoberg, H., 1993, "The Process of Separation of Fine Mineral Particles by Flotation with Hydrophobic Polymeric Carrier", **Int. J. Mine. Process.**, 37, pp. 109-122.

Rubio, J. and Kitchener, J. A., 1977, "New Basis for Selective Flocculation of Mineral Slimes", **Transactions, IMM**, Sec. C, Vol. 86, pp. 97-100.

Ruehrvein, R. A. and Ward, D. W., 1952, **Soil Sci.**, 73, pp. 485-491.

Singh, P. K., Adler, J., Moudgil, B. M. and Singh, R., 1998, "Selective Flocculation of Apatite and Dolomite Fines: Loss of Selectivity due to Surface Contamination During Grinding", **SME Annual Meeting Preprint**.

Sjoberg, S., et al, 1985, "Equilibrium and Structural Studies of Silicon (IV) and Aluminium (III) in Aqueous Solution. II. Polysilicate Formation in Alkaline Aqueous Solution. A combined potentiometric and ^{29}Si NMR Study, **Acta Chem. Scand. A**, Vol. 39, pp. 93-107.

Smani, S., Blazy, P. and Cases, J. M. , 1975, "Beneficiation of sedimentary Moroccan Phosphate Ores 1. Electrochemical Properties of Some Minerals of the Apatite Group, 2. Electrochemical Phenomena at the Calcite-Aqueous Solution Interface, 3. Selective Flotation and Recovery", **Trans. SME-AIME**, 258, pp. 168-180.

Smith, P. G. and Warren, L. J., 1989, "Entrainment of Particles into Flotation Froths", **Mineral Processing and Extractive Metallurgy**, Vol. 5, pp. 123-145.

Smith, W. V. and Ewart, R. H., 1948, "Kinetics of Emulsion Polymerization", **J. Chem. Phys.**, Vol. 16, No. 6, pp. 592-599.

Smith, W. V., 1949, "Chain Initiation in Styrene Emulsion", **J. Am. Chem. Soc.**, Vol. 71, pp. 4077-4082.

Somasundaran, P. and Agar, G. E., 1967, "The Zero Point of Charge of Calcite", **J. Colloid Interface Sci.**, Vol. 24, pp. 433-440.

Somasundaran, P., Ofoviamankonah, J. and Ananthapadmabhan, K. P., 1985, "Mineral-Solution Equilibria in Sparingly Soluble Mineral Systems", **Colloids and Surfaces**, 15, pp. 309-333.

Somasundaran, P., 1968, "Zeta Potential of Apatite in Aqueous Solutions and Its Change During Equilibration", **J. Colloid Interface Sci.**, Vol. 27, pp. 659-666.

Somasundaran, P., 1980, "Principles of Flocculation, Dispersion, and Selective Flocculation", in: **Fine Particle Processing, Proc. Int. Symp.** Ed. P. Somasundaran, Vol. 2, AIME, New York, pp. 947-976.

Sperry, P. R., Hopfenberg, H. B. and Thomas, N. C., 1981, "Flocculation of Latex by Water-Soluble Polymers: Experimental Confirmation of a Nonbridging, Nonadsorptive, Volume-Restriction Mechanism", **J. Colloid Interface Sci.**, 82(1), pp.63-71.

Sresty, G. C., Raja, A. and Somasundaran, P., 1978, "Selective Flocculation of Mineral Slimes Using Polymers", in: **Recent Developments in Separation Science**, Eds. N. Li, Vol. IV, CRC Press, pp. 93-105.

Sturm, W. and Morgan, J., 1981, **J Aquatic Chemistry**, 2nd edition, New York, Wiley-Interscience, table 5.1.

Tadros, Th. F., 1996, "Correlation of Viscoelastic Properties of Stable and Flocculated Suspensions with their Interparticle Interactions", **Advances in Colloid and Interface Sci.**, 68, pp. 97-200.

Trahar, W. J. 1981, "A Rational Interpretation of the Role of Particle Size in Flotation", **Int. J. Miner. Process.**, Vol. 8, 289-327.

van de Ven, T. G. M., Dabros, T. and Czarnecki, J., 1983, "Flexible Bonds between Latex Particles and Solid Surfaces", **J. Colloid Interface Sci.**, Vol. 93, No. 2, pp. 580-581.

van den Hul, H. J. and Vanderhoff, J. W., 1968, "Well Characterized Monodisperse Latexes", **J. Colloid Interface Sci.**, 28, pp. 336-337.

Vanderhoff, J. W., 1981, "Well-Characterized Monodisperse Polystyrene Latexes as Model Colloids", **Emulsion Polymers and Emulsion Polymerization**, Eds. D. R. Bassett and A. E. Hamielec, ACS Symposium Series Number 165, Washington, D. C., pp. 61- 83.

Vanderhoff, J. W., 1983, "The Making of a Polymer Colloid", **Science and Technology of Polymer Colloids. Preparation and Reaction Engineering**, Vol. I, Eds. G. W. Poehlein, R. H. Ottewill and J. W. Goodwin, NATO ASI Series, Martinus Nijhoff Publishers, The Netherlands, pp. 1-39.

Vanderhoff, J. W., van den Hul., H. J., Tausk, R. J. M. and Overbeek, J. T. G., 1970, "Preparation of Monodisperse Latexes with Well-Characterized Surfaces", in: **Clean Surfaces: Their Preparation and Characterization for Interfacial Studies**, Ed. G. Goldfinger, Marcel Dekker, New York, pp. 15-44.

Vijayendran, B. R., Boone, T. and Gajria, C., 1981, "Some Studies on Vinyl Acrylic Latex-Surfactant Interactions" **Emulsion Polymerization of Vinyl Acetate**, Eds. M. S. El-Aasser and J. W. Vanderhoff, Applied Science, London, pp. 253-283.

Vurdela, R. M. and Laskowski, J. S., 1987, "Positively Charged Colloidal Species in Aqueous Anionic Surfactant Solutions", **Colloid Surf.** Vol. 22, pp. 77-80.

Wang, S. S. N. , 1977, "Flotation Agents for the Beneficiation of Phosphate Ores", **U.S. Patent, 4034863.**

Wang, S. S. N. and Huliganga, E. F., 1979, "Froth Flotation of Phosphate Ores", **U.S. Patent, 4158623**.

Warren, L. J., 1992, "Shear-flocculation", in: **Colloid Chemistry in Mineral Processing**, Eds. J. S. Laskowski and J. Ralston, Elsevier, Amsterdam, pp. 309-329.

Wensel, R. W., Vernon, M. S., Penaloza, M., Cross, W. M., Winter, R. M. and Kellar, J. J., 1994, "Adsorption Behavior of Oleate on Brucite as Revealed by FT-IR Spectroscopy", **SME Preprint 94-102**.

Wilkinson, M. C. and Fairhurst, D., 1981, "A New Technique for the Cleaning of Polymer Latices", **J. Colloid and Interface Sci.**, 79, pp. 272-277.

Xu, Z. H. and Yoon, R., 1989, "The Role of Hydrophobic Interaction in Coagulation", **J. Colloid Interface Sci.**, Vol. 132, pp. 532-541.

Xu, Z. H. and Yoon, R., 1990, "A Study of Hydrophobic Coagulation", **J. Colloid Interface Sci.**, Vol. 134, pp. 427-434.

Yarar, B. and Kitchener, J. A., 1970, "Selective Flocculation of Minerals", **Transactions, IMM**, Sec. C, Vol. 79, pp. 23-33.

Yotsumoto, H. and Yoon, R., 1993, "Application of Extended DLVO Theory, I. Stability of Rutile Suspensions", **J. Colloid Interface Sci.**, Vol. 157, pp. 426-433.

Young, C. A. and Miller, J. D., 1993, "Comparison of Oleate Adsorption at Calcite and Fluorite Surfaces: An In-Situ FT-IR/IRS and MLRS Study", **SME Annual Meeting**, Preprint Number, 93-224.

Young, R. J. and Lovell, P. A., 1991, **Introduction to Polymers**, Chapman and Hall, London.

Young, R. S., 1971, **Chemical Analysis in Extractive Metallurgy**, Griffin, London.

Yu, S. and Attia, Y. A., 1987, "Review of Selective Flocculation in Mineral Separations", **Flocculation in Biotechnology and Separation Systems**, Eds. Y. A. Attia, Elsevier, Amsterdam, pp. 601-637.

Yu, Z. M., 1998, **Flocculation, Hydrophobic Agglomeration and Filtration of Ultrafine Coal**, Ph. D Dissertation.

Zhang, P., Snow, R., El-Shall, H. and Bogan, M., 1998, "Recovery of Phosphate from Florida Beneficiation Slimes, II. Dispersion as the First Step", **SME Preprint 98-79**.

Zhang, P., Snow, R., and Bogan, M., 1998, "Recovery of Phosphate from Florida Beneficiation Slimes, III. Small Hydrocyclone as the First Step", **SME Preprint, 98-80**.

Zheng, X., Smith, R. W., Mehta, R. K., Misra, M. and Raichur, A. M., 1997, "Anionic Flotation of Apatite from Dolomite Modified by the presence of a Bacterium", **SME Preprint 97-98**.

Zimehl, R. and Lagaly, G., 1986, "Coagulation of Latex Dispersions by Inorganic Salts: Structural Effect", **Progress in Colloid & Polymer Science**, Vol. 72, pp. 28-36.

Zimmels, Y. and Lin, I. J., 1974, "Stepwise Association Properties of Some Surfactant Aqueous Solution", **Colloids Polym. Sci.**, Vol. 252, pp. 594-612.

APPENDIX I

Calculation of mobility μ , $\text{m}^2 \text{sec}^{-1} \text{volt}^{-1}$

$$\text{mobility } \mu = \frac{v}{E}$$

v - particle velocity, m/sec, $v = \frac{L}{t}$, L - graticule, m, t - second

E - field strength, volt / m, $E = \frac{V}{l}$,

V - potential difference applied to the electrodes, volt,

l - effective interelectrode distance, m,

$$\mu = \frac{vl}{V} \text{ m}^2 \text{sec}^{-1} \text{volt}^{-1}$$

The effective interelectrode distance $l = RKA$

R - interelectrode resistance, Ω

K - conductivity of suspension, s/m

A - cross sectional area, m^2

$$A = dh$$

d - thickness of the cell, m

h - width of the cell, m

For the particular cell, $d = 8.070 \times 10^{-4}$ m, $h = 9.730 \times 10^{-3}$ m

$$A = dh = 7.852 \times 10^{-6} \text{ m}^2$$

In 0.1 M KCl solution, and temperature of 25°C , interelectrode resistance $R = 6000 \Omega$,

$K = 0.1315$ s/m,

The effective interelectrode distance $l = RKA = 6000 \times 0.1315 \times 7.852 \times 10^{-6} = 6.195 \times 10^{-2}$ m

For each measurement, record particle velocity, and the potential difference applied to the electrodes, and use the equation $\mu = \frac{vl}{V}$ to calculate the mobility.

Conversion of mobility to zeta potential (ζ)

$$\mu = \frac{\epsilon\zeta}{4\pi\eta} f(\kappa a)$$

ϵ - permittivity of the suspending liquid, for water at 25°C, 8.716×10^{-9} F/m

ζ - zeta potential, volt

η - suspension viscosity, for water at 25°C, 8.903×10^{-4} Ns / m²

κ - reciprocal of double layer thickness, m⁻¹

a - radius of the particle, m

If $\kappa a > 100$, $f(\kappa a) = 1$

$$\mu = \frac{\epsilon\zeta}{4\pi\eta}$$

This is so called Smoluchowski equation.

$$\zeta = \frac{4\pi\eta}{\epsilon} \mu$$

$$\text{at } 25^\circ\text{C, } \zeta = \frac{4 \times 3.14 \times 8.903 \times 10^{-4}}{8.716 \times 10^{-9}} \mu = 12.83 \times 10^5 \mu$$

ζ - volt

μ - m² sec⁻¹ volt⁻¹

If $\kappa a < 0.1$ then the Hückel equation would be relevant

$$f(\kappa a) = \frac{2}{3}$$

$$\mu = \frac{\varepsilon \zeta}{4\pi\eta} \frac{2}{3} = \frac{\varepsilon \zeta}{6\pi\eta}$$

This is so called Hückel equation.

$$\zeta = \frac{4\pi\eta}{\varepsilon} \mu \frac{3}{2} = \frac{6\pi\eta}{\varepsilon} \mu$$

This will hardly ever be useful in the case of water as suspending medium since even water with no added electrolyte has $\kappa = 10^8 \text{ m}^{-1}$.

When $\kappa a < 0.1$, $a < 10^{-9} \text{ m} = 1 \text{ nm}$

If $0.1 < \kappa a < 100$ the Henry equation should be used

$$\mu = \frac{\varepsilon \zeta}{6\pi\eta} [1 + f(\kappa a)]$$

For calculation of $f(\kappa a)$, refer to Wiersema, Loeb and Overbeek, J. Coll. Sci., 22(1966), 78.

In this study, the particle size of mineral sample is around 10-38 μm . According to the calculation shown below, $\kappa a > 100$, thus the Smoluchowski equation can be used to calculate zeta potentials of mineral samples. The detailed calculation is shown as follows.

The calculation of reciprocal of double layer thickness κ :

$$\kappa = \sqrt{\frac{8\pi e^2 n z^2}{\varepsilon k T}}$$

e - electronic charge, -1.6×10^{-19} coulomb

n - number of ions / m^3 , $n = N c$

N - Avogadro number, 6.023×10^{23} particles/mol

c - concentration of electrolyte kmol/m^3

k - Boltzmann constant, 1.38×10^{-23} J/T

t - absolute temperature, °K

at 25°C, $\varepsilon = 8.716 \times 10^{-9}$, $t = 298^\circ\text{K}$, $z=1$, $c=10^{-3}$ kmol/m³

$$\kappa = \sqrt{\frac{8 \times 3.14 (-1.6 \times 10^{-19})^2 \times 6.023 \times 10^{23} \frac{1}{10^{-3}} \times 10^{-3} \times 1}{8.716 \times 10^{-9} \times 1.38 \times 10^{-23} \times 298}}$$

$$= 1.041 \times 10^8 \text{ m}^{-1}$$

when $a = 38 \mu\text{m}$, $\kappa a = 1.041 \times 10^8 \times 38 \times 10^{-6} = 3956 > 100$

when $a = 10 \mu\text{m}$, $\kappa a = 1.041 \times 10^8 \times 10 \times 10^{-6} = 1041 > 100$

APPENDIX II

Standard deviation s can be calculated from the following equation:

$$s = \sqrt{\frac{\sum (Y_i - \bar{Y})^2}{(r-1)}} \quad (\text{AII.1})$$

where $\bar{Y} = \frac{\sum Y_i}{r}$ is the average response from r replicate runs, and \sum represents the sum over i from 1 to r .

For the apatite-calcite system, the calculated standard deviation s_R^2 on the three replicate centerpoints

Recovery, %	85.4	87.5	89.6
Grade, %	30.0	31.3	31.5

is 4.3 for the recovery and 0.70 for the grade.

The standard deviation s^2 for the other two replicate points,

Recovery, %	64.1	67.2
Grade, %	22.5	23.6

is 4.8 for the recovery and 0.6 for the grade.

The standard deviation from the above two sources can be combined, or pooled, to give a firmer estimate of error. The pooled variance for k separate estimates of error, s_i , each with r_i replicates, is

$$s^2 = \frac{\sum (r_i - 1) s_i^2}{\sum (r_i - 1)} \quad (\text{AII.2})$$

where \sum denotes the summation over i from 1 to k . $\sum (r_i - 1)$ represents the total degree of freedom. According to equation AII.2, the pooled variance s which combines the error estimate from the above two sources is 2.1 for the recovery and 0.8 for the grade.

For the apatite-silica system, the standard deviation s , estimated on the three replicate centerpoints,

Recovery, %	88.4	90.7	88.3
Grade, %	30.7	31.8	32.4

is 1.3 for the recovery and 0.9 for the grade.

Estimation of main effects:

A main effect is estimated from the difference between the average high- and low- factor-level responses:

$$\text{Main effect of } X_i = \frac{\sum (\text{responses at high } X_i) - \sum (\text{responses at low } X_i)}{(\text{half the number of factorial runs})} \quad (\text{AII.3})$$

Estimation of interaction effects:

The calculation for interaction effects follows the same procedure as that for main effects. The interaction effect is calculated as the average response difference between one half of the factorial runs and the other half.

Assessment of significance of main effects:

The precision of estimation of main effects is generally stated in the form of a confidence interval, which is an interval to include the "true" effect at a stated confidence level. The most common confidence levels are 90, 95 and 99%. The confidence-interval width is a function of the response error estimates, the number of data in the estimate, and the number

of degree of freedom in the response error estimate for a main effect. The confidence interval is :

$$\text{(Main effect estimate)} \pm ts \frac{1}{\sqrt{\frac{N}{4}}} \quad \text{(AII.4)}$$

where s = response error estimate with ν degree of freedom; N = number of factorial runs in the design; and t = student's t statistic with ν degree of freedom at stated confidence level. Values of the multiplier t can be obtained from Table XI in Murphy's (1977) paper. The table is indexed by the confidence level and the number of degrees of freedom corresponding to the estimate s . If the confidence interval does not include zero, it can be said that effect is significantly different zero at the stated confidence level.

For the apatite-calcite system, the 95% confidence interval is calculated as follows:

$$\text{for the recovery, } t = 3.181 \text{ at } \nu = 3, \quad ts \frac{1}{\sqrt{\frac{N}{4}}} = 3.181 \times 2.1 / \sqrt{2} = 4.7$$

$$\text{for the grade, } t = 3.181 \text{ at } \nu = 3, \quad ts \frac{1}{\sqrt{\frac{N}{4}}} = 3.181 \times 0.8 / \sqrt{2} = 1.8$$

For the apatite-silica system, the 95% confidence interval is calculated as follows:

$$\text{for the recovery, } t = 4.303 \text{ at } \nu = 2, \quad ts \frac{1}{\sqrt{\frac{N}{4}}} = 4.303 \times 1.4 / \sqrt{2} = 4.3$$

$$\text{for the grade, } t = 4.303 \text{ at } \nu = 2, \quad ts \frac{1}{\sqrt{\frac{N}{4}}} = 4.303 \times 0.9 / \sqrt{2} = 2.7$$

Estimation of curvature effects

The overall curvature effect is estimated as the difference between the average of the centerpoints responses and the average of the factorial points. A confidence interval for the curvature effect is calculated as:

$$\text{Curvature effect} \pm t_s \sqrt{\frac{C+N}{NC}} \quad (\text{AII.5})$$

where C = number of centerpoints, and N = the number of factorial points in the design.

For the apatite-calcite system:

The average of the recovery for the three centerpoints is 87.5% and the average of the recovery for the eight factorial points is 66.6%. Thus the curvature effect for the recovery is 20.9%. The average of the grade for the three centerpoints is 30.9% and the average of the grade for the eight factorial points is 31.0%. Thus the curvature effect for the grade is 0.1.

The 95% confidence interval for the curvature effect is calculated as follows:

$$\text{for the recovery, } t_s \sqrt{\frac{C+N}{NC}} = 2.365 \times 2.1 \times \sqrt{\frac{11}{24}} = 3.4$$

$$\text{for the grade, } t_s \sqrt{\frac{C+N}{NC}} = 2.365 \times 0.8 \times \sqrt{\frac{11}{24}} = 1.3$$

Therefore the curvature effects at the 95% confidence interval are 20.9 ± 3.4 for the recovery, and 0.1 ± 1.3 for the grade.

For the apatite-silica system:

The average of the recovery for the three centerpoints is 89.1% and the average of the recovery for the eight factorial points is 82.7%. Thus the curvature effect for the recovery is 6.4%. The average of the grade for the three centerpoints is 31.6% and the average of the grade for the eight factorial points is 30.8%. Thus the curvature effect for the grade is 0.8 %.

The 95% confidence interval for the curvature effect is calculated as follows:

$$\text{for the recovery, } ts\sqrt{\frac{C+N}{NC}} = 2.365 \times 1.3 \times \sqrt{\frac{11}{24}} = 2.2$$

$$\text{for the grade, } ts\sqrt{\frac{C+N}{NC}} = 2.365 \times 0.86 \times \sqrt{\frac{11}{24}} = 1.4$$

Therefore the curvature effects at the 95% confidence interval are 6.4 ± 2.2 for the recovery and 0.8 ± 1.4 for the grade.